Isolation and Structure Elucidation of Bioactive Chemical Constituents from *Vitex pinnata*, *Artocarpus nobilis*, *Barleria prionitis*, *Buxus natalensis* and *Coprinus micaceus*.

By

Shamsul Haq Zahid

Thesis Submitted to the Faculty of Graduate Studies

In Partial Fulfillment for the Degree of

MASTER OF SCIENCE

Department of Chemistry

University of Manitoba

Winnipeg, Manitoba, Canada

Copyright © 2009 by Shamsul Haq Zahid

THE UNIVERSITY OF MANITOBA

FACULTY OF GRADUATE STUDIES

*****

COPYRIGHT PERMISSION

Isolation and Structure Elucidation of Bioactive Chemical Constituents from *Vitex pinnata*, *Artocarpus nobilis*, *Barleria prionitis*, *Buxus natalensis* and *Coprinus micaceus*

By

Shamsul Haq Zahid

A Thesis/Practicum submitted to the Faculty of Graduate Studies of The University of Manitoba in partial fulfillment of the requirement of the degree

Of

Master of Science

Shamsul Haq Zahid©2009

Permission has been granted to the University of Manitoba Libraries to lend a copy of this thesis/practicum, to Library and Archives Canada (LAC) to lend a copy of this thesis/practicum, and to LAC's agent (UMI/ProQuest) to microfilm, sell copies and to publish an abstract of this thesis/practicum.

This reproduction or copy of this thesis has been made available by authority of the copyright owner solely for the purpose of private study and research, and may only be reproduced and copied as permitted by copyright laws or with express written authorization from the copyright owner.

Acknowledgements

First of all, I bow down my head before Almighty God, Who provided me wisdom and opportunity to perform this research. I am thankful to Him for blessing me with several successes in life. I am grateful to Dr. Athar Ata, for accepting me in his lab as a graduate student and for his supervision, guidance, advice and crucial contribution throughout this research work. Thanks are due to the Chemistry professors at the University of Winnipeg as well as at the University of Manitoba for their teachings. I would also like to record my gratitude to the examining committee members who spent their precious time to evaluate this thesis.

Most of the experimental work of this thesis was completed at the Chemistry department, University of Winnipeg. I wish to express my appreciation to all faculty and staff members at the University of Winnipeg especially Gunders Reinsfield, Peter Balagus, Ramin Vakili and Ed Segstro for their technical support.

I also wish to acknowledge Dr. Paul Holloway, Biology Department, (University of winnipeg), for his assistance in performing bioassays. I am also thankful to Dr. Kirk Marat of the NMR facility, University of Manitoba in doing NMR experiments. I gratefully acknowledge Dr. Radhika Samaresekera of Industrial Technology Institute, Sri Lanka and Dr. Richert Geggan of the Chemistry department, Durban University, South Africa for providing the plant extracts for this research. Collective and individual acknowledgements are owned to all my lab fellows during this study as well as apology that I could not mention personally one by one.

Finally, I am thankful to my parents for their moral support and for creating thrust of acquiring knowledge in me. I am also grateful to my wife, Sarfraz Akhter and my

children, Rimsha Zahid, Sufian Muhammad Zahid and Razeena Zahid who spend many evenings without me.

Abstract

This thesis describes phytochemical studies on four medicinally important plants, *Vitex pinnata*, *Artocarpus nobilis*, *Barleria prionitis*, *Buxus natalensis* and one saprophytic fungus, *Coprinus micaceus*. These findings are summarized as follows:

1. Chemical studies on the crude methanolic extract of *Vitex pinnata* yielded one new iridoid glucoside, 6″-glucosepeduncullariside (**88**) and three known natural products, peduncullariside (**89**), agnuside (**90**) and *p*-hydroxy benzoic acid (**91**). Compounds **88-91** were found to exhibit weak to moderate GST/AChE inhibitory activities and antioxidant activity.
2. Phytochemical investigations on the crude ethanolic extract of *Artocarpus nobilis* resulted in the isolation of two new triterpenoids, [artocarpurate A (**109**), atocarpurate B (**110**)]; four known triterpenoids, [cyclolaudenyl acetate (**111**), lupeol acetate (**112**), β-amyrine acetate (**113**), 12,13-dihydromicromeric acid (**114**)]; and two known flavonoids [artonins E (**115**) and artobiloxanthone (**116**)]. All of these compounds exhibited different levels of anti-AChE and anti-GST properties. Compounds **115** and **116** were found to be more potent GST inhibitors than the standard GST inhibitor sodium taurocholate whereas compound **113** showed good AChE inhibitory activitity ($IC_{50} = 11.5 \pm 2.58$).
3. Our studies on the crude ethanolic extract of aerial parts of *Barleria prionitis* afforded five known natural products, 8-*O*-acetylshanzhiside methyl ester (**127**), shanzhiside methyl ester (**128**), lupeol (**129**), betulinic acid (**130**) and pipataline (**131**). Pipataline was isolated in enough quantity to prepare three different analogues of this natural product by doing reactions on C-7/C-8 double bond and

evaluate them for the aforementioned bioactivities. We were interested to see the role of this double bond in the moderate bioactivity of this compound. In this study, we discovered that by the addition of an amino group at C-7 position, acetylcholinesterase inhibitory activity was improved from IC_{50} value of 135.09 ± 0.501 μM to 36.75 ± 0.272 μM.

4. Phytochemical studies on *Buxus natalensis* have resulted in the isolation of one new steroidal alkaloid, natalensamine-A (**156**). Compound **156** showed weak AChE inhibitory activity.
5. Chemical studies on the methanolic extract of *Coprinus micaceus* yielded two compounds, micaceol (**179**) and (Z, Z)-4-oxo-2, 5-heptadienedioic acid (**180**). Compound **179** was found to be new while **180** was isolated for the first time as a natural product. Compound **179** showed weak antibacterial activity against *Staphylococcus aureus* and *Corynebacterium xerosis* while compound **180** was inactive in this bioassay. Compound **180** showed weak GST inhibitory activity while compound **179** was inactive in this bioassay.

Dedicated to my family

For their patience and endurance

CONTENTS

		Page
Acknowledgements		**iii**
Abstract		**v**
List of Abbreviations		**xiv**
List of Tables		**xvii**
List of Schemes		**xix**
List of Appendices		**xx**
Chapter 1: General introduction		**1**
1.1	Natural products	**1**
1.2	Modern drug discovery process from terrestrial plants	**4**
1.3	Enzyme inhibitors as promising approach for the discovery of new leads	**12**
1.3.1	Acetylcholinestrase, its role in nervous system and inhibition	**13**
1.3.2	Glutathione *S*-transferase and its role in drug resistance	**19**
1.4	References	**25**
Chapter 2: Phytochemical studies on *Vitex pinnata*		**33**
2.1	Introduction	**33**
2.2	Results and discussion	**37**
2.2.1	Isolation of compounds **88-91**	**37**
2.2.2	Structure elucidation of 6″-glucosepeduncullariside (**88**)	**37**
2.2.3	Structure elucidation of pedunculariside (**89**)	**41**
2.2.4	Structure elucidation of agnuside (**90**)	**43**
2.2.5	Structure elucidation of *p*-hydroxy benzoic acid (**91**)	**45**

2.2.6 Biological activities of compounds **88-91** **46**

2.3 Experimental **47**

2.3.1 General experimental conditions **47**

2.3.2 Plant material **47**

2.3.3 Extraction and isolation **48**

2.3.4 6″-glucosepeduncularisside (**88**) **50**

2.3.5 Pedunculariside (**89**) **50**

2.3.6 Agnuside (**90**) **50**

2.3.7 *p*-Hydroxy benzoic acid (**91**) **50**

2.4 Enzyme inhibition assays **50**

2.4.1 Glutathione *S*-transferase inhibition assay **50**

2.4.2 Acetylcholinesterease assay **51**

2.4.3 Antioxidant assay **52**

2.5 References **53**

Chapter 3: Phytochemical studies on *Artocarpus nobilis* **56**

3.1 Introduction **56**

3.2 Results and discussion **60**

3.2.1 Isolation of compounds **109** to **116** **60**

3.2.2 Structure elucidation of artocarpuate A (**109**) **60**

3.2.3 Structure elucidation of artocarpuate B (**110**) **65**

3.2.4 Structure elucidation of cyclolaudenyl acetate (**111**) **69**

3.2.5 Structure elucidation of lupeol acetate (**112**) **73**

3.2.6 Structure elucidation of β-amyrine acetate (**113**) **77**

3.2.7 Structure elucidation of 12,13-dihydromicromeric acid (**114**) **80**

3.2.8 Structure elucidation of artonins E (**115**) **83**

3.2.9 Structure elucidation of artobiloxanthone (**116**) **87**

3.2.10 Biologic al activities of compounds **109-116** **90**

3.3 Experimental **91**

3.3.1 General experimental conditions **91**

3.3.2 Plant material **91**

3.3.3 Extraction and isolation **91**

3.3.4 Artocarpuate A (**109**) **95**

3.3.5 Artocarpuate B (**110**) **95**

3.3.6 Cyclolaudenyl acetate (**111**) **95**

3.3.7 Lupeol acetate (**112**) **95**

3.3.8 β-amyrine acetate (**113**) **95**

3.3.9 12,13-dihydromicromeric acid (**114**) **95**

3.3.10 Artonins E (**115**) **96**

3.3.11 Artobiloxanthone (**116**) **96**

3.4 Enzyme inhibition assays **96**

3.4.1 Glutathione *S*-transferase inhibition assay **96**

3.4.2 Acetylcholinesterease assay **96**

3.4.3 Antioxidant assay **96**

3.5 References **97**

Chapter 4: Phytochemical studies on *Barleria prionitis* **101**

4.1 Introduction **101**

4.2	Results and discussion	**104**
4.2.1	Isolation of compounds **127-131**	**104**
4.2.2	Structure elucidation of barlerin (**127**)	**104**
4.2.3	Structure elucidation of shanzhiside methyl ester (**128**)	**108**
4.2.4	Structure elucidation of lupeol (Lup-20(29)-ene-3β-ol) (**129**)	**110**
4.2.5	Structure elucidation of betulinic acid (**130**)	**112**
4.2.6	Structure elucidation of pipataline (**131**)	**114**
4.2.7	Derivatization of pipataline	**116**
	4.2.7.1 7,8-epoxypipataline (**132**)	**116**
	4.2.7.2 7-Amino-8-hydroxypipataline (**133**)	**117**
	4.2.7.3 7,8-dibromopipataline (**134**)	**118**
4.2.8	Enzyme inhibitory activities of compounds **127-134**	**119**
4.3	Experimental	**121**
4.3.1	General experimental conditions	**121**
4.3.2	Plant material	**121**
4.3.3	Extraction and isolation	**121**
4.3.4	Barlerin (**127**)	**126**
4.3.5	Shanzhiside methyl ester (**128**)	**126**
4.3.6	Lupeol (Lup-20(29)-ene-3β-ol) (**129**)	**126**
4.3.7	Betulinic acid (**130**)	**126**
4.3.8	Pipataline (**131**)	**126**
4.3.9	Epoxidation of pipataline (**132**)	**126**
4.3.10	S ynthesis of 7-amino-8-hydroxy pipataline (**133**)	**127**

4.3.11 Bromination of pipatal ine (**134**) **128**

4.4 Enzyme inhibition assays **129**

4.4.1 Glutathione *S*-transferase inhibition assay **129**

4.4.2 Acetylcholinesterease assay **129**

4.5 References **130**

Chapter 5: Phytochemical studies on *Buxus natalensis* **133**

5.1 Introduction **133**

5.2 Results and discussion **139**

5.2.1 Isolation of compound (**156**) **139**

5.2.2 Structure elucidation of natalensamine-A (**156**) **139**

5.2.3 AChE inhibitory activity of natalensamine-A (**156**) **144**

5.3 Experimental **145**

5.3.1 General experimental conditions **145**

5.3.2 Plant material **145**

5.3.3 Extraction and isolation **139**

5.3.4 Natalensamine-A (**156**) **148**

5.4 Enzyme inhibition assay **148**

5.4.1 Acetylcholinestrase assay **148**

5.5 References **149**

Chapter 6: Chemical studies on *Coprinus micaceus* **151**

6.1 Introduction **151**

6.2 Results and discussion **157**

6.2.1 Isolation of compounds **179** and **180** **157**

6.2.2 Structure elucidation of micaceol (**179**) **157**

6.2.3 Structure elucidation of (Z, Z)-4-oxo-2,5-heptadienedioic acid(**180**) **162**

6.3 Bioactivity of chemical constituents of *Coprinus micaceus* **164**

6.3.1 Anti-bacterial activity **164**

6.3.2 Glutathione *S*-transferase inhibitory activity **164**

6.4 Experimental **165**

6.4.1 General experimental conditions **165**

6.4.2 Collection of mushroom **165**

6.4.3 Extraction and isolation **165**

6.4.4 Micaceol (**179**) **167**

6.4.5 (Z, Z)-4-oxo-2,5-heptapadienedioic acid (**180**) **167**

6.4.6 Enzyme inhibition assays **167**

6.4.6.1 Glutathione *S*-transferase inhibition assay **167**

6.4.6.2 Anti-bacterial assay **167**

6.5 References **170**

Chapter 7: Conclusions **173**

LIST OF ABBREVIATIONS

Abbreviation	Name
2° CC	Secondary column chromatography
ACh	Acetylcholine
AChE	Acetylcholinesterase
AChEI	Acetylcholinesterase inhibitor
ACN	Acetonitrile
AD	Alzheimer disease
AIDS	Acquired immune deficiency syndrome
ATCC	American Type Culture Collection
BChE	Butyrylcholinesterase
BCNU	1,3-bis(2-chloroethyl)-1-nitrosourea
BPO	Benzoyl peroxide
$CDCl_3$	Deuterated Chloroform
CDNB	1-chloro-2,4-dinitrobenzene
CD_3OD	Deuterated methanol
CIMS	Chemical ionization mass spectrum
CNS	Central nervous system
CHS	Chalcone synthase
CHI	Chalcone isomerase
CH_2Cl_2	Dichloromethane
COSY	Correlation spectroscopy
DEPT	Distortionless Enhancement by Polarization Transfer

DNA	Deoxyribonucleic acid
DPPH	2,2-Diphenyl-1-picrylhydrazyl
DMSO	Dimethyl sulfoxide
DTNB	5-5-dithio-bis (2-nitrobenzoic acid)
EC_{50}	Effective concentratin by 50%
EIMS	Electron impact mass spectrum
EtOAc	Ethyl acetate
GSH	Glutathione
GST	Glutathione *S*-transferase
HIV	Human Immunodeficiency Virus
HMBC	Heteronuclear Multiple-Bond Correlation
HPLC	High performance liquid chromatography
HSQC	Heteronuclear Single Quantum Correlation
IC_{50}	Inhibition concentration by 50 %
iNOS	Inducible nitric oxide synthase
IR	Infrared
LC_{50}	Lethal concentration by 50%
LD_{50}	Lethal dose by 50%
LDL	Low-density lipoprotein
MH	Muller-Hinton
MS	Mass Spectroscopy
MDR	Multi Drug Resistance
NMR	Nuclear magnetic resonance
NMDA	*N*-methyl *D*-aspartate

OD	Optical density
PAS	Peripheral anionic site
PLA	Phenylalanine ammonia lyase
RSV	Respiratory Syncytial Virus
SARS	Severe Acute Respiratory Syndrome
TLC	Thin layer chromatography
THF	Tetrahydrofuran
UV	Ultra violet

LIST OF TABLES **Page**

Table 2.1 ^{1}H and ^{13}C-NMR data of **88**, recorded at 300 and 75 MHz, respectively 40

Table 2.2 ^{1}H and ^{13}C-NMR data of **89**, recorded at 300 and 75 MHz, respectively **42**

Table 2.3 ^{1}H and ^{13}C-NMR data of **90**, recorded at 300 and 75 MHz, respectively **44**

Table 2.4 ^{1}H and ^{13}C-NMR data of **91,** recorded at 300 and 75 MHz, respectively **46**

Table 2.5 GST, AChE and antioxidant activities of compounds **88** to **91** **46**

Table 3.1 ^{1}H and ^{13}C-NMR data of **109**, recorded at 300 and 75 MHz, respectively **64**

Table 3.2 ^{1}H and ^{13}C-NMR data of **110**, recorded at 300 and 75 MHz, respectively **68**

Table 3.3 ^{1}H and ^{13}C-NMR data of **111,** recorded at 300 and 75 MHz, respectively **72**

Table 3.4 ^{1}H and ^{13}C-NMR data of **112**, recorded at 300 and 75 MHz, respectively **76**

Table 3.5 ^{1}H and ^{13}C-NMR data of **113**, recorded at 300 and 75 MHz, respectively **79**

Table 3.6 ^{1}H and ^{13}C-NMR data of **114**, recorded at 300 and 75 MHz, respectively **82**

Table 3.7 ^{1}H and ^{13}C-NMR data of **115**, recorded at 300 and 75 MHz, respectively **86**

Table 3.8 ^{1}H and ^{13}C-NMR data of **116**, recorded at 300 and 75 MHz, respectively **89**

Table 3.9 AChE, GST and antioxidant activities of compounds **109** to **116** **90**

Table 4.1 ^{1}H and ^{13}C-NMR data of **127**, recorded at 300 and 75 MHz, respectively **107**

Table 4.2 ^{1}H and ^{13}C-NMR data of **128**, recorded at 300 and 75 MHz, respectively **109**

Table 4.3 ^{1}H and ^{13}C-NMR data of **129,** recorded at 300 and 75 MHz, respectively **111**

Table 4.4 ^{1}H and ^{13}C-NMR data of **130**, recorded at 300 and 75 MHz, respectively **113**

Table 4.5 ^{1}H and ^{13}C-NMR data of **131**, recorded at 300 and 75 MHz, respectively **115**

Table 4.6 AChE and GST inhibitory activities of compounds **127** to **134** **120**

Table 5.1 ^{1}H and ^{13}C-NMR data of **156,** recorded at 300 and 75 MHz, respectively **143**

Table 6.1 Antibacterial data of crude methanolic extract of *C. micaceus* **156**

Table 6.2 ^{1}H and ^{13}C-NMR data of **179,** recorded at 500 and 125 MHz, respectively **161**

Table 6.3 ^{1}H and ^{13}C-NMR data of **180,** recorded at 500 and 125 MHz, respectively **163**

LIST OF SCHEMES **Page**

Scheme 1.1 Flow sheet diagram for isolation of bioactive compounds **5**

Scheme 1.2 Catalytic hydrolysis of acetylcholine **14**

Scheme 1.3 Reaction mechanism of the hydrolysis of ACh catalyzed by AChE **14**

Scheme 1.4 A general reaction catalyzed by GST; R-X = electrophilic substrate **20**

Scheme 1.5 Michael-type addition and reduction reactions catalyzed by GST **20**

Scheme 1.6 Mechanism of inhibition by haloenol lactones **23**

Scheme 1.7 Mode of action of latent cytotoxin TLK286 **24**

Scheme 2.1 Biogenesis of iridoid glycoside from *Vitex pinnata* **35**

Scheme 2.2 Isolation procedure for compounds **88-91** **49**

Scheme 3.1 Isolation procedure for compounds **109-110** **92**

Scheme 3.2 Isolation procedure for compounds **111-114** **93**

Scheme 3.3 Isolation procedure for compounds **115-116** **94**

Scheme 4.1 Isolation procedure for compound **129** **123**

Scheme 4.2 Isolation procedure for compounds **130** and **131** **124**

Scheme 4.3 Isolation procedure for compounds **127** and **128** **125**

Scheme 5.1 Plausible biosynthesis of Buxus alkaloids **137**

Scheme 5.2 Isolation procedure for natalensamine-A (**156**) **147**

Scheme 6.1 Isolation procedure for compounds **179** and **180** **166**

List of APPENDICES (Spectra of all compounds) **Page**

6″-glucosepednucullariside (**88**) I

Peduncullariside (**89**) III

Agnuside (**90**) V

p-Hydroxy benzoic acid (**91**) VII

Artocarpurate A (**109**) IX

Atocarpurate B (**110**) XI

Cyclolaudenyl acetate (**111**) XIII

Lupeol acetate (**112**) XV

β-amyrine acetate (**113**) XVII

12, 13-dihydromicromeric acid (**114**) XIX

Artonins E (**115**) XXI

Artobiloxanthone (**116**) XXIII

Balerin (8-*O*-acetylshanzhiside methyl ester) (**127**) XXV

Shanzhiside methyl ester (**128**) XXVII

Lupeol (**129**) XXIX

Betulinic acid (**130**) XXXI

Pipataline (**131**) XXXIII

7, 8-epoxypipataline (**132**) XXXV

7-amino-8-hydroxy pipataline (**133**) XXXVII

7, 8-dibromopipataline (**134**) XXIX

Natalensamine-A (**156**) XLI

Micaceol (**179**) XLIII

(Z, Z)-4-oxo-2, 5-heptadienedioic acid (**180**) XLVI

CHAPTER 1

General Introduction

1.1 Natural products

Natural products are produced by living organisms including plants, animals, marine organisms and microorganisms for their survival against predators. The aforementioned living organisms produce two kinds of metabolites: primary metabolites and secondary metabolites. Primary metabolites, including carbohydrates, proteins and lipids are the building blocks of life. The secondary metabolites, including alkaloides, terpenoids, steroids, coumarins, saponins, phenols and phenolic glycosides are produced by these organisms for their self-deterrence[1,2]. The plants produce these compounds in response to ecological stress have shown their potential as various pharmaceuticals. These potentials led humans to use these plants to treat various ailments. For instance, terrestrial plants or their extracts such as licorice (*Glycyrrhiza glabra*), myrrh (*Commiphora* species), and poppy capsule latex (*Papaver somniferum*) have been used in herbal preparations as herbal drugs since ancient times for the treatment of ailments in various parts of the world[3]. Based on this ethanomedical importance of plants, chemists developed an interest in exploring the active phytochemicals from these plants. For instance, phytochemical studies on opium poppy (*Papaver somniferum*) yielded morphine (**1**), codeine (**2**), noscapine (**3**), and papaverine (**4**) as active ingredients and developed as single chemical drug which are still in use as clinically approved drugs. Morphine, codeine and noscapine are used as analgesics while papaverine is used for gastrointestinal disorders[2,4].

In the beginning of 19th century pharmaceutical companies started to use organic extracts to produce relatively crude therapeutic formulations. Later on in the mid-twentieth century with the discovery of antibiotics, use of fairly purified molecules became more typical for the formulation of drugs.

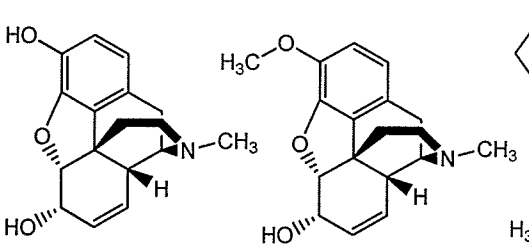

(1)

(2)

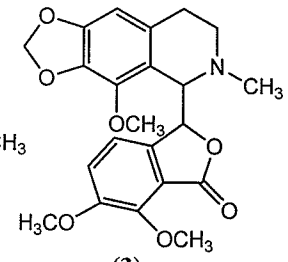

(3)

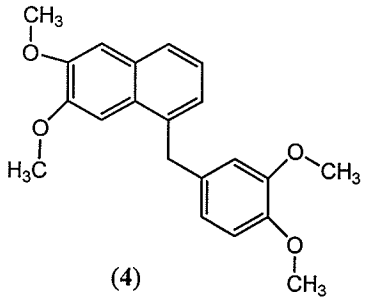

(4)

Natural products have been the major sources of chemical diversity as templates in the drug discovery program over the past century[5]. Many natural products and their derivatives have been successfully developed as drugs for the treatment of human diseases in almost all therapeutic areas[6]. For example, the presently used antimalarial drug artemether (**5**), a synthetic analogue of artemisinin (**6**), is effective against both chloroquinine-resistant and chloroquinine-sensitive strains of *Plasmodium falciparum* and against cerebral malaria[7]. Artemisinin was isolated from the Chinese herb "*Artemisia annua*", which has been used for over 2000 years by the Chinese to cure malaria[8].

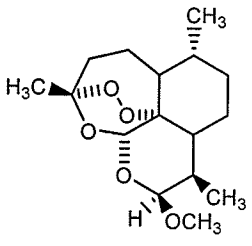

(5)

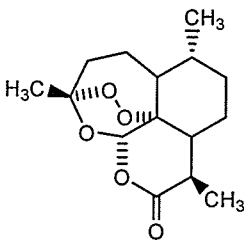

(6)

The antifungal drug anidulafungin (**7**) is a semi-synthetic derivative of echinocandin B (**8**), a fungal metabolite of *Aspergillus rugulovalvus*[9].

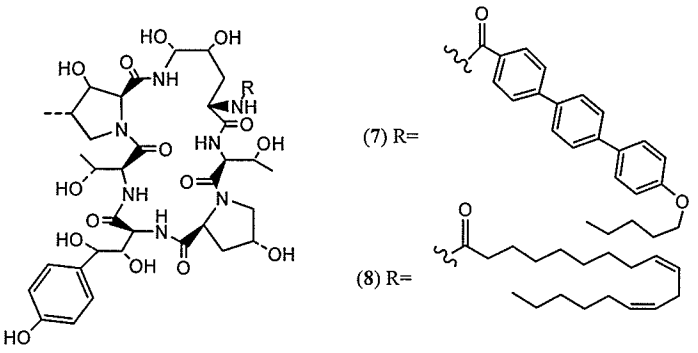

(7) R=

(8) R=

A secondary metabolite, Δ^9-tetrahydrocannabinol (**9**), isolated from *Cannabis sativa* L. exhibits both anti-emetic and anticancer properties[10]. During the course of structure activity relationship its two synthetic analogs, dexanabinol (**10**) and ajulemic acid (**11**) were found to possess neuroprotective and anti-inflammatory properties, respectively. Dexanabinol has shown neuroprotective properties by inhibiting NMDA glutamate receptors along with anti-inflammatory and anti-oxidant activities[11]. Ajulemic acid (**11**) has been discovered as a drug to treat acute and chronic pain and is in phase III clinical trials[12].

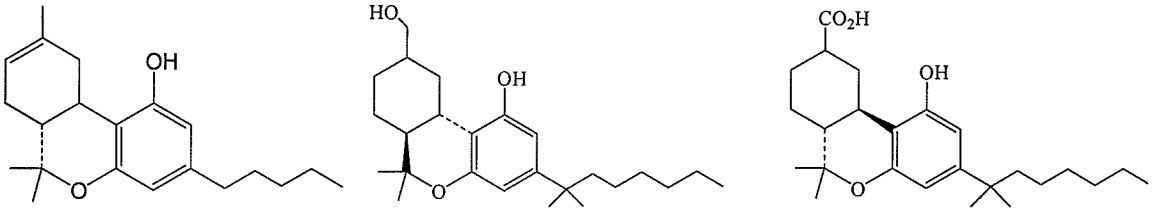

(**9**) (**10**) (**11**)

During the past few decades most of the pharmaceutical companies have significantly reduced their research budgets in natural product discovery program due to the introduction of new techniques like biotechnology and combinatorial chemistry for the discovery of new bioactive compounds[13]. Unfortunately, biotechnology companies working in the fields of combinatorial biosynthesis and genetic engineering for the discovery of novel bioactive molecules were unable to produce significant results and this failure forced pharmaceutical companies to move back towards natural products. Natural products offer structurely diverse libraries. These diverse natural products are

now part of innovative strategies to determine their interaction with macromolecules to inhibit their catalytic property in order to modulate cellular process such as immune response, signal transduction, mitosis and apoptosis[14]. This property of natural products provides a rational to use natural products as leads in drug discovery program.

These days, natural product chemists are involved in performing phytochemical studies on plants having biomedical importance in folk medicine history. These studies have yielded several biomedical agents including paclitaxel (**12**) and emetine (**13**). Paclitaxel (Taxol®) (**12**), which was isolated from bark extract of the pacific yew tree (*Taxus brevifolia*), is an important drug used in the treatment of cancer. Paclitaxel is an effective drug of choice for the treatment of lung, ovarian and breast cancer. Similarly, the isoquinoline alkaloid emetine (**13**), isolated from *Cephaelis ipecacuanha*, has been used for many years for the treatment of abscesses caused by the spread of *Escherichia histolytica* infections[15].

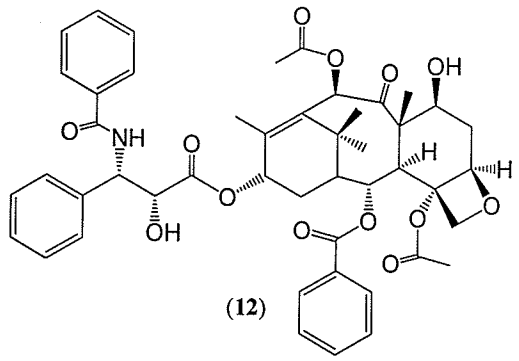

(12)

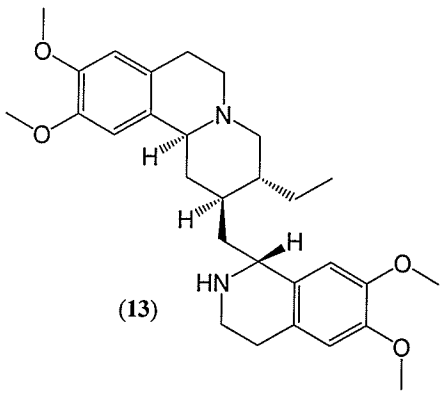

(13)

1.2 Modern drug discovery process from terrestrial plants

In China and India plants have been and continue to be used in organized traditional medical systems such as Ayurveda, Unani and Kampo for thousands of years[13,16-17]. These systems mainly focus on multi-component mixtures[18] and are playing an imperative role in health care. According to the World Health Organization report,

approximately 80% of the world's population relies on traditional medicines for their primary health care[19]. Plant products play an essential role in the health care systems of the remaining 20% of the population residing in developed countries. Data of prescribed drugs from 1959 to 1980 dispensed from community pharmacies in the United States showed that 25% of these drugs contained active ingredients derived from vascular plants[20]. In 1997 a study using US-based prescription data from 1993, showed that over 50% of the most-prescribed drugs in the US had a natural product either as a drug, or as a template in the synthesis or design of biologically active agents[21].

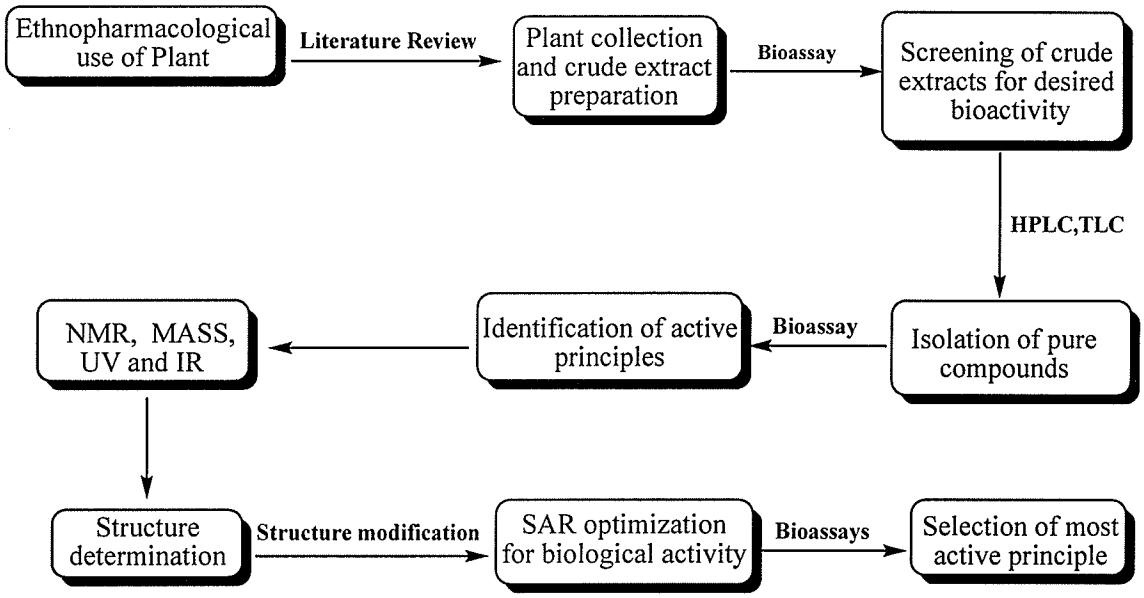

Scheme 1.1 Flow sheet diagram for the isolation of bioactive compounds

Currently, the isolation of an active agent relies on bioactivity-oriented isolation methods. The flow sheet diagram (Scheme **1.1**) describes this methodology, which involves the selection of plants in the light of available literature on desired bioactivity and subsequently compounds are purified and evaluated for their bioactivity. Bioactive compounds are structurely modified to understand structure activity relationship

(SAR) and more potent analogs are selected for further studies for drug development. This methodology has afforded many important bioactive molecules. For example, the important anticancer agent, camptothecin (**14**) from *Camptotheca acuminata*[22] was discovered by following bioassay guided isolation methdology. In 1995, Pisha and his coworkers reported the cytotoxic effects of betulinic acid (**15**) on the human melanoma cell line[23] MEL-1, 2 and 4 with IC_{50} values ranged from 0.5–1.6 μg/ml and on neuroblastoma cell lines with IC_{50} ranged from 14–17 μg/ml[24]. *In vitro* cytotoxic effects of betulinic acid (**15**) were found to be more potent on primary cancer cells isolated from glioblastoma multiforme than doxorubicin (**17**), cisplatin (**18**) and vincristine (**19**)[25]. Betulinic acid (**15**) has also been reported as a potent anti-HIV agent and was discovered to inhibit HIV-replication in H9 lymphocytes with an EC_{50} value of 1.4 μM[26].

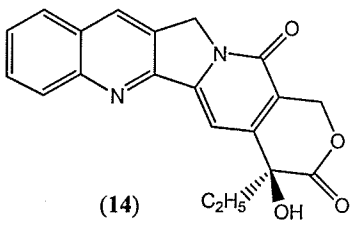

(**14**)

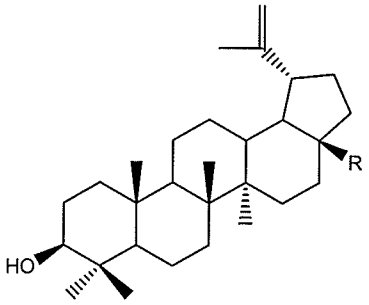

(**15**) R = COOH (**16**) R = CH_3

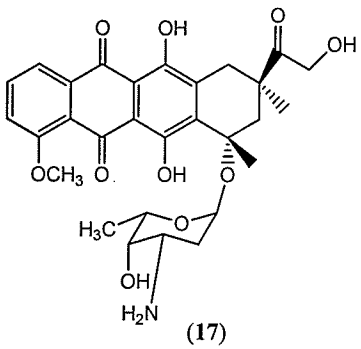

(**17**)

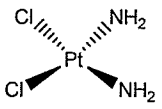

(**18**)

Lupeol (**16**), another chemopreventative agent, is found in various edible fruits (*e.g.* mango)[27] and medicinal herbs[28]. It suppresses benzoylperoxide (BPO) induced skin toxicity by activating a series of antioxidant enzymes. This involves inactivation of BPO such as catalase, glutathione peroxidase, glutathione-disulfide reductase and glutathione-*S*-transferase. Based on these findings, the use of lupeol (**16**) in the case of illnesses induced by free radicals has been recomended[29].

Derivatives of boswellic acid (**20**, **21**), are triterpenoids found in the resin of the Indian tree, *Boswellia serrata*. This plant is widely used for its anti-inflammatory and anti-arthritic effects in Indian folk medicine[30].

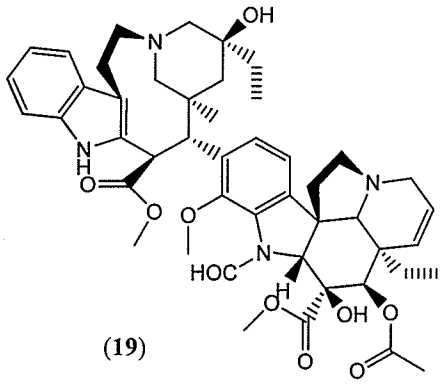

(**19**)

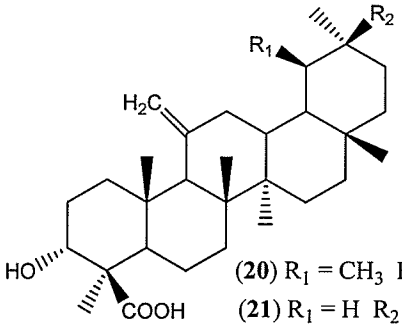

(**20**) $R_1 = CH_3$ $R_2 = H$
(**21**) $R_1 = H$ $R_2 = CH_3$

In 1998, Tanaka *et al.* reported triterpenoidal DNA polymerase inhibitors, fomitellic acids A (**22**) and B (**23**) from basidiomycete, *Fomitella fraxinea*[31]. Both acids **22** and **23** have shown inhibitory effects against DNA polymerase α, rat polymerase β and mild inhibition of plant DNA polymerase II, HIV reverse transcriptase as well as cytotoxic effects on cancer cell lines NUGC-3 (acid **22**, LD_{50} = 38μM) and PC-12 (acid **22**, LD_{50} = 23μM, acid **23**, LD_{50} = 62μM)[32]. Some triterpenoids have been reported to possess the ability to inhibit the classic course of the complement system e. g. ganoderiol F (**24**), isolated from the mushroom *Ganoderma lucidum* has shown anti-inflamatory properties with an IC_{50} value of 4.8 μM[33].

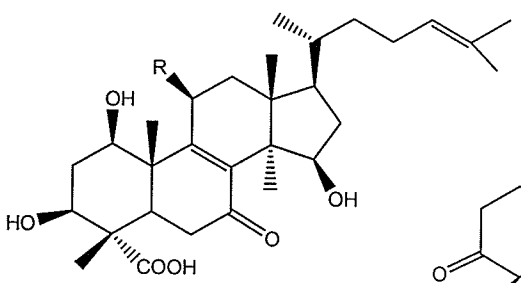

(22) R = OH (23) R = H

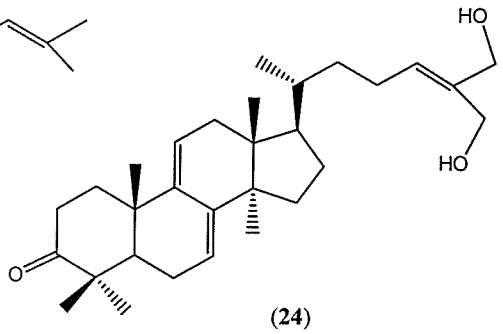

(24)

In the last few decades *Buxus* steroidal alkaloids have shown interesting pharmacological activities such as antimicrobial, antimalarial, antituberculosis[34], anti-HIV[35] and anti-cholinesterase effects[36]. For example four steroidal alkaloids, cyclovirobuxeine-F (**25**), *N*-benzoyl-*O*-acetylbuxa longifoline (**26**), buxasamarine (**27**) and cyclobuxamidine (**28**), isolated from *Buxus longifolia*, have shown weak antibacterial activity against *Salmonella typhi*, *Shigella flexneri* and *Pseudomonas aeruginosa*[37].

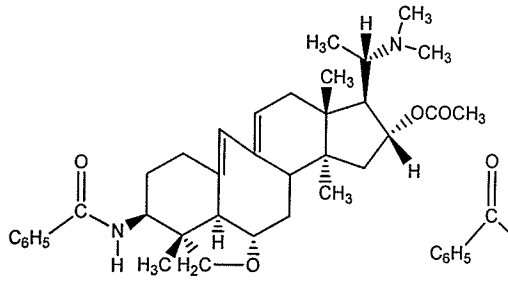

(25)

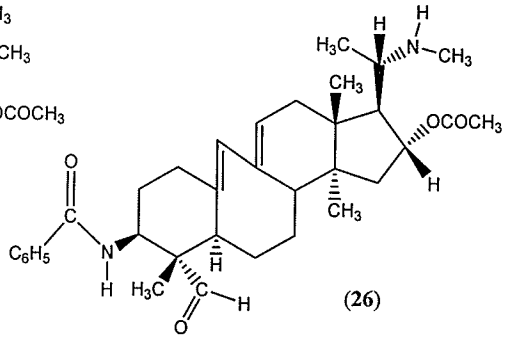

(26)

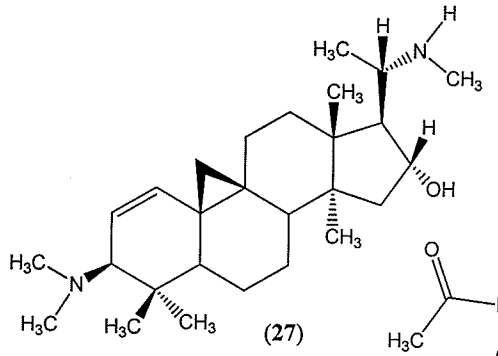

(27)

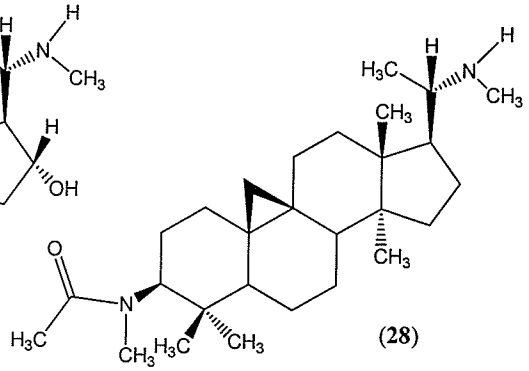

(28)

Some naturally occurring molecules hold multiple functions and are useful in combating certain kind of diseases, for example, Alzheimer's disease, which is caused

by multiple factors such as amyloid-β peptide (α,β) and tau protein aggregation, excessive transition metals, oxidative stress and reduced acetylcholine (ACh) level in brain[38]. In the last decade many attempts were made to incorporate more than one pharmacophore in a single molecule to design multifunctional agents to hit more than one target in Alzheimer's disease (AD). These multifunctional molecules were found to be very effective in *in vitro* studies but the complex pharmacokinetics and higher toxicity level became the major obstacle in their further drug development.

Flavonoids are one of the most important dietary phytochemicals which can act as multifunctional molecules, and may exert beneficial effects in the central nervous system by protecting neurons against stress-induced injury by suppressing neuroinflammation and by promoting neurocognitive performance, through changes in synaptic plasticity as supported by the dietary supplementation studies[39]. These studies revealed that flavonoids-rich plant or food extracts have potential influence on cognition and learning in humans and animals[39,40]; presumably by protecting neurons, enhancing existing neuronal function, or by stimulating neuronal regeneration. Their neuroprotective potential was noted in both oxidative stress[41] and neuron cell death[41]. Flavonoid-rich *Ginkgo biloba* extracts were investigated in this regard and found to be beneficial in neuromodulatory effects, particularly in connection with age related dementias and Alzheimer's disease[42,43]. Flavonoids comprise the most common group of polyphenolic compounds in the human diet and are found ubiquitously in plants. Major dietary sources of flavonoids include fruits, vegetables, tea, wine, cereals and fruit juices [44].

The main dietary groups of flavonoids are:

I Flavonols e.g. kaempferol (**29**), quercetin (**30**) are found in onions, leeks, broccoli[44].

II Flavones e.g. apigenin (**31**), luteolin (**32**) are found in parsley and celery[44].

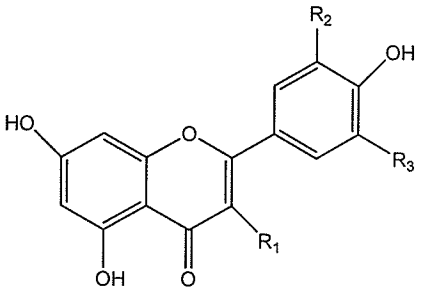

	R_1	R_2	R_3
(**29**)	OH	H	H
(**30**)	OH	OH	H
(**31**)	H	H	H
(**32**)	H	OH	H

III Isoflavones e.g. daidzein (**33**), genistein (**34**) are mainly found in soy and soy products[44].

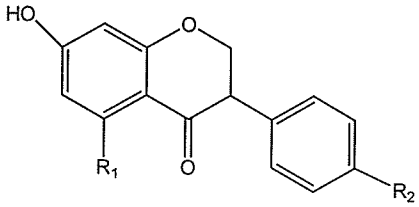

	R_1	R_2
(**33**)	OH	H
(**34**)	OH	OH

IV Flavanones e.g. hesperetin (**35**), naringenin (**36**) are mainly found in citrus fruit and tomatoes[44].

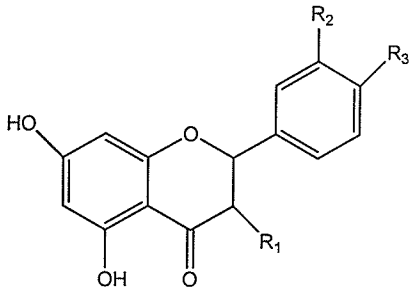

	R_1	R_2	R_3
(**35**)	H	OCH_3	H
(**36**)	H	H	OH

V Favanols e.g. catechin (**37**), epicatechin (**38**), epigallocatechin (**39**), epigallocatechin gallate (**40**) are abundant in green tea, red wine and chocolate[44].

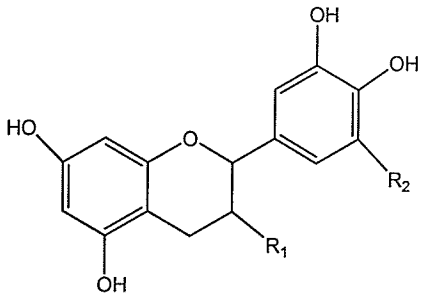

	R_1	R_2
(**37**)	OH	H
(**38**)	OH	H
(**39**)	OH	OH
(**40**)	gallate	OH

VI Anthocyanidins e.g. pelargonidin (**41**), cyaniding (**42**), malvidin (**43**), whose sources include red wine and berry fruits[44].

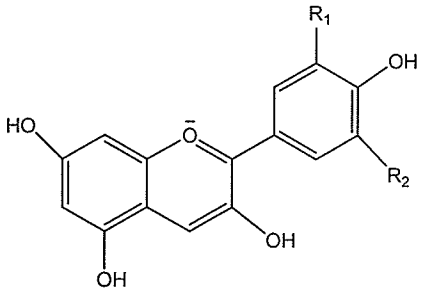

	R_1	R_2
(**41**)	H	H
(**42**)	OH	H
(**43**)	OCH_3	OCH_3

Antioxidant properties of flavonoids have been attributed either through their reducing capacities or through their influences on the intracellular redox status[45,46]. It has been studied that flavonoids exert their neuroprotective actions by **A**: the modulation of intracellular signaling cascades which control neuronal survival, death and differentiation; **B**: affecting gene expression; and **C**: interactions with mitochondria[47,48].

Iridoids are another class of naturally occurring polyhydroxy compounds and are usually found in plants as glycosides. They are present in a number of folk medicinal plants used as bitter tonics, sedatives, antipyretics, cough medicines, remedies for wounds, skin disorders and as hypotensives[49]. Recently Consolacion *et al.* reported the iridoidal natural product (**44**), exhibiting antimicrobial activity against *E. coli*, *Pseudomonas aeruginosa*, *Staphylococcus aureus* and *Trichophyton mentagrophytes*[50]. Three acylated iridoid glycosides (**45-47**) were found to exhibit antioxidant activities. All three compounds (**45-47**) showed activities in superoxide free-radical scavenging test with IC_{50} values of 24.3, 32.0, and 31.9 μM, respectively and in a DPPH-radidcal scavenging test with IC_{50} values of 15.2, 10.9, and 11.4 μM, respectively[51].

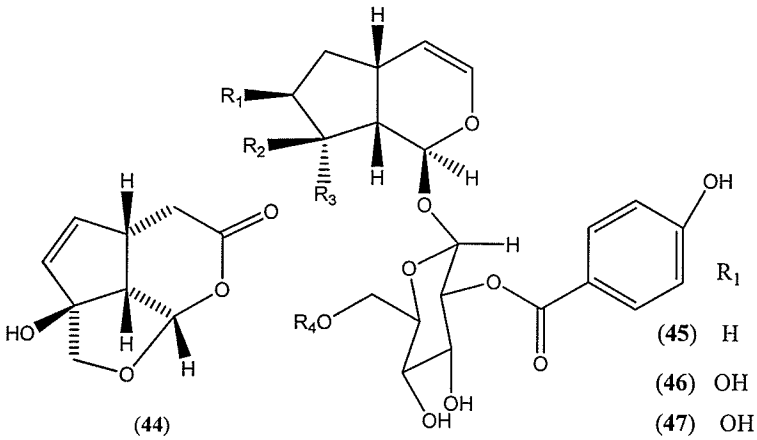

(44)

	R_1	R_2	R_3	R_4
(45)	H	OH	CH_3	trans-caffeoyl
(46)	OH		$=CH_2$	trans-caffeoyl
(47)	OH	H	CH_3	trans-caffeoy l

1.3 Enzyme inhibitors as a promising approach for the discovery of new leads

Enzymes are natural proteins that catalyze chemical reactions and play a major role in regulating cellular processes including, metabolism, signal transduction and growth of an organism. Any change in these metabolic processes can lead to a disease. Understanding of the course of the disease at a molecular level helps to correct the problem before hand. Enzyme inhibitors play an important role in the drug discovery process. For instance, galanthamine isolated from *Galanthus woronowii* (Amaryllidaceae) is an acetylcholinestrase inhibitor and a prescribed drug used for the treatment of mild to moderate Alzheimer's disease[52]. During the years 1998 to 2000 ninety-seven new drugs were introduced in the world drug market. One third of these drugs were enzyme inhibitors[53].

Enzyme inhibitors are grouped into two major classes, namely irreversible inhibitors (compounds that completely block the activity of an enzyme) and reversible inhibitors (compounds that retard the activity of an enzyme). With the use of enzyme inhibitors, enzymes are incapable to perform their function and thus help to cure the ailment. For example, generation of excess uric acid leads to a disease known as gout. An enzyme xanthine oxidase is involved in the conversion of xanthine to uric acid. Inhibition of

xanthine oxidase can result in an antihyperuricemic effect. Allopurinol (**48**) is used as a xanthine oxidase inhibitor to reduce the level of uric acid in blood plasma. Arglabin (**49**) and exemestane (**50**) are some other enzyme inhibitors used as drugs to cure cancer[54].

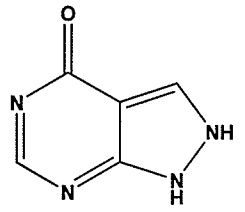

(48)

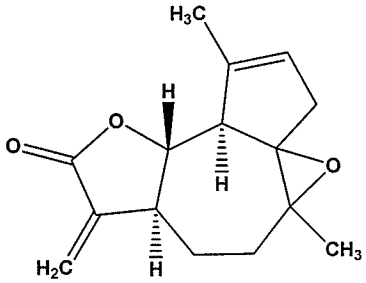

(49)

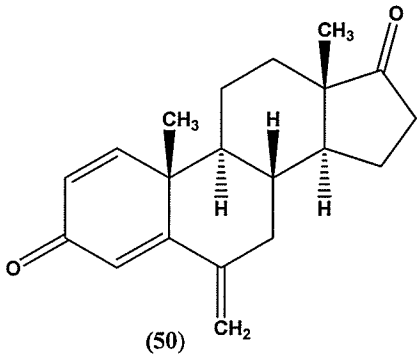

(50)

1.3.1 Acetylcholinestrase, its role in nervous system and inhibition

Acetylcholine (ACh) (**51**) serves as one of the neurotransmitters. Its certain level is required for the proper function of brain.

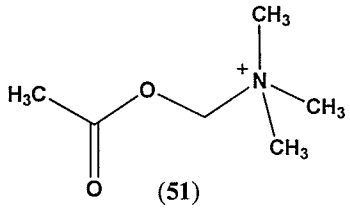

(51)

It is sensitive to two major types of receptors namely, muscarinic receptors and nicotinic receptors. The binding of muscarinic receptors with ACh causes stimulation to the parasympathetic nervous system that results in a decrease in heart rate and blood pressure, constriction of bronchi, increase in salivation, promotion of digestion and increase in intestinal peristalsis, release of fluids from the bladder, and accommodation of the eyes for near vision, with contraction of the pupils.

The nicotinic receptors are found in the central nervous system (CNS) and in the motor end plates which are the synapses between nerves and skeletal muscle. In the CNS, ACh stimulation of the nicotinic receptors is associated with cognitive processes

and memory, while in skeletal muscles it causes contraction. ACh is stored in the nerve terminals, commonly known as vesicles from where it is released at the depolarization of nerve terminals, and the ACh thus released enters the synapse and binds to the receptor. This released ACh has a very short half-life due to the presence of large amounts of acetylcholinesterase (AChE), an enzyme that hydrolyses ACh into choline and acetic acid (shown in Scheme **1.2**). This results in the brain leading to several diseases including Alzheimer's disease.

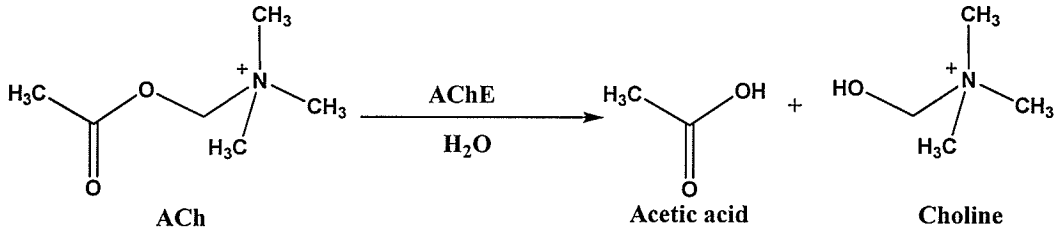

Scheme 1.2 Catalytic hydrolysis of acetylcholine

Structurally, AChE consists of a complex protein of the α/β hydrolase fold type having an overall ellipsoid shape, which contains about 20 A° deep groove, called the gorge. Hydrolysis of ACh takes place at the bottom of the gorge through a complex mechanism[55] as shown in Scheme **1.3**.

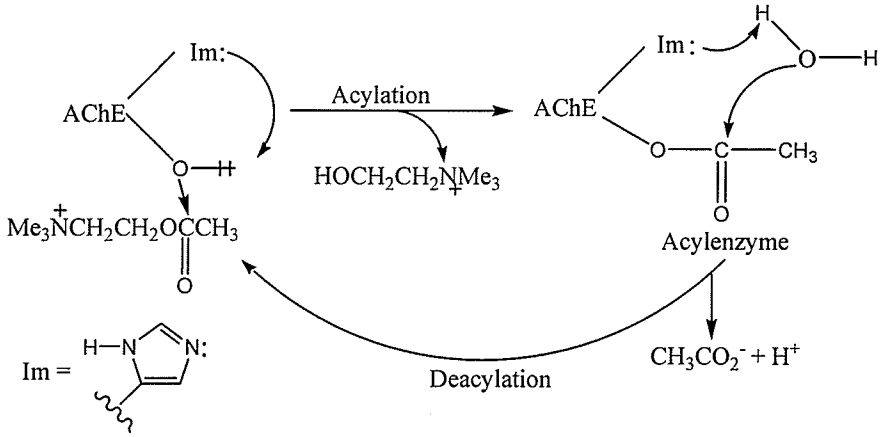

Scheme 1.3 Reaction mechanism of the hydrolysis of ACh castalysed by AChE

AChE and inhibitor interaction have been investigated throughly[56] due to its pharmaceutical and pesticidal importance. Acetylcholinestrase inhibitors (AChEIs) can be divided into two major groups: those which bind to the active site at the bottom of the gorge, and those which bind to the peripheral anionic site (PAS). Alkaloidal inhibitors bind through positively charged nitrogen to the oxyanion area at the bottom of the gorge, especially the Trp84, and a region, separated by a lipophilic area from the positive charge, which can form hydrogen bonds with the Ser200 residue and others like His440[57]. The use of AChEIs for the treatment of glaucoma was an old application. The other major use of naturally occurring AChEIs was for the treatment of myasthenia gravis, where muscle weakness occurs because of insufficient ACh levels at the neuromuscular junction.

The advent of the hypothesis that Alzheimer's disease (AD) can be treated by enhancing ACh level in the brain[58] provides a new application for AChEIs. Moreover AChE is also considered responsible for the deposition of extracellular plaques of β-amyloid. These deposits are characteristic of the abnormal histology of the forebrain of patients with Alzheimer's disease[59]. The AChE inhibitor, rivastigmine, which acts in the central nervous system (CNS) is used clinically, and is an analogue of another AChE inhibitor physostigmine, which has been developed to cross the blood–brain barrier[60]. Recently another AChE inhibitor, galantamine, was licensed for use in early stages of Alzheimer's disease. This drug is popular in this respect, especially because it appears to have nicotinergic effects which increase its effectiveness in treating AD[52]. Some alkaloids, such as ungimorine (**52**) isolated from a *Narcissus* cultivar[61] and hamayne (**53**), crinamine (**54**), and haemanthamine (**55**) isolated from two Nigerian

Crinum species had a weaker AChE inhibitory effects (IC_{50} values ranged from 86-50 μM)[62].

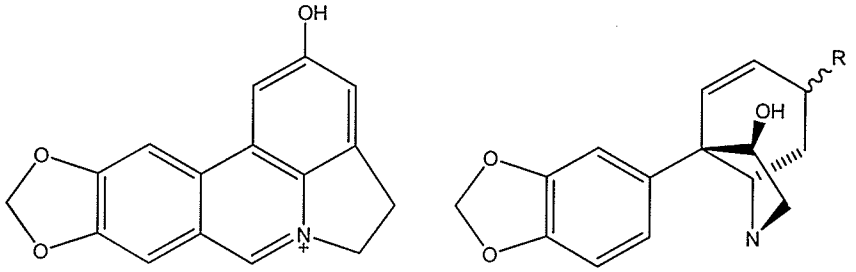

(52) (53) R= β-OH (54) R= α-OCH3 (55) R= β-OCH3

Huperzine A (**56**) is one of the alkaloids isolated from the clubmoss *Huperzia serrata* (Lycopodiaceae) is used in various formulae in traditional Chinese medicine to treat memory loss, promote circulation and for fever and inflammation[63]. Huperzine A is related to the quinolizidine alkaloids and it reversibly inhibits acetylcholinestrase *in vitro*[64,65] and *in vivo* [66].

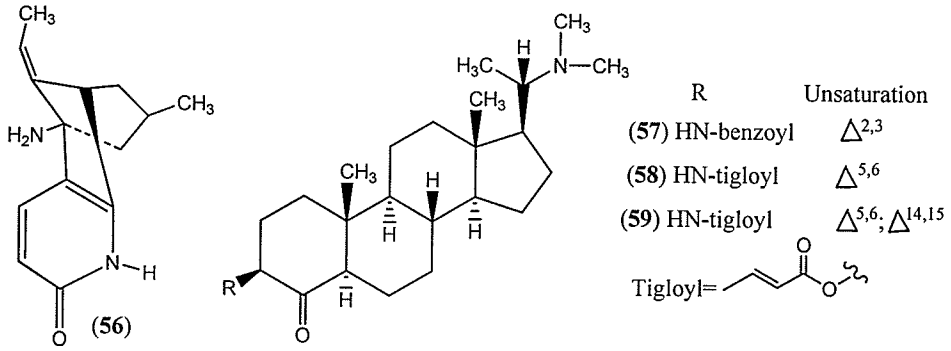

(56)

R	Unsaturation
(57) HN-benzoyl	$\Delta^{2,3}$
(58) HN-tigloyl	$\Delta^{5,6}$
(59) HN-tigloyl	$\Delta^{5,6};\Delta^{14,15}$

Tigloyl=

Some pregnane-type alkaloids from *Sarcococca saligna* have shown anti-AChE activity[67]. Axillaridine-A (**57**), sarsalignone (**58**) and sarsalignenone (**59**) have been investigated and found to be active against AChE (IC_{50} = 5.21, 7.02, 5.83 μM respectively). The lower inhibitory activity has also been observed with some compounds, such as 2β-hydroxyepipachysamine-D (**60**) and axillarine-C (**61**) (78.2, 227.9 μM respectively), maybe because of steric hindrance, since these compounds contain benzamide moieties at position C-3. The presence of a hydroxyl group at C-2

was also associated with the low inhibitory activity and was considered to result in unfavorable interactions[68].

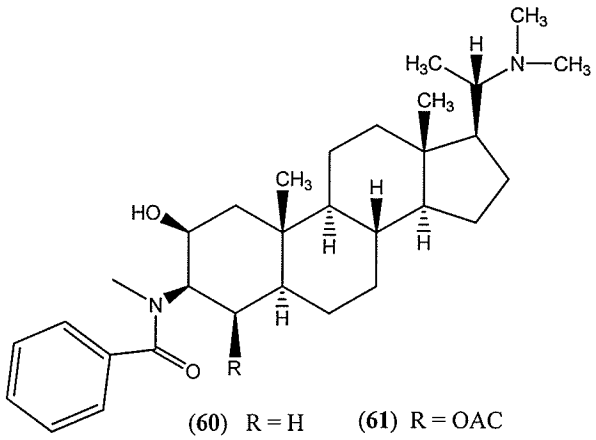

(**60**) R = H (**61**) R = OAC

In another report the steroidal alkaloids, isosarcodine (**62**), sarcorine (**63**), sarcodine (**64**), sarcocine (**65**), and alkaloid-C (**66**), also purified from *Sarcococca saligna* (Buxaceae), were reported as acetylcholinestrase inhibitors with IC_{50} values of 10.31, 69.99, 49.77, 20.0 and 42.2μM, respectively[69].

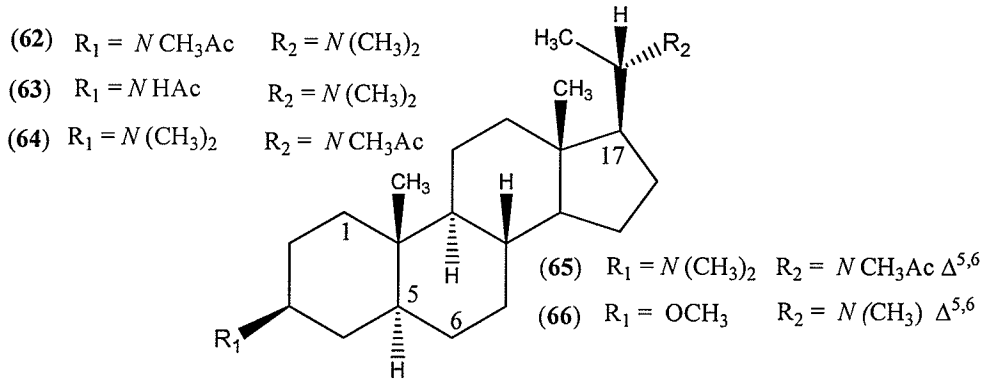

(**62**) R_1 = *N* CH_3Ac R_2 = *N* $(CH_3)_2$
(**63**) R_1 = *N* HAc R_2 = *N* $(CH_3)_2$
(**64**) R_1 = *N* $(CH_3)_2$ R_2 = *N* CH_3Ac

(**65**) R_1 = *N* $(CH_3)_2$ R_2 = *N* CH_3Ac $\Delta^{5,6}$
(**66**) R_1 = OCH_3 R_2 = *N* (CH_3) $\Delta^{5,6}$

The plants of Buxaceae family are one of the most regarded herbs used in Ayurvedic medicine. Several alkaloids from this family have been investigated as cholinesterase inhibitors. For instance, hyricamine (**67**) and buxidine (**68**) isolated from *Buxus hyrcana*, gave *in vitro* IC_{50} of 83.0 and 210.6 μM against AChE[70].

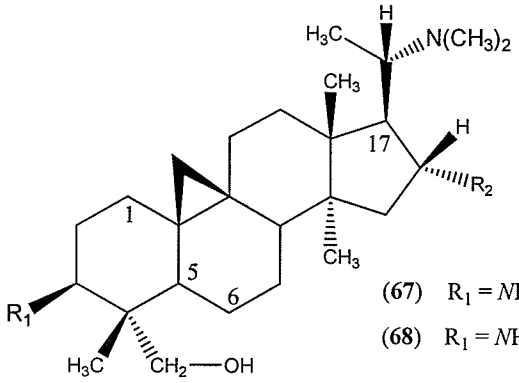

(**67**) R_1 = *N*H-tigloyl R_2 = OAC

(**68**) R_1 = *N*H-benzoyl R_2 = OH $\Delta^{6,7}$

The triterpenes were the first reported AChE inhibitors, partly from studies on chemical interactions between plant volatiles and insects[71] and partly from investigations based on English ethnopharmacology that terpene containing plants were good for the memory[72]. Chung and his coworkers screened 139 different plant species to search for AChE inhibitors, and found that *Origanum majorana* (Lamiaceae) had the best AChE inhibitory activity. A detailed phytochemical investigation on this plant resulted in the isolation of ursolic acid (**69**), an AChE inhibitor with IC_{50} value of 75 μM[73]. Taraxerol (**70**) has a similar structure and was shown to be one of the active compounds, with an IC_{50} value of 79 μM when an extract of the twigs of *Vaccinium oldhami* was investigated[74].

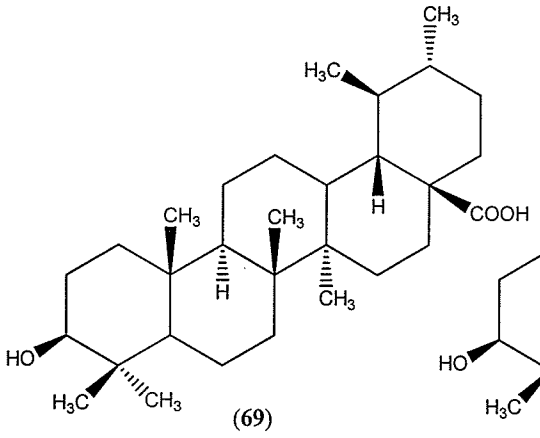

(**69**)

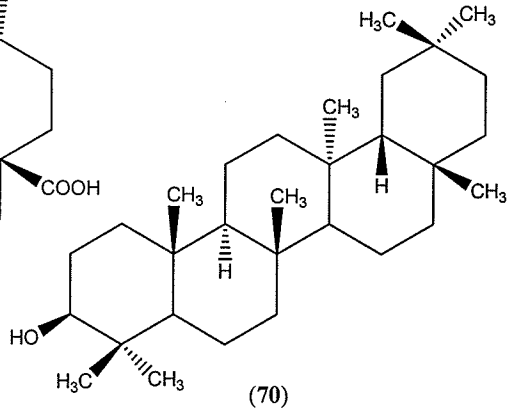

(**70**)

In the last 20 years phenolic compounds like flavonides have gained the most popularity due to their unique biological activities and a few compounds of this class

have been shown to have anti AChE effects. The flavanone naringenin (**36**) from *Citrus junos* (Rutaceae) ameliorated scopolamine-induced amnesia in mice, which may be related to anti-AChE effect, since naringenin was shown to dose-dependently inhibit AChE *in vitro*[75]. Another flavanone, hispidone (**71**), isolated from *Onosma hispida* (Boraginaceae) was found to inhibit AChE with IC_{50} value 11.6μM[76].

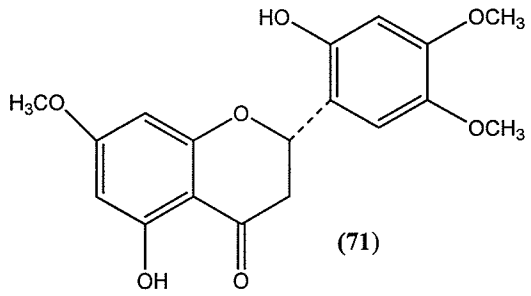

(71)

1.3.2 Glutathione *S*-transferase and its role in drug resistance

Glutathione *S*-transferases (GST) are a family of phase II detoxification enzymes, which catalyze the conjugation of glutathione (GSH) with a broad spectrum of xenobiotics, rendering toxic compounds more water soluble and therefore more easily eliminated. Thus, GST plays a vital role in the detoxification of potential carcinogenic substances[77] and potential alkylating agents including pharmacologically active compound[78] through glutathione conjugation and subsequently mercapturic acid formation[79].

GST catalyzes the formation of thioester bond between GSH and cytotoxic molecules at its electric core, rendering the molecule chemically less reactive by lowering pK_a of nucleophilic cysteine of GSH from about 9.5 in aqueous solution to neutral value[80]. Since most of the anticancer drugs are potent electrophiles and therefore act as substrates for GST[81,82]. A typical GSH-conjugation reaction catalysed by GST is shown in Scheme **1.4**.

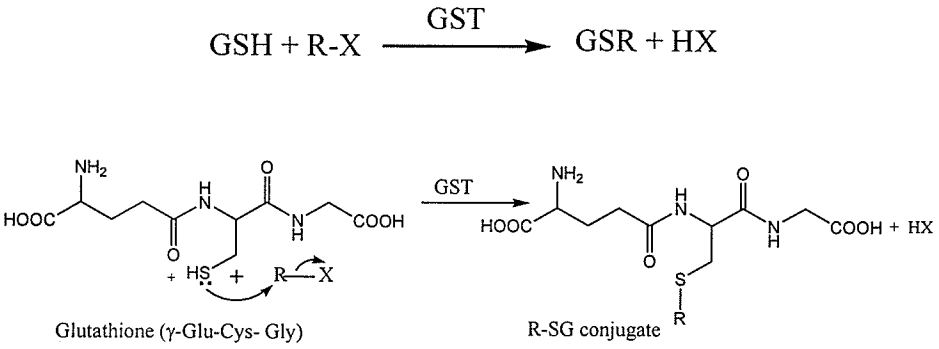

Scheme 1.4 A general reaction catalyzed by GST; R-X = electrophilic substrate

Based on the immunogenicity and primary structure of GSTs, they are divided into two groups; the endoplasmic reticulum-membrane bound microsomal GSTs and cytosolic GSTs. The cytosolic GSTs are divided into eight classes, namely alpha (A), mu (M), pi (P), theta (T), zeta (Z), kappa (K), sigma (S) and omega (O)[83]. The existence of GSTs into various isoenzyme classes provide a broader spectrum of substrates specificity for detoxification of most of the chemical moieties. Various types of these GST isoenzyme catalyzed reactions have been identified including Michael type addition, nucleophilic aromatic substitution, nucleophilic addition to epoxide, cis-trans double bond isomerization, positional double bond isomerization and peroxide reduction. Some of these reactions are schematized in Scheme **1.5**[84].

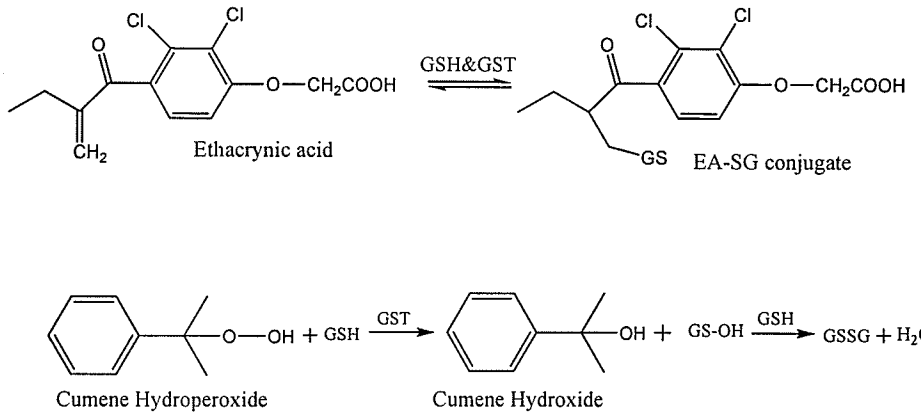

Scheme 1.5 Michael-type addition and reduction reactions catalysed by GST

Besides above stated detoxification mechanism, GSTs also perform other functions such as clearance of oxidative stress products, modulation of cell proliferation and apoptosis signaling pathways. This multifunction ability of GSTs leads to several possible therapeutic uses for isoform specific GST inhibitors. Recent detailed investigations show that alkylating agents during chemotherapy are directly related with the over expression of GSTs, which cause resistance against chemotherapy[85]. This relationship stimulates the utilization of such agents that can inhibit GST in combination with anticancer drugs to circumvent this resistance and to enhance the effect of chemotherapy.

The GST isoenzymes cover a broad range of substrate specificity of a wide variety of xenobiotic substances including carcinogens and anti-cancer drugs. That is why many research groups have been engaged to investigate the rational between reduced cytotoxic drug treatment efficacy and GST activity. It was discovered that most of the anticancer agents conjugate with GSH by GST isoenzymes and are efficiently excreted from the body[86]. For example, GSTs-α have been discovered to be involved in resistance against nitrogen mustards[87], GST-μ offers resistance to nitrosoureas[88,89], GST-π produce resistance against alkylating agents (Ifosfamide and thiotepa)[90,91], which depicts clear picture that GSTs are directly involve in multi drug resistance (MDR)[80,92,93]. Therefore a rationale has been established to use such agents that can selectively inhibit specific GSTs as adjuvant in anticancer chemotherapy[84,94]. In the past few decades several attempts have been made to discover specific GST inhibitors for enhanced activity of the desired anticancer drugs.

Although, broad classes of both competitive and non competitive inhibitors exist but in spite of a number of serious efforts, GST inhibitors which are isozyme specific,

non-toxic, and active *in vivo* have yet not been developed. So far the only known *in vivo* active GSTs inhibitors are ethacrynic acid (EA) and few glutathione derived structures[90,95,96].

According to Ploemen *et al.* studies[96], EA (**72**) inhibits GST competitively and non-competitively. It inhibits all classes of GSTs competitively towards 1-chloro-2,4-dinitrobenzene (CDNB) and non competitively towards GSH[97].

Like EA, a GSH analog, γ-glutamyl *S*-(benzyl) cysteinyl-R-(-)-phenyl glycine diethyl ester (TER 199) (**73**), has been shown to be an effective inhibitor of GST[94]. It is also an effective modulator of alkylating agents. In contrast to EA, **73** is an isozyme specific inhibitor of GST π[98], which affects GSH homeostasis results depletion of GSH and inhibits GST π activity[98].

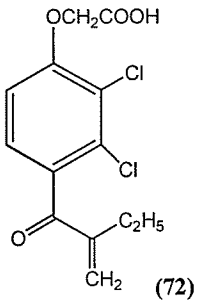

(72)

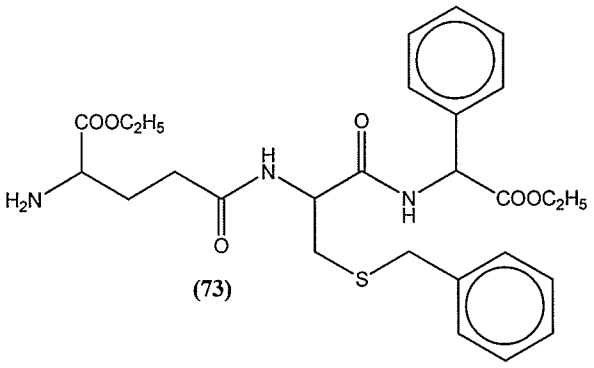

(73)

Some researchers attempted to prepare non-peptide GST with increased peptidase stability. For example, haloenol lactones are known to enhance the cytotoxic effect of cisplatin by acting as GST P1-1 inactivators[99]. Several haloenol lactones represented by Scheme **1.6** were developed to identify more potent selective compounds as GST P1-1 inactivators[90]. These inhibitors are active site-directed chemically modified reagents that form thioester linkages with Cys-47 of GST P1-1, with potent inhibitory catalytic activity and are now being further modified to enhance their efficacy[90].

GST activatable prodrugs have been designed on the basis of GSTs ability to hydrolyze or to cleave GSH-conjugates[100,101]. GSH thioesters and isothiocyanates act as substrates for 'reverse' GST catalysis.

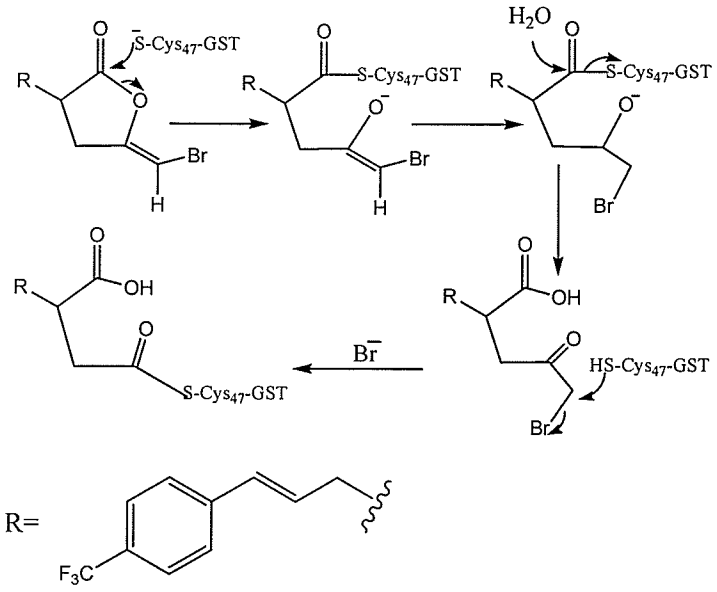

Scheme 1.6 Mechanism of inhibition by haloenol lactones.

Several research groups have utilized these reverse reactions for GST-activated pro-drugs that release electrophilic toxins or other chemical species. The best known example for this strategy is TLK286, a GSH analog containing a phosphoramidate sulfonyl moiety that undergoes enzyme-dependent release of a DNA alkylating agent and a GS-vinyl sulfone[102-104]. It is speculated that the active site Tyr of GSTP1-1 acts as a general base to promote the β-elimination that yields the alkylating agent (Scheme **1.7**).

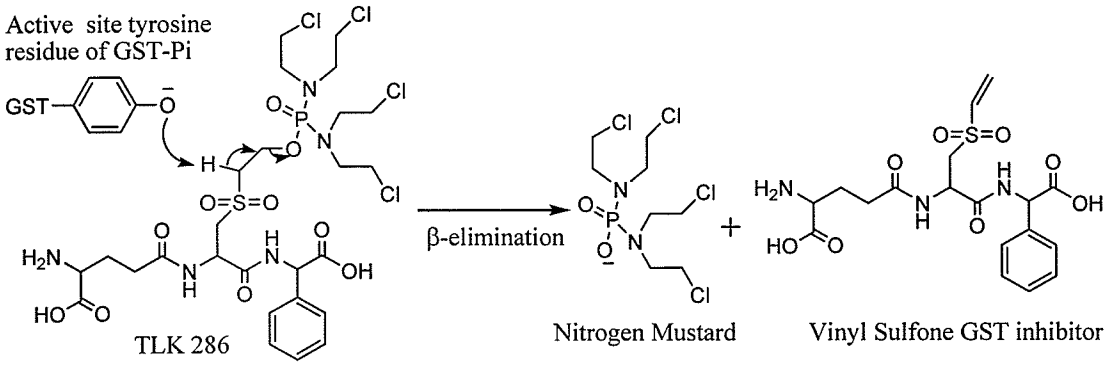

Scheme 1.7 Mode of action of latent cytotoxin TLK286.

Naturally occurring polyphenols are classic ligandin-type inhibitors, for example quercetin (**30**) and tocopherols (**74**), found in plants or even as food constituents. These are hydrophobic aromatic compounds with potential anionic character and are particularly common in grapes, some vegetables and some teas. These and other dietary constituents have received great attention due to their ability to induce various GSTs and their potential anti-carcinogenic properties. In addition, these compounds have the ability to directly inhibit some GSTs, mainly GST-π[105].

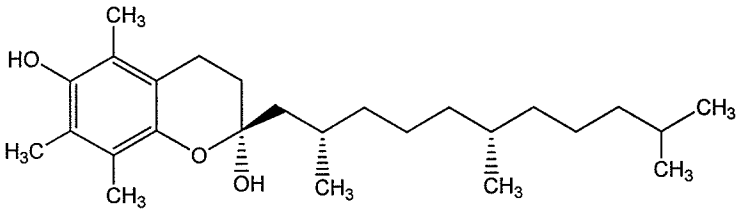

(74)

Natural products provide a source of lead compounds for drug discovery program. Keeping in view *Vitex pinnata*, *Artocarpus nobilis, Barleria prionitis, Buxus natalensis* and *Coprinous micaceous* were investigated to isolate natural products and to evaluate them for AChE and GST inhibitory activities. Chapters **2** to **6** describe details of bioassay guided isolation and characterization of GST and AChE inhibitors from the above mentioned natural sources.

1.4 References

[1] Taiz, L.; Zeiger, E. *Plant Physiology*, Sunderland, M A., USA, **2002**.

[2] Dewick, P. M. *Medicinal Natural Products*: *A biosynthetic approach*." 2nd ed., John Wiley & Sons, **2001**.

[3] Newman, D. J.; Cragg, G. M.; Snader, K. M.; *Nat. Prod. Rep.*, **2000**, 17 , 215.

[4] Mann, J. *Murder, Magic and Medicine*, Oxford University Press, Oxford, **2000**.

[5] Harborne, J. B.; Baxter, H. *Chemical Dictionary of Economic Plants*, John Wiley & Sons, Chichester, UK, **2006**.

[6] Newman, D. J.; Cragg, G. M. *J. Nat. Prod.*, **2007**, 70, 461.

[7] Shu, Y. Z. *J. Nat. Prod.*, **1998**, 6 1, 1053.

[8] Klayman, D. L.; Lin, A. J.; Acton, N.; Scovill, J. P.; Hoch, J. M.; Milhous, W. K.; Theoharides, A. D.; Dobek, A. S. *J. Nat. Prod.*, **1984**, 47, 715.

[9] Murdoch, D.; Plosker, G. L. *Drugs*, **2004**, 64, 2249.

[10] Gaoni, Y.; Mechoulam, R. *J. Am. Chem. Soc.*, **1964**, 86, 1646.

[11] Biegon, A. *Curr. Pharm. Des.*, **2004**, 10, 2177.

[12] Burstein, S. H.; Andette, C. A.; Breurr, A.; Devane, W. A.; Colodner, S.; Doyle, S. A.; Mechoulam, R. *J. Med. Chem.*, **1992**, 35, 3135.

[13] Chang, H. M.; But, P. P. H. *Pharmacology and Applications of Chinese Materia Medica*, World Scientific Publishing, Singapore, **1986**, vols 1 & 2.

[14] Koehn, F. E.; Carter, G. T. *Nat. Rev. Drug Discov.*, **2005**, 4, 206.

[15] Kong, J. M.; Goh, N. K.; Chia, L. S.; Chia, T. F. *Acta. Pharmaco. Sin.*, **2003**, 24, 7.

[16] Kapoor, L. D. *CRC Handbook of Ayurvedic Medicinal Plants*, CRC Press, Boca Raton, **1990**.

[17] Schultes, R. E., Raffauf, R. F., *The Healing Forest*, Dioscorides Press, Portland, **1990**.

[18] Fabricant, D. S.; Fransworth, N. R. *Environ. Health Prespcet.*, **2001**, 109, 69.

[19] Farnsworth, N. R.; Akerele, O.; Bingel, A. S.; Soejarto, D. D.; Guo, Z. *Bull.* WHO, **1985**, 63, 965.

[20] Arvigo, R.; Balick, M. *Rainforest Remedies*, Lotus Press, Twin Lakes, **1993**.

[21] Grifo, F.; Newman, D.; Fairfield, A. S.; Bhattacharya, B.; Grupenhoff, J. T. *The Origins of Prescription Drugs*, ed. Grifo, F. and Rosenthal, J. Island Press, Washington, D.C., **1997**, 131.

[22] Kinghorn, A. D. *The Discovery of Natural Products with Therapeutic Potential.* Boston, MA : Butterworth-Heinemann, **1994**, 81.

[23] Pisha, E.; Chai, H.; Lee, I. S.; Chagwedera, T. E.; Farnsworth, N. R.; Cordell, G. A.; Beecher, C.W.; Fong, H. H.; Kinghorn, A. D.; Brown, D. M. *Nat. Med.*, **1995**, 1, 1046.

[24] Schmidt, M. L.; Kuzmanoff, K. L.; Ling-Indeck, V.; Pezzuto, J. M. *Eur. J. Cancer*, **1997**, 33, 2007.

[25] Jeremias, I.; Steiner, H. H.; Debatin, A.; Herold-Mende, C.; Benner, A.; *Acta Neurochir.*, **2004**, 146, 721.

[26] Fujioka, T.; Kashiwada, Y. *J. Nat. Prod.*, **1994**, 57, 243.

[27] Anjaneyulu, V.; Prasad, K. H.; Rao, G. S.; *Indian J. Pharm. Sci.*, **1982**, 44, 58.

[28] Oliveira, M.; Carvalho, M.; Silva. C.; Werle, A. A.; *J. Braz. Chem. Soc.*, **2002**, 13, 119.

[29] Saleem, M.; Alam, A.; Arifin, S.; Shah, M. S.; Ahmed, B.; Sultana, S.; *Pharmacol. Res.*, **2001**, 43, 127.

[30] Glaser, T.; Winter, S.; Groscurth, P.; Safayhi, H.; Sailer, E. R.; Ammon, H. P.; Schabet, M.; Weller, M. *Br. J. Cancer*, **1999**, 80, 756.

[31] Tanaka, N.; Kitamura, A.; Mizushina, Y.; Sugawara, F.; Sakaguchi, K. *J. Nat. Prod.*, **1998**, 61, 193.

[32] Mizushina, Y.; Iida, A.; Ohta, K.; Sugawara, F.; Sakaguchi, K. *Biochem. J.*, **2000**, 350, 757.

[33] Min, B. S.; Gao, J. J.; Hattori, M.; Lee, H. K.; Kim, Y. H. *Planta Med.*, **2001**, 67, 811.

[34] Cordel, G. A. *Introduction to Alkaloids: A Biogenetic Approach*, Wiley Interscience, New York, **1981**.

[35] Durant, J.; Dellamonica, p.; Reboult, A. PCT Int. Appl. WO9300916, **1993**, Jan. 21. *Chem. Abstr.* **1993**, 118, 139823u.

[36] Langjae, R.; Bussarawit, S.; Yuenyongsawas, S.; Ingkaninan, K.; Piubrukarn, A. *Steroids*, **2007**, 72, 682.

[37] Atta-ur-Rahman, Noor-e-ain, F.; Choudhary, M. I.; Parveen, Z. *J. Nat. Prod.*, **1997**, 60, 976.

[38] Hong-Fang, J.; Hong-Yu, Zhang. *J. Mol. Structure, THEOCHEM*, **2006**, 767, 3.

[39] Galli, R. L.; Shukitt-Hale, B.; Youdim, K. A.; Joseph, J. A. *Ann. N. Y. Acad. Sci.*, **2002**, 959, 128.

[40] Kuriyama, S.; Hozawa, A.; Ohmori, K.; Shimazu, T.; Matsui, T.; Ebihara, S.; Awata, S.; Nagatomi, R.; Arai, H.; Tsuji, I. *Am. J. Clin. Nutr.*, **2006**, 83, 355.

[41] Inanami, O.; Watanabe, Y.; Syuto.; B.; Nakano, M.; Tsuji, M.; Kuwabara, M. *Free. Radic. Res.*, **1998**, 29, 359.

[42] Luo, Y.; Smith, J. V.; Paramasivam, V.; Burdick, A.; Curry, K. J.; Buford, J. P.; Khan, I.; Netzer, W. J.; Xu, H.; Butko, P. *Proc. Natl. Acad. Sci.*, USA, **2002**, 99, 12197.

[43] Zimmermann, M.; Colciaghi, F.; Cattabeni, F.; Di-Luca, M. *Cell Mol. Biol.*, **2002**, 48, 613.

[44] Manach, C.; Scalbert, A.; Morand, C.; Remesy, C.; Jimenez, L. *Am. J. Clin. Nut.*, **2004**, 79, 727.

[45] Rice-Evans, C. *Curr. Med. Chem.*, **2001**, 8, 797.

[46] Rice-Evans, C. *Free Radic. Biol. Med.*, **1996**, 20, 933.

[47] Schroeter, H.; Boyd, C.; Spencer, J. P. E.; Williams, R. J.; Cadenas, E.; Rice-Evans, C. *Neurobiol. Aging.*, **2002**, 23, 861.

[48] Spencer, J. P. E.; Rice-Evans, C.; Williams, R. J. *J. Biol. Chem.*, **2003,** 278, 34783.

[49] Biswanath, D.; Sudhan, D.; Yoshihiro, H. *Chem. pharm. Bull.*, **2007**, 55, 159.

[50] Consolacion, Y.; Leslie-Elline, N.; Pimenta, John, A.; Ridepout. *Nat. Prod. Res.*, **2007**, 21, 1078.

[51] Sridhar, C.; Subbaraju, G. V.; Venkateswarlu, Y.; Venugopal, R. T. *J. Nat. Prod.*, **2004**, 67, 2012.

[52] Woodruff-Pak, D. S.; Vogel, R. W.; Wenk, G. L. *Proc. Natl. Acad. Sci.*, USA, **2001**, 98, 2089.

[53] Newman, D. J., Cragg, G. M., Snader, K. M. *J. Nat. Prod.*, **2003**, 66, 1022.

[54] Shaikenov, T. E.; Adekenov, S. M.; Williams, R. M.; Prashad, N.; Baker, F. L.; Madden, T. L.; Newman, R. *Oncol. Rep.*, **2001**, 8, 173.

[55] Deniel, M.; Quinn, *Chem. Rev.*, **1987**, 87, 955.

[56] Greenblatt, H. M.; Dvir, H.; Silman, I.; Sussman, J. L. *J. Mol. Neurosci.*, **2003**, 20, 369.

[57] Harel, M.; Kleywegt, G. J.; Ravelli, R. B.; Silman, I.; Sussman, J. L. *Structure*, **1995**, 3, 1355.

[58] Perry, E. K.; Perry, R. H.; Tomlinson, B. E.; Blessed, G. *Br. Med. J.*, **1978,** 2, 1457.

[59] Roberson, M. R.; Harrell, L. E. *Brain Res. Rev.*, **1997**, 25, 50.

[60] Holmstedt, B. *Plants in the Development of Modern Medicine*, Ed. Swain, T. Harvard University Press, Cambridge, MA, USA, **1972**, 303.

[61] Ingkaninan, K.; Hazekamp, A.; De-Best, C. M.; Irth, H.; Tjaden, U. R.; van der Heijden, R.; van der Greef, J.; Verpoorte, R. *J. Nat. Prod.*, **2000**, 63, 803.

[62] Andrade, M. T.; Lima, J. A.; Pinto, A. C.; Rezende, C. M.; Carvalho, M. P.; Epifanio, R. A. *Bioorg. Med. Chem.*, **2005**, 13, 4092.

[63] Skolnick, A. A. *J. Am. Med. Soc.*, **1997**, 277, 776.

[64] Wang, Y. E.; Yue, D. X.; Tang, X. C. *Acta Pharm. Sin.*, **1986**, 7, 110.

[65] Kozikowski, A. P.; Ding, Q.; Saxena, A.; Bhupendra, P. *Bioorg. Med.Chem.*, **1996**, 6, 259.

[66] Bai, D. L.; Tang, X. C.; He, X. C. *Curr. Med. Chem.*, **2000**, 7, 355.

[67] Khalid, A.; Zaheer-ul-Haq, Anjum, S.; Khan, M. R.; Atta-ur-Rahman, Choudhary, M. I. *Bioorg. Med. Chem.*, **2004**, 12, 1995.

[68] Khalid, A.; Azim, M. K.; Parveen, S.; Atta-ur-Rahman, Choudhary, M. I. *Biochem. Biophys. Res. Commun.*, **2005**, 331, 1528.

[69] Khalid, A.; Zaheer-ul-Haq, Ghayur, M. N.; Feroz, F.; Atta-ur-Rahman, Gilani, A. H.; Choudhary, M. I. *J. Steroid, Biochem. Mol. Biol.*, **2004**, 92, 477.

[70] Choudhary, M. I.; Shahnaz, S.; Parveen, S.; Khalid, A.; Ayatollahi, S. A. M.; Atta-ur-Rahman, Pervez, M. *Chem. & biodivers.*, **2006**, 3, 1039.

[71] Ryan, M. F.; Byrne, O. *J. Chem. Ecol.*, **1988**, 14, 1965.

[72] Perry, E. K.; Pickering, A. T.; Wang, W.W.; Houghton, P. J.; Perry, N. S. L. *J. Alt. Complementary Med.*, **1998**, 4, 419.

[73] Chung, Y. K.; Heo, H. J.; Kim, E. K.; Kim, H. K.; Huh, T. L.; Lim, Y.; Kim, S. K.; Shin, D. H. *Mol. Cells*, **2001**, 11, 137.

[74] Lee, J. H.; Lee, K. T.; Yang, J. H.; Baek, N. L.; Kim, D. K. *Arch. Pharm. Res.*, **2004**, 27, 53.

[75] Heo, H. J.; Kim, M. J.; Lee, J. M.; Choi, S. J.; Cho, H. Y.; Hong, B. S.; Kim, H. K.; Kim, E.; Shin, D. H. *Dementia Geriatr. Connit. Disord.*, **2004**, 17, 151.

[76] Ahmad, I.; Anis, I.; Malik, A.; Nawaz, S. A.; Choudhary, M. I. *Chem. Pharm. Bull.*, **2003**, 51, 412.

[77] Bongers, V.; Snow, G. B.; Braakhuis, B. J. M.; *Oral Oncal. Eur. J. Cancer,* **1995**, 31B, 349.

[78] William, H. H.; Michael, J. P.; William, B. J. *J. Biol. Chem.*, **1974**, 249, 7130.

[79] James, H. K.; Willian, H. H.; Willian, B. J. *J. Biol. Chem.*, **1976**, 251, 6183.

[80] Hayes, J. D.; Pulford, D. J. *Crit. Rev. Biochem. Mol. Biol.*, **1995**, 30, 445.

[81] Tew, K. D.; Houghton, P. J.; Houghton, J. A. *Preclinical and Clinical Modulation of Anticancer Drugs*, CRC Press, Boca Raton, FL, **1993**, 13–77.

[82] Schimke, R.T. *Cell*, **1984**, 37, 705.

[83] Erika, L. A.; Robert, P. L.; Theodore, K. B.; Christophe, L. M. J.; Verlinde, Serrine S. L.; Terrence, J. M.; David, L. E. *Chemico-Biological Interactions*, **2004**, 151, 21.

[84] Mahajan, S.; Atkins, W. M. *Cell. Mol. Life Sci.*, **2005**, 62, 1221.

[85] Chasseaud, L. F. *Adv. Can. Res.*, **1979**, 29, 175.

[86] Turella, P.; Cerella, C.; Filomeni, G.; Bullo, A.; Francesca, D. M.; Federici, G.; Ricci, G.; Caccuri, A. M.; *Cancer Res.*, **2005**, 65, 3751.

[87] Townsend, D. M.; Tew, K. D. *Oncogene*, **2003**, 22, 7369.

[88] Berhane, K.; Hao, X. Y.; Egyhazy, S.; Hansson, J.; Ringborg, U.; Mannervik, B. *Cancer Res.*, **1993**, 53, 4257.

[89] Skalski, V.; Yarosh, B. D.; Batist, G.; Gros, P.; Feindel, W.; Kopriva, D.; Panasci, *Mol. Pharmacol.*, **1990**, 38, 299.

[90] Dirven, H. A.; Megens, L.; Oudshoorn, M. J.; Dingemanse, M. A.; van-Ommen, B.; van-Bladeren, P. J. *Chem. Res. Toxicol.*, **1995**, 8, 979.

[91] Dirven, H. A.; Dictus, E. L.; Broeders, N. L.; van-Ommen, B.; van-Bladeren, P. J. *Cancer Res.*, **1995**, 55,1701.

[92] Tsuchida, S.; Sato, K. *Crit. Rev. Biochem. Mol. Biol.*, 1992, 27, 337.

[93] Tew, K. D. *Cancer Res.*, **1994**, 54, 4313.

[94] Schultz, M.; Dutta, S.; Tew, K. D. *Adv. Drug. Delv. Rew.*, **1997**, 26, 91.

[95] van-Iersel, M. L.; Ploemen, J. P.; Lo-Bello, M.; Federici, G.; van-Bladeren, P. J. *Chem. Biol. Interact.*, **1997**, 108, 67.

[96] van-Iersel, M. L.; Ploemen, J. P.; Struik, I.; van-Amersfoort, C.; Keyzer, A. E.; Schefferlie, J. G.; van-Bladeren, P. J. *Chem. Biol. Interact.*, **1996**, 102, 117.

[97] Ploemen, J. H. T. M.; Ommen, B. V.; Bladeren, P. J. V.; *Biochem. Pharmacol.*, **1990**, 40, 1631.

[98] Schimke, R. T. *Cell*, **1984**, 37, 705.

[99] Lyttle, M. H.; Hocker, M. D.; Hui, H. C.; Caldwell, C. G.; Aaron, D. T.; Engqvist-Goldstein, A.; Flatgaard, J. E.; Bauer, K. E. *J. Med. Chem.*, **1994**, 37, 189.

[100] Zhang, Y.; Kolm, R. H.; Mannervik, B.; Talalay, P. *Biochem. Biophys. Res. Commun.*, **1995**, 206, 748.

[101] Dietze, E. C.; Grillo, M. P.; Kalhorn, T.; Nieslanik, B. S.; Jochheim, C. M.; Atkins, W. M. *Biochemistry*, **1998**, 37, 14948.

[102] Morgan, A. S.; Sanderson, P. E.; Borch, R. F.; Tew, K. D.; Niitsu, Y.; Takayama, T. *Cancer Res.*, **1998**, 58, 2568.

[103] Izbicka, E.; Lawrence, R.; Cerna, C.; Von-Hoff, D. D.; Sanderson, P. E. *Anticancer Drugs*, **1997**, 8 , 345.

[104] Townsend, D. M.; Shen, H.; Staros, A. L.; Gate, L.; Tew, K. D. *Mol. Cancer Ther.*, **2002**, 1, 1089.

[105] Rosen, L. S.; Laxa, B.; Boulos, L.; Wiggins, L.; Keck, J. G.; Jameson, A. J. *Clin. Cancer Res.*, **2004**, 10, 3689.

CHAPTER 2

Phytochemical studies on *Vitex pinnata*

2.1 Introduction

The genus *Vitex* (Verbenaceae) comprises of various species including *Vitex negundo*, *V. agnus-castus*, *V. polygama*, *V. cannabifolia, V. limonifolia, V. rotundifolia, V. altissima, V. canescens, V. trifolia, V. triora, V. odorata, V. montevidensis* and *V. pinnata.* The plants of this genus are abundant in the tropical and sub-tropical regions of India[1]. For instance, 14 species of this genus including *V. pinnata* are found in India[2]. Plants belonging to this genus have ethnomedicinal applications in South-East Asia. For instance, *V. negundo* is one of the most common plants used in Indian and Chinese traditional medicine. The oil from the fruits of this plant is used to treat bronchitis[3]. An aqueous extract of leaves is used to cure catarrhal fever and has been reported to possess anti-inflammatory, anti-oxidant, anti-genotoxic, anti-fertility and central nervous system depressant and anti-histamine release activity[4]. Various parts of *V. agnus-castus* are used as diuretic, digestive, anti-fungal and stomach ache relief agent by Anatolians and Brazilians[5,6]. The hot aqueous extract of leaves of *V. cannabifolia* is used to treat malaria and dysentery by Chinese[7]. Other plants from genus *Vitex* have also been reported to possess anti-viral[8], anti-cancer[9], anti-inflammatory[10], hepatoprotective[11] and anti-bacterial[12] activities.

Previous phytochemical investigations on the genus *Vitex* have resulted in the isolation of iridoids[13-16], monoterpenes[17], diterpenoids[18-19], flavonoids, [20], steroids, ecdysteroids[21], and *C*-glycoside[4]. Examples include 2`-*p*-hydroxybenzoyl mussaenosidic (**75**)[13], agnuside (**76**)[14], pedunculariside (**77**) [14], eucommiol (**78**)[15],

iridolactone (**79**) [15], ferruginol (**80**)[18], abietatrien-3β-ol (**81**)[18], luteolin (**82**)[20], artemetin (**83**)[20], isorhamnetin (**84**)[20], 20-hydroxyecdysone (**85**)[22], 24-epi-abutasterone (**86**)[22] and shidasterone (**87**)[22] were purified from different plants of *Vitex* species.

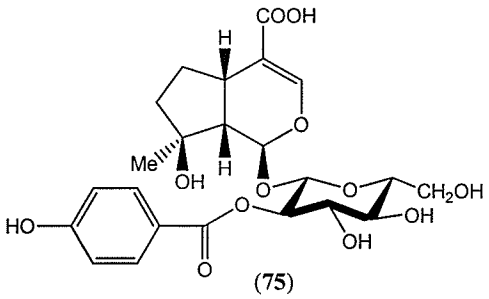

(**75**)

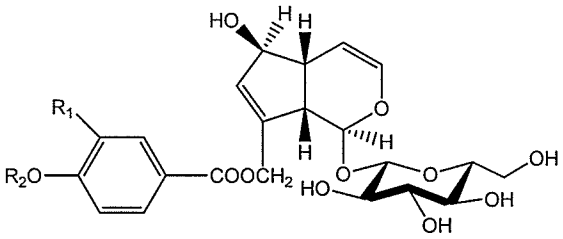

(**76**) $R_1 = R_2 = H$ (**77**) $R_1 = OCH_3$, $R_2 = H$

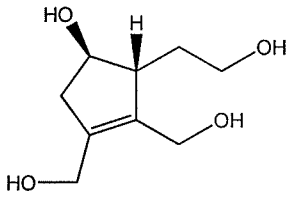

(78)

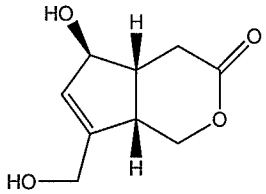

(79)

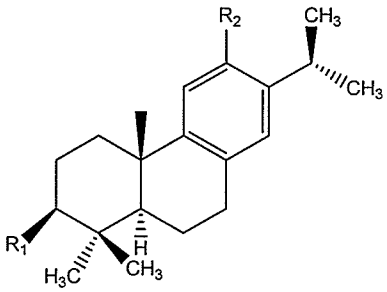

(**80**) $R_1 = H$, $R_2 = OH$ (**81**) $R_1 = OH$, $R_2 = H$

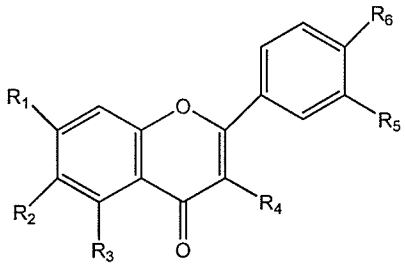

(**82**) $R_1=R_3=R_5=R_6= OH$, $R_2=R_4= H$

(**83**) $R_1=R_2=R_4=R_5=R_6= OCH_3$, $R_3= OH$

(**84**) $R_1=R_3=R_4=R_6= OH$, $R_5= OCH_3$, $R_2= H$

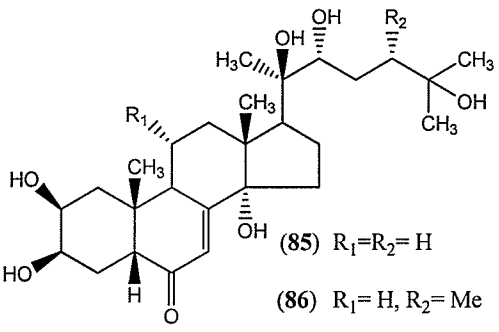

(**85**) $R_1=R_2= H$

(**86**) $R_1= H$, $R_2= Me$

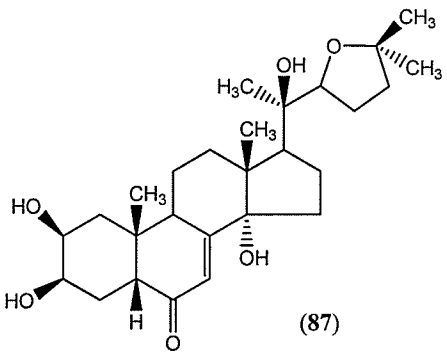

(**87**)

2.1.1 Biogensis of iridoid glycosides

Iridoid glycosides are monoterpenes composed of a pentacyclic ring which is fused with a pyran ring and sugar moieties attached to it. Biogenetically they are derived from mevalonic acid forming geraniol as an intermediate. This intermediate undergoes a series of hydroxylation and oxidation reactions to afford a dialdehyde molecule that after cyclization yields iridodial. This hemiacetal is a precursor to iridoids which then undergoes glucosylation to produce iridoid glycoside[23-24] as outlined in Scheme **2.1**.

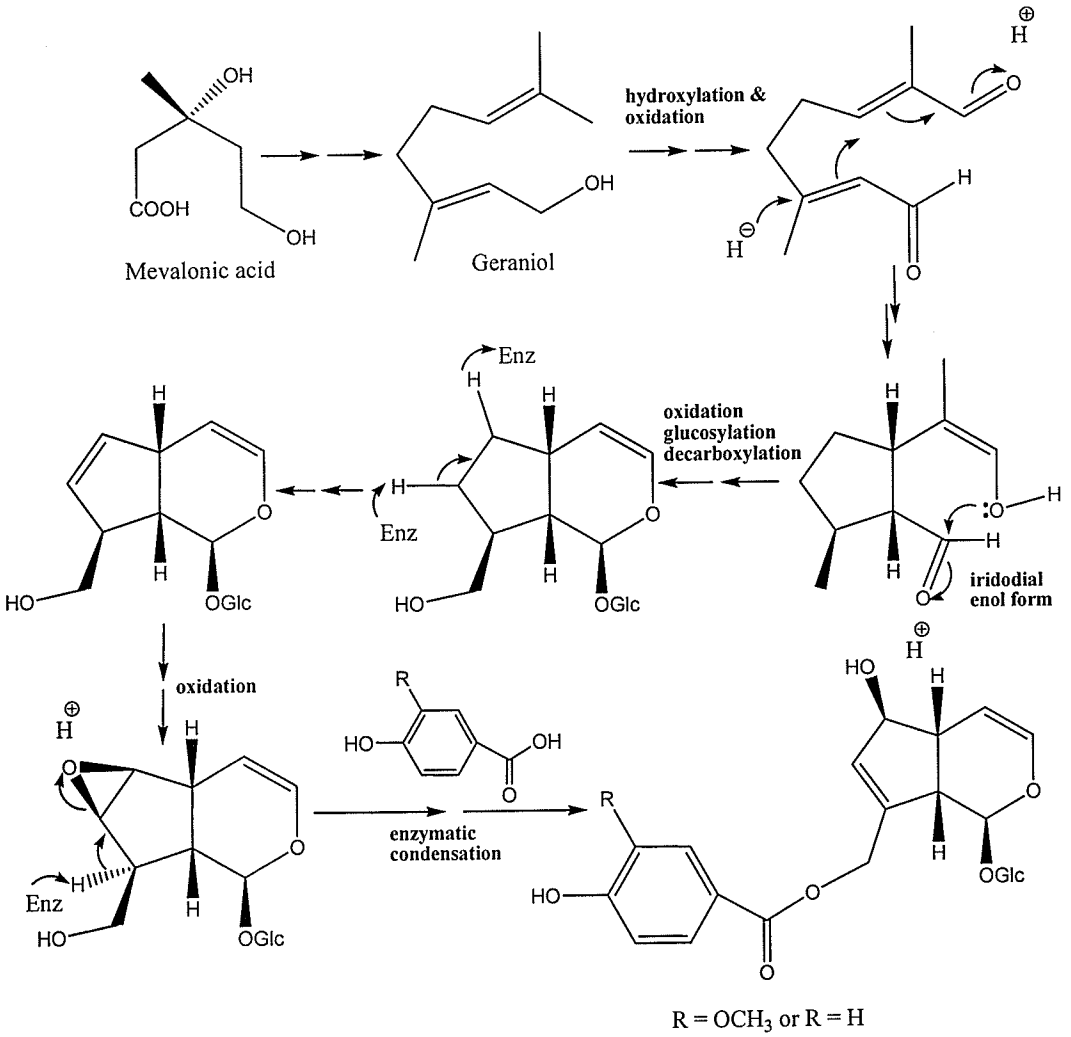

Scheme 2.1 Plausible pathway towards the biosynthesis of iridoid glycoside from *V. pinnata*

Vitex pinnata Linn (syn V. pubescens Vahl.) is a moderately sized tree of tropical Asia belonging to the family Verbenaceae[1,2]. This plant has been reported to have various ethanomedicinal applications[25-27]. For instance, the hot water extract of the bark of *V. pinnata* is used to cure stomach pain and in post child-birth recovery. Leaves are used to cure fever and wounds while the bark scrapings are applied to wounds and used as charm for convulsions[28]. On the basis of these folk pharmaceutical uses, phytochemical studies on *V. pinnata* Linn of Sri Lankan origin were carried out. These studies resulted in the isolation of compounds **88-91**. Compounds **88-91** exhibited anti-AChE, anti-GST and antioxidant activities.

2.2 Results and discussion

2.2.1 Isolation of compounds 88 to 91

The crude methanolic extract was subjected to various chromatographic techniques including column chromatography and preparative TLC which resulted in the isolation of one new iridoid glycoside, 6″-glucosepeduncullariside (**88**) along with three known compounds, peduncullariside (**89**), agnuside (**90**) and *p*-hydroxy benzoic acid (**91**) (for detailed purification procedure, see experimental section).

2.2.2 Structure elucidation of 6″-glucosepeduncullariside (88)

Compound (**88**) exhibited UV absorption bands at 291.4 nm and 262.8 nm indicating the presence of a substituted benzoyl group. The IR spectrum suggested the presence of hydroxyl (3421cm^{-1}), carbonyl (1715cm^{-1}), olefinic (1654 cm^{-1}), and aromatic (1508, 1451cm^{-1}) functionalities. High resolution FABMS showed the molecular ion peak at *m/z* 658.2085 (calcd. 658.2109). A combination of MS, ^{1}H and ^{13}C-NMR data provided the molecular formula $C_{29}H_{38}O_{17}$ for **88**.

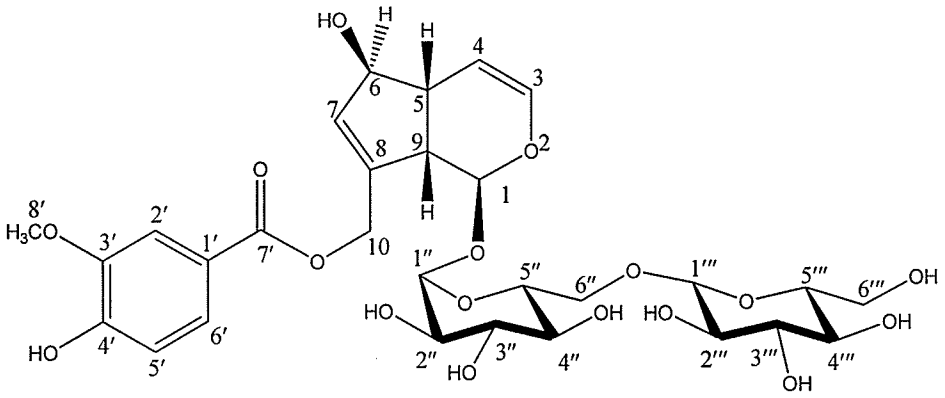

(**88**)

The ^{1}H-NMR spectrum (CD_3OD, 300MHz) of **88** exhibited (Table **2.1**) two sets of double doublets at δ 6.36 (J = 6.0, 1.8) and δ 5.10 (J = 6.0, 3.9) assigned to H-3 and

H-4, respectively. A one-proton multiplet at δ 4.15, bonded to a carbon (δ 82.9) showed by HSQC spectrum, was assigned to H-6. Another one-proton multiplet resonated at δ 2.70, a one-proton broad singlet at δ 5.85 and a one-proton triplet at δ 3.0 (J = 7.2, 14.4) were assigned to H-5, H-7 and H-9, respectively. These signals are characteristic for iridoids and suggested that compound **88** had an iridoid skeleton. Three downfield signals at δ 7.63 (dd, J = 8.1, 2.1), δ 7.59 (d, J = 2.1), δ 6.89 (d, J = 8.1) along with a singlet at δ 3.90 revealed the presence of a 3-methoxy-4-hydroxy-benzoyl moiety in the molecule[14]. Two sets of doublets centered at δ 4.70 (d, J = 7.9) and δ 4.38 (d, J = 7.8) along with signals resonating between δ 3.36-3.80 indicated the presence of two sugar moieties in the molecule. These spectral data revealed that the natural product is like 6″-glucosepeduncullariside. This assumption was further supported by the ^{13}C-NMR spectrum that showed the resonance of two anomeric carbons at δ 100.2 and 104.2.

The COSY-45° spectrum showed vicinal coupling of acetal proton, H-1 (δ 5.15) with H-9 (δ 3.0). The latter proton was further coupled to H-5 (δ 2.70). H-3 (δ 6.36) and H-4 (δ 5.10) showed cross peaks with each other. The latter proton showed coupling with H-5 (δ 2.70). H-5 also exhibited coupling with H-6 (δ 4.15) that in turn showed COSY-45° interaction with H-7 (δ 5.85).

The ^{13}C-NMR (CD_3OD, 75MHz) spectrum of **88** displayed twenty nine signals. DEPT and broad-band ^{13}C-NMR spectrum showed the presence of one methyl, three methylene, twenty methine and five quaternary carbons. The HSQC spectrum was also helpful to determine ^{1}H/^{13}C one-bond shift correlation of all protonated carbons. The complete ^{1}H and ^{13}C-NMR chemical shift assignments of **88** are shown in Table **2.1**.

The HMBC spectrum of **88** exhibited long-range correlations of the C-3 methine proton (δ 6.36) with C-1 (δ 97.9), C-4 (δ 105.6) and C-5 (δ 46.3). The C-7 methine proton (δ 5.85) also exhibited cross peaks with C-5 (δ 46.3), C-6 (δ 82.9) and C-8 (δ 143.0). The C-10 methylene protons (δ 4.9) showed $^{1}H/^{13}C$ long-range correlations with C-8 (δ 143.0) and C-7′ (δ 168.0). The C-6′ methine proton of benzene ring (δ 7.63) showed connectivity with C-7′ (δ 168.0) and H-5′ (δ 6.89) exhibited cross peak with C-1′ (δ 122.4). The cross peaks between C-1 methine proton (δ 5.15) and C-1″ (δ 100.2) were also observed in the HMBC spectrum. These HMBC spectral data indicated that compound **88** had penduncullariside having a glucose moiety at C-6″. This was confirmed by the HMBC interaction of H-1‴ (δ 4.38) with C-6″ (δ 66.3). The down field chemical values of C-6″ also indicated the presence of second glucose moiety at C-6″. The observed HMBC interactions in compound **88** are shown in **88a.**

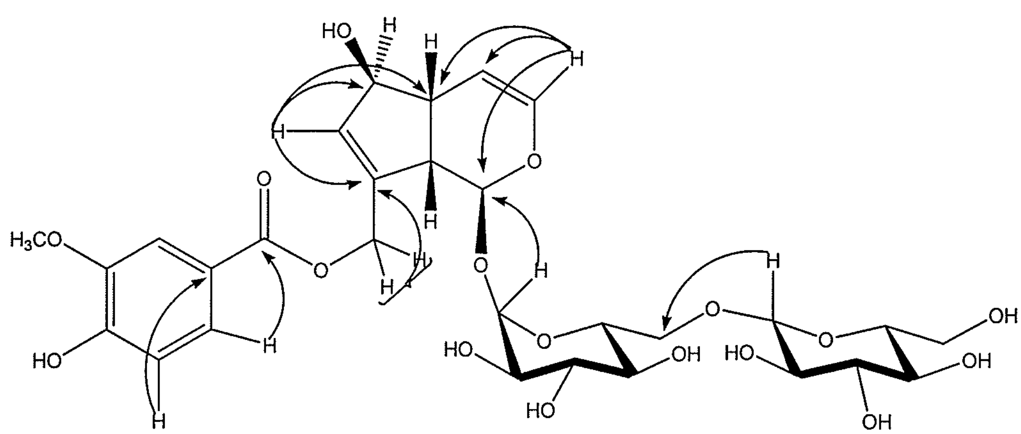

(88a)

The stereochemistry at C-1, C-5, C-6 and C-9 was found to be same as reported for penduncullariside. The chemical shift values of these chiral centers were the same as those of penduncullariside, reported in the literature[14-15]. Both sugars had β-linkage as indicated by the large coupling constants of anomeric protons. These spectral data led us to characterize compound **88** as 6″-glucosepedunculariside.

Table 2.1 ^{1}H and ^{13}C-NMR data of **88**, recorded at 300 and 75 MHz, respectively.

Carbon No.	^{1}H-NMR (δ)	^{13}C-NMR (δ)	DEPT Multiplicity
1	5.15, *d,* (7.2)	97.9	CH
3	6.36, *dd,*(6.0, 1.8)	141.8	CH
4	5.10, *dd,* (6.0, 3.9)	105.6	CH
5	2.70, *m*	46.3	CH
6	4.15, *overlap*	82.9	CH
7	5.85, *brs*	132.7	CH
8	-	143.0	C
9	3.0, *t* (7.2, 14.4)	47.8	CH
10	4.90, *brs*	62.9	CH_2
1'	-	122.4	C
2'	7.59, *d,* (2.1)	113.6	CH
3'	-	153.0	C
4'	-	148.0	C
5'	6.89, *d,* (8.1)	116.3	CH
6'	7.63, *dd,* (8.1, 2.1)	125.4	CH
7'	-	168.0	C
8'	3.90, *s*	56.6	CH_3
1"	4.70, *d,* (7.9)	100.2	CH
2"	3.24, *m*	75.0	CH
3"	3.36, *m*	78.0	CH
4"	3.28, *overlap*	71.6	CH
5"	3.28, *overlap*	78.4	CH
6"	3.77, *dd,* (11.0, 5.0)	66.3	CH_2
	3.87, *dd,* (12.0, 2.0)		
1"'	4.38, *d,* (7.8)	104.2	CH
2"'	3.37, *m*	74.9	CH
3"'	3.62, *m*	78.4	CH
4"'	3.29, *overlap*	71.7	CH
5"'	3.63, *m*	77.9	CH
6"'	3.67, *m*	63.9	CH_2
	3.79, *m*		

Solvent: CD_3OD

2.2.3 Structure elucidation of pedunculariside (89)

The UV and IR spectral data of **89** were similar to those of previously discussed for compound **88** indicating the presence of the same chromophore and functional groups as those were for **88**. A combination of MS, ^{1}H and ^{13}C-NMR spectral data indicated the molecular formula $C_{23}H_{28}O_{12}$.

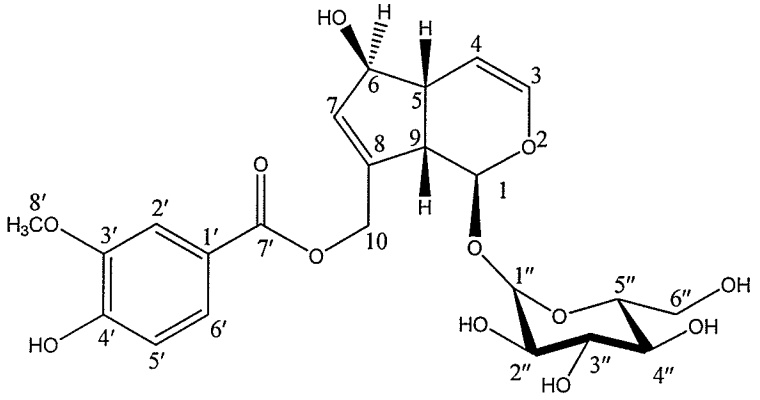

(**89**)

The ^{1}H-NMR spectrum (CD_3OD, 300MHz) of compound **89** was distinctly similar to that of compound **88** except that the ^{1}H-NMR spectrum of the former showed the resonance of one anomeric proton at δ 4.70. This suggested the presence of one sugar moiety in **89**.

The ^{13}C-NMR (CD_3OD, 75MHz) spectrum of compound **89** showed the resonance of all twenty-three carbons. The chemical shift values of all carbons of **89** were distinctly similar to that of compound **88** except for the absence of an additional sugar moiety signals in the former. The complete ^{1}H and ^{13}C-NMR chemical shift assignments of **89** are shown in Table **2.2.**

These spectral data led us to propose structure **89** for this reported iridoidal glycoside. The ^{1}H and ^{13}C-NMR spectral data of **89** were identical to those of pedunculariside as reported in the literature[7,14-15]. This compound was previously isolated from

V.cannabifolia[7], *V. penduncularis*[14] and *V. rotundifolia*[15] and it was the first report of compound **89** from *V. pinnata.*

Table 2.2 ^{1}H and ^{13}C-NMR data of **89**, recorded at 300 and 75 MHz, respectively.

Carbon No.	^{1}H-NMR (δ)	^{13}C-NMR (δ)	DEPT Multiplicity
1	5.15, *d,* (7.2)	97.9	CH
3	6.36, *dd,*(6.0, 1.8)	141.8	CH
4	5.10, *dd,* (6.0, 3.9)	105.6	CH
5	2.70, *m*	46.3	CH
6	4.15, *overlap*	82.9	CH
7	5.85, *brs*	132.7	CH
8	-	143.0	C
9	3.0, *t* (7.2, 14.2)	47.8	CH
10	4.90, *brs*	62.9	CH_2
1'	-	122.4	C
2'	7.59, *d,* (2.1)	113.7	CH
3'	-	153.0	C
4'	-	148.0	C
5'	6.89, *d,* (8.1)	116.2	CH
6'	7.63, *dd,* (8.1, 2.1)	125.4	CH
7'	-	168.0	C
8'	3.90, *s*	56.6	CH_3
1"	4.70, *d,* (7.9)	100.3	CH
2"	3.24, *m*	75.0	CH
3"	3.36, *m*	78.1	CH
4"	3.28, *overlap*	71.6	CH
5"	3.28, *overlap*	78.4	CH
6"	3.77, *dd,* (11.0, 5.0)	63.9	CH_2
	3.87, *dd,* (12.0, 2.0)		

Solvent: CD_3OD

2.2.4 Structure elucidation of agnuside (90)

Both UV and IR spectra of compound **90** look similar to those of **88** and **89**.

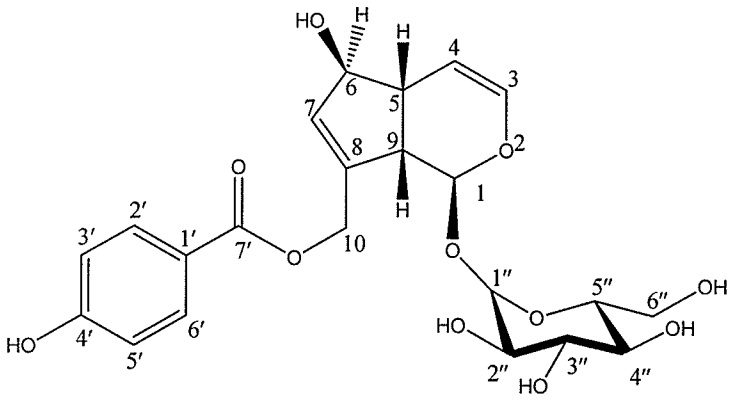

(90)

The ^{1}H-NMR spectrum (CD_3OD, 300MHz) of compound **90** was identical to that of compound **89** with an exception that **90** showed the lack of O-CH_3 signal. The presence of two AB doublets at δ 7.94 (2H, d, J = 9.0 Hz) and δ 6.85 (2H, d, J = 9.0 Hz) suggested the presence of OH group at C-4`.

The ^{13}C-NMR (CD_3OD, 75MHz) spectrum of **90** showed the resonance of all twenty two carbons. The complete ^{13}C-NMR chemical shift assignments of **90** are shown in Table **2.3**.

The ^{1}H and ^{13}C-NMR spectral data of **90** were identical to those of agnuside, reported in the literature[7,14,15,29]. This compound was previously isolated from *V. cannabifolia*[7], *V. penduncularis*[14], *V. rotundifolia*[15], and *V. limonifolia*[29] and was isolated for the first time from this plant.

Table 2.3 ^{1}H and ^{13}C-NMR data of **90**, recorded at 300 and 75 MHz, respectively.

Carbon No.	^{1}H-NMR (δ)	^{13}C-NMR (δ)	DEPT Multiplicity
1	5.05, *d,* (7.2)	98.1	CH
3	6.36, *dd,*(6.0, 1.8)	141.9	CH
4	5.10, *dd,* (6.0, 3.9)	105.4	CH
5	2.70, *m*	46.5	CH
6	4.15, *overlap*	83.0	CH
7	5.85, *brs*	132.6	CH
8	-	143.0	C
9	3.0, *t* (7.2, 14.4)	48.3	CH
10	4.90, *brs*	62.9	CH_2
1'	-	122.2	C
2'	7.94, *d*, (9.0)	133.0	CH
3'	6.85, *d*, (9.0)	116.4	CH
4'	-	163.9	C
5'	6.85, *d*, (9.0)	116.4	CH
6'	7.94, *d*, (9.0)	133.0	CH
7'	-	167.9	C
1"	4.70, *d*, (7.9)	100.3	CH
2"	3.24, *m*	75.0	CH
3"	3.36, *m*	78.1	CH
4"	3.28, *overlap*	71.6	CH
5"	3.28, *overlap*	78.4	CH
6"	3.77, *dd*, (11.0, 5.0)	63.8	CH_2
	3.85, *dd*, (12.0, 2.0)		

Solvent: CD_3OD

2.2.5 Structure elucidation of *p*-hydroxy benzoic acid (91)

The UV spectrum of **91** showed absorption maxima at 321.0 and 249.8 nm. The EIMS of **91** showed the molecular ion peak (M^+) at *m/z* 138. A base peak at *m/z* 121 was observed due to the loss of a hydroxyl group from the molecular ion. Another ion at *m/z* 93 was attributed to the cleavage of carboxylic group. A combination of mass, ^1H and ^{13}C-NMR led us to derive molecular formula $C_7H_6O_3$.

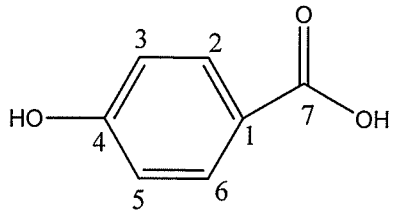

(91)

The ^1H-NMR spectrum (CD_3OD, 200MHz) displayed two AB doublets at δ 6.71 (J = 6.0 Hz) and 7.79 (J = 6.0 Hz), integrating for two protons each, were due to the four methine protons of the di-substituted benzene ring.

The ^{13}C-NMR (CD_3OD, 50MHz) spectrum of **91** showed signals for all seven carbons. The carbonyl carbon (C-7) resonated at δ 170.4. An Attached Proton Test (APT) spectrum showed the presence of four methine and three quaternary carbons in compound **91**. The complete assignments of all ^1H and ^{13}C-NMR of **91** are shown in Table **2.4**. These spectral data identified compound **91** as *p*-hydroxy benzoic acid.

Table 2.4 ^{1}H and ^{13}C-NMR data (CD_3OD) of **91**, recorded at 300 and 75 MHz, respectively.

Carbon NO.	^{1}H-NMR(δ)	^{13}C-NMR (δ)	†Multiplicity
1	----	122.6	C
2	7.79 *d*, (6.0)	133.1	CH
3	6.71 *d*, (6.0)	116.1	CH
4	----	163.3	C
5	6.71 *d*, (6.0)	116.1	CH
6	7.79 *d*, (6.0)	133.1	CH
7	----	170.4	C

Solvent: CD_3OD

2.2.6 Biological activities of compounds 88-91

Compounds **88-91** wer e evaluated for AChE and GST inhibition and antioxidant activities. All of these compounds were weakly active in these bioassays and these are summarized in Table **2.5**.

Table 2.5 GST, AChE and antioxidant activities of compounds **88** to **91.**

Compound	GST activity IC_{50} (μM)	AChE activity IC_{50} (μM)	Anti-oxidant activity IC_{50} (μM)
88	131.49 ± 16.95	344.42 ± 36.73	192.50 ± 8.30
89	391.57 ± 12.90	288.0 ± 41.90	192.56 ± 8.83
90	219.24 ± 14.0	457.57 ±78.32	383.79 ± 28.68
91	NA	NA	248.36 ± 1.87

NA = Non active

2.3 Experimental

2.3.1 General experimental conditions

All solvents (methanol, ethyl acetate, chloroform, dichloromethane, hexane) and Ellman's reagent, DTNB [5-5′-dithio-bis (2-nitrobenzoic acid)], used in this research were bought from VWR-USA. The IR spectra were recorded on *Bomem Hartmann and Braum (BM Series)* spectrometer while the UV spectra were acquired on Shimadzu UV-250 IPC spectrometer. The ^{1}H, ^{13}C-NMR, COSY, HSQC, HMBC, 1D NOE and NOESY spectra were recorded on Varian Inova 200 and Bruker Avance/DPX 300 spectrometer. Chemical shifts (δ) were recorded in ppm and referenced to solvents. EI/CI MS data were obtained on Hewlett Packard 5989B mass spectrometers. HRFABMS spectrum was recorded on INCOSSO, FINNIGA-MAT Mass spectrometer. Thin layer chromatography was carried out on silica gel GF_{254} precoated plates purchased from Merck whereas column chromatography was performed on silica gel (200-400 mesh). Electric-eel acetylcholinestrase (EC 3.1.1.7), acetylthiocholine iodide, 2,2′-diphenyl-1-picrylhydrazyl (DPPH˙), α-tocopherol and quercetin, sodium taurocholate and Equine liver GST were purchased from Sigma-Aldrich. Glutathione (GSH) and 1-chloro-2,4-dinitrobenzene (CDNB) were purchased from MP Biomedicals.

2.3.2 Plant material

The stem bark of *V. pinnata* Linn was collected by Dr. Radhika Samarasekra of the Industrial Technology Institute (ITI) Colombo, Sri Lanka and a voucher specimen was deposited in the herbarium of this institute.

2.3.3 Extraction and isolation

The air dried stem bark (1.815 Kg) of *V.pinnata* was extracted three times with ethanol at room temperature. This ethanolic extract was concentrated under reduced pressure to yield a brownish gummy material. The crude extract was subjected to various chromatographic methods including column and thin layer chromatography to purify compounds **88-91**. The isolation procedure for these compounds is outlined in Scheme **2.2**.

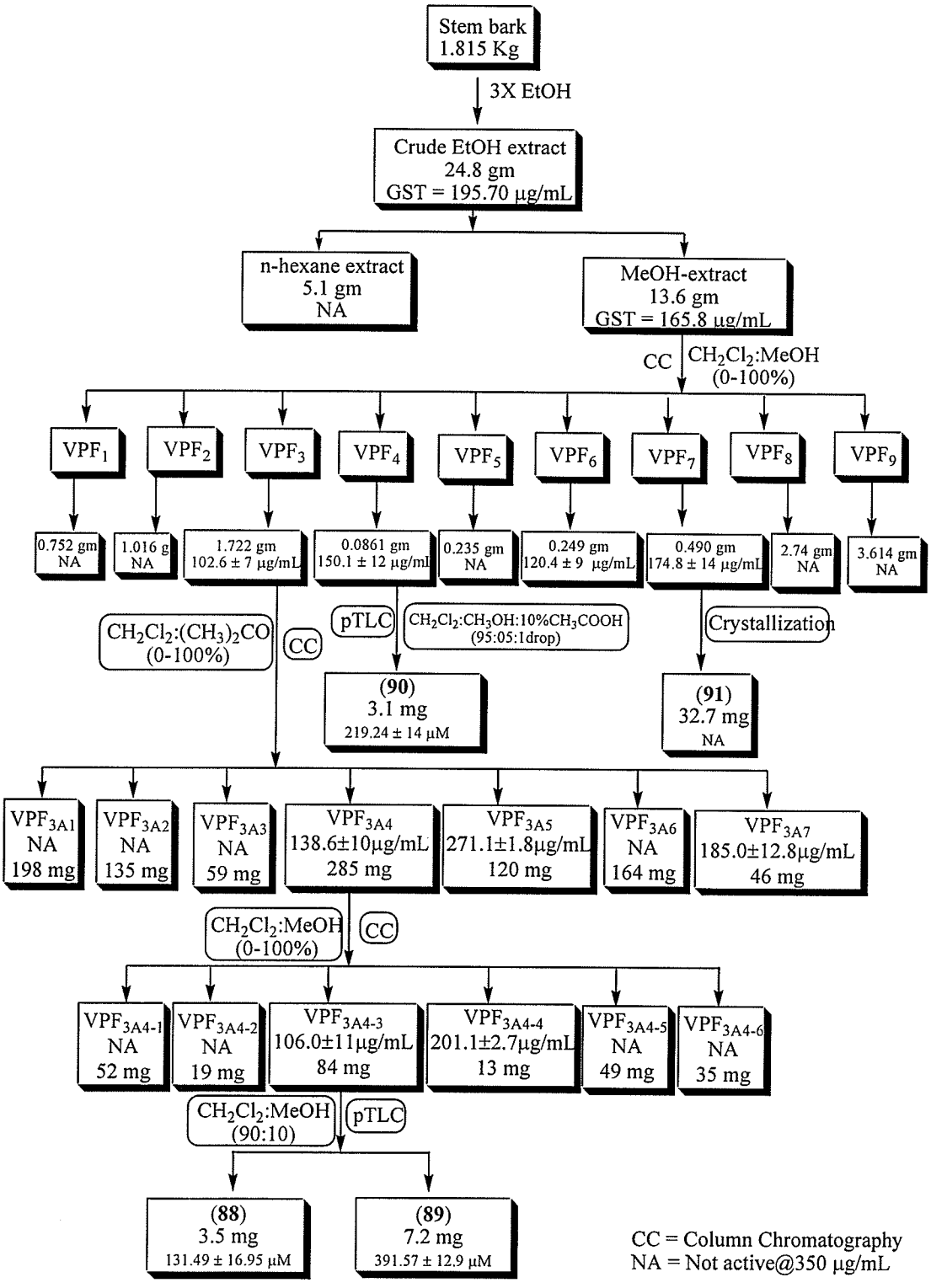

Scheme 2.2 Isolation procedure for compounds **88 – 91**

2.3.4 6″-glucosepeduncullariside (88)

White amorphous solid, 3.5 mg, 0.00019% yield, R_f = 0.23 (CH_2Cl_2-MeOH, 9:1); $C_{29}H_{38}O_{17}$; UV λ_{max} (MeOH) = 291.0 and 262.4 nm; IR (solid film) ν_{max} = 3421, 1715, 1654, 1508 and 1451cm^{-1}; for ^{1}H and ^{13}C-NMR spectral data see Table **2.1**.

2.3.5 Peduncullariside (89)

Off-white amorphous solid, 7.2 mg, 0.00039% yield, R_f= 0.35 (CH_2Cl_2-MeOH, 9:1); $C_{23}H_{28}O_{12}$; UV λ_{max} (MeOH) = 204.0 and 198.8 nm; for ^{1}H and ^{13}C-NMR spectral data see Table **2.2**.

2.3.6 Agnuside (90)

White amorphous solid, 3.1 mg, 0.00017% yield, R_f = 0.33 (CH_2Cl_2-MeOH, 9.5:0.5, 1 drop of 10% CH_3COOH); $C_{22}H_{26}O_{11}$; UV λ_{max} (MeOH) = 258.4 and 200.6 nm; for ^{1}H and ^{13}C-NMR spectral data see Table **2.3**.

2.3.7 *p*-hydroxy benzoic acid (91)

Transparent crystalline solid, 32.7 mg, 0.0018% yield; $C_7H_6O_3$; UV λ_{max} (MeOH) = 321.0 and 249.8 nm; for^{1}H and ^{13}C-NMR spectral data see Table **2.4**.

2.4 Enzyme inhibition assays

2.4.1 Glutathione *S*-transferase inhibition assay

Glutathion *S*-transferase inhibitory activity was measured by following the Habig spectrophotometer method[30]. In a t ypical assay specific concentrations of compound/crude extract were incubated with 133µl of phosphate buffer (pH 6.5), 2µl of GST (with initial effective assay activity of 0.12106 UmL^{-1}) and 25 µl of 1mM CDNB for ten minutes at 25°C. After incubation period, 40 µl of 1mM GSH was added and the product of conjugation was measured at 340 nm in 96-well microplate reader (KC-4 Biokinetic reader, Bio-TEK instrumentation, USA.) The inhibitory

activity of GST was calculated with reference to a control assay (assay carried out under similar conditions with out test compound). The percentage inhibition was calculated by following formula: [(*E* - *S*) / *S*] x 100, where *E* is the activity of the enzyme with out test compound/extract and *S* is the activity of enzyme with test compound/extract. The compound/extract concentration providing IC_{50} was calculated from the graph plotting inhibition percentage against compound/extract concentration. All assays were performed in triplicate.

2.4.2 Acetylcholinesterease assay

The inhibitory activity of acetylcholinesterease was measured by following Ellman's methodology[31] with slight modifications. In order to evaluate the inhibitory activity of all purified compounds (**88-91**) the assay was carried out at room temperature in 100 mM sodium phosphate buffer at pH 7.8. In a typical assay, 126µl buffer, 50µl of 0.01M DTNB [5-5′-dithio-bis (2-nitrobenzoic acid)], 2µl enzyme and 2µl test compound solution were mixed and incubated for 30 minutes. The reaction was then initiated by the addition of 20µl of 0.075M acetylthiocholine. Hydrolysis of acetylthiocholine was monitored by the formation of yellow 5-thio-2-nitrobenzoate anion as a result of the reaction of DTNB with thiocholine, released by the enzymatic hydrolysis of acetylthiocholine at a wavelength of 406 nm. All assays were carried out in triplicate in 96-well microplate reader (KC-4 Biokinetic reader, Bio-TEK instrumentation, USA). The percentage inhibition was calculated by following the formula: [(*E* - *S*) / *S*] x 100, where *E* is the activity of the enzyme with out test compound and *S* is the activity of enzyme with test compound. The IC_{50} values were calculated by plotting a concentration response curve.

2.4.3 Antioxidant assay

The antioxidant activity of all purified compounds (**88-91**) was evaluated on the basis of radical scavenging activity of stable free radical 2,2′-diphenyl-1-picrylhydrazyl ($DPPH^{\cdot}$)[32]. A solution of $DPPH^{\cdot}$ was prepared at 2.5 mg/mL in methanol and was stored at 4 °C in dark. The stock solutions of all compounds along with α-tocopherol and quercetin as standards were also prepared by dissolving 1 mg of each in 1mL of methanol and were diluted to varying concentrations in 96-well microplates. Then freshly prepared $DPPH^{\cdot}$ solution (final concentration 0.3 mM) was added to each well. The reaction mixture was shaken vigorously to ensure proper mixing and allowed to stand for 30 minutes in dark at room temperature. The decrease in absorbance was recorded at 517 nm using UV-Vis microplate reader (KC-4 Biokinetic reader, Bio-TEK instrumentation, USA). A methanolic solution of $DPPH^{\cdot}$ served as a control while sample solution without $DPPH^{\cdot}$ served as negative control. The scavenging activity was calculated using the following equation: % Inhibition = $[(A° - A^1)/A°)] \times 100$, Where $A°$: absorbance of $DPPH^{\cdot}$ solution without sample, A^1: absorbance of $DPPH^{\cdot}$ solution in the presence of sample. A concentration response curve was plotted to calculate the IC_{50} values. All tests were run in triplicate.

2.5 References

[1] The Wealth of India. *A Dictionary of Indian Raw Materials and Industrial Products*; CSIR: New Delhi, **1976**, 10, 520-526.

[2] Chopra, R. N.; Nayar, S. L.; Chopra, I. C. In *Glossary of Indian Medicinal Plants*; CSIR: New Delhi, **1956**, 256-257.

[3] Peigen, X.; Keji, C.; *Phytother. Res.*, **1988**, 2, 55.

[4] Sathiamoorthy, B.; Gupta, P.; Kumar, M.; Aswhok, K.; Chaturvedi, P. K.; Maurya, R. *Bioorg. Med. Chem. Lett.*, **2007**, 17, 239.

[5] Balbao, J. G.; Lim-Sylianco, C. Y. Phillip. *J. Sci.*, **1993**, 122, 1.

[6] Barbosa, L. C. A.; Demuner, A. J.; Howarth, O. W.; Pereira, N. S; Veloso, D. P. *Fitoterapia*, **1995**, 66, 279.

[7] Yamasaki, T.; kawabata, T.; Masuoka, C.; Kinjo, J.; Ikeda, T.; Nohara, T. *J. Nat. Med.*, **2008**, 62, 47.

[8] Goncalves, J. L.; Leitao, S. G.; delle Monache, F.; Miranda, M. M.; Santos, M. G.; Romanos, M. T.; Wigg, M. D. *Phytomedicine,* **2001**, 8, 477.

[9] Ko, W. G.; Kang, T. H.; Lee, S. J.; Kim, Y. C.; Lee, B. H. *Phytother.Res.*, **2001**, 15, 535.

[10] Chawla, A. S.; Sharma, A. K.; Handa, S. S.; Dhar, K. L. *J. Nat. Prod.*, **1992**, 55, 163.

[11] Avadhoot, Y.; Rana, A. C. *Arch. Pharm. Res.*, **1991**, 14, 96.

[12] Kawazoe, K.; Yutani, A.; Tamemoto, K.; Yuasa, S.; Shibata, H.; Higuti, T.; Takaishi, Y. *J. Nat. Prod.*, **2001**, 64, 588.

[13] Sehgal, C. K.; Taneja, S. C.; Dhar, K. L.; Atal, C. K. *Phytochemistry,* **1982**, 21, 363.

[14] Suksamrarn, A.; kumpun, S.; kirtikara, K.; yingyoungnarongkul, B.; Suksamrarn, S. *Planta Medica*, **2002**, 68, 72.

[15] Ono, M.; Ito, Y.; Kubo, S.; Nohara, T. *Chem. Pharm. Bull.*, **1997**, 45, 1094.

[16] Kuruuzum-Uz, A.; Stroch, K.; Demirezer, L. O.; Zeeck, A. *Phytochemistry,* **2003**, 63, 959.

[17] Watanabe, K.; Takada, Y.; Matsuo, N.; Nishimura, H. *Biosci. Biotech. Biochem.*, **1995**, 59, 1979.

[18] Ono, M.; Yamamoto, M.; Masuoka, C.; Ito, Y.; Yamashita, M.; Nohara, T. *J. Nat. Prod.*, **1999**, 62, 1532.

[19] Ono, M.; Sawamura, H.; Ito, Y.; Mizuki, K.; Nohara, T. *Phytochemistry,* **2000**, 55, 873.

[20] Hirobe, C.; Qiao, Z. S.; Takeya, K.; Itokawa, H. *Phytochemistry*, **1997**, 46, 521.

[21] Suksamrarn, A.; Promrangsan, N.; Tintasirikul, A. *Phytochemistry,* **2000**, 53, 921.

[22] Suksamrarn, A.; Promrangsan, N.; Chitkul, B.; Homvisasevongsa, S.; Sirikate, A. *Phytochemistry,* **1997**, 45, 1149.

[23] Dewick, P. M. *Medicinal Natural Products*: *A biosynthetic approach.*" 2nd ed., John Wiley & Sons, 2001.

[24] Damtoft, S.; Franzyk, H.; Jensen, S. R. *Phytochemistry*, **1993**, 34, 1291.

[25] Dharmasiri, M. G.; Jayakody, J. R. D. C.; Galhena, G.; Liyanage, S. S. P.; Ratnasooriya, W. D. *J. Ethnopharmacol.*, **2003**, 87, 199.

[26] Zheng, G. M.; Luo, Z. M.; Chen, D. M. *Guangdong Gongye Dexue Xuebao*, **1999**, 16, 41.

[27] Chawla, A. S.; Sharma, A. K.; Handa, S. S.; Dhar, K. L. *Indian J. Chem.*, Sect. B. **1991**, 30B, 773.

[28] Burkill, I. H. *A dictionary of the economic products of the Malay Peninsula*, Ministry of Agriculture and Cooperatives, Kuala Lumpur, **1966**, 2, 2280.

[29] Suksamrarn, S.; Kumcharoen, S.; Suksamrarn, A. *Planta Medica*, **1999**, 65, 392.

[30] Habig, W. H.; Pabst, M. J.; Jakoby, W. B. *J. Biol. Chem.*, **1974**, 25, 7130.

[31] Ellman, G. L.; Courtney, K. D.; Andrews, V.; Featherstone, R. M. *Biochem. Pharmacol.*, **1961**, 7, 88.

[32] Lee, S. K.; Zakaria, H. M.; Cheng, H. S.; Luyengi, L.; Gamez, E. J. C.; Metha, R.; Kinghorn, A. D.; Pezzuto, J. M. *Combinat. Chem. High Throughput Screen*, **1998**, 1, 35.

CHAPTER 3

Phytochemical studies on *Artocarpus nobilis*

3.1 Introduction

Artocarpus nobilis Thw. (Moraceae) is a moderate sized tree and is the only endemic species of the genus *Artocarpus* found in Sri Lanka[1]. The genus *Artocarpus* comprises of about 1400 species[2]. Plants of this genus have several ethnopharmaceutical applications to treat inflammations, malarial fever, ulcers, abress and diarrhea in Southeast Asia[3,4]. The roots of *A. altilis* are used for the treatment of venereal diseases and cancer[5] in Thailand. In Taiwan, the stem and roots are used traditionally as curative agents for the treatment of liver cirrhosis and hypertension[6]. The crude extracts of different species of *Artocarpus* have also been reported to have various biological activities. For example, the CH_2Cl_2 extract of roots of *A. altilis* have shown antitubercular activity against *Mycobacterium tuberculosis* with a minimum inhibitory concentration of 25μg/mL. The extract also exhibited antiplasmodial activity (IC_{50} = 3.5 μg/mL) against the parasite *Plasmodium falciparum*[6]. Recently the crude extract of *A. lakoocha* was found to be effective for the treatment of taeniasis[7] and the chloroform extract of the heartwood of *A. communis* have been reported to exhibit inducible nitric oxide synthase (iNOS) inhibitory activity with an IC_{50} value of 10.0 μg/mL[8].

Previous phytochemical studies on various plants of genus *Artocarpus*, resulted in the isolation of flavonoids, stilbenoids and terpenoids[9-16]. These constituents have been reported to exhibit antioxidant, antimalarial, cytotoxic and antibacterial activities[9]. For instance, the flavonoids artocarpone A (**92**), artocarpone B (**93**), artoindonesianine R

(**94**), artonine A (**95**), cycloheterophyllin (**96**), artoindonesianine A-2 (**97**), heterophyllin (**98**), and heteroflavanone C (**99**) isolated from *A. champeden* have been reported as antimalarial agents with IC_{50} values of 0.12, 0.18, 0.66, 0.55, 0.02, 1.31, 1.04, and 0.001 μM, respectively[10]. A large number of cytotoxic flavonoids have also been reported from *A. champeden.* For instance, artoindonesianin U (**100**), artoindonesianin L (**101**) cyclocommunol (**102**), cyclocommunin (**103**) and cycloartocarpin (**104**) isolated from *A. champeden* have shown cytotoxic activities with LC_{50} values of 2.0, 0.06, 9.0, 4.7 and 1.9 μg/mL[11-15].

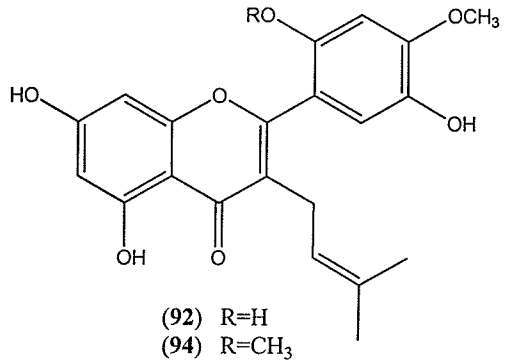

(**92**) R=H
(**94**) R=CH_3

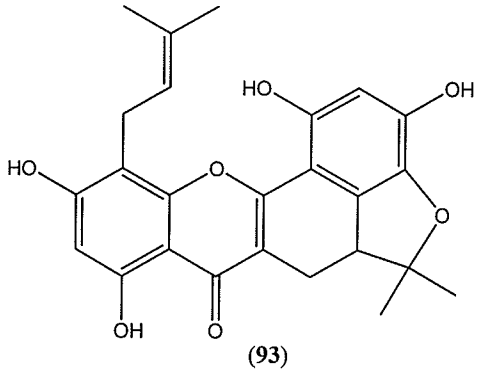

(**93**)

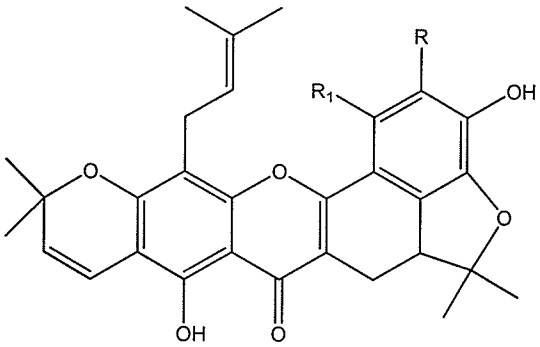

(**95**) R=H, R_1=OH
(**96**) R=OH, R_1=H

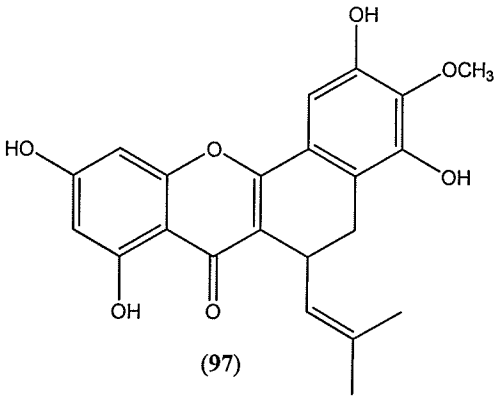

(**97**)

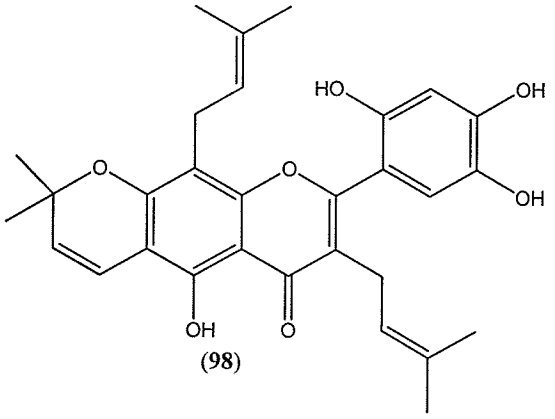

(98)

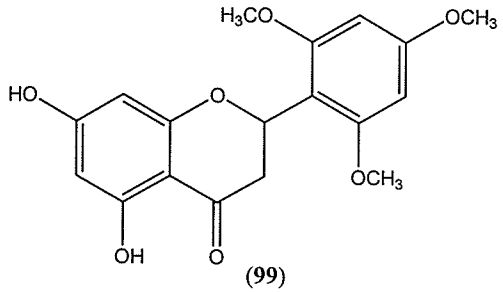

(99)

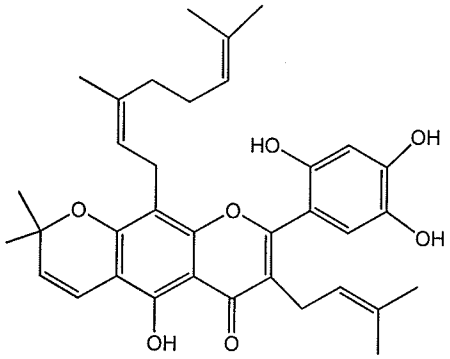

(100)

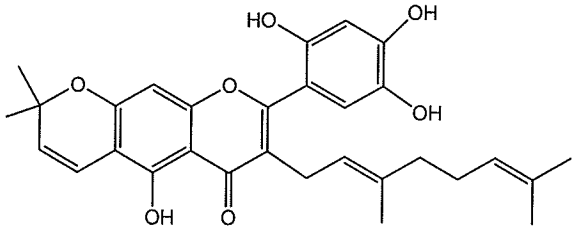

(101)

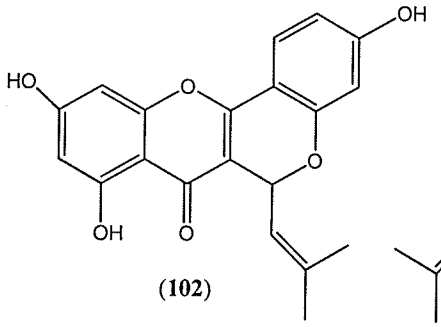

(102)

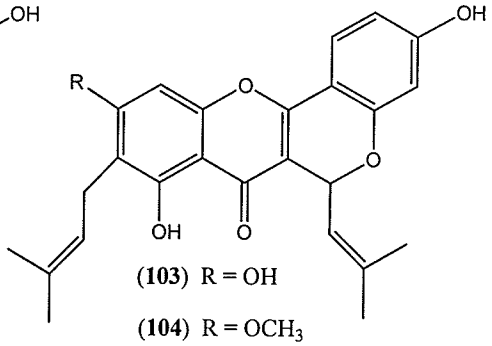

(103) R = OH

(104) R = OCH_3

Phytochemical investigations on the non-polar fractions of *Artocarpus* species have resulted in the isolation of lanosterole type triterpenes. For example, triterpenes, cycloartenone (**105**), 24-methylenecycloartanone (**106**), cycloeucalenol (**107**), and glutinol (**108**) have been reported from the *n*-hexane extract of the tree bark of *A. champeden*[16].

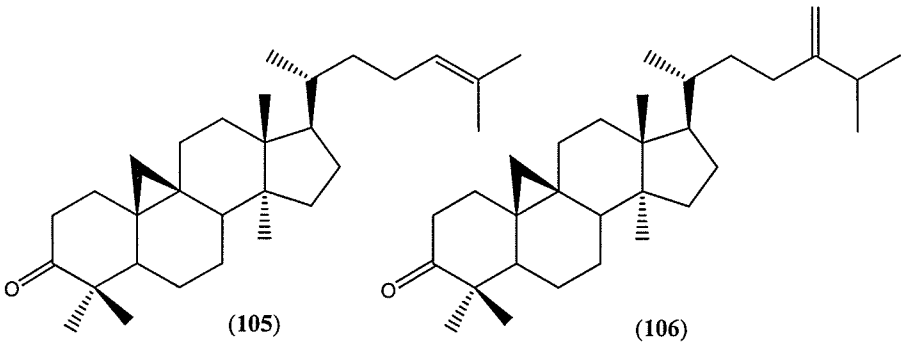

(105) (106)

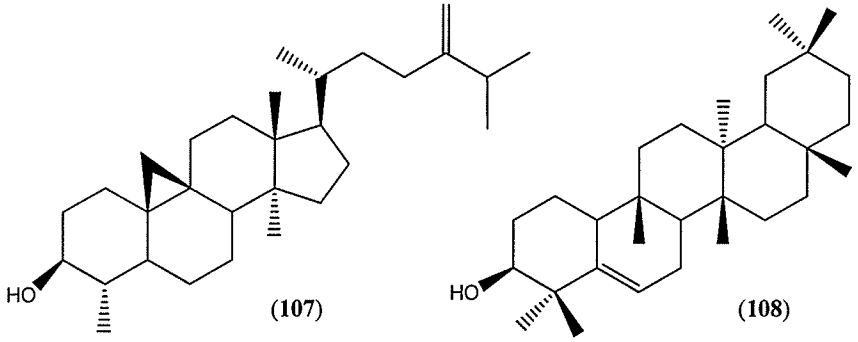

(107) (108)

3.2 Results and discussion

3.2.1 Isolation of compounds 109 to 116

Phytochemical studies on the crude ethanolic extract of *A. nobilis* resulted in the isolation of six triterpenoids, artocarpuate A (**109**), artocarpuate B (**110**), cyclolaudenyl acetate (**111**), lupeol acetate (**112**), β-amyrine acetate (**113**), 12,13-dihydromicromeric acid (**114**) along with two flavonoids, artonins E (**115**) and artobiloxanthone (**116**) (for purification see experimental section). Compounds **109** and **110** were new and **111-116** were known natural products. All of these compounds exhibited different levels of AChE and GST inhibitory activities. Structures of all of these compounds were established with the aid of extensive spectroscopic studies and are discussed below.

3.2.2 Structure elucidation of artocarpuate A (109)

The UV spectrum of artocarpuate A (**109**) displayed terminal absorption, indicating the lack of any conjugated π bond. The IR spectrum displayed intense absorption bands at 1734 (C=O) and 1636 (C=C) cm^{-1}. The CIMS of **109** showed the $[M+H]^+$ ion at *m/z* 399. The HREIMS exhibited the molecular ion peak at *m/z* 398.2824 (calcd. 398.2821) corresponding to the molecular formula $C_{26}H_{38}O_3$. This indicated the presence of eight degrees of unsaturation in compound **109** and these were accounted for by the cycloartane triterpenoidal skeleton having a double bond in ring B and two carbonyl groups.

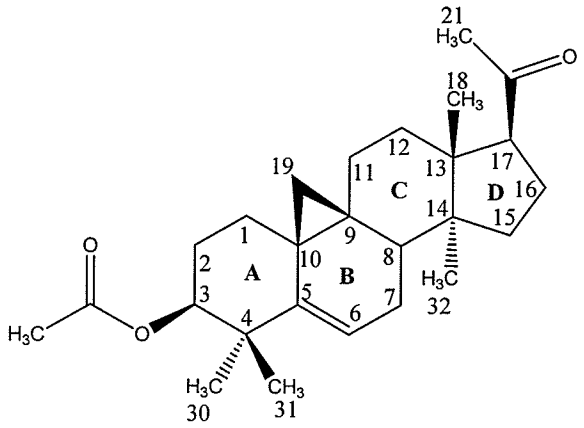

(109)

The ^{1}H-NMR spectrum ($CDCl_3$, 300 MHz) of **109** showed a set of AB doublets at δ 0.33 and 0.57 (J = 4.0 Hz) due to H_2-19. Four three-proton singlets at δ 0.90, 0.94, 0.84 and 1.04 were assigned to H_3-30, H_3-31, H_3-32 and H_3-18, respectively. H_3-21 resonated as a three-proton singlet at δ 2.17. Another three-proton singlet at δ 2.05 was ascribed to the acetyl methy protons of an acetyl group, substituted at C-3. A double doublet, integrating for one proton, appeared at δ 4.56 (dd, $J_{1,2}$ = 6.0 and $J_{1,3}$ = 11.4 Hz) was ascribed to H-3. Its downfield chemical shift value was indicative of the presence of geminal ester functionality. A downfield broad singlet at δ 5.12 was ascribed to H-6.

The COSY-45° and TOCSY spectra showed the presence of four isolated spin systems in compound **109**. The first spin system was traced from H-3 (δ 4.56), which showed cross-peaks with H_2-2 (δ 2.15 and 2.02) and H_2-2 in turn exhibited vicinal couplings with H_2-1 (δ 1.30 and 1.55). The second spin system consisted of a fragment starting from H-6 (δ 5.12) and ending at H-8 (δ 1.49). The H-6 (δ 5.12) displayed ^{1}H-^{1}H spin corelations with H_2-7 (δ 1.38 and 1.63) which in turn showed COSY-45° interactions with H-8 (δ 1.49). The third spin system was traced from the vicinal couplings of H_2-11 (δ 1.13 and 2.01) with H_2-12 (δ 1.68 and 2.10). The fourth spin system

consisted of ring D. H-17 (δ 1.59) showed vicinal couplings with H_2-16 (δ 1.35 and 1.90). The latter in turn showed cross peaks with H_2-15 (δ 1.25 and 1.41).

The ^{13}C-NMR spectrum ($CDCl_3$, 75 MHz) of **109** showed signals for all 26 carbons. The olefinic signals resonating at δ 134.4 and 119.3 were due to C-5 and C-6 carbons, respectively. An attached proton test (APT) experiment was performed to establish the multiplicity of each signal in the broad-band ^{13}C-NMR spectrum. The APT spectrum revealed the presence of six methyl, eight methylene, four methine and eight quaternary carbons in compound **109**. The HSQC spectrum was recorded to determine the ^{1}H/^{13}C one-bond shift correlations of all protonated carbons. The complete ^{1}H and ^{13}C-NMR chmical shift assignments are shown in Table **3.1**.

A combination of ^{1}H, ^{13}C, COSY, HSQC, HMBC and mass spectral data suggested that compound **109** had a cycloartane-type structure with a degraded C-20 side chain and an ester moiety at C-3, as most of the signals in the ^{1}H and ^{13}C-NMR spectra were identical to those of cycloartane-type triterpenoids[17-19]. The HMBC spectral data were used to confirm structure **109**. Important HMBC interactions are shown around structure **109a**.

After establishing a gross structure for compound **109**, the NOESY spectrum was used to determine the relative stereochemistry at all chiral centers present in this compound. H-3 (δ 4.56) showed an NOE with H_3-30 (δ 0.90). H-17 (δ 1.59) showed an NOE with the H_3-32 (δ 0.84). H_3-31 (δ 0.94) exhibited cross peaks with H-8 (δ 1.49), which further showed an NOE with H_3-18 (δ 1.04). It has been reported that H-3, H_3-30 and H_3-32 have invariably α-orientations while H-8, H_3-18 and H_3-31 have β-orientation in this class of natural products[40]. These NOESY spectral observations led us to assume α-stereochemistry for H-3, H-17, H_3-30 and H_3-32 and β- stereochemistry for H-8,

H_3-18 and H_3-31. Based on these spectroscopic studies, structure **109** was established for this new natural product.

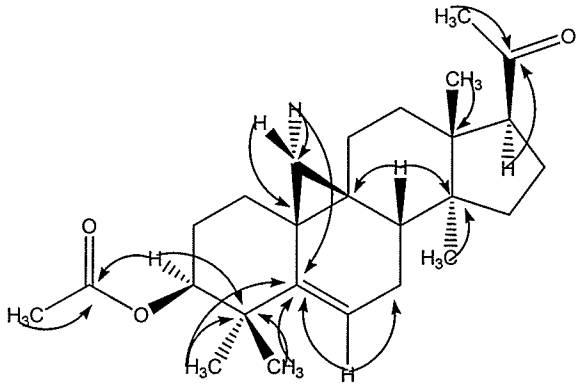

(109a)

Table 3.1 ^{1}H and ^{13}C-NMR data of **109**, recorded at 300 and 75 MHz, respectively.

Carbon No.	$\delta^{1}H$-NMR	$\delta^{13}C$-NMR	Multiplicity
1	1.30, 1.55, *m*	32.0	CH_2
2	2.15, 2.02, *m*	29.6	CH_2
3	4.56 *dd,* (6.0, 11.4)	80.6	CH
4	----	39.4	C
5	----	134.4	C
6	5.12, brs	119.3	CH
7	1.38, 1.63, *m*	26.4	CH_2
8	1.49, *m*	47.8	CH
9	----	20.2	C
10	----	26.8	C
11	1.13, 2.01, *m*	25.9	CH_2
12	1.68, 2.10, *m*	32.6	CH_2
13	----	40.6	C
14	----	48.7	C
15	1.25, 1.41, *m*	35.5	CH_2
16	1.35, 1.90, *m*	29.1	CH_2
17	1.59, *m*	52.2	CH
18	1.04, *s*	18.0	CH_3
19	0.33, 0.57, *d*(4.0)	30.8	CH_2
20	----	207.0	CH
21	2.17, *s*	19.2	CH_3
30	0.90, *s*	15.1	CH_3
31	0.94, *s*	14.1	CH_3
32	0.84, *s*	20.9	CH_3
$OCOCH_3$	-----	171.2	C
$OCOCH_3$	2.05, *s*	20.9	CH_3

Solvent: $CDCl_3$

3.2.3 Structure elucidation of artocarpuate B (110)

The UV and IR spectra of artocarpuate B (**110**) were nearly identical to that of **109** except that the IR spectrum of the former showed an intense absorption band at 3421cm^{-1} due to a hydroxyl group. The CIMS showed a $[M+H]^+$ ion peak at *mlz* 503. The HREIMS also exhibited a molecular ion peak at *m/z* 502.3999 (calcd. 502.4022) corresponding to the molecular formula $C_{32}H_{54}O_4$, indicating the presence of six double bond equivalents in the molecule.

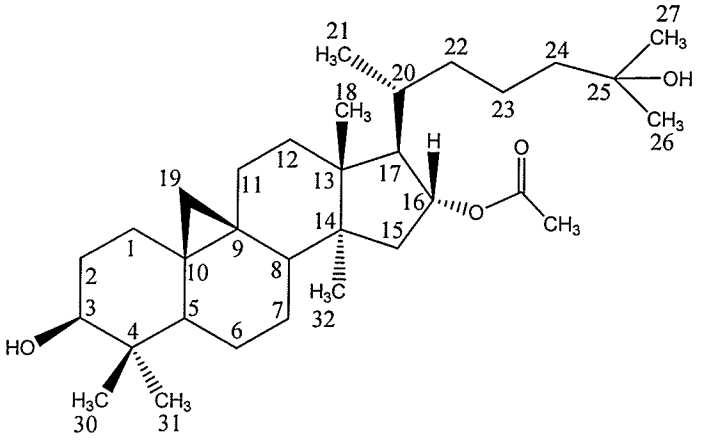

(110)

The ^{1}H-NMR spectrum ($CDCl_3$, 300 MHz) of compound **110** showed two signals at δ 3.60 (H-3) and 4.56 (H-16), respectively. The downfield chemical shift values of H-3 and H-16 were indicative of the presence of geminal hydroxyl and acetoxy functionalities at C-3 and C-16, respectively. The rest of the ^{1}H-NMR spectrum of **110** was similar to that of compound **109** with the exception of signals due to the C-20 side cahin. A doublet, integrating for three protons, resonating at δ 0.98 (J = 6.0 Hz) was assigned to H_3-21. Additionally, two singlets, integrating for three protons each, at δ 1.38 and 1.58 due to H_3-26 and H_3-27 were also observed in the ^{1}H NMR spectrum of **110**.

The analysis of ^{1}H-^{1}H COSY-45° and TOSCY spectra of **110** revealed the presence of a side chain at C-20 in this molecule. H-3 (δ 3.60) showed cross peaks with H_2-2 (δ 1.50 and 2.17) in the COSY-45° spectrum. H_3-21 (δ 0.98) showed ^{1}H-^{1}H spin couplings with H-20 (δ 1.91). The latter exhibited cross peaks with H_2-22 (δ 1.19 and 1.26) and H-17 (δ 1.62). H-17 showed vicinal coupling with H-16 (δ 4.56) which in turn exhibited cross peaks with H_2-l5 (δ 1.22 and 1.37). H_2-22 showed vicinal couplings with H_2-23 (δ 1.02 and 1.30), which further showed COSY-45° interactions with H_2-24 (δ 1.28 and 1.34). The remaining ^{1}H-^{1}H spin correlations in the COSY-45° and TOCSY spectra were the same as observed for compound **109**.

The ^{13}C-NMR spectrum ($CDCl_3$, 75 MHz) of **110** was similar to that of **109** except for the additional signals for the C-20 side chain and the difference in the chemical shift values for C-3, C-5, C-6, C-16, and C-20 which resonated at δ 77.3, 47.2, 20.8, 80.1, and 35.7, respectively. Another aliphatic downfield signal at δ 77.4 was assigned to C-25, and its down field resonance was due to the presence of hydroxyl functionality. The presence of a hydroxyl moiety at C-25 was also confirmed from the HMBC spectrum of **110**, which exhibited long-range heteronuclear couplings of H_3-26 (δ 1.38) and H_3-27 (δ 1.58) with C-25 (δ 77.4). Complete ^{1}H and ^{13}C-NMR chemical shift assignments of **110** are given in Table **3.2**.

The NOESY spectrum of **110** indicated that the stereochemistry at C-3, C-5, C-8, C-10, C-13, C-14, and C-20 was similar to those of compound **109**. The H-16 (δ 4.56) showed an NOE with H_3-18 (δ 1.04), suggesting a β-orientation of H-16 and α-orientation for C-16/OAc. The stereochemistry at C-20 was established by the comparison of ^{1}H and ^{13}C-NMR chemical shift values of C-20 with those of

compounds of this series, reported in the literature[21]. Based on these spectroscopic studies, structure **110** was proposed for this new natural product.

Table 3.2 ^{1}H and ^{13}C-NMR data of **110**, recorded at 300 and 75 MHz, respectively.

Carbon No.	$\delta^{1}H$-NMR	$\delta^{13}C$-NMR	DEPT Multiplicity
1	1.31, 1.52, *m*	32.1	CH_2
2	1.52, 2.17, *m*	29.8	CH_2
3	3.60 *dd,* (6.2, 9.8)	77.3	CH
4	----	40.6	C
5	1.89, *m*	47.2	CH
6	0.82, 1.68, *m*	20.8	CH_2
7	1.16, 1.35, *m*	26.2	CH_2
8	1.50, *m*	48.2	CH
9	----	20.5	C
10	----	26.5	C
11	1.12, 2.05, *m*	25.8	CH_2
12	1.60, 2.09, *m*	34.9	CH_2
13	----	40.5	C
14	----	48.5	C
15	1.22, 1.37, *m*	34.7	CH_2
16	4.56, *m*	80.1	CH
17	1.62, *m*	51.5	CH
18	1.04, *s*	18.6	CH_3
19	0.34, 0.55, *d* (4.1)	30.4	CH_2
20	1.91, *m*	35.7	CH
21	0.98, *d* (6.0)	20.1	CH_3
22	1.19, 1.26, *m*	33.8	CH_2
23	1.02, 1.30, *m*	23.9	CH_2
24	1.28, 1.34, *m*	29.4	CH_2
25	----	77.4	C
26	1.38, *s*	18.8	CH_3
27	1.58, *s*	19.5	CH_3
30	0.91, *s*	16.3	CH_3
31	0.84, *s*	14.6	CH_3
32	0.88, *s*	17.4	CH_3
$O\underline{C}O\underline{C}H_3$	-----	173.5	C
$OCO\underline{CH_3}$	2.03, *s*	21.3	CH_3

Solvent: $CDCl_3$

3.2.3 Structure elucidation of cyclolaudenyl acetate (111)

The UV spectrum of cyclolaudenyl acetate (**111**) showed terminal absorption indicating the absence of any conjugated π system. The IR spectrum suggested the presence of carbonyl (1732cm^{-1}) and olefinic (1454 cm^{-1}) functionalities. The EIMS of compound **111** showed a molecular ion peak at *m/z* 482 while the CIMS showed a $[M+H]^+$ ion at *m/z* 483. An ion at *m/z* 467 was due to the loss of a methyl group from the molecular ion. A combination of MS, ^{1}H and ^{13}C-NMR spectral data provided the molecular formula, $C_{33}H_{54}O_2$, for this compound.

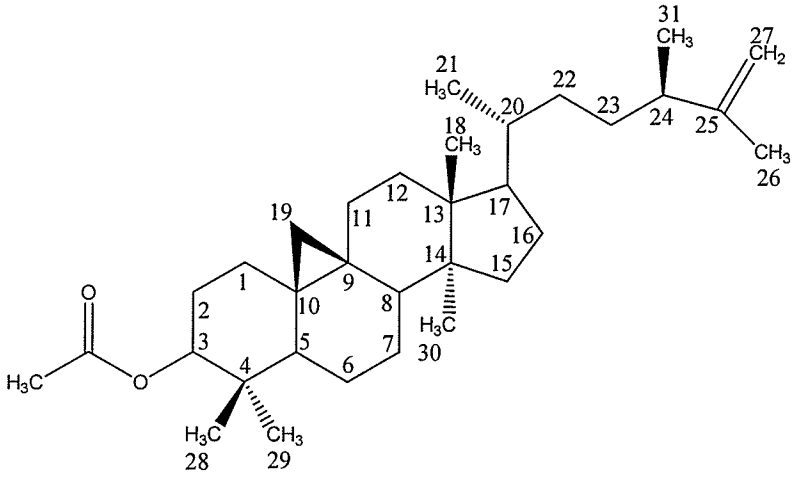

(111)

The ^{1}H-NMR spectrum ($CDCl_3$, 300 MHz) of **111** showed a set of AB doublets at δ 0.33 and 0.59 (J = 4.0 Hz) due to H_2-19. Four singlets at δ 0.85, 0.87, 0.89 and 0.90, integrating for three protons each, were due to H_3-28, H_3-30, H_3-29 and H_3-18, respectively. One singlet resonating at δ 1.65, integrating for three protons, was due to H_3-26. Another three-proton singlet at δ 2.05 was due to the acetyl methyl protons of an acetoxy group substituted at C-3. Two doublets, integrating for three protons each, resonating at δ 0.98 and 1.01 were assigned to H_3-21 and H_3-31. A broad singlet, integrating for two protons, resonated at δ 4.68 was assigned to H_2-27$^{22\text{-}23}$. A double

doublet, integrating for one proton, resonating at δ 4.55 (dd, $J_{1,2}$ = 5.3 and $J_{1,3}$ = 10.3 Hz) was ascribed to H-3.

The COSY-45° spectrum of **111** showed cross peaks between H-3 (δ 4.55) and H_2-2 (δ 1.68 and 1.90). The latter showed cross peaks with H_2-1 (δ1.39 and 1.65). H-5 (δ 1.35) showed cross peaks with H_2-6 (δ 0.84 and 1.58). The latter exhibited cross peaks with H_2-7 (δ1.28 and 1.39), which in turn displayed a cross peak with H-8 (1.67). H_2-11 (δ 2.26 and 1.05) and H_2-12 (δ 1.88 and 1.57) also showed cross peaks with each other. The remaining ^{1}H-^{1}H spin correlations in the COSY-45° spectrum were the same as observed for compound **110**.

The broad-band decoupled ^{13}C-NMR spectrum ($CDCl_3$, 75 MHz) of **111** showed signals for all 33 carbons. The DEPT spectrum showed the presence of eight methyl, twelve methylene, six methine, and seven quaternary carbons in **111** (Table **3.3**). The HSQC spectrum was recorded to determine the ^{1}H/^{13}C one-bond shift correlations of all protonated carbons.

The HMBC spectrum of **111** exhibited long-range shift correlations of C-19 methylene protons (δ 0.33 and 0.59) with C-1 (δ 32.8), C-5 (47.8), C-9 (20.2) and C-11 (26.4). The C-28 methyl protons (δ 0.85) exhibited cross peaks with C-3 (δ 80.6) and C-4 (δ 39.4) while the C-29 methyl protons (δ 0.89) showed connectivity with C-3 (δ 80.6) and C-5 (δ 47.8). The C-30 methyl protons (δ 0.87) displayed cross peaks with C-8 (δ 47.1), C-14 (δ 48.8) and C-15 (δ 35.5) carbons. The C-27 methylene protons (δ 4.68) exhibited cross peak with C-24 (δ 41.6) while C-26 methyl protons (δ 1.65) showed interactions with C-24 (41.6), C-25 (150.2) and C-27 (109.3). The C-31 methyl protons (δ 1.01) displayed cross peaks with C-23 (δ 31.5), C-24 (δ 41.6) and C-25 (δ 150.2) carbons. All of these above mentioned HMBC interactions helped to

establish the gross structure of **111**. The important HMBC interactions are shown in the figure **111a**.

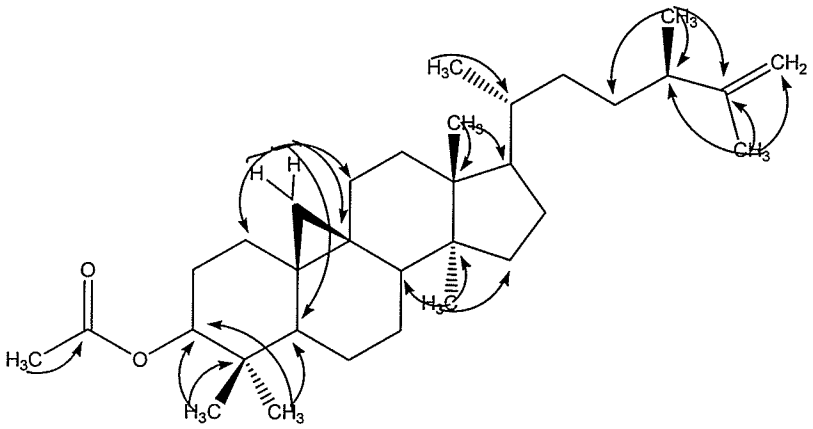

(111a)

Based on these spectral data, this compound was identified as cyclolaudenyl acetate as the ^{1}H and ^{13}C-NMR spectral data of **111** was identical to those of cyclolaudenyl acetate reported in the literature[22-24]. This compound was previously reported from *Tillandsia fasciculate*[22] and *Polypodium formosanum*[23-24]. This compound was isolated for the first time from *A. nobilis.*

Table 3.3 ^{1}H and ^{13}C-NMR data of **111,** recorded at 300 and 75 MHz, respectively.

Carbon No.	δ^{1}H-NMR	δ^{13}C-NMR	DEPT Multiplicity
1	1.39, 1.69, *m*	32.6	CH_2
2	1.68, 1.90, *m*	28.0	CH_2
3	4.55 *dd,* (5.3, 10.3)	80.6	CH
4	----	39.4	C
5	1.35, *brs*	47.8	CH
6	0.84, 1.58, *m*	25.8	CH_2
7	1.28, 1.39, *m*	26.8	CH_2
8	1.67, *m*	47.1	CH
9	----	20.2	C
10	----	33.8	C
11	1.05, 2.26, *m*	26.4	CH_2
12	1.57, 1.88, *m*	29.7	CH_2
13	----	45.2	C
14	----	48.8	C
15	1.30, *m*	35.5	CH_2
16	1.51, 1.82, *m*	31.4	CH_2
17	1.40, *m*	52.2	CH
18	0.90, *s*	18.6	CH_3
19	0.33, 0.59, *m*	20.9	CH_2
20	1.32, *m*	36.0	CH
21	0.98, d (6.2)	18.3	CH_3
22	0.93, 1.38, *m*	33.9	CH_2
23	1.02, *m*	31.5	CH_2
24	----	41.6	C
25	----	150.2	C
26	1.65, *s*	19.6	CH_3
27	4.68, *brs*	109.3	CH_2
28	0.85, *s*	17.9	CH_3
29	0.89, *s*	25.4	CH_3
30	0.87, *s*	15.1	CH_3
31	1.01, d (6.8)	20.1	CH_3
$OCOCH_3$	-----	171.0	C
$OCOCH_3$	2.05, *s*	21.3	CH_3

Solvent: $CDCl_3$

3.2.5 Structure elucidation of lupeol acetate (112)

The UV spectrum of compound **112** showed a terminal absorption (λ_{max} 220.5 nm) indicative of the absence of a conjugated π system. The IR spectrum showed intense absorption bands at 1732 (C=O) and 1640 (C=C) cm^{-1}. The EIMS of compound **112** showed the molecular ion peak at *m/z* 468. This mass was further confirmed by the CIMS that showed a $[M+H]^+$ peak at *m/z* 469. A fragment at *m/z* 453 was due to the loss of a methyl group from the molecular ion. A combination of mass along with ^1H and ^{13}C-NMR spectral data provided the molecular formula, $C_{32}H_{52}O_2$, for this compound.

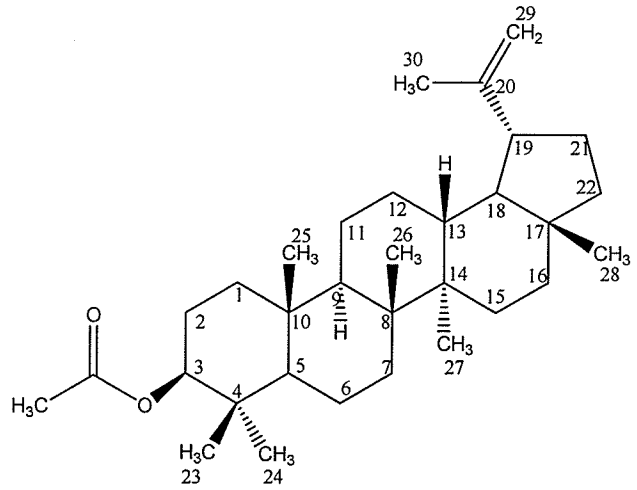

(112)

The ^1H-NMR spectrum ($CDCl_3$, 300 MHz) of **112** showed the resonance of seven tertiary methyl groups at δ 0.77, 0.83, 0.85, 0.87, 0.94, 1.04 and 1.69 due to H_3-25, H_3-23, H_3-24, H_3-26, H_3-27, H_3-28 and H_3-30, respectively. Another three-proton singlet at δ 2.05 was ascribed to the acetyl methyl protons of an ester group, substituted at C-3. Two broad singlets, integrating for one-proton each, resonated at δ 4.57 and 4.68, were assigned to H_2-29. A double doublet, integrating for one proton,

at δ 4.47 (dd, $J_{1,2}$ = 5.3 and $J_{1,3}$ = 10.4 Hz) was ascribed to H-3. Another one-proton multiplet resonated at δ 2.35 was assigned to the H-19.

The COSY-45° spectrum of **112** showed cross peaks between H-3 (δ 4.47) and H_2-2 (δ 1.65 and 0.98). The latter showed cross peaks with H_2-1 (δ 0.95 and 1.71). H-9 (δ 1.39) showed cross peaks with H_2-11 protons (δ 1.27 and 1.40). H_2-11 exhibited cross peaks with H_2-12 (δ 1.08 and 1.67), which in turn displayed a cross peak with H-13 (δ 1.65).

H-19 (δ 2.35) showed COSY interactions with H-18 (δ 1.39) and H_2-21 (δ 1.35 and 1.95), which in turn showed cross peaks with H_2-22 (δ 1.23 and 1.41). H_2-29 (δ 4.57 and 4.68) showed an allylic coupling with H_3-30 (δ 1.69).

The broad-band decoupled ^{13}C-NMR spectrum ($CDCl_3$, 75 MHz) of **112** showed signals for all 32 carbons. The ^{13}C-NMR and DEPT spectral data showed the presence of eight methyl, eleven methylene, six methine, and seven quaternary carbons in this compound. The complete ^{1}H and ^{13}C-NMR assignments are shown in Table **3.4.** The HSQC spectrum was recorded to determine the ^{1}H/^{13}C one-bond shift correlations of all protonated carbons.

The HMBC spectrum of **112** was useful for the chemical shift assignments of the quaternary carbons and to establish the overall structure. H-3 methine proton (δ 4.47) exhibited cross-peaks with C-2 (δ 27.40) and C-4 (δ 38.4) carbons. H_3-24 (δ 0.85) exhibited cross peaks with C-3 (δ 80.9) and C-4 (δ 38.4) while H_3-25 (δ 0.77) showed connectivity with C-5 (δ 55.3) and C-9 (δ 50.3) carbons. H_3-28 (δ 1.04) displayed cross peaks with C-16 (δ 35.5) and C-17 (δ 42.9) carbons. H_2-29 (δ 4.57 and 4.68) exhibited cross peaks with C-30 (δ 18.1) and C-19 (δ 47.9). Important HMBC interactions are shown in the figure **112a**.

The UV, MS, ^{1}H, and ^{13}C-NMR spectral data of **112** matched nicely with those of lupeol acetate, reported in literature[25-29]. These spectral data led to the identification of compound **112** as lupeol acetate. This compound has been previously reported from *Hieracium plumulosum*[25], *Ixeris chinesis*[26], *Pyrus communis*[27] *Maytenus cuzcoina*[28], *Campanula lactiflora*[29]. This is a first report of lupeol acetate from *A. nobilis*.

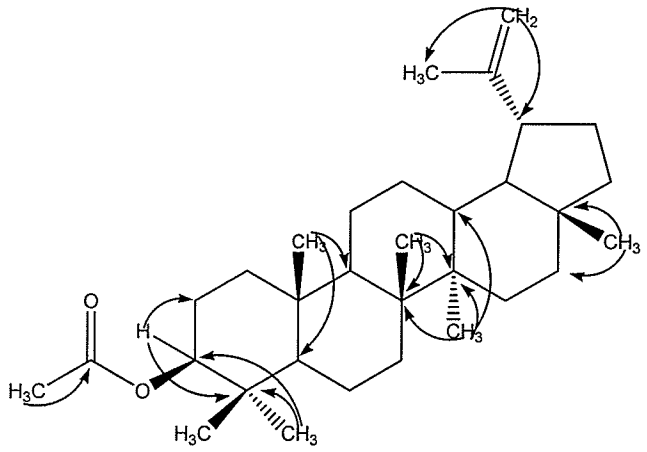

(112a)

Table 3.4 ^{1}H and ^{13}C-NMR data of **112**, recorded at 300 and 75 MHz, respectively.

Carbon No	$\delta^{1}H$-NMR	$\delta^{13}C$-NMR	Multiplicity
1	0.95, 1.71, *m*	38.3	CH_2
2	0.98, 1.65, *m*	27.4	CH_2
3	4.47, *dd,* (5.3,	80.9	CH
4	----	38.4	C
5	0.82, *m*	55.3	CH
6	1.45, 1.49, *m*	19.2	CH_2
7	1.36, 1.36, *m*	34.2	CH_2
8	----	39.8	C
9	1.39, *m*	50.3	CH
10	----	38.0	C
11	1.27, 1.40, *m*	20.9	CH_2
12	1.08, 1.67, *m*	29.8	CH_2
13	1.65, *m*	38.0	CH
14	----	42.7	C
15	1.06, 1.66, *m*	25.0	CH_2
16	1.36, 1.45, *m*	35.5	CH_2
17	----	42.9	C
18	1.39, *m*	48.2	CH
19	2.35, *m*	47.9	CH
20	----	150.9	C
21	1.35, 1.95, *m*	29.8	CH_2
22	1.23, 1.41, *m*	39.9	CH_2
23	0.83, *s*	15.9	CH_3
24	0.85, *s*	27.9	CH_3
25	0.77, *s*	16.1	CH_3
26	0.87, *s*	14.5	CH_3
27	0.94, *s*	16.4	CH_3
28	1.04, *s*	17.9	CH_3
29	4.57, 4.68, *brs*	109.3	CH_2
30	1.69, *s*	18.1	CH_3
$O\underline{CO}CH_3$	----	171.0	C
$OCO\underline{CH_3}$	2.05, *s*	21.3	CH_3

Solvent: $CDCl_3$

3.2.6 Structure elucidation of β-amyrine acetate (113)

The UV spectrum of compound **113** showed the lack of conjugated π system. The IR spectrum of **113** showed intense absorption bands at 1731 (C=O) and 1646 (C=C) cm^{-1}. The EIMS of **113** showed a molecular ion peak at *m/z* 468 while the CIMS showed a $[M+H]^+$ ion peak at *m/z* 469. An ion at *m/z* 453 was due to the loss of a methyl group from the molecular ion. Another fragment at *m/z* 409 showed the loss of an acetate ion (CH_3COO^-) from the molecular ion. A combination of mass, ^1H and ^{13}C-NMR spectral data provided its molecular formula, $C_{32}H_{52}O_2$.

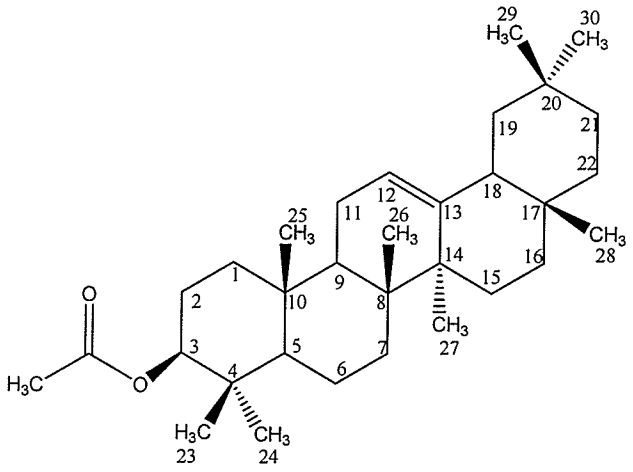

(113)

The ^1H-NMR spectrum ($CDCl_3$, 300 MHz) of **113** showed two singlets at δ 0.87 and 0.97, integrating for six protons each, was due to H_3-23, H_3-25, H_3-29 and H_3-30, respectively. Four three-proton singlets at δ 0.83, 0.88, 1.14 and 1.26, were ascribed to H_3-28, H_3-24, H_3-26 and H_3-27, respectively. The C-3 acetyl methyl protons resonated at δ 2.05. A downfield triplet, integrating for one proton, at δ 5.18 was assigned to H-12. A double doublet, integrating for one proton, resonating at δ 4.45 (dd, $J_{1,2}$ = 4.6 and $J_{1,3}$ = 11.3 Hz) was ascribed to H-3. The ^1H-^1H chemical shift assignments were confirmed from COSY-45° spectrum.

The broad-band ^{13}C-NMR spectrum ($CDCl_3$, 75 MHz) of **113** showed signals for all 32 carbons. The comparison of broad-band ^{13}C-NMR and DEPT spectra revealed the presence of nine methyl, ten methylene, five methine and eight quaternary carbons in compound **113**. The HSQC spectrum was recorded to determine the ^{1}H/^{13}C one-bond shift correlations of all protonated carbons. The complete ^{1}H and ^{13}C-NMR chmical shift assignments are shown in Table **3.5**. Two dimensional NMR spectra (COSY, HSQC, HMBC and NOESY) were used to determine the structural formula of **113**. The MS, ^{1}H and ^{13}C-NMR spectral data of **113** were identical to those of β-amyrine acetate reported in the literature[30-32]. This helped to identify compound **113** as β-amyrine acetate. This compound was previously isolated from *Winchia calophylla*[30-31] and *Koelpinia linearis*[32]. This is the first report about the isolation of β-amyrine acetate from *A. nobilis*.

Table 3.5 ^{1}H and ^{13}C-NMR data of **113**, recorded at 300 and 75 MHz, respectively.

Carbon No.	$\delta^{1}H$-NMR	$\delta^{13}C$-NMR	DEPT Multiplicity
1	1.21, 1.82, *m*	37.6	CH_2
2	1.02, 1.67, *m*	26.1	CH_2
3	4.45, *dd,* (4.6,	80.9	CH
4	----	39.7	C
5	0.86, *m*	55.2	CH
6	1.39, 1.58, *m*	18.2	CH_2
7	1.32, 1.53, *m*	32.5	CH_2
8	----	38.2	C
9	1.71, *m*	47.5	CH
10	----	37.1	C
11	1.61, 1.90, *m*	23.5	CH_2
12	5.18, *t,* (3.4)	121.6	CH
13	----	145.1	C
14	----	41.6	C
15	1.22, 1.89, *m*	29.6	CH_2
16	1.45, 1.96, *m*	31.0	CH_2
17	----	33.3	C
18	2.30, *m*	47.2	CH
19	1.53, 1.85, *m*	46.7	CH_2
20	----	32.4	C
21	1.24, 1.47, *m*	34.6	CH_2
22	1.55, 1.83, *m*	36.8	CH_2
23	0.87, *s*	23.6	CH_3
24	0.88, *s*	28.0	CH_3
25	0.87, *s*	16.6	CH_3
26	1.14, *s*	25.9	CH_3
27	1.26, *s*	26.9	CH_3
28	0.83, *s*	28.3	CH_3
29	0.97, *s*	16.8	CH_3
30	0.97, *s*	15.5	CH_3
$O\underline{CO}CH_3$	-----	171.0	C
$OCO\underline{CH_3}$	2.05, *s*	21.2	CH_3

Solvent: $CDCl_3$

3.2.7 Structure elucidation of 12, 13-dihydromicromeric acid (114)

The EIMS of **114** exhibited molecular ion peak at *m/z* 456. A combination of ^{1}H, ^{13}C-NMR and EIMS spectral data suggested the molecular formula $C_{30}H_{48}O_3$ for **114**. It indicated seven double bond equivalents; five of them were adjusted in pentacyclic triterpene carbon framework and one each, for the olefinic and carboxylic group.

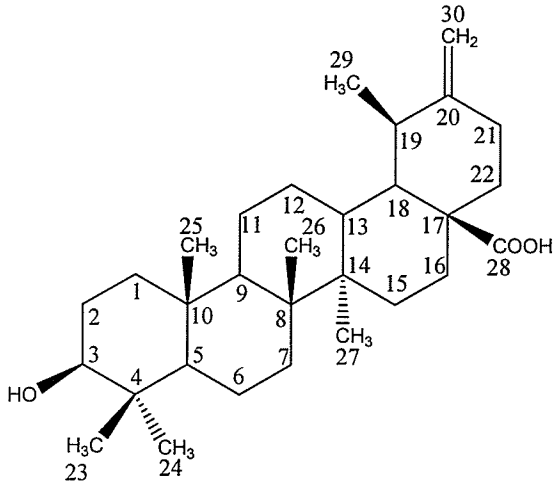

(114)

The ^{1}H-NMR spectrum (DMSO-d_6, 300 MHz) of **114** displayed one broad singlet at δ 0.86, integrating for nine protons was due to H_3-24, H_3-25 and H_3-29, respectively[33]. Three singlets resonating at δ 0.65, 0.76, 0.98, integrating for three protons each, were assigned to H_3-26, H_3-27 and H_3-23, respectively. A one-proton multiplet, resonating at δ 3.36 was ascribed to H-3. Another one-proton multiplet at δ 2.20 was assigned to H-18. Two broad singlets integrating for one proton each, resonating at δ 4.58 and 4.69, were assigned to H_2-30.

The ^{13}C-NMR spectrum (DMSO-d_6, 75 MHz) of **114** showed the presence of thirty carbons. The assignments of the carbon chemical shifts were made by comparison with chemical shift values of ursane-type triterpenes[33-36]. Three downfield signals at

δ 177.2, 150.2 and 109.5 were assigned to C-28, C-20 and C-30, respectively. The complete ^{1}H and ^{13}C-NMR chemical shift assignments of **114** are shown in Table **3.6**. Mass, ^{1}H and ^{13}C-NMR spectral data of **114** were identical to those of 12,13-dihydromicromeric acid, isolated from *Zizyphus valgaris*[33] and *Cyclolepis genistoides*[34]. Based on these spectroscopic data and comparison with literature data[33-36], structure **114** was proposed for this known natural product. This is a first report for the purification of triterpene 12,13-dihydromicromeric acid from *A. nobilis*.

Table 3.6 ^{1}H and ^{13}C-NMR data of **114**, recorded at 300 and 75 MHz, respectively

Carbon No.	$\delta^{1}H$-NMR	$\delta^{13}C$-NMR	Multiplicity
1	1.23, 1.97, *m*	38.4	CH_2
2	1.01, 1.83, *m*	25.0	CH_2
3	3.36 *m*	76.7	CH
4	----	38.2	C
5	1.48, *m*	54.8	CH
6	1.64, 1. 80, *m*	18.9	CH_2
7	1.32, 1.61, *m*	33.8	CH_2
8	----	40.3	C
9	1.42, *m*	48.4	CH
10	----	37.5	C
11	1.56, 1.95, *m*	20.4	CH_2
12	1.23, 1.24, *m*	27.1	CH_2
13	1.12, *m*	41.9	CH
14	----	46.6	C
15	1.26, 1.91, *m*	28.0	CH_2
16	1.51, 1.94, *m*	29.1	CH_2
17	----	49.8	C
18	2.20, *m*	55.3	CH
19	2.41, *d*, (10.3)	39.0	CH
20	----	150.2	C
21	1.34, 2.37, *m*	31.6	CH_2
22	1.75, 1.83, *m*	36.7	CH_2
23	0.98, *s*	30.0	CH_3
24	0.86, *s*	15.9	CH_3
25	0.86, *s*	14.3	CH_3
26	0.65, *s*	15.7	CH_3
27	0.76, *s*	15.8	CH_3
28	----	177.2	C
29	0.86, *brs*	17.9	CH_3
30	4.58, 4.69, *brs*	109.5	CH_2

Solvent: DMSO-d_6

3.2.8 Structure elucidation of artonins E (115)

The UV spectrum of **115** exhibited absorption bands at 222, 266, and 358 nm. The IR spectrum suggested the presence of hydroxyl (3429 cm^{-1}), carbonyl (1655 cm^{-1}) and olefinic (1560 cm^{-1}) functionalities. The EIMS of compound **115** showed molecular ion peak at *m/z* 436 and the CIMS showed $[M+H]^+$ ion peak at *m/z* 437. A fragment at *m/z* 421 was due to the loss of a methyl group from the molecular ion. The EIMS of **115** also showed two significant fragment ions at *m/z* 393 and *m/z* 203 which suggested that a 2,2-dimethylpyrane ring was located in the A ring[37], and a prenyl group at the C-3 position[38]. A combination of MS along with ^1H and ^{13}C-NMR spectral data provided its molecular formula $C_{25}H_{24}O_7$.

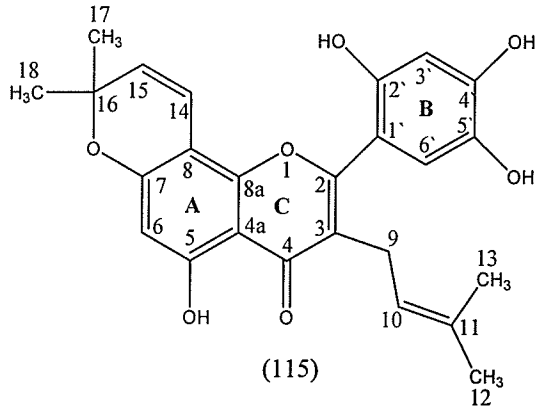

(115)

The ^1H-NMR spectrum (acetone-d_6, 300MHz) (Table **3.7**) displayed a six-proton singlet at δ 1.43 due to H_3-17 and H_3-18. Two singlets resonating at δ 1.46 and 1.57, integrating for three protons each, were assigned to H_3-12 and H_3-13, respectively. A broad doublet resonating at δ 3.15 (brd, J = 7.2 Hz) was assigned to H_2-9. A multiplet resonating at δ 5.11 was assigned to H-10 where as two doublets resonating at δ 5.62 (d, J = 10.0 Hz), and 6.60 (d, J = 10.0 Hz), integrating for one proton each, were assigned to H-15 and H-14, respectively. Three downfield singlets resonating at

δ 6.13, 6.58 and 6.89, integrating for one proton each, were assigned to H-6, H-3` and H-6`, respectively. A singlet at δ 13.25 was assigned to a C-5 hydroxyl group.

In COSY-45° spectrum, H_3-12 (δ 1.46) and H_3-13 (δ 1.57) showed allylic coupling with H-10 (δ 5.11) which was further coupled with H-9 (δ 3.15). The olefinic protons, H-14 (δ 6.60) and H-15 (δ 5.62) showed cross peaks with each other.

The ^{13}C-NMR (acetone-d_6, 75MHz) spectrum of **115** displayed all twenty five signals. The ^{13}C-NMR and DEPT spectra revealed the presence of four methyl, one methylene, six methine and fourteen quaternary carbons in compound **115**. The HSQC spectrum was also recorded to assign the protons to their respective carbon atoms. The complete ^{1}H and ^{13}C-NMR chemical shift assignments of **115** are shown in Table **3.7**.

The HMBC spectrum of **115** was recorded to confirm the substitution of various functional groups. H_3-17 (δ 1.43) showed long-range connectivities with C-16 (δ 78.0) and C-15 (δ 127.6). H_3-12 (δ 1.46) and H_3-13 (δ 1.57) displayed interactions with C-10 (δ 121.5) and C-11 (δ 131.3). H_2-9 (δ 3.15) showed cross peaks with C-4 (δ 181.8), C-3 (δ 119.9) and C-2 (δ 161.6). H-6 (δ 6.13) displayed long-range correlations with C-5 (δ 158.5) and C-7 (δ 160.9). H-15 (δ 5.62) showed HMBC interactions with C-14 (δ 114.2) and C-16 (δ 78.0). The cross peaks between H-3` (δ 6.58) and C-4′ (δ 148.5), C-2′ (δ 148.8) and C-1′ (δ 109.2) were also observed. The methine proton of C-6` (δ 6.89) exhibited cross-peaks with C-5` (δ 138.0), C-4` (δ 148.5) and C-2 (δ 161.5). The observed HMBC interactions in compound **115** are shown in **115a.**

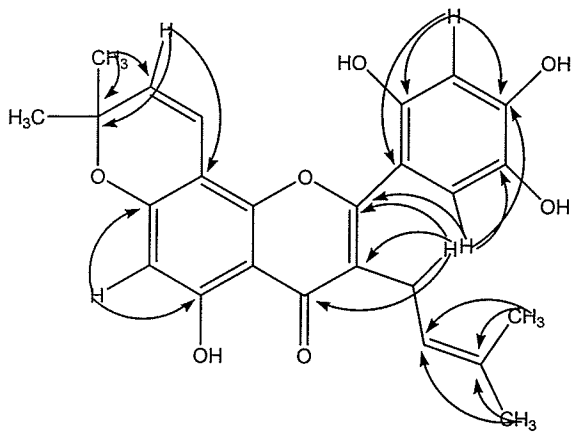

(115a)

The ^{1}H and ^{13}C-NMR spectral data of **115** were similar to those of artonins E reported in the literature[59-63]. Previously artonins E was isolated from *Artocarpus communis* Frost[59], *A. lanceifolius*[60], *A. chama*[61], *A. nobilis*[62] and *A. altilis*[63]. Based on these spectroscopic data structure **115** was proposed for this known natural product.

Table 3.7 ^{1}H and ^{13}C-NMR data of **115**, recorded at 300 and 75 MHz, respectively.

Carbon No.	$\delta^{1}H$-NMR	$\delta^{13}C$-NMR	DEPT Multiplicity
2	----	161.6	C
3	----	119.9	C
4	----	181.8	C
4a	----	103.8	C
5	----	160.9	C
6	6.13, *s*	98.8	CH
7	----	158.5	C
8	----	100.4	C
8a	----	151.7	C
9	3.15, *brd*, (7.2 Hz)	23.7	CH_2
10	5.11, *m*	121.5	CH
11	----	131.3	C
12	1.46, *s*	25.5	CH_3
13	1.57, *s*	17.4	CH_3
14	6.60, *d*, (10.0 Hz)	114.2	CH
15	5.62, *d*, (10.0 Hz)	127.6	CH
16	----	78.0	C
17	1.43, *s*	27.6	CH_3
18	1.43, *s*	27.6	CH_3
1`	----	109.2	C
2`	----	148.8	C
3`	6.58, *s*	104.2	CH
4`	----	148.5	C
5`	----	138.0	C
6`	6.89, *s*	116.1	CH

Solvent: Acetone-d_6

3.2.9 Structure elucidation of artobiloxanthone (116)

The UV spectrum of artobiloxanthone (**116**) displayed maximum absorption bands at 220, 265, and 360 nm. The IR spectrum showed hydroxyl (3320 cm^{-1}), carbonyl (1680 cm^{-1}) and benzene (1530, 1480 cm^{-1}) functionalities. The EIMS of compound **116** showed molecular ion peak at *m/z* 434. An ion at *m/z* 419 was observed due to the loss of a methyl group from the molecular ion. A combination of MS, ^{1}H and ^{13}C-NMR spectral data provided the molecular formula, $C_{25}H_{22}O_7$, for **116**.

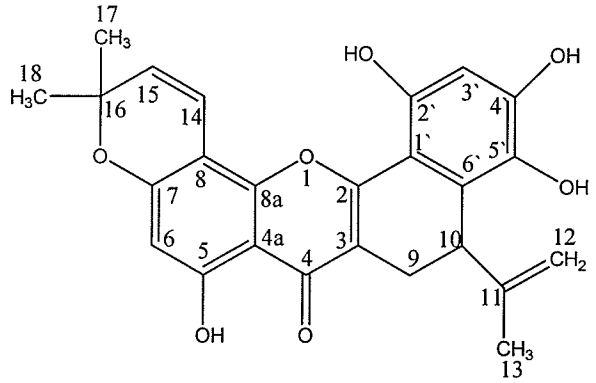

(116)

The ^{1}H-NMR spectrum (acetone-d_6, 300MHz) displayed three singlets resonating at δ 1.43, 1.46 and 1.78, integrating for three protons each, were assigned to H_3-17, H_3-18 and H_3-13, respectively. Two sets of double doublets, resonating at δ 2.45 (dd, J = 16.2, 8.0 Hz) and 3.43 (dd, J = 16.2, 1.8 Hz) were assigned to H_2-9. A broad doublet resonating at δ 3.99 (d, J = 8.0 Hz), was assigned to H-10 whereas two one-proton broad singlets resonating at δ 4.30 and 4.68, were assigned to H_2-12. Two downfield doublets resonated at δ 5.65 (d, J = 10.2 Hz), and 6.95 (d, J = 10.2 Hz), integrating for one proton each, were assigned to H-15 and H-14, respectively. Two downfield singlets resonated at δ 6.11 and 6.59, integrating for one proton each, were assigned to H-6 and H-3` respectively. A singlet at δ 13.35 was assigned to C-5

hydroxyl group. The ^{1}H-NMR chemical shift assignments were further confirmed by performing the COSY-45° experiment.

The ^{13}C-NMR and DEPT experiments revealed the presence of three methyl, two methylene, five methine, and fifteen quaternary carbons. The complete ^{1}H and ^{13}C-NMR chemical shift assignments of **116** are shown in Table **3.8**.

Based on these spectral studies compound **116** was characterized as artobiloxanthone as ^{1}H and ^{13}C-NMR spectral data were matched to those of artobiloxanthone reported in literature[42,44-45]. This compound was previously isolated from *A. lanceifolius*[44] and *A. nobilis*[42,45].

Table 3.8 ^{1}H and ^{13}C-NMR data of **116**, recorded at 300 and 75 MHz, respectively.

Carbon No.	δ^{1}H-NMR	δ^{13}C-NMR	DEPT Multiplicity
2	----	161.3	C
3	----	111.1	C
4	----	180.9	C
4a	----	151.2	C
5	----	101.6	C
6	6.11, *s*	99.4	CH
7	----	162.2	C
8	----	159.1	C
8a	----	106.7	C
9	2.45, *dd*, (16.2, 8.0)	21.9	CH_2
	3.43, *dd*, (16.2, 1.8)		
10	3.99, *d*, (8.0)	37.8	CH
11	----	136.3	C
12	4.30, 4.68, br*s*	111.5	CH_2
13	1.78, *s*	21.6	CH_3
14	6.95, *d*, (10.2)	115.7	CH
15	5.65, *d*, (10.2)	127.5	CH
16	----	78.3	C
17	1.43, *s*	27.8	CH_3
18	1.46, *s*	28.1	CH_3
1`	----	115.7	C
2`	----	151.9	C
3`	6.59, *s*	103.3	CH
4`	----	150.5	C
5`	----	144.9	C
6`	----	129.6	C

Solvent: Acetone-d_6

3.2.10 Biological activities of compounds 109-116

Compounds **109** to **116** were evaluated for anti-AChE activity. Compounds **111-113** and **115-116** were evaluated for anti-GST activity and compounds **115-116** were also tested for antioxidant activity. AChE and GST inhibition data of compounds **109-116** along with antioxidant data of compounds **115-116** are listed in Table **3.9**. AChE inhibition data indicated that all of these compounds were weakly active in this assay as compared to glanthamine, a prescribed drug used to treat AD. In GST inhibition assays, compound **115** and **116** were significantly active than sodium taurocholate, a standard GST inhibitor. Compounds **115** and **116** were also significantly active in antioxidant assays.

Table 3.9 AChE, GST and antioxidant activities (IC_{50} = μM) of compounds **109** to **116**

Compound	AChE ± SEM	GST ± SEM	Antioxidant activity ± SEM
109	195.06 ± 4.29	NE	NE
110	146.14 ± 12.53	NE	NE
111	251.38 ± 24.11	314.27 ± 12.29	NE
112	68.52 ± 2.74	143.92 ± 1.56	NE
113	11.5 ± 2.58	256.83 ± 10.18	NE
114	104.07 ± 8.62	NE	NE
115	32.0 ± 2.09	0.11 ± 0.03	5.26 ± 0.69
116	43.0 ± 7.33	0.97 ± 0.06	14.05 ± 1.04
α-tocopherol	NE	NE	95.8 ± 0.5
qurecetin	NE	NE	17.30 ± 0.20
glanthamine	0.52 ± 0.01 μM	NE	NE
Na-taurocholate	NE	395.0 ± 9.537	NE

SEM = Standard error of mean of three assays

NE = Not evaluated

3.3 Experimental

3.3.1 General experimental conditions

All the general experimental conditions were the same as described in chapter **2,** page 47 except High Performance Liquid Chromatography (HPLC) was carried out for the purification of compounds **111-116** on a *Waters* HPLC system equipped with photodiode array (PDA) detector (*Waters* 2996) using a 5 μm *Zobrax* ODS column (9.4 x 250 mm) and 5 μm C_{18} *Waters* column (4.6 x 150 mm).

3.3.2 Plant material:

The bark of *Artocarpus nobilis* (2.2 kg) was collected from Malwana, Sri Lanka. This plant was identified by Dr. Radhika Samarasekera, Natural Products Development Group, Industrial Technology Institute, Colombo, Sri Lanka, and a voucher specimen was deposited at the Industrial Technology Institute, Sri Lanka.

3.3.3 Extraction and isolation

The air dried bark (2.185 kg) of *A. nobilis* was extracted with 95 % ethanol at room temperature. Filtration and evaporation of the solvent *in vacuo* afforded a gum (68.22 g). This gum was loaded onto a silica gel column, which was eluted with hexane-ethyl acetate (0 - 100 %) and ethyl acetate-methanol (0 - 100 %) to afford 128 fractions and fractions of similar R_f values were pooled together, which yielded fractions F_1-F_{32}. A primary fraction-F_3 (6.43 g) was rechromatographed over a silica gel column using gradient elution with hexane-ethyl acetate (0-100 %) to afford 24 fractions. Compounds **109-116** were purified from fractions F_3, F_5, F_{15} and F_{27} with the help of different chromatographic techniques. A detailed isolation procedure for compounds **109-116** is shown in Schemes **3.1** to **3.3**.

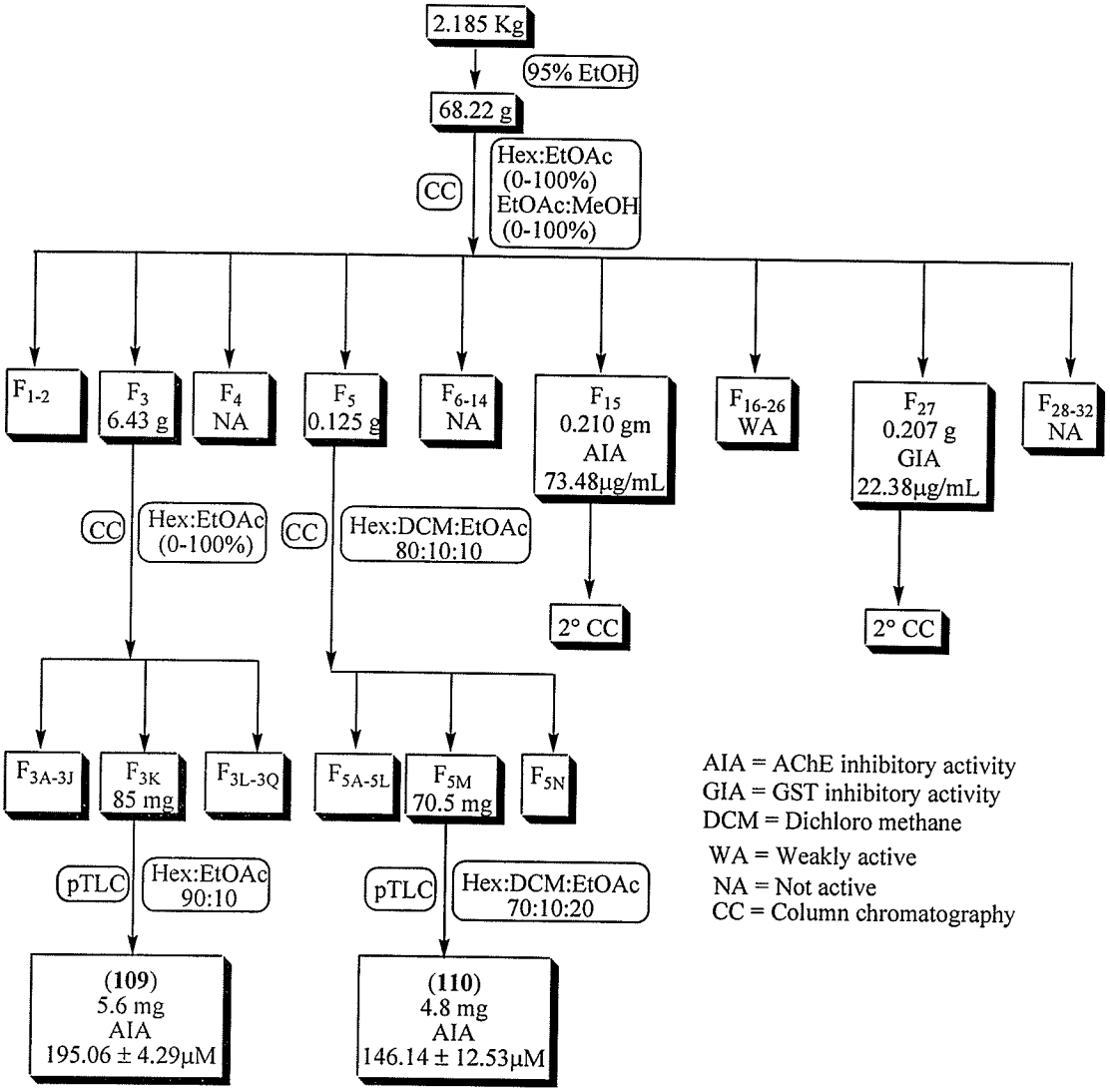

Scheme 3.1 Isolation procedure for compounds **109 -110**

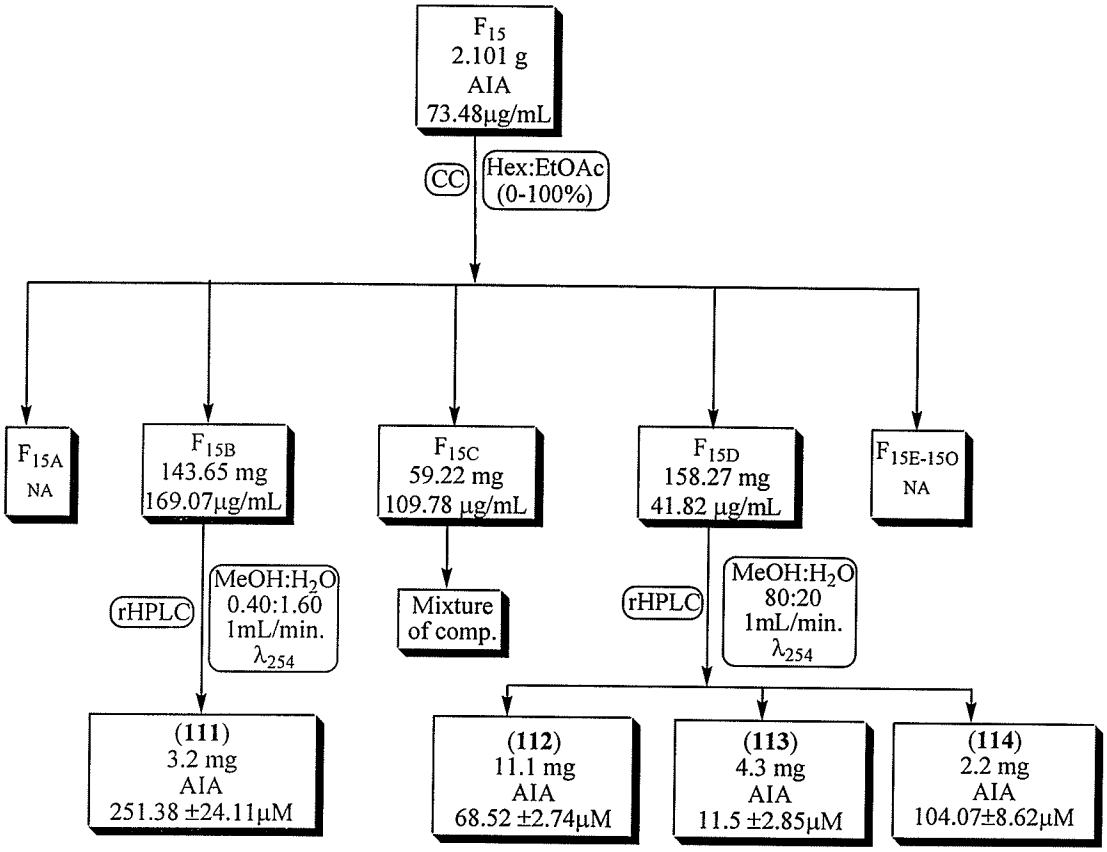

Scheme 3.2 Isolation procedure for compounds **111-114**

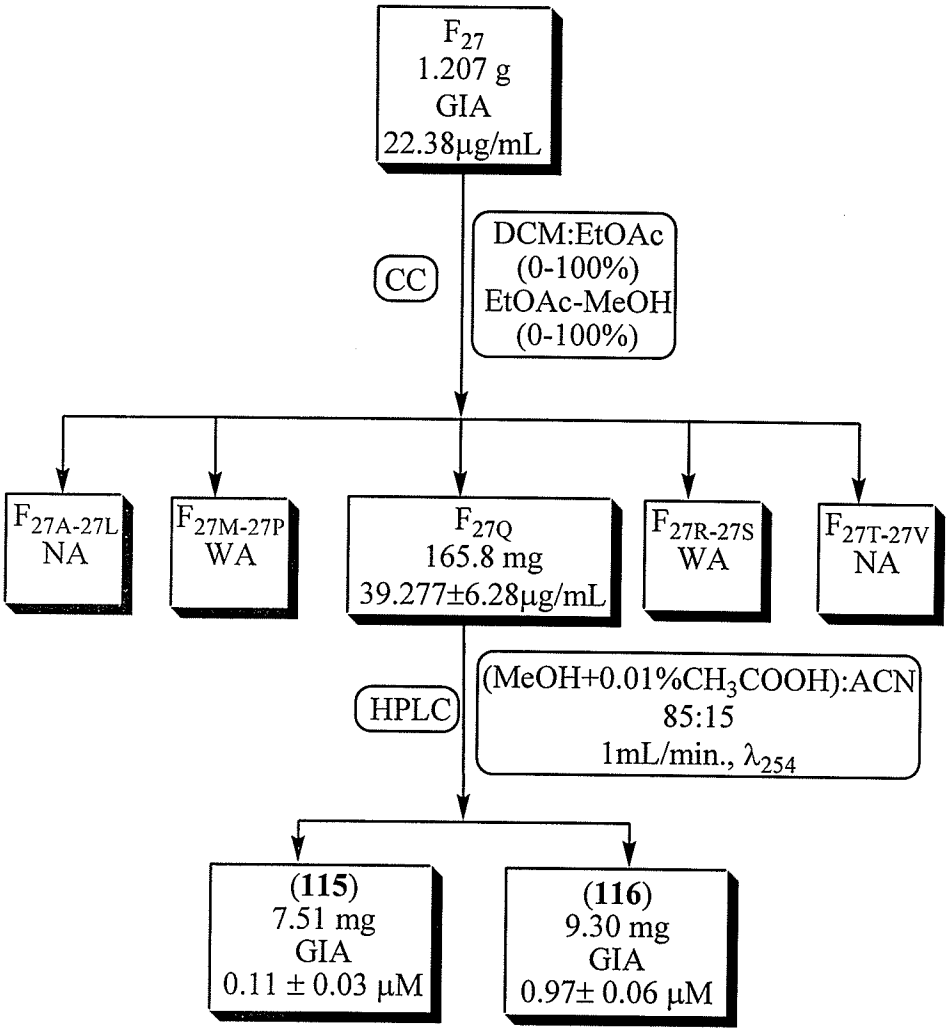

Scheme 3.3 Isolation procedure for compounds **115-116**

3.3.4 Artocarpuate A (109)

Colorless amorphous solid, 5.6 mg, yield 0.00025%, R_f = 0.48 (9:1, hexane-ethyl acetate); $C_{26}H_{38}O_3$; UV λ_{max} (MeOH) = 226.2 nm; IR (solid film) ν_{max} = 1734, 1636 cm^{-1}; for ^1H and ^{13}C-NMR spectral data see Table **3.1**.

3.3.5 Artocarpuate B (110)

Light greenish oily liquid, 4.8 mg, yield 0.00022%, R_f = 0.45 (6:1:2, hexane-dichloromethane-EtOAc); $C_{32}H_{54}O_4$; UV λ_{max} (MeOH) = 204.0 nm; IR (solid film) ν_{max} = 3421, 1733 cm^{-1}; for ^1H and ^{13}C-NMR spectral data see Table **3.2**.

3.3.6 Cyclolaudenyl acetate (111)

Transparent amorphous solid, 3.2 mg, yield 0.00015%, R_t = 7.25 (0.40:1.60, MeOH-H_2O, 1mL/min); $C_{33}H_{54}O_2$; UV λ_{max} (MeOH) = 220.5 nm; IR (solid film) ν_{max} = 1732, 1454 cm^{-1}; for ^1H and ^{13}C-NMR spectral data see Table **3.3**.

3.3.7 Lupeol acetate (112)

White crystalline solid, 11.1mg, yield 0.00051%, R_t = 24.57 (80% MeOH-H_2O, 1mL/min); $C_{32}H_{52}O_2$; UV λ_{max} (MeOH) = 220.5 nm; IR (solid film) ν_{max} = 1732, 1640 cm^{-1}; for ^1H and ^{13}C-NMR spectral data see Table **3.4**.

3.3.8 β-amyrine acetate (113)

Opaque amorphous solid, 4.2 mg, yield 0.00019%, R_t = 25.83 (80% MeOH-H_2O, 1mL/min); $C_{32}H_{52}O_2$; UV λ_{max} (MeOH) = 220.5 nm; IR (solid film) ν_{max} = 1731, 1646 cm^{-1}; for ^1H and ^{13}C-NMR spectral data see Table **3.5**.

3.3.9 12, 13-dihydromicromeric acid (114)

Transparent amorphous solid, 2.2 mg, yield 0.0001%, R_t = 18.79 (80% MeOH-H_2O, 1mL/min); $C_{30}H_{48}O_3$; for ^1H and ^{13}C-NMR spectral data see Table **3.6**.

3.3.10 Artonins E (115)

Orange red amorphous solid, 7.51 mg, yield 0.00034%, R_t = 3.67 (MeOH- mixture of 0.01% CH_3COOH & ACN 85:15, 1mL/min); $C_{25}H_{24}O_7$; UV λ_{max} (MeOH) = 222, 266, and 358 nm; IR (solid film) ν_{max} = 3429, 1655, 1560 cm^{-1}; for ^1H and ^{13}C-NMR spectral data see Table **3.7**.

3.3.11 Artobiloxanthone (116)

Dark orange amorphous solid, 9.13 mg, yield 0.00042%, R_t = 13.51(MeOH- mixture of 0.01% CH_3COOH & ACN 85:15, 1mL/min); $C_{25}H_{22}O_7$; UV λ_{max} (MeOH) = 220, 265, and 360 nm; IR (solid film) ν_{max} = 3320, 1680, 1530, 1480 cm^{-1}; for ^1H and ^{13}C-NMR spectral data see Table **3.8**.

3.4 Enzyme inhibition assays

3.4.1 Glutathione *S*-transferase inhibition assay

The GST assay was conducted as described in chapter **2**, page 50.

3.4.2 Acetylcholinesterease assay

The AChE assay was conducted as described in chapter **2**, page 51.

3.4.3 Antioxidant assay

The antioxidant assay was conducted as described in chapter **2**, page 52.

3.5 References

[1] Mageswaran, R.; Sultanbawa, M. U. S.; Manickavasagar, M. M. *Proc. Ceylon Assoc. Adv. Sci.,* **1970**, 26, 78.

[2] Jarrett, F. M. *Studies in Artocarpus and allied genera, A Revision of Artocarpus subgenus Pseudojaca*, Arnold Arbo, J. **1960**, 4, 73.

[3] Heyne, K. *The useful Indonesian plants*, Research and Development Agency, The Ministry of Forestry, Jakarta, **1987**, 659.

[4] Perry, L. M. *Medicinal plants of East and Southeast Asia: attributed properties and uses.* MIT Press, Cambridge, **1980**, 269.

[5] Wutthithammaweach W. *Encyclopedia of herb; compilation of Thai pharmaceuticals,* 1st Ed., Odion store, Bangkok, **1997**, 123.

[6] Chen, C. C.; Huang, Y. L.; Ou, J. C. *J. Nat. Prod.*, **1993**, 56, 1594.

[7] Charoenlarp, P.; Radomyos, P.; Bunnag, D. *J. Med. Assoc. Thai.,* **1989**, 72, 71.

[8] Han, A. R.; Kang, Y. J.; Windono, T.; Lee, S. K.; Seo, E. K. *J. Nat. Prod.,* **2006,** 69, 719.

[9] Nomura, T.; Hano, Y.; Aida, M. *Heterocycles*, **1998**, 47, 1179.

[10] Widyawaruyanti, A.; Subhan, Kalauni, S. K.; Awale, S.; Nindatu, M.; Zaini, N. C.; Syafruddin, D.; Asih. P. B. S.; Tezuka, Y.; Kadota, S.; *J. Nat. Med.*, **2007**, 61, 410.

[11] Syah, Y. M.; Achmad, S. A.; Ghisalberti, E. L.; Hakim, E. H.; Mujahidin, D. *Fitoterapia*, **2004**, 75, 134.

[12] Nomura, T. *Fortschr. Chem. Org. Naturst.*, **1988**, 53, 87.

[13] Lin, C. N.; Shieh, W. L. *Phytochemistry*, **1992**, 31, 2922.

[14] Rao, A. V. R.; Varadan, M.; Venkataraman, K. *Indian J. Chem.*, **1971**, 9, 7.

[15] Ajizah, A. *Some flavonoids from the heartwood of Artocarpus champeden.* Ph.D. Thesis, Department of Chemistry, Bandung Institute of Technology, **2001**.

[16] Achmad, S. A.; Hakim, E. H.; Juliawaty, L. D.; Makmur, L.; Suyatno, *J. Nat. Prod.*, **1996**, 59, 878.

[17] Pinto, F. C.; Ascenso, J. R.; Ferrieira, M. J. U. *Proc. Phytochem. Soc. Eur.*, **2002**, 47, 73.

[18] Pavanasasivam, G.; Sultanbawa, M. S. *Phytochemistry*, **1973**, 12, 2725.

[19] Clement, J. A. Zhou, B.; Johnson, R. K.; Kingston, D. G. I. *Magn. Reson. Chem.,* **2003**, 41, 644.

[20] Corey, E. J.; Matsuda, S. P. T.; Bartel, B. *Proc. Natl. Acad. Sci. USA.*, **1993**, 90, 11628.

[21] Zhnag, X. T.; Zhnag, L. H.; Ye, W. C.; Zhnag, X. L.; Yin, Z. Q.; Shou, S. X.; Yao, X. S. *Chem. Pharm. Bull.*, **2006**, 54, 107.

[22] Cantillo-Ciau, Z.; Brito-Loeza,W.; Quijano, L. *J. Nat. Prod.*, **2001**, 64, 953.

[23] Ageta, H.; Arai, Y. *Phytochemistry*, **1984**, 23, 2875.

[24] Ageta, H.; Arai, Y. *Chem. Lett.*, **1982**, 6, 881.

[25] Argay, G.; Kalman, A.; Kapor, A.; Ribar, B.; Petrovic, S.; Gorunovic, M. *J. Mol. Stru.*, **1997**, 435, 169.

[26] Shiojima, K.; Suzuki, H.; Kodera, N.; Ageta, H.; Chang, H. C.; Chen, Y. P. *Chem. Pharm. Bull.*, **1996**, 44, 509.

[27] Mehta, B. K.; Verma, M.; Jafri, M.; Neogi, R.; Desiraju, S. *Nat. Prod. Res.*, **2003**, 17, 459.

[28] Nunez, M.; J.; Reyes, C. P.; Jimenez, I. A.; Moujir, L.; Bazzocchi, I. L. *J. Nat. Prod.*, **2005**, 68, 1018.

[29] Yayli, N.; Yildirim, N.; Dogan, N.; Usta, A.; Altun, L. *J. Asian Nat. Prod. Res.*, **2005**, 7, 771.

[30] Wei-Ming, Z.; Yue-Mao, S.; Xin, H.; Gue-Ying, Z.; Xiao-sheng, Y.; Xiao-Jiang, H. *Acta Botanica Sinica*, **2002**, 44, 354.

[31] Seebacher, W.; Simic, N.; Weis, R.; Saf, R.; Kunert, O. *Mag. Res. Chem.*, **2003**, 41, 636.

[32] Koul, S.; Razdan, T. K.; Andotra, C. S.; Kalla, A. K.; Taneja, S. C.; Dhar, K. L. *Phytochemistry*, **2000**, 53, 305.

[33] Hayat, N.; Mukhtar, S. H.; Ansari, M.; Ali, T.; Naveed, Bhat, Z. A. *Pharmaceu. Bio.*, **2005**, 43, 392.

[34] De Heluani, C. S.; De Boggiato, M. V.; Catalan, C. A. N.; Diaz, J. G.; Gedris, T. E.; Herz, W. *Phytochemistry*, **1997**, 45, 801.

[35] Ali, M.; Gupta, J.; Neguerulla, A. V.; Perez-Alenso, *Pharmazie*, **1998**, 53, 718.

[36] Mahato, S. B.; Kundu, A. P. *Phytochemistry*, **1994**, 37, 1517.

[37] Nomura, T.; Fukai, T.; Yamada, S.; Katayanagi, M. *Chem. Pharm. Bull.*, **1978**, 26, 1394.

[38] Takayama, M.; Fukai, T.; Nomura, T. *Mass spectroscopy*, **1989**, 37, 129.

[39] Hano, Y.; Yamagami, Y.; Kobayashi, M.; Isohata, R.; Nomura, T. *Heterocycles*, **1990**, 31, 877.

[40] Shugeng, C. A. O.; Mark, S. B.; Antony, D. B. *Nat. Prod. Res.*, **2002**, 17, 79.

[41] Wang, Y. H.; Hou, A. J.; Chen, L.; Chen, D. F.; Sun, H. D.; Zhao, Q. S.; Kenneth, F.; Bastow, Nakanish, Y.; Wang, X. H.; Lee, K. H. *J. Nat. Prod.*, **2004**, 67, 757.

[42] Jayasinghe, U. L. B.; Samarakoon, T. B.; Kumarihamy, B. M. M.; Hara, N.; Fujimoto, Y. *Fitoterapia*, **2008**, 79, 37.

[43] Boonphong, S.; Baramee, A.; Kittakoop, P.; Puangsombat, P. *Chiang Mai. J. Sci.*, **2007**, 34, 339.

[44] Hakim, E. H.; Asnizar,; Yurnawilis,; Aimi, N.; Kitajima, M.; Takayama, H. *Fitoterapia*, **2002**, 73, 668.

[45] Sultanbawa, M. U. S.; Surendrakumar, S. *Phytochemistry*, **1989**, 28, 599.

CHAPTER 4

Phytochemical studies on *Barleria prionitis*

4.1 Introduction

Barleria prionitis Linn (Acanthaceae) is a medicinal plant found in tropical regions of Asia, Africa and the Pacific[1,2]. This is an annual medium sized shrub of 1-3 feet high and is widely planted as an ornamental and hedge plant[2]. In India and Sri Lanka this plant is known as "Vajradanti or Katsreya" and "Karunta" respectively. In Australia, this plant is considered a weed and is found in North Queensland, Darwin, Lambell's, Lagoon, Berry Springs, the Victoria River District, Katherine, and Mataranka in the Northern Territory[3,4].

The various parts of *B. prionitis* are used as folk pharmaceuticals in Asia[2]. For example, the leaves are used for the treatment of piles and skin irritation[5], joint pains, toothache, in healing of wounds[6]. The aerial parts are used as an anti-arthritic, anti-inflammatory[7] and anti-fertility agent[8] in India. The whole plant extract is also incorporated into herbal cosmetics and hair products to promote skin and scalp health due to its antiseptic properties. In India, Sri Lanka and Thailand, hot aqueous extract of leaves and flowers of *B. prionitis* are taken orally to treat fever. In Thailand, the extract of green shoots of *B. prionitis* is used as a herbal medicine to cure whooping cough and asthma in infants and children[9] which is caused by respiratory syncytial virus (RSV) infection of the lungs[10]. The crude extract of this plant has also been reported to have inhibitory activity against RSV strain A2 (EC_{50} 6.8 μg/mL)[11]. The extracts of *B. prionitis* have been reported to suppress the growth of fungi *Trichophyton mentagrophytes in vitro*[12]. The aqueous bioactive fractions of

B. prionitis have been reported to contain hepatoprotective, anti-stress and immunorestorative properties[13].

Previous phytochemical studies on *B. prionitis* have resulted in the isolation of iridoid glycosides[11,14-16], luteolin glycosides[4] and phenolic glycosides[11]. Gupta and Saxena in 1984 reported lutolin-7-O-β-D-glucoside (**117**)[4] from the roots of *B. prionitis*. Recently Chen *et al.* isolated anti-viral iridoid glycosides (**118-119**) and a phenolic glycoside (**120**) from the aerial parts of this plant[11]. In this study a 3:1 mixture of compounds **119** and **120** displayed antiviral activity against RSV (A2 strain) with an EC_{50} value of 2.46 μg/mL. The coumaroyl moiety in the iridoid nucleus is considered an important structural feature for anti RSV activity. Another member of this genus *B. lupulina*, which has similar kinds of biological activities as stated for *B. prionitis*, is the most chemically investigated plant. Many iridoid glucosides have been reported from this plant, such as: 6-*O*-*trans*-*P*-coumaroyl-8-*O*-acetylshanzhiside methyl ester (**119**), 6-*O*-*cis*-*P*-coumaroyl-8-*O*-acetylshanzhiside methyl ester (**120**), shanzhiside methyl ester (**121**), 6,8-*O*-diacetyl-shanzhiside methyl ester (acetylbarlerin) (**122**)[17], 6-*O*-acetylshanzhiside methyl ester (**123**), ipolamiidoside (**124**)[18], 6-*O*-*P*-methoxy-*cis*-cinnamoyl-8-*O*-acetylshanzhiside methyl ester (**125**), 6-*O*-*P*-methoxy-*trans*-cinnamoyl-8-*O*-acetylshanzhiside methyl ester (**126**)[19].

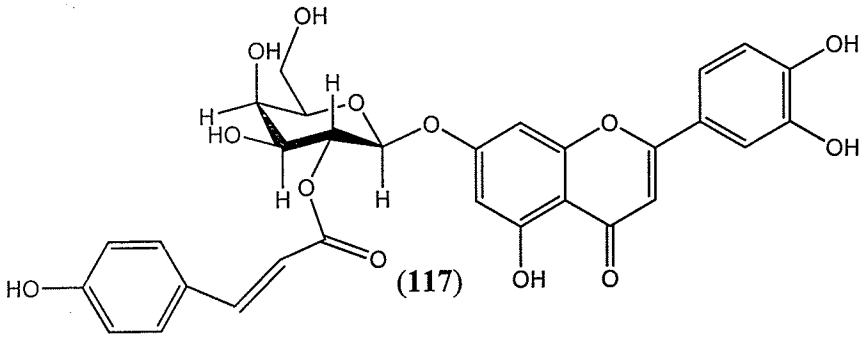

(**117**)

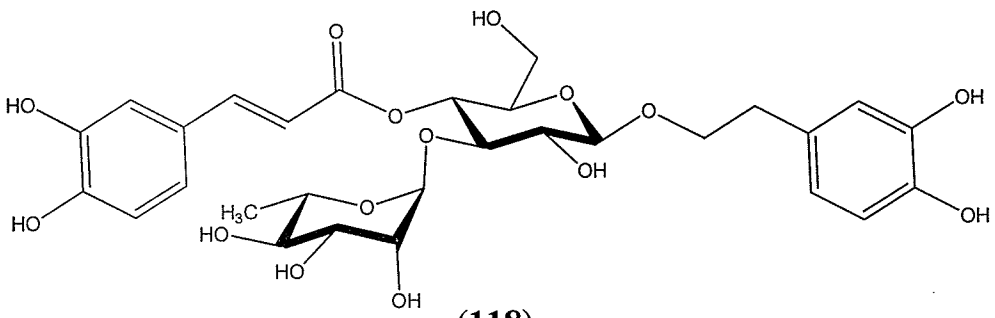

(118)

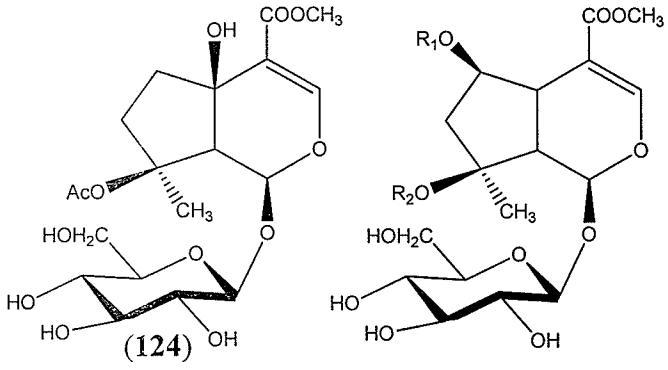

(124)

	R_1	R_2
(119)	*P-cis*-coumaroyl	Ac
(120)	*P-trans*-coumaroyl	Ac
(121)	H	H
(122)	Ac	H
(123)	Ac	Ac
(125)	*P*-OMe-*cis*-cinnamoyl	Ac
(126)	*P*-OMe-*trans*-cinnamoyl	Ac

Based on the medicinal importance and ethnomedical uses, a chemical investigation on the crude ethanolic extract of the aerial parts of *B. prionitis*, collected in Sri Lanka was undertaken and purified compounds were evaluated for acetylcholinesterase (AChE) and glutathione *S*-transferase (GST) inhibitory activities.

4.2 Results and discussion

4.2.1 Isolation of compounds 127-131

The crude ethanolic extract of *B. prionitis* was evaluated for acetylcholinesterase inhibitory activity (IC_{50} = 215.4 ± 22.1 µg/mL). The repeated silica gel column chromatography followed by preparatory TLC of crude ethanolic extract of aerial parts of *B. prionitis* led to the isolation of two known iridoid glycosides, barlerin (8-*O*-acetylshanzhiside methyl ester) (**127**) and shanzhiside methyl ester (**128**); along with two triterpenoids, lupeol (**129**), betulinic acid (**130**); and an aromatic hydrocarbon, pipataline (**131**). All of these compounds were identified with the aid of NMR spectroscopic studies. This chapter describes the isolation of compounds (**127-131**), preparation of three derivatives (**132-134**) of pipataline (**131**) and their biological activities (anti-GST and anti-AChE).

4.2.2 Structure elucidation of barlerin (8-*O*-acetylshanzhiside methyl ester) (127)

Barlerin (**127**) showed UV absorption band at 231.0 nm revealed the presence of α,β-unsaturated carbonyl moiety within molecule[20-21]. The IR spectrum suggested the presence of hydroxyl (3330cm^{-1}), carbonyl (1707cm^{-1}), and olefinic (1576 cm^{-1}) functionalities. A combination of ^{1}H and ^{13}C-NMR data provided the molecular formula, $C_{19}H_{28}O_{12}$ of **127**.

The ^{1}H-NMR spectrum (CD_3OD, 300 MHz) (Table **4.1**) displayed a doublet, resonating at δ 7.45 (d, J = 1.5) was assigned to H-3. A multiplet at δ 4.35 showed HSQC cross peak with a carbon at δ 76.1 and was ascribed to H-6, whereas two double doublets at δ 3.02 (dd, J = 1.5, 9.0), and 2.88 (dd, J = 2.5, 9.0) were assigned to H-5, and H-9, respectively. A doublet at δ 5.90 (d, J = 2.5) and a broad singlet at δ 2.04 were assigned to H-1 and H-7, respectively. These ^{1}H-NMR data indicated that

compound **127** had an iridoid aglycon. The ^{1}H-NMR spectral data also suggested the presence of a glucose moiety as anomeric proton resonated at δ 4.65 (d, J = 8.0). Rest of the glucose protons resonated between δ 3.15 and 3.90. Signals due to acetyl methyl and carboxy methyl protons were also observed at δ 2.02 and 3.74, respectively in the ^{1}H-NMR spectrum. These signals were assigned to the methyl protons of C-8 and C-11 groups, respectively.

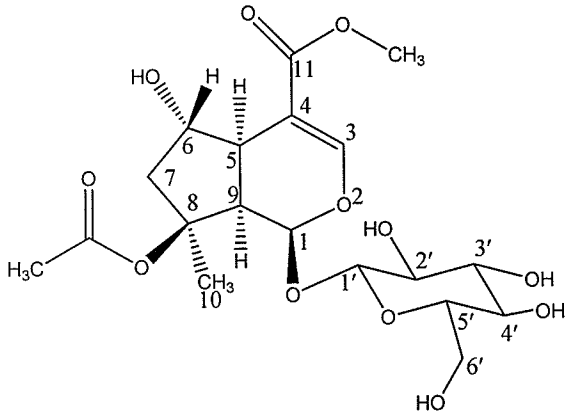

(**127**)

The COSY-45° spectrum showed the presence of two isolated spin systems in compound **127**. The first spin system was traced from H-3 (δ 7.45) which showed allylic coupling with H-5 (δ 3.02). H-1(δ 5.90) showed coupling with H-9 (δ 2.88). The latter proton was further coupled to H-5 (δ 3.02). H-5 in turn exhibited coupling with H-6 (δ 4.35) which showed a cross peak with H-7 (δ 2.04, 2.20). The second spin system was due to a glucose moiety.

The broad-band ^{13}C-NMR (CD_3OD, 75MHz) spectrum of **127** displayed nineteen signals. Multiplicity of each carbon signal was determined by DEPT experiment. The complete ^{1}H and ^{13}C-NMR chemical shift assignments and ^{1}H/^{13}C one-bond shift of **127**, as determined from HSQC are shown in Table **4.1**.

The HMBC spectrum of **127** showed cross-peaks between the olefinic C-3 methine proton (δ 7.45) and C-1 (δ 95.8), C-4 (δ 109.9), C-5 (δ 42.4) and C-11 (δ 173.2). The C-10 methyl protons (δ 1.52) showed HMBC interactions with C-7 (δ 48.3), C-8 (δ 89.9) and C-9 (δ 47.8). The cross peaks between C-1 methine proton (δ 5.90) and C-1′ (δ 100.5) were also observed in the HMBC spectrum indicating the connection of a glucose moiety, while on the other side the C-1 methine proton (δ 5.90) also displayed interactions with C-3 (δ 153.6) and C-9 (δ 47.8). Important HMBC interactions in compound **127** are shown in **127a.**

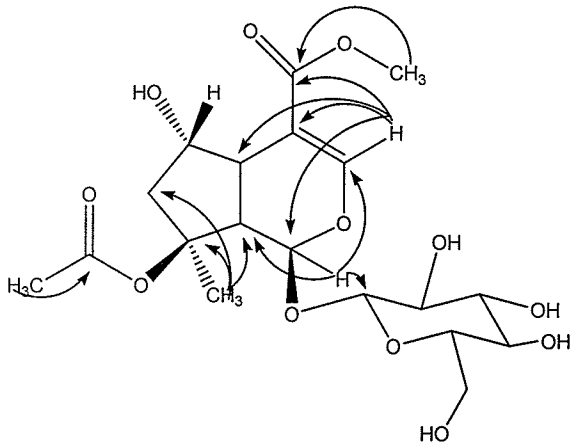

(127a)

The stereochemistry of **127** was determined by the interpretation of 1D NOE and ^{1}H-NMR spectral data of iridoids. Irradiation of H-1 resulted in an enhancement of H-5, H-9 and H_3-10. This indicated a *cis* relationship among these protons. An extensive literature survey indicated that in iridoids H-1 is α-oriented[22]. This *cis* relationship indicated the α-orientation of H-1, H-5 and H-9. This was also supported by the axial-eqatorial coupling constant between H-1/H-9[23].

The ^{1}H and ^{13}C-NMR spectral data of **127** were identical to that of the barlerin, reported in literature[20-20,24-26]. This compound has been isolated from a number of plants including *B. prionitis*[11], *Lamium garganicum*[20], *Arbutus unedo*[21], *Eremostachys*

glabra[24], *Penstemon mucronarus*[25] and *P. secundiflorus*[26] previously. Based on these spectroscopic data structure **127** was proposed for this known natural product.

Table 4.1 ^{1}H and ^{13}C-NMR data of **127**, recorded at 300 and 75 MHz, respectively.

Carbon No.	^{1}H-NMR (δ)	^{13}C-NMR (δ)	DEPT Multiplicity
1	5.90, *d*, (2.5)	95.8	CH
3	7.45, *d*, (1.5)	153.6	CH
4	----	109.9	C
5	3.02, *dd*, (1.5, 9.0)	42.4	CH
6	4.35, *m*	76.1	CH
7	2.04, 2.20, *brs*	48.3	CH_2
8	----	89.9	C
9	2.88, *dd*, (2.5, 9.0)	47.8	CH
10	1.52, *s*	22.4	CH_3
O<u>CO</u>CH_3-8	----	180.4	C
OCO<u>CH_3</u>-8	2.02, *s*	24.3	CH_3
11	----	173.2	C
OMe-11	3.74, *s*	51.9	CH_3
1'	4.65, *d*, (8.0)	100.5	CH
2'	3.15, *dd*, (8.0, 9.0)	74.8	CH
3'	3.35, *t*, (9.0)	78.5	CH
4'	3.20, *t*, (9.0)	71.7	CH
5'	3.30, *m*	78.1	CH
6'	3.90, *dd*, (8.9.0, 4.5)	63.0	CH_2
	3.65, *dd*, (9.0, 4.2)		

Solvent: CD_3OD

4.2.3 Structure elucidation of shanzhiside methyl ester (128)

The UV and IR spectra of **128** were nearly identical to those of **127** which suggested the presence of the same functional groups as those which were in **127**. A combination of mass, ^{1}H and ^{13}C-NMR spectral data of **128** provided its molecular formula $C_{17}H_{26}O_{11}$, which indicated the presence of five degrees of unsaturation in this compound.

The ^{1}H-NMR spectrum (CD_3OD, 300MHz) of **128** was nearly identical to that of compound **127** except that the former showed the resonance of C-10 methyl protons at δ 1.34. This indicated the absence of an acetoxy group. This was further confirmed by the absence of acetyl methyl protons in the ^{1}H-NMR spectrum of **128**. A detailed analysis of ^{1}H-^{1}H COSY-45° spectrum of **128** revealed the presence of identical spin systems as those were observed in **127**.

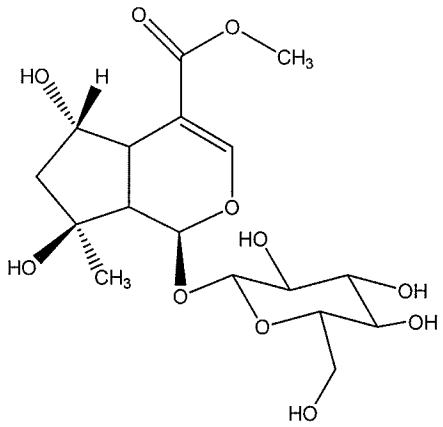

(**128**)

The ^{13}C-NMR (CD_3OD, 75MHz) spectrum of compound **128** showed the resonance of all seventeen carbons and exhibited nearly identical chemical shift values for all carbons as those of carbons in **127**. Multiplicity of each carbon signal was determined

by DEPT experiment. The complete ^{1}H and ^{13}C-NMR chemical shift assignments of **128** are shown in Table **4.2.**

The ^{1}H and ^{13}C-NMR spectral data of **128** were identical to those of shanzhiside methyl ester as reported in the literature[20-21,24-26]. On the basis of the above spectral data and comparison of this spectral data with reported literature[20-21,24-26], the structure of compound **128** was identified as shanzhiside methyl ester. This compound was previously isolated from *Lamium garganicum* subspeci. *Laevigatum*[20], *Arbutus Unedo*[21], *Eremostachys glabra*[24], *Penstemon Mucronarus*[25], *P. Secundiflorus*[26] and *B. prionitis*[27].

Table 4.2 ^{1}H and ^{13}C-NMR data of **128**, recorded at 300 and 75 MHz, respectively.

Carbon No.	^{1}H-NMR (δ)	^{13}C-NMR (δ)	DEPT Multiplicity
1	5.60, *d*, (2.6)	95.4	CH
3	7.41, *brs*	153.4	CH
4	----	112.0	C
5	3.0, *dd*, (3.3, 10.2)	42.0	CH
6	4.1, *m*	78.9	CH
7	1.85,2.01, *dd*, (2.3, 10.1)	48.7	CH_2
8	----	79.6	C
9	2.60, *dd*, (2.6, 10.2)	52.4	CH
10	1.34, *s*	25.2	CH_3
11	----	170.3	C
$COO\underline{CH_3}$	3.74, *s*	52.3	CH_3
1'	4.65, *d*, (7.9)	100.4	CH
2'	3.18, *dd*, (7.9, 9.0)	74.4	CH
3'	3.35, *t*, (9.0)	78.0	CH
4'	3.20, *t*, (9.0)	72.2	CH
5'	3.34, *m*	78.5	CH
6'	3.90, *dd*, (10.8, 4.5)	63.4	CH_2
	3.65, *dd*, (10.8, 4.2)		

Solvent: CD_3OD

4.2.4 Structure elucidation of lupeol (Lup-20(29)-ene-3β-ol) (129)

The UV, IR, ^{1}H and ^{13}C-NMR spectral data of **129** was nearly identical to that of compound **112** with the exception of C-3 signal in ^{1}H and ^{13}C-NMR spectral data. H-3 resonated at δ 3.20 (dd, $J_{1,2}$ = 5.4 and $J_{1,3}$ = 10.5 Hz) and was found to be coupled with C-3 (δ 79.0) in HSQC spectrum. The ^{1}H and ^{13}C-NMR spectra of **129** did not show the resonance of acetyl group.

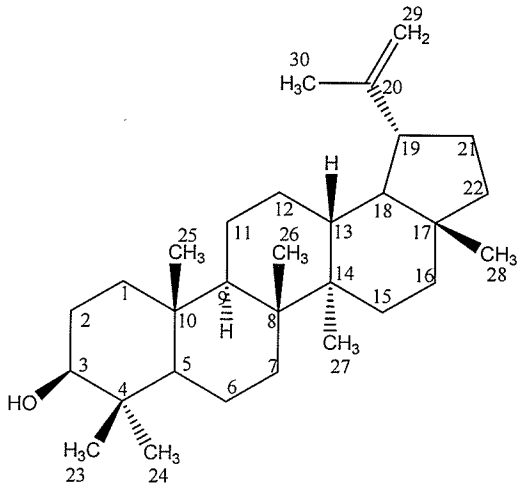

(**129**)

The EIMS of **129** showed the molecular ion peak at *m/z* 426. All of these spectral data indicated that compound **129** was a C-3 hydroxy derivative of **112**. These spectral studies led us to characterize compound **129** as lupeol, as the UV, IR, ^{1}H, ^{13}C and MS spectral data of **129** were consistent with those of lupeol as reported in the literature[28-32]. Complete ^{1}H and ^{13}C-NMR chemical shift assignments of **129** are shown in Table **4.3**. This compound was isolated for the first time from this plant.

Table 4.3 ^{1}H and ^{13}C-NMR data of **129,** recorded at 300 and 75MHz, respectively.

Carbon No.	$\delta^{1}H$-NMR	$\delta^{13}C$-NMR	DEPT Multiplicity
1	1.01, 1.65, *m*	38.6	CH_2
2	1.62, 1.62, *m*	27.3	CH_2
3	3.20, *dd*, (5.4, 10.5)	79.0	CH
4	----	38.8	C
5	0.80, *m*	55.2	CH
6	1.48, 1.49, *m*	18.3	CH_2
7	1.38, 1.38, *m*	34.2	CH_2
8	----	40.8	C
9	1.35, *m*	50.4	CH
10	----	37.1	C
11	1.30, 1.40, *m*	20.9	CH_2
12	1.08, 1.67, *m*	29.8	CH_2
13	1.66, *m*	38.0	CH
14	----	42.8	C
15	1.0, 1.68, *m*	25.1	CH_2
16	1.36, 1.45, *m*	35.5	CH_2
17	----	42.9	C
18	1.37, *m*	48.2	CH
19	2.30, *m*	47.9	CH
20	----	150.9	C
21	1.32, 1.92, *m*	29.6	CH_2
22	1.19, 1.37, *m*	39.9	CH_2
23	0.75, *s*	15.9	CH_3
24	0.77, *s*	27.9	CH_3
25	0.82, *s*	16.1	CH_3
26	0.94, *s*	14.5	CH_3
27	0.96, *s*	15.3	CH_3
28	1.02, *s*	17.9	CH_3
29	4.52, 4.68, *brs*	109.3	CH_2
30	1.68, *s*	19.2	CH_3

Solvent: $CDCl_3$

4.2.5 Structure elucidation of betulinic acid (130)

The UV spectrum of **130** was identical to that of **129**. The EIMS of **130** showed a molecular ion peak at *m/z* 456. Another ion at *m/z* 439 showed the loss of a hydroxyl group from the molecular ion indicating the presence of carboxylic acid functionality.

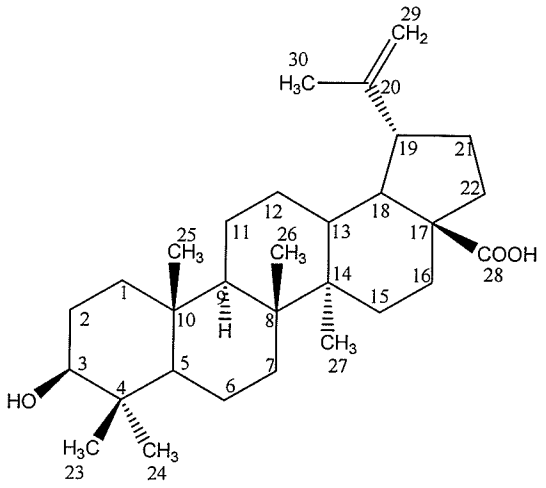

(130)

The ^{1}H and ^{13}C-NMR spectra of **130** were distinctly similar to those of compound **129** except that these spectral data did not show the resonance of C-28 methyl group. This signal was resonated downfield at δ 178.5. A combination of ^{13}C-NMR and IR spectral data indicated the presence of a carboxylic acid group at C-17. The EIMS, ^{1}H and ^{13}C-NMR spectral data of **130** matched nicely with those of reported in literature[33]. Complete ^{1}H and ^{13}C-NMR spectral data of **130** are shown in Table **4.4**. These spectral studies led us to identify compound **130** as betulinic acid.

Table 4.4 ^{1}H and ^{13}C-NMR data of **130**, recorded at 300 and 75 MHz, respectively.

Carbon No.	$\delta^{1}H$-NMR	$\delta^{13}C$-NMR	DEPT Multiplicity
1	1.0, 1.67, *m*	38.6	CH_2
2	1.64, 1.64, *m*	27.4	CH_2
3	3.20, *dd*, (5.6, 10.7)	79.0	CH
4	----	38.8	C
5	0.85, *m*	55.2	CH
6	1.46, 1.53, *m*	18.3	CH_2
7	1.37, 1.37, *m*	34.2	CH_2
8	----	39.9	C
9	1.32, *m*	50.4	CH
10	----	35.5	C
11	1.33, 1.50, *m*	39.9	CH_2
12	1.03, 1.57, *m*	27.9	CH_2
13	1.68, *m*	38.0	CH
14	----	42.9	C
15	1.02, 1.68, *m*	25.1	CH_2
16	1.31, 1.48, *m*	31.9	CH_2
17	----	42.8	C
18	1.34, *m*	48.2	CH
19	2.38, *m*	47.9	CH
20	----	150.9	C
21	1.30, 1.95, *m*	29.6	CH_2
22	1.20, 1.39 *m*	40.8	CH_2
23	0.75, *s*	16.1	CH_3
24	0.79, *s*	27.9	CH_3
25	0.95 *s*	17.9	CH_3
26	0.97, *s*	19.2	CH_3
27	1.09, *s*	20.9	CH_3
28	----	178.5	C
29	4.52, 4.70, *brs*	109.3	CH_2
30	1.69, *s*	19.6	CH_3

Solvent: $CDCl_3$

4.2.6 Structure elucidation of pipataline (131)

The IR spectrum of **131** showed an intense absorption band at 1502 (C=C) cm^{-1}, whereas the EIMS of **131** showed a molecular ion peak at *m/z* 288, which was further confirmed by CIMS that showed the $[M+H]^+$ peak at *m/z* 289. A combination of MS, ^1H and ^{13}C-NMR spectral data of **131** provided its molecular formula, $C_{19}H_{28}O_2$.

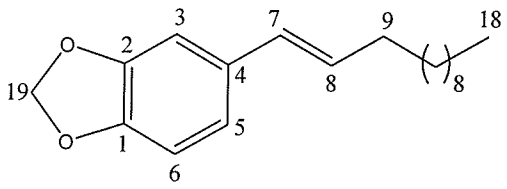

(131)

The ^1H-NMR spectrum ($CDCl_3$, 300 MHz) of **131** showed the presence of two signals at δ 6.25 (d, J = 16.0 Hz) and 6.07 (dt, J = 16.0, 6.8, 3.0 Hz) assigned to H-7 and H-8, respectively. A singlet observed at δ 6.89 was due to H-3 whereas two doublets at δ 6.74 (d, J =1.7 Hz) and δ 6.75 (d, J =1.7 Hz) were assigned to H-5 and H-6, respectively. A downfield broad singlet resonating at δ 5.93 was due to the methylene dioxy protons whereas a multiplet at δ 2.17 was ascribed to the allylic H_2-9. H_2-10 to H_2-17 were observed at δ 1.34 whereas H_3-18 resonated as a triplet at δ 0.88 (t, J = 6.5 Hz).

The COSY-45° spectrum of **131** showed a cross peak between H-5 (δ 6.74) and H-6 (δ 6.75) whereas H-5 in turn showed *meta*-coupling with H-3 (δ 6.89). An olefinic H-7 (δ 6.25) displayed cross peaks with H-8 (δ 6.07) which in turn showed vicinal coupling with allylic H_2-9 (δ 2.17).

The broad-band ^{13}C-NMR spectrum ($CDCl_3$, 75 MHz) of **131** showed the resonance of all nineteen carbons. A combination of broad-band ^{13}C-NMR and DEPT spectra indicated the presence of one methyl, ten methylene, five methine, and three

quaternary carbons in **131**. The complete ^{1}H and ^{13}C-NMR chemical shift assignments of the molecule **131** are presented in Table **4.5**.

The HSQC and HMBC spectra of **131** were recorded in order to determine the structural formula. The ^{1}H and ^{13}C-NMR spectral data were found to be similar to those of pipataline reported in the literature[34]. This led us to identify compound **131** as pipataline which was previously isolated from *piper peepuloides*[34].

Table 4.5 ^{1}H and ^{13}C-NMR data of **131**, recorded at 300 and 75 MHz, respectively.

Carbon No.	$\delta^{1}H$-NMR	$\delta^{13}C$-NMR	DEPT Multiplicity
1	----	147.8	C
2	----	146.4	C
3	6.89, *s*	124.2	CH
4	----	132.4	C
5	6.74, *d*, (1.7)	120.1	CH
6	6.75, *d*, (1.7)	105.3	CH
7	6.25, *d*, (16.0)	129.5	CH
8	6.07, *dt*, (16.0,6.8,3.0)	129.1	CH
9	2.17, *m*	33.1	CH_2
10	(H_{10} to H_{17}) = 1.34, *s*	32.9	CH_2
11		31.8	CH_2
12		29.1	CH_2
13		29.5	CH_2
14		29.5	CH_2
15		29.4	CH_2
16		29.2	CH_2
17		22.6	CH_2
18	0.88, *t*, (6.5)	14.1	CH_3
19	5.93, *s*	100.8	CH_2

Solvent: $CDCl_3$

4.2.7 Derivatization of pipataline

Compound **131** was isolated in bulk quantity and exhibited moderate AChE and GST inhibitory activities. In order to determine the role of the double bond Δ^{7-8} of this compound in the aforementioned bioactivities, three derivatives (**132-134**) were prepared. Details of synthesis of **132-134** and their spectroscopic data are discussed in experimental section (page 121-123). The effect of different constituents on C-7 and C-8 of **131** and role of unsaturation for AChE and GST inhibitory activity is discussed in sections **4.2.11** of this chapter.

4.2.7.1 7, 8-Epoxypipataline (132)

The oxidation of pipataline (**131**) with *m*-chloroperbenzoic acid resulted epoxide[35] (**132**). The EIMS of **132** showed the molecular ion peak at *m/z* 304 while the parent compound (**131**) had a molecular ion peak at *m/z* 288 which clearly demonstrated the difference of oxygen mass (**132**) with the formation of epoxide.

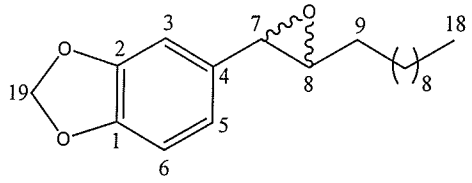

(**132**)

The ^{1}H-NMR spectrum of **132** was identical to that of **131** except the up-field resonance of C-7 and C-8 at δ 3.37 (d, J = 2.0 Hz, H-7) and 2.88 (ddd, J = 8.4, 2.4, 2.0 Hz, H-8), respectively. The ^{13}C-NMR spectrum ($CDCl_3$, 50 MHz) of **132** showed the resonances of C-7 and C-8 at δ 63.0 and 58.6, respectively. These spectroscopic studies helped to identify compound (**132**) as 7, 8-epoxypipataline.

4.2.7.2 7-Amino-8-hydroxypipataline (133)

Compound **133** was synthesized by reacting compound **132** with a 28% solution of NH_3 using a household microwave[35]. In this case only one product was observed due to the regioselective nucleophilic attack at benzylic carbon (C/7).

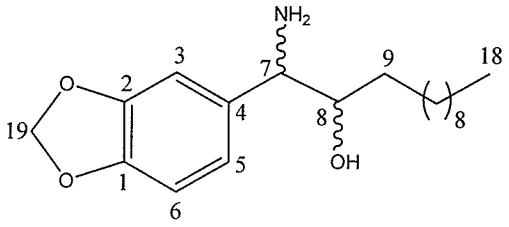

(**133**)

The formation of compound **133** was confirmed by recording the mass, ^1H and ^{13}C-NMR spectra. The EIMS of **133** exhibited the molecular ion peak at *m/z* 321. The ^1H-NMR spectrum of compound **133** showed the resonances of H-7 and H-8 at δ 3.70 (d, J = 2.3 Hz) and δ 2.87 (dt, J = 9.7, 3.2, 2.3 Hz) respectively. An exchangeable OH proton appeared at δ 5.50. The ^{13}C-NMR spectrum ($CDCl_3$, 50 MHz) of **133** showed the resonances of C-7 and C-8 at δ 60.4 and 75.7 respectively. These spectroscopic studies aided the characterization of compound (**133**) as 7-amino-8-hydroxypipataline.

4.2.7.3 7, 8-Dibromopipataline (134)

Bromination of pipataline (**131**) was carried out with bromine that furnished 7,8-dibromoypipataline (**134**) as a brown solid[36]. The EIMS of **134** exhibited the M^+ at *m/z* 448 and M^++2 at *m/z* 450. The isotopic ion peaks resulting from the loss of one bromine atom was observed at *m/z* 367 and 369 while the loss of both bromine atoms was observed at *m/z* 286 and 288 in the EIMS of **134**. The molecular ion peak was further confirmed by recording the CIMS. This type of double ion peak pattern confirmed the formation of brominated product.

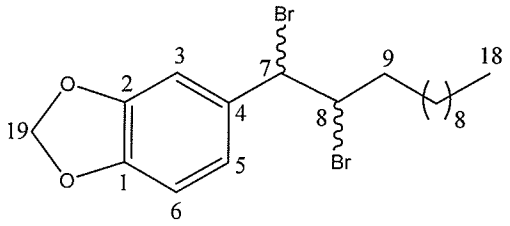

(**134**)

The ^{1}H-NMR spectrum of compound **134** was similar to that of compound **131** except the resonance of C-7/C-8. The ^{1}H-NMR spectrum of compound **134** showed H-7 at δ 5.58 (d, J = 7.0 Hz) and H-8 at δ 4.39 (dt, J = 7.0, 5.4, 3.4Hz), respectively. The^{13}C-NMR spectrum ($CDCl_3$, 50 MHz) of **134** showed the resonances of C-7 and C-8 at δ 57.4 and 55.3 respectively. These spectroscopic studies helped to identify compound **134** as 7,8-dibromopipataline.

4.2.8 Enzyme inhibitory activities of compounds 127-134

All of the purified natural constituents of *B. Prionitis* and derivatives were evaluated in AChE and GST inhibition assays.

4.2.8.1 AChE inhibitory activity of compounds 127-134

The compounds (**127-134**) exhibited moderate AChE inhibitory activity. The IC_{50} values of these compounds are listed in Table **4.6**. Pipataline (**131**) exhibited anti-AChE activity with an IC_{50} value of 135.09 μM. Pipataline (**131**) was isolated in enough quantity to prepare its three derivatives in order to study role of double bond Δ^{7-8} in the side chain. To achieve this goal, its three derivatives (**132-134**) were prepared. Compounds (**132-134**) were also evaluated for anti-AChE activity and it was discovered that the AChE inhibitory activity of **131** was increased by the introduction of amino functionality at C-7.

4.2.8.2 GST inhibitory activity of compounds 127-134

Compounds **127-134** exhibited moderate to weak GST inhibitory activity as listed in Table **4.6**. Pipataline (**131**) showed better bioactivity compared to compounds **127-130** and **132-134**.

Table 4.6 AChE and GST inhibitory activities (IC_{50} = μM) of compounds **127** to **134**

Compounds	**AChE ± SEM**	**GST ± SEM**
8-*O*-acetylshanzhiside methyl ester (**127**)	211.40 ± 11.47	107.71 ± 2.511
Shanzhiside methyl ester (**128**)	145.50 ± 5.33	85.32 ± 7.011
lupeol (**129**)	89.97 ± 0.121	60.00 ± 0.270
Betulinic acid (**130**)	318.59 ± 5.33	NA
pipataline (**131**)	135.09 ± 0.501	57.0 ± 0.370
7,8-epoxypipataline (**132**)	164.00 ± 0.112	86.9 ± 0.215
7-amino-8-hydroxy pipataline (**133**)	36.75 ± 0.272	53.2 ± 0.225
7,8-dibromopipataline (**134**)	208.0 ± 0.372	90.4 ± 0.470
Galanthamine	0.5 ± 0.011	----------
Sodium taurocholate	----------	395.0 ± 9.537

SEM = Standard error of mean of three assays

NA = No activity at 102.9 μg/mL

4.3 Experimental

4.3.1 General experimental conditions

General experimental conditions for this part of research were same as those described in chapter 2, page 47.

4.3.2 Plant material

The aerial parts of *B. prionitis Linn* were collected from Gampaha, Western province of Sri Lanka in September 2004. Dr. Radhika Samarasakera identified this plant, and a voucher specimen was deposited in the herbarium of ITI, Colombo, Sri Lanka.

4.3.3 Extraction and isolation

The air dried ground aerial parts of *B. Prionitis* (1.25 Kg) were macerated in 95% ethanol (5.7 L) for 72 hours. The extract was filtered and evaporated *in vacuo* to afford 42.5 g. The crude extract showed acetylcholinestrase inhibitory activity with an IC_{50} value of 215.4 ± 22.105 μg/mL. The extract was fractionated by column chromatography over silica gel (200-400 mesh) using hexane-ethyl acetate (0-100%) and ethyl acetate-methanol (0-100%) which yielded 152 fractions which were pooled on the basis of similarity in R_f values on analytical TLC. All of the fractions (F_1-F_{41}) obtained were evaluated for acetylcholinestrase inhibitory activity. The fractions F_6, F_8, F_{11}, F_{12}, F_{13}, F_{14}, F_{22}, F_{23}, F_{24} and F_{34} displayed AChE inhibitory activity with IC_{50} value of 195.5, 133.47, 371.2, 271.93, 312.9, 149.79, 215.7, 313.3, 251.11 and 327.51 μg/mL, respectively. These bioactive fractions were subjected to various chromatographic techniques as outlined in Schemes **4.1-4.3**. A bioactive fraction, F_6, afforded compound **129** (transparent crystalline solid, 5.2 mg, 0.00042% yield, R_f 0.67 in 75:25 hexane-ethyl acetate) by column chromatography and followed by peparatory TLC. Another bioactive fraction F_8 yielded compound **130** (white gummy

solid, 7.3 mg, 0.00058% yield, R_f 0.5 in 75:25 hexane ethylacetate) on column chromatography followed by pTLC. The bioactive fraction F_{14} (0.302 g) obtained on elution of primary silica gel column with hexane-ethyl acetate (60:40) yielded compound **131** (white amorphous solid, 15.1 mg, 0.0012% yield, R_f 0.7 in 60:40 hexane-ethylacetate) by repeated column chromatography and preparatory thin layer chromatography. The bioactive fraction F_{22} (1.613 g) obtained on elution of primary silica gel column was again subjected to silica gel column chromatography using $CHCl_3$-methanol (0-100%) yielded another fraction F_{22M} (172.2 mg) which was again chromatographed on silica gel column by using CH_2Cl_2-methanol (0-100%) to afford another fraction F_{22M7}. The fraction F_{22M7} was subjected to pTLC and developed in $CHCl_3$-Methanol (85:15) seven times in the same solvent to afford two compounds **127** (white amorphous solid, 5.1 mg, 0.00041% yield, R_f 0.21) and **128** (white amorphous solid, 3.7 mg, 0.00029% yield, R_f 0.53).

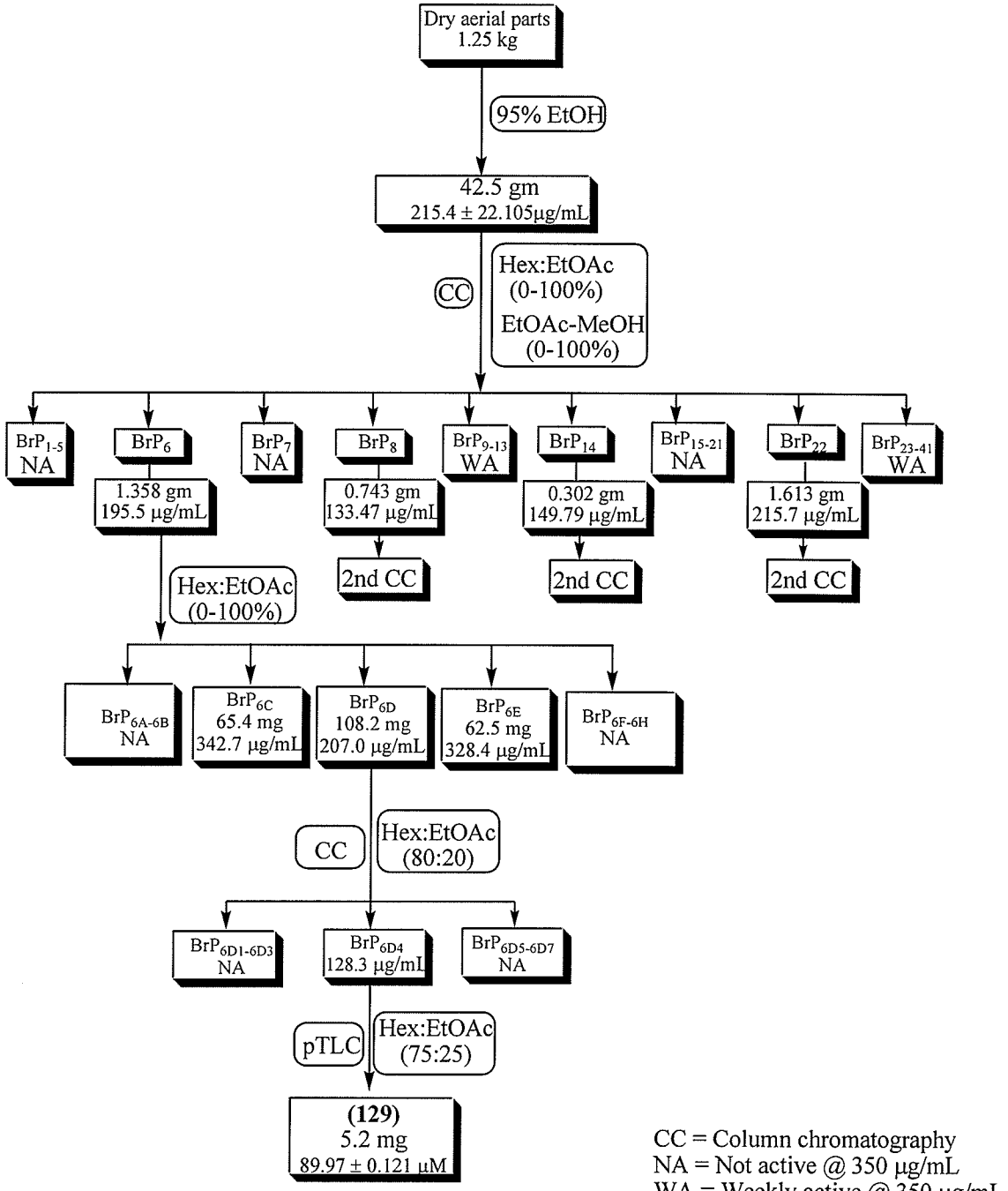

Scheme 4.1 Isolation procedure for compound **129**

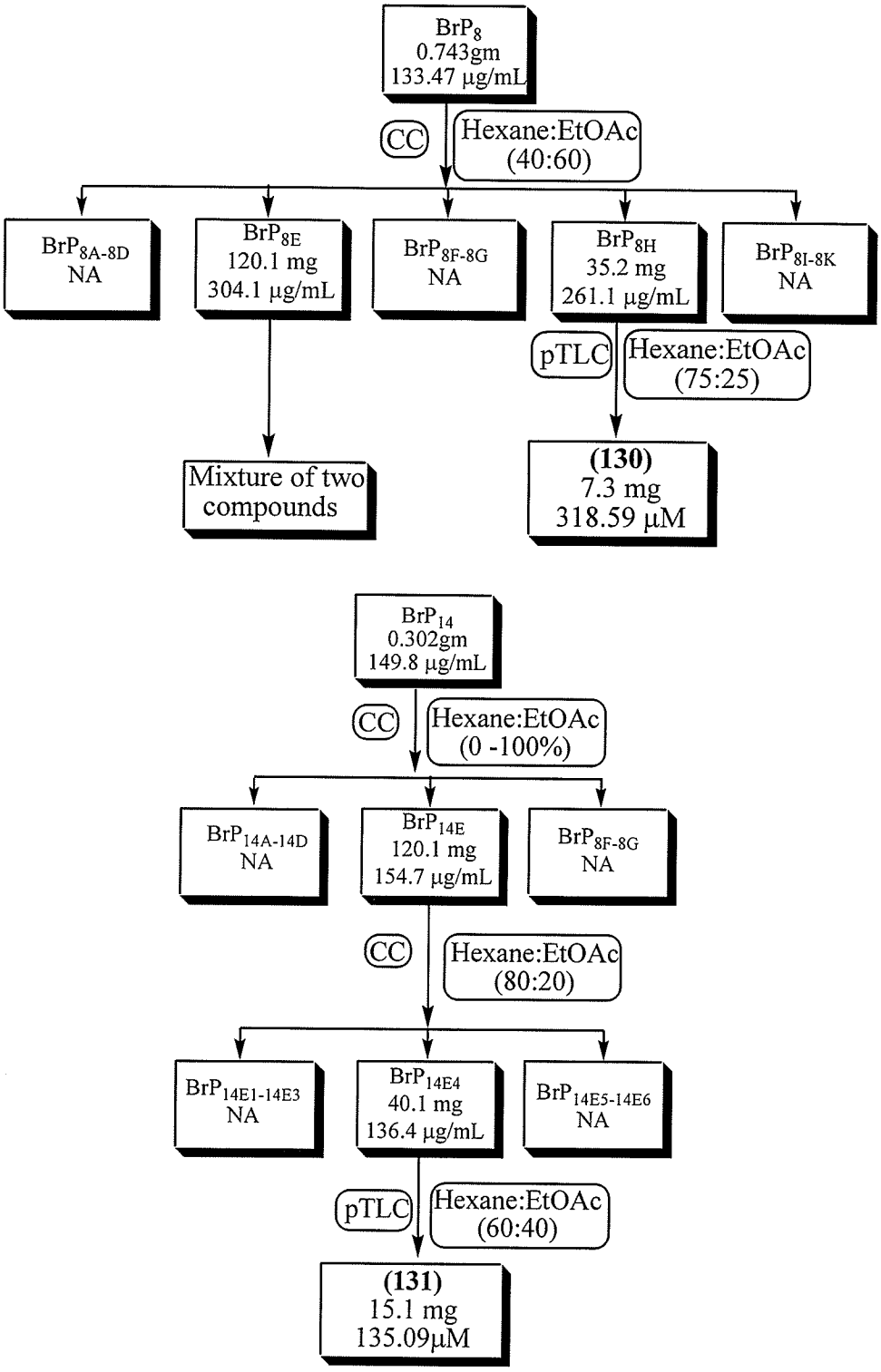

NA = Not active @ 350 µg/mL

WA = Weekly active @ 350 µg/mL

Scheme 4.2 Isolation procedure for compounds **130** and **131**

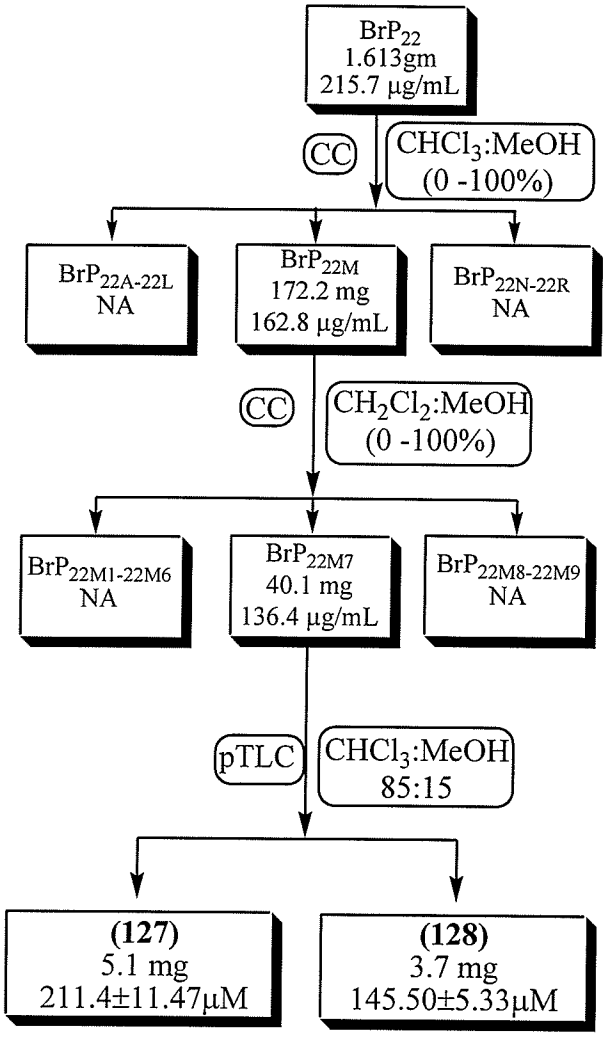

NA = Not active @ 350 µg/mL

WA = Weekly active @ 350 µg/mL

Scheme 4.3 Isolation procedure for compounds **127** and **128**

4.3.4 Barlerin (8-*O*-acetylshanzhiside methyl ester) (127)

White amorphous solid, 5.1 mg, 0.00041% yield, R_f = 0.21 (85:15, $CHCl_3$-MeOH); $C_{19}H_{28}O_{12}$; UV λ_{max} (MeOH) = 231.0 nm; IR (solid film) ν_{max} = 3330, 1707 and 1576, 1420 cm^{-1}; for ^1H and ^{13}C-NMR spectral data see Table **4.1**.

4.3.5 Shanzhiside methyl ester (128)

White amorphous solid, 3.7 mg, 0.00029% yield, R_f = 0.53 (85:15, $CHCl_3$-MeOH); $C_{17}H_{26}O_{11}$; UV λ_{max} (MeOH) = 233.6 nm; IR (solid film) ν_{max} = 3321, 1694 and 1414 cm^{-1}; for ^1H and ^{13}C-NMR spectral data see Table **4.2**.

4.3.6 Lupeol (lup-20(29)-ene-3β-ol) (129)

Transparent crystalline solid, 5.2 mg, 0.00042% yield, R_f = 0.67 (75:25, hexane-ethyl acetate); $C_{30}H_{50}O$; UV λ_{max} (MeOH) = 220.5 nm; for ^1H and ^{13}C-NMR spectral data see Table **4.3**.

4.3.7 Betulinic acid (130)

White gummy solid, 7.3 mg, 0.00058% yield, R_f = 0.5 (75:25, hexane:ethyl acetate); $C_{30}H_{48}O_3$; UV λ_{max} (MeOH) = 225.5 nm; for ^1H and ^{13}C-NMR spectral data see Table **4.4**.

4.3.8 Pipataline (131)

White amorphous solid, 15.1 mg, 0.0012% yield, R_f = 0.7 (60:40, hexane:ethyl acetate); $C_{19}H_{28}O_2$; IR (solid film) ν_{max} = 1501.9 cm^{-1}; for ^1H and ^{13}C-NMR spectral data see Table **4.5**.

4.3.9 Epoxidation of pipataline (131)

This reaction was carried out by using a procedure described by Sello[37] to prepare compound (**132**). Pipataline (**131**) (3 mg) dissolved in 10 mL of CH_2Cl_2 was mixed with an equal amount of water containing 1.0 g of $NaHCO_3$. Then 3.58 mg of

m-chloroperbenzoic acid was continuously added to this reaction mixture. The reaction mixture was stirred at room temperature for 24 hours after which Na_2SO_3 (10 mL) was added to the reaction mixture, which was then extracted with 2x10 mL of CH_2Cl_2. The combined organic phase was washed with 2x25 mL aqueous $NaHCO_3$ and water and dried over anhydrous $MgSO_4$. Filtration and evaporation of the solvent under vacuum gave **132** as a white powder.

Spectral data of 7,8-epoxypipataline (132)

White solid, 2.5 mg, 83% yield; $C_{19}H_{28}O_3$; ^{1}H-NMR (CD_3OD, 300MHz) δ = 6.89 (1H, s , H-3), 6.73 (2H, dd, J = 8.0, 1.7 Hz, H-5, H-6), 5.93 (2H, s , H-19), 3.37 (1H, d, J = 2.0 Hz, H-7), 2.88 (1H, ddd, J = 8.4, 2.4, 2.0 Hz, H-8), 2.17 (2H, s , H-9), 1.34 (16H, s , H-10 to H-17), 0.88 (3H, t, J = 6.5 Hz, H-18); ^{13}C-NMR ($CDCl_3$, 50 MHz) (δppm): 147.8 (-C-, C-1), 146.4 (-C-, C-2), 124.2 (CH, C-3), 132.4 (-C-, C-4), 120.1 (CH, C-5), 105.3 (CH, C-6), 63.0 (CH, C-7), 58.6 (CH, C-8), 33.1 (CH_2, C-9), 32.9 (CH_2, C-10), 31.8 (CH_2, C-11), 29.1 (CH_2, C-12), 29.5 (CH_2, C-13), 29.5 (CH_2, C-14), 9.4 (CH_2, C-15), 29.2 (CH_2, C-16), 22.6 (CH_2, C-17), 14.1 (CH_3, C-18), 100.8 (CH_2, C-19). EIMS *m/z* (rel. int.%): 304 $[M]^+$ (9), 288 $[M\text{-}O]^+$ (1.5), 163 (41), 150 (100).

4.3.10 Synthesis of 7-amino-8-hydroxy pipataline (133)

7,8 Epoxy pipataline **132** (2.5 mg) and 28% NH_3 (5 mL) were added in to a 20 mL vial[35]. This vial was closed and placed in a modified household microwave at the chosen power (1200 KW). The reaction was carried out for two min and 10 sec with 5 sec intervals. After cooling, the solution was extracted with ethyl acetate (3x10mL) and the organic layer was dried over anhydrous Na_2SO_4. The solvent was evaporated under reduced pressure to afford **133** as a colorless solid.

Spectral data of 7-amino-8-hydroxy pipataline (133)

Colorless solid, 2.1 mg, 84% yield; $C_{19}H_{31}NO_3$; ^{1}H-NMR (CD_3OD, 300MHz) δ = 6.89 (1H, s , H-3), 6.73 (2H, dd, J = 8.0, 1.7 Hz, H-5, H-6), 5.93 (2H, s , H-19), 3.70 (1H, d, J = 2.3 Hz, H-7), 2.87 (1H, dt, J = 9.7, 3.2, 2.3 Hz, H-8), 2.17 (2H, s, H-9), 1.34 (16H, s , H-10 to H-17), 0.88 (3H, t, J = 6.5 Hz, H-18); ^{13}C-NMR ($CDCl_3$, 50 MHz) (δppm): 147.8 (-C-, C-1), 146.4 (-C-, C-2), 124.2 (CH, C-3), 132.4 (-C-, C-4), 120.1 (CH, C-5), 105.3 (CH, C-6), 75.7 (CH, C-7), 60.4 (CH, C-8), 33.1 (CH_2, C-9), 32.9 (CH_2, C-10), 31.8 (CH_2, C-11), 29.1 (CH_2, C-12), 29.5 (CH_2, C-13), 29.5 (CH_2, C-14), 29.4 (CH_2, C-15), 29.2 (CH_2, C-16), 22.6 (CH_2, C-17), 14.1 (CH_3, C-18), 100.8 (CH_2, C-19). ElMS *m/z* (rel. int.%): 321 $[M]^+$ (1.5), 305 $[M\text{-}NH_2]^+$, (49), 304 $[M\text{-}OH]^+$, (20), 288 $[M\text{-}OH\text{-}NH_2]^+$ (70), 179 (17), 151 (90), 135 (100).

4.3.11 Bromination of pipataline (134)

Pipataline (**131**) (3 mg) was dissolved in ethyl acetate (5 mL) and the reaction mixture was stirred with Br_2 (0.5 mL) under UV (λ = 366 nm) for 24 hours[36]. After 24 hours, the reaction was stopped by adding water. This reaction mixture was extracted with ethyl acetate (3x10mL). The ethyl acetate layer was dried over anhydrous Na_2SO_4. The solvent was evaporated under reduced pressure to yield **134** as a brown solid.

Spectral data of 7, 8-dibromopipataline (134)

Brown solid, 2.8 mg, 93% yield; $C_{19}H_{28}Br_2O_2$; δ = 6.89 (1H, s , H-3), 6.73 (2H, dd, J = 8.0, 1.7 Hz, H-5, H-6), 5.93 (2H, s , H-19), 5.58 (1H, d, J = 7.0 Hz, H-7), 4.39 (1H, dt, J = 7.0, 5.4, 3.4 Hz, H-8), 2.17 (2H, s , H-9), 1.34 (16H, s , H-10 to H-17), 0.88 (3H, t, J = 6.5 Hz, H-18); ^{13}C-NMR ($CDCl_3$, 50 MHz) (δ in ppm): 147.8 (-C-, C-1), 146.4 (-C-, C-2), 124.2 (CH, C-3), 132.4 (-C-, C-4), 120.1 (CH, C-5), 105.3 (CH, C-6), 57.4 (CH, C-7), 55.3 (CH, C-8), 33.1 (CH_2, C-9), 32.9 (CH_2, C-10), 31.8

(CH_2, C-11), 29.1 (CH_2, C-12), 29.5 (CH_2, C-13), 29.5 (CH_2, C-14), 29.4 (CH_2, C-15), 29.2 (CH_2, C-16), 22.6 (CH_2, C-17), 14.1 (CH_3, C-18), 100.8 (CH_2, C-19). EIMS *m/z* (reI. int.%): 448 $[M]^+$ (5), 450 $[M+2]^+$ (8), 367 $[M-Br]^+$ (9), 288 $[M-Br_2]^+$ (3), 228 (22), 212 (62), 135 (46), 160 (100).

4.4 Enzyme inhibition assays

4.4.1 Glutathione *S*-transferase inhibition assay

The GST assay was conducted as described in chapter **2**, page 50.

4.4.2 Acetylcholinesterease assay

The AChE assay was conducted as described in chapter **2**, page 51.

4.5 References

[1] Airy Shaw, H. K.; Willis, J. C. *A Dictionary of Flowering Plants and Ferns*, 8th ed. University Press, Cambridge, **1973**.

[2] Burkill, H. M. *The useful plants of West Tropical Africa*, Royal Botanic Garden, Kew, UK, **1985**, 960.

[3] Chopra, R. N.; Nayar, S. L.; Chopra, I. C. *Glossary of Indian Medicinal Plants*, CSIR: New Delhi, **1965**, 33.

[4] Gupta, H. M.; Saxena, V. K. *Nat. Acad. Sci. Lett.*, **1984**, 7, 187.

[5] Singh H. *Anc. Sci. Life*, **1988**, 8, 167.

[6] Parrotta, J. A. *Healing plants of Peninsular India*, CABI, Wellington, UK & New York, **2001**, 917.

[7] Sing, B.; Bani, S.; Gupta, D. K.; Chandan, B. K.; Kaul, A.; *J. Ethanopharmacol.*, **2003**, 85, 187.

[8] Gupta, R. S.; Kumar, P.; Dixti, V. P.; Dobhal, M. P. *J. Ethanopharmacol.*, **2000**, 70, 111.

[9] Alam, M. M.; Anis, M. *J. Ethnopharmacol.*, **1987**, 19, 85.

[10] Hall, C. B., McCarthy, C. A. In *Infectious Diseases*, Mandell, G. L., Bennett, J. E., Dolin, R., Eds.; Church Livingstone, New York, **1995**, 1501.

[11] Chen, J. L.; Blanc, P.; Stoddart, C. A.; Bogan, M.; Rozhon, E. J.; Parkinson, N.; Ye, Z.; Cooper, R.; Balick, M.; Nanakorn, W.; Kernan, M. R. *J. Nat. Prod.*, **1998**, 61, 1295.

[12] Panwar, H. S.; Nauriyal, M. M.; Joshi, H. C. *Veteri. Res. Bull.*, **1979**, 2, 164.

[13] Suri, J. L.; Banerjee, S. K.; Taneja, S. C.; Chandra, S.; Anand, A. S.; Prabhakar, A.; Jaggi, B. S.; Sing, B.; Saxena, A. K.; Chandan, B. K.; Krishan, B.; Handa, S. S.; Swami, S. *U. S. Pat. Appl. Publ.*, **2003**, 20030181397, 9.

[14] Harborne, J. B., Sankara, S.; Nair, A. G. R. *Phytochemistry*, **1971**, 10, 2822.

[15] Damtoft, S.; Jensen, S. R.; Nielsen, B. J. *Tetrahedron Lett.*, **1982**, 23, 4155.

[16] Taneja, S. C.; Tiwari, H. P. *Tetrahedron Lett.*, **1975**, 24, 1995.

[17] Suksamran, A. *J. Nat. Prod.*, **1986**, 49, 179.

[18] Byrne, L. T.; Sasse, J. M.; Skelton, B. W.; Suksamran, A.; White, A. H. *Aust. J. Chem.*, **1987**, 40, 785.

[19] Tuntiwachwuttikul, P.; Pancharoen, O.; Taylor, W. C. *Phytochemistry*, **1998**, 49, 163.

[20] Ersoz, T.; Kaya, D.; Yalcin, F. N.; Kazaz, C.; Palaska, E.; Charlotte, H.; Gotfredsen, Soren, R.; Jensen, Calis, I. *Turk. J. Chem.*, **2007**, 31, 155.

[21] Davini, E.; Esposito, P.; zIavarone, C.; Trogolo, C. *Phytochemistry*, **1981**, 20, 1583.

[22] Boros, C. A.; Stermitz, F. R. *J. Nat. Prod.*, **1991**, *54*, 1173.

[23] Foderado, T. A.; Stermitz, F. R. *Tetrahedron Lett.*, **1992**, 33, 2953.

[24] Delazar, A.; Byres, M.; Gibbons, S.; Kumarasamy, Y.; Modarres, M.; Nahar, L.; Shoeb, M.; Sarker, S. D. *J. Nat. Prod.*, **2004**, 67, 1584.

[25] Robert, E.; Krull, Frank, R.; Stermitz. *Phytochemistry*, **1998**, 49, 2413.

[26] Robert, E.; Krull, Frank, R.; Stermitz, Franzyk, H.; Jensen, S. R. *Phytochemistry*, **1998**, 49, 1605.

[27] Abdel-Hafiz, M. A.; Ahmed, A. S. *Bull. Pharmaceut. Sci.* Assiut. Univ., **1990**, 13, 65.

[28] Mehta, B. K.; Verma, M.; Jafri, M.; Neogi, R.; Desiraju, S. *Nat. Prod. Res.*, **2003**, 17, 459.

[29] Nunez, M.; J.; Reyes, C. P.; Jimenez, I. A.; Moujir, L.; Bazzocchi, I. L. *J. Nat. Prod.*, **2005**, 68, 1018.

[30] Yayli, N.; Yildirim, N.; Dogan, N.; Usta, A.; Altun, L. *J. Asian Nat. Prod. Res.*, **2005**, 7, 771.

[31] Gutierrez, R. M. P. *J. Chil. Chem. Soc.*, **2005**, 50, 587.

[32] Yuruker, A.; Orjala, J.; Sticher, O.; Rali, T. *Phytochemistry*, **1998**, 48, 863.

[33] Peng, C.; Bodenhausen, G.; Qiu, S.; Fong, H. H. S.; Farnsworth, N. R.; Yuan, S.; Zheng, C. *Magn. Reson. Chem.*, **1998**, 36, 267.

[34] Atal, C. K.; Dhar, K. L.; Pelter, A. *Chem. Ind.*, **1967**, 52, 2173.

[35] Sello, G.; Orsini, F.; Bernasconi, P. D.; Gennaro. *Tetrahedron Asymm.*, **2006**, 17, 372.

[36] Motsarev, G. V.; Inshakova, V. T.; Kolbasov, V. I.; Dzhagatspanyan, R. V.; Snegova, A. D. *Zhurnal Obshchei Khimii*, **1971**, 41, 114.

CHAPTER 5

Phytochemical studies on *Buxus natalensis*

5.1 Introduction

The family Buxaceae is composed of a large number of species that are found in temperate regions of both hemispheres and at only higher elevations in the tropics. These species include *Buxus sempervirens, B. papillosa, B. hildebrandtii, B. microphyla, B. madagascarica* and *B. natalensis.* These plants have been used for several decades to treat various ailments such as malaria, rheumatism, depression and skin infections[1]. For example, the crude ethanolic extract of *B. sempervirens* has been used in the treatment of the Human Immunodeficiency Virus (HIV) infections. This extract has also exhibited a delayed progression in HIV infected asymptomatic patients[2,3]. An extensive literature survey shows that chemical investigations on *Buxus* species have resulted in the isolation of more than 200 steroidal alkaloids[4].

Buxus alkaloids have a unique steroid-triterpenoidal structure and these alkaloids have shown interesting pharmacological activities. For example cyclovirobuxine-D (**135**) has shown activity against heart disorders[5] and cycloprotobuxine-A (**136**) has shown a protective effect against cardiac arrhythmia induced by oubain (LD_{50} 5mg/kg) and a positive inotropic effect on isolated guinea pig myocardium[1,6-7].

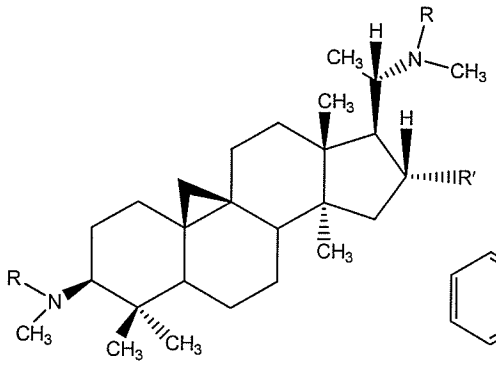

(**135**) R = H, R′ = OH
(**136**) R = CH_3, R′ = H

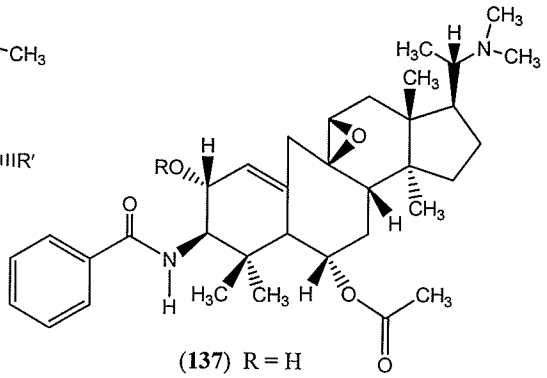

(**137**) R = H
(**138**) R = OAc

Alkaloids, buxoxybenzamide (**137**) and buxapapillinine (**138**), isolated from *B. sempervirens* were reported to exhibited 86%, 57%, 57% and 86%, 71% and 57% phytotoxic activity against *Lemna minor* L. at 500, 50, and 5 ppm, respectively[8]. Cyclovirobuxine F (**139**), *N*-benzoyl-*O*-acetylbuxalongifoline (**140**), buxasamarine (**141**), and cyclobuxamidine (**142**), purified from *B. longifolia,* displayed weak antibacterial activity against *Salmonella typhi, Shigella flexneri, Pseudomonas aeruginosa* and *Escherichia coli*[9].

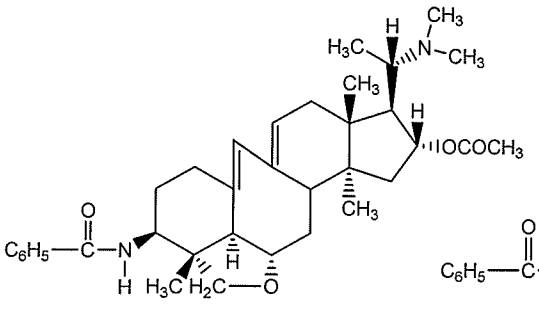

(**139**)

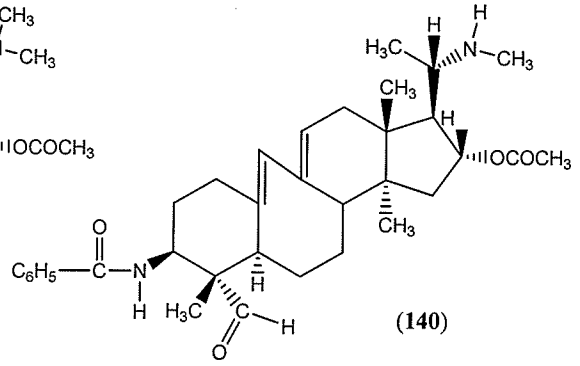

(**140**)

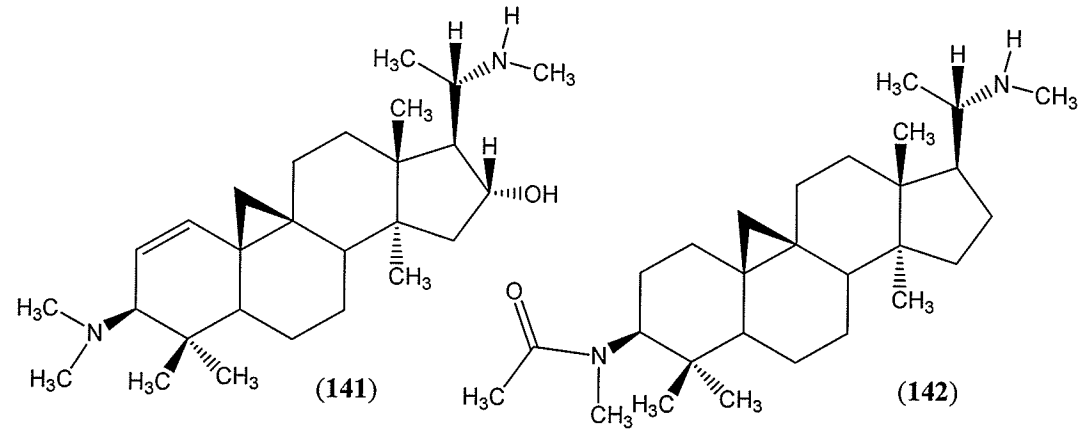

(141) (142)

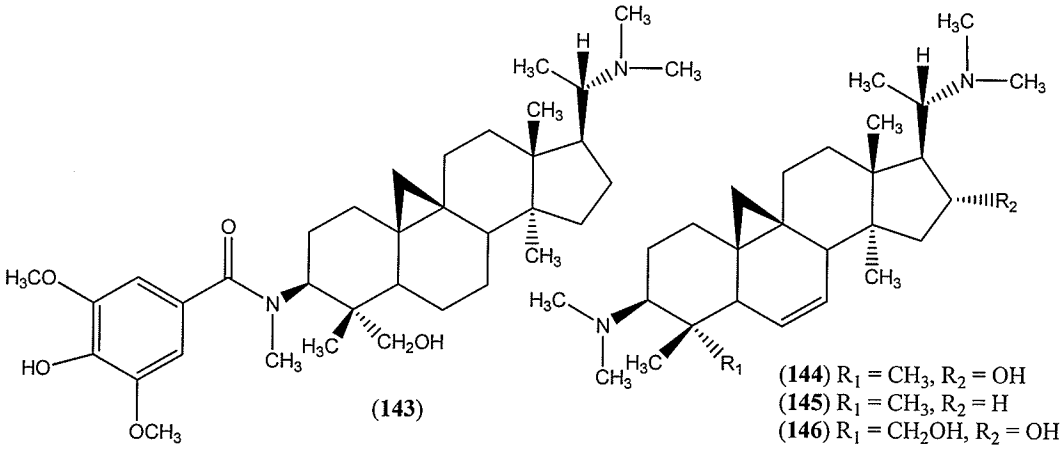

(143)

(144) $R_1 = CH_3$, $R_2 = OH$
(145) $R_1 = CH_3$, $R_2 = H$
(146) $R_1 = CH_2OH$, $R_2 = OH$

Buxus alkaloids have also demonstrated their potentials as anti-acetylcholinesterase[10] and anti-butyrylcholinesterase[11] properties. For instance, buxakashmiramine (**143**), cyclovirobuxine-A (**144**), cycloprotobuxine-C (**145**), cyclomicrophylline-A (**146**) buxamines B (**147**) and C (**148**), purified from *B. papilosa* and *B. hyrcana*, have been reported to inhibit AChE concentration dependently with IC_{50} values of 25.4, 105.7, 38.4, 235.0, 74.0 and 7.5 μM respectively[12-13]. The difference in anticholinestrase activity of compound **147** and **148** was explained by docking studies, which showed that **148** penetrated deeper into the AChE gorge than **147**, and that the positioning of the C-3 tertiary amino group resembles the quaternary ammonium group of AChE better than the secondary amino group of **147**[12]. Seven alkaloids,

homomoenjodaramine (**149**), moenjodaramine (**150**), 7-deoxy-O^6-buxafurandiene (**151**), hyrcanone (**152**), buxabenzacinine (**153**), N_b-dimethylcycloxobuxoviricine (**154**) and buxandrine (**155**) isolated from *B. hyrcana*, (Buxaceae) have been reported to inhibit AChE with varing degrees of activities having IC_{50} value of 19.2, 50.8, 13, 145, 468, 310 and 175.4 μM respectively[14-16].

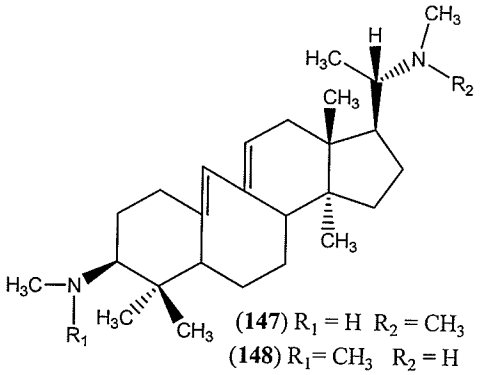

(**147**) $R_1 = H$ $R_2 = CH_3$
(**148**) $R_1 = CH_3$ $R_2 = H$

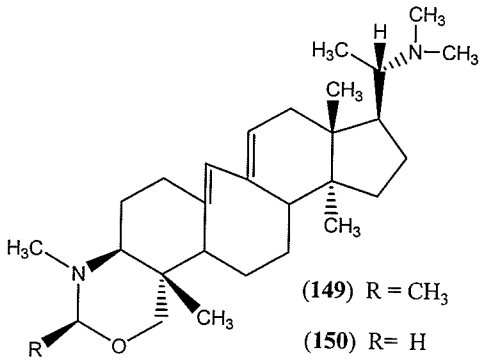

(**149**) $R = CH_3$
(**150**) R= H

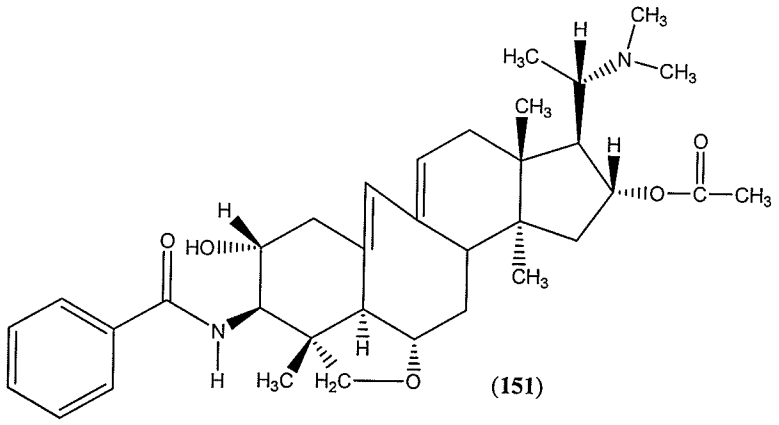

(**151**)

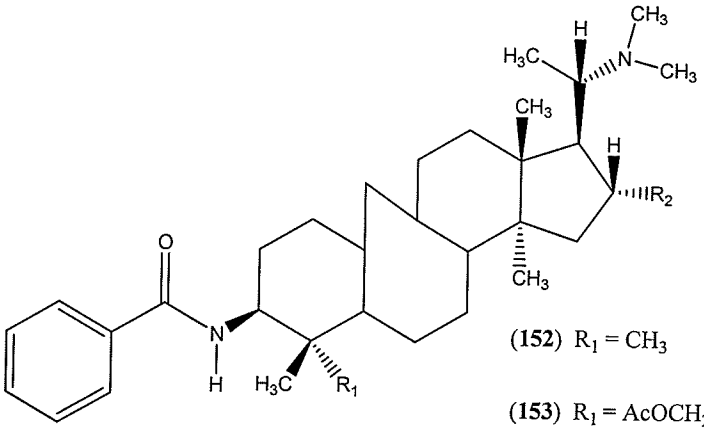

(**152**) $R_1 = CH_3$ $R_2 = H$ $\Delta^{1,10}$ 11-C=O

(**153**) $R_1 = AcOCH_2$ $R_2 = OH$ $\Delta^{1,10}$ $\Delta^{9,11}$

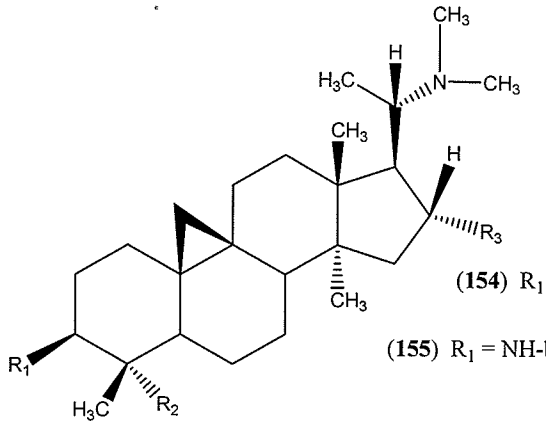

(**154**) R_1 = C=O $R_2 = CH_3$ R_3 = OH $\Delta^{1,2}$

(**155**) R_1 = NH-benzoyl $R_2 = HOCH_2$ R_3 = OAc $\Delta^{6,7}$

Structures of *Buxus* alkaloids contain the buxane (9,19-cyclobuxus) or the 9,10-seco-buxa-9(11), 10(19) diene skeleton which have a substitution pattern at C-4 and C-14. Biosynthetically lanosterol or cycloartenol type triterpenes are considered to be precursors of *Buxus* alkaloids which are formed by the cyclization of squalene either by oxidative or non-oxidative pathways[1,17-18]. These transformations might involve in the formation of 20-ketosteroid intermediates by oxidative cleavage of the C-20 side chain. This intermediate might under go another oxidation reaction at C-3 to afford 3,20-diketosteroid. *Buxus* alkaloids may have been derived from this intermediate as outlined in Scheme **5.1**

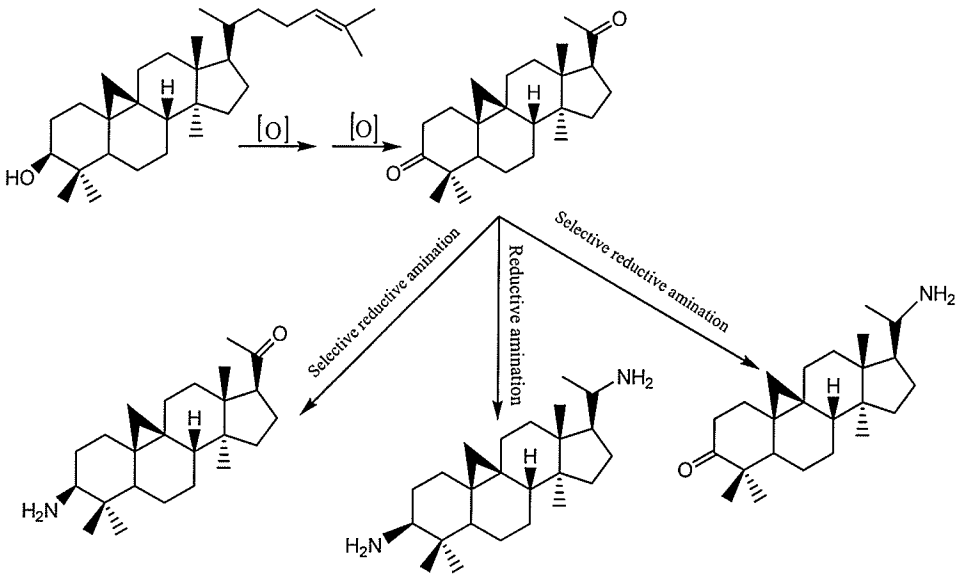

Scheme 5.1 Plausible biosynthesis of *Buxus* alkaloids

Keeping the pharmacological importance of *Buxus* alkaloids in view, the present project was designed to isolate alkaloids from *B. natalensis* and to evaluate them for enzyme inhibitory activity including AChE. To the best of our knowledge, no report on phytochemical studies of this plant has been reported in the literature.

5.2 Results and discussion

5.2.1 Isolation of compound 156

Compound (**156**) was isolated as a colorless gum after column and thin layer chromatography of crude methanolic extract of *B. natalensis* (for details see the experimental section). This compound was characterized by using extensive NMR spectral data. Compound **156** was found to exhibit anti-AChE activity.

5.2.2 Structure elucidation of natalensamine-A (156)

The UV spectrum of **156** showed an absorption maximum at 206 nm indicating the absence of conjugated π system. The IR spectrum of compound **156** suggested the presence of hydroxyl (3436) and olefinic (1551cm^{-1}) functionalities [19]. The EIMS of **156** showed the molecular ion peak at *m/z* 444. A combination of ^{1}H, ^{13}C-NMR and mass spectral data provided the molecular formula, $C_{28}H_{48}N_2O_2$, of this compound. An ion at *m/z* 429 arose due to the loss of a methyl group from the molecular ion. A base peak at *m/z* 72 indicated a trimethyl-imminium cation formed by the cleavage of C-17/C-20 bond with charge retention on the nitrogen side chain[20].

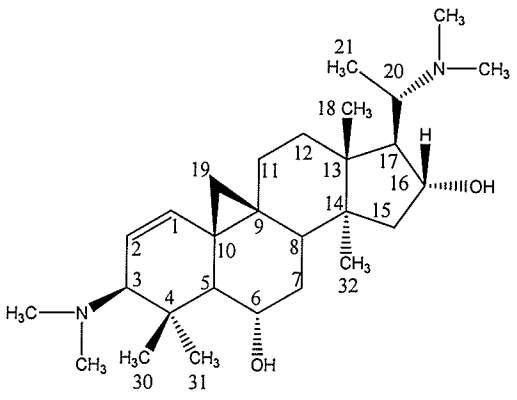

(156)

The ^{1}H-NMR ($CDCl_3$, 300MHz) spectrum of **156** displayed four three-proton singlets at δ 0.83, 0.86, 0.89 and 1.02 due to H_3-18, H_3-32, H_3-31 and H_3-30, respectively. A

secondary methyl H_3-21 resonated as a doublet at δ 0.85 (d, J = 6.5 Hz). Two six-proton singlets at δ 2.23 and 2.56 were due to *N,N*-dimethyl protons substituted at C-20 and C-3, respectively. A set of AB doublets, resonating at δ -0.02 and 0.68 (d, $J_{19\alpha,\ 19\beta}$ = 4.5 Hz), were due to the H_2-19. A doublet at δ 2.52 (d, J = 7.4 Hz) was assigned to H-3 while a multiplet appeared at δ 2.62 was due to H-20. Two multiplets, integrating for one proton each, resonating at δ 3.72 and 4.08 were due to H-6 and H-16. Their downfield chemical shift values were indicative of the presence of geminal hydroxyl groups. A downfield doublet at δ 5.52 (d, J = 10.2 Hz) was ascribed to H-1 whereas H-2 resonated as a multiplet at δ 5.39.

The COSY-45° spectrum of **156** showed the presence of five isolated spin systems in it. The first spin system started with H-1 (δ 5.52) that exhibited coupling with H-2 (δ 5.39) which in turn showed cross peak with H-3 (δ 2.52). In the second spin system, H-5 (δ 1.90) displayed cross peaks with H-6 (δ 3.72) that exhibited coupling with H_2-7 (δ 1.55, 2.12). The latter was coupled with H-8 (δ 1.87). The third spin system showed only geminal coupling between H-19α (δ -0.02) and H-19β (δ 0.68). H_2-11 (δ 1.29, 1.72) exhibited vicinal coupling with H_2-12 (δ 1.53, 1.79) in the fourth spin system. The fifth spin system showed strong cross peaks of H-16 (δ 4.08) with H-15 (δ 2.08, 1.45) and H-17 (δ 1.89). H-17 further showed cross peak with H-20 (δ 2.62) that in turn exhibited coupling with H-21 (δ 0.85). All of these spin systems present in compound **156** are shown around structure **156a**.

The broad-band ^{13}C-NMR ($CDCl_3$, 75MHz) spectrum of **156** displayed signals for twenty eight carbons. The DEPT spectra suggested the presence of nine methyl, five methylene and nine methine carbons. Subtraction of DEPT spectra from the broad-band ^{13}C-NMR spectrum revealed the presence of five quaternary carbons in

compound **156.** The HSQC spectrum was recorded to determine $^{1}H/^{13}C$ one bond shift correlations of all protonated carbon atoms in compound **156**. Complete ^{1}H and ^{13}C-NMR chemical shift assignments are shown in Table **5.1**.

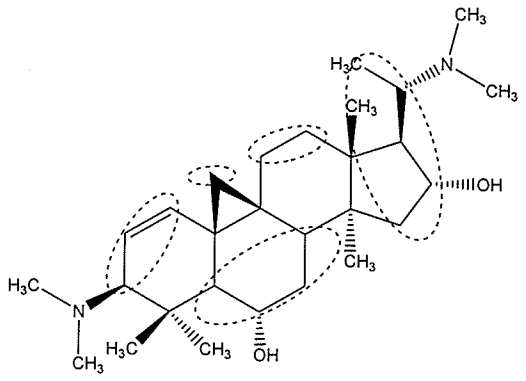

(156 a)

The HMBC spectrum was used to establish the gross structure **156** from spin systems deduced from the COSY-45° spectrum. H-1 (δ 5.52) showed HMBC interactions with C-2 (δ 128.9) and C-10 (δ 27.0) where as H-2 (δ 5.39) exhibited cross peaks with C-1 (δ 126.1) and C-4 (δ 41.5) carbons. H-3 (δ 2.52) displayed long-range correlation with C-2 (δ 128.9). H_3-30 (δ 1.02) showed cross peaks with C-3 (δ 66.1), C-4 (δ 41.5) and C-31(δ 18.8) whereas H_3-31 (δ 0.90) showed long-range correlations with C-4 (δ 41.5), C-5 (δ 56.5) and C-30 (δ 26.9). H_2-19 (δ –0.02, 0.68) showed HMBC interactions with C-5 (δ 56.5), C-8 (δ 49.7), C-9 (δ 19.8), C-10 (δ 27.0), and C-11(δ 24.8) carbons. H_3-18 (δ 0.83) showed long-range heteronuclear shift correlations with C-12 (δ 31.7), C-13 (δ 45.2), C-14 (δ 48.6) and C-17 (δ 49.7) carbons. H-16 (δ 4.08) geminal to hydroxyl group, exhibited cross peaks with C-17 (δ 49.7) and C-20 (δ 62.7). These HMBC interaction data indicated that compound **156** had a *Buxus* alkaloidal skeleton. Important HMBC correlations are shown in structure **156b.**

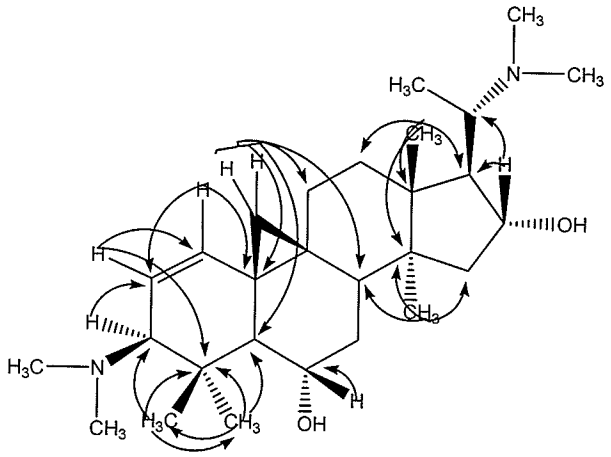

(156b)

Stereochemical assignments at C-3, C-6, C-13, C-14, C-16, C-17 and C-20 were made on biosynthetic considerations and on chemical shift correlations with the previously reported *Buxus* alkaloids of the series[9, 21-23].

The ^{1}H and ^{13}C-NMR spectral data of **156** were identical to those of buxasamarine isolated from *B. longifolia*[9] except that NMR and mass spectral data of **156** showed the presence of *N,N*- dimethyl group at C-20 and hydroxyl group at C-6. Based on these spectroscopic data structure **156** was proposed for this new natural product and was `named as natalensamine-A.

Table 5.1 ^{1}H and ^{13}C-NMR data of **156,** recorded at 300 and 75 MHz, respectively.

Carbon No.	^{1}H-NMR (δ)	^{13}C-NMR (δ)	DEPT Multiplicity
1	5.52, *d*, (10.2)	126.1	CH
2	5.39, *m*	128.9	CH
3	2.52, *d*, (7.4)	66.1	CH
4	----	41.5	C
5	1.90, *m*	56.5	CH
6	3.72, *m*	77.5	CH
7	1.55, 2.12, *m*	32.2	CH_2
8	1.87, *m*	49.7	CH
9	---	19.8	C
10	---	27.0	C
11	1.29, 1.72, *m*	24.8	CH_2
12	1.53, 1.79, *m*	31.7	CH_2
13	---	45.2	C
14	---	48.6	C
15	1.45, 2.08, *m*	38.5	CH_2
16	4.08, *m*	78.6	CH
17	1.89, *m*	49.7	CH
18	0.83, *s*	15.3	CH_3
19	-0.02, 0.68, *d*, (4.5)	18.3	CH_2
20	2.62, *m*	62.7	CH
21	0.85, *d*, (6.5)	10.3	CH_3
30	1.02, *s*	26.9	CH_3
31	0.90, *s*	18.8	CH_3
32	0.86, *s*	18.4	CH_3
N_a-$(CH_3)_2$	2.56, *s*	39.5	CH_3
N_b-$(CH_3)_2$	2.23, *s*	43.4	CH_3

Solvent: $CDCl_3$

5.2.3 AChE inhibitory activity of natalensamine-A (156)

Compound **156** exhibited weak AChE inhibitory activity with an IC_{50} value of 58.937 ± 1.551 μM. This bioactivity was weak when compared with a standard AChE inhibitor glanthamine (IC_{50} 0.5 ± 0.017 μM). Structurally, natalensamine-A was similar to that of **144-146** except for the different position of the double bond and different substituents at C-4 and C-16. The most active among all of these was cycloprotobuxine-C (**145**) (IC_{50} 38.4 μM) that did not a have hydroxyl moiety at C-16. The AChE inhibitory activity of **156** was lower than cycloprotobuxine-C which may be due to the presence of hydroxyl group at C-16. On the other hand natalensamine-A was a stronger inhibitor compared with cyclovirobuxeine-A (IC_{50} 105.7 μM). This might be due to the presence of a Δ^{1-2} double bond that might have provided better interaction with the enzyme compared to cyclovirobuxine-A.

5.3 Experimental

5.3.1General experimental conditions

General experimental conditions for this part of research were the same as previously discussed in chapters **2-4.**

5.3.2 Plant material

This plant was collected from Umhlanga Rocks, South Affrica by Richard J. P. Cannell Department of Chemistry, Durban University, South Africa in February 2007 and was identified by Yashica Singh, Curator, South African National Biodiversity Institute, South Africa. A voucher specimen (132176) was deposited in the South African National Biodervisity Institute, Durban, South Africa.

5.3.3 Extraction and isolation

The roots of *B. natalensis* Linn were peeled off (2.25 Kg) using a steel knife, dried under shade and grounded into a fine powder (1.7542 Kg powder). The powder was extracted three times with equal volumes of ethanol (2.0 L) at room temperature. The extract was concentrated to a reddish brown gum (173.19 g) under reduced pressure. The crude ethanolic extract was defatted with hexane and extracted with methanol. Both hexane and methanolic extracts were subjected to acetylcholinestrase inhibitory assay. The hexane extract was inactive while the methanolic extract (122.30 g) showed positive results with an IC_{50} value of 113.20 ±26.15 μg/mL in this assay. The extract was dissolved in 30% methanol (V/V) and was fractionated at different pH values. A fraction obtained at pH 7.0 (28.21g) showed acetylcholinestrase inhibition with an IC_{50} value of 127.20 ± 5.2 μg/mL and was loaded onto a silica gel column (200-400 mesh, Merk). The column was eluted with hexane-EtOAc (0-100%) followed by EtOAc:MeOH (0-100%) to afford various fractions. These fractions were

pooled on the basis of analytical TLC results and were screened in the AChE inhibition assay. Fraction F_{11} (AChE inhibitory activity with IC_{50} value of 80.49 ± 6.17 μg/mL) yielded another fraction F_{11C} by column chromatography using CH_2Cl_2:EtOAc (0-100%) as the mobile phase. This fraction was subjected to preparatory TLC to afford four minor compounds and one major compound natalensamine-A (**156**), as shown in Scheme **5.2** (7.1904 mg, 0.00041% yield, Isopropanol:CH_2Cl_2, 28:2, R_f 0.21) which was evaluated for AChE inhibitory activity. The minor compounds were not isolated in sufficient quantities for spectral analysis.

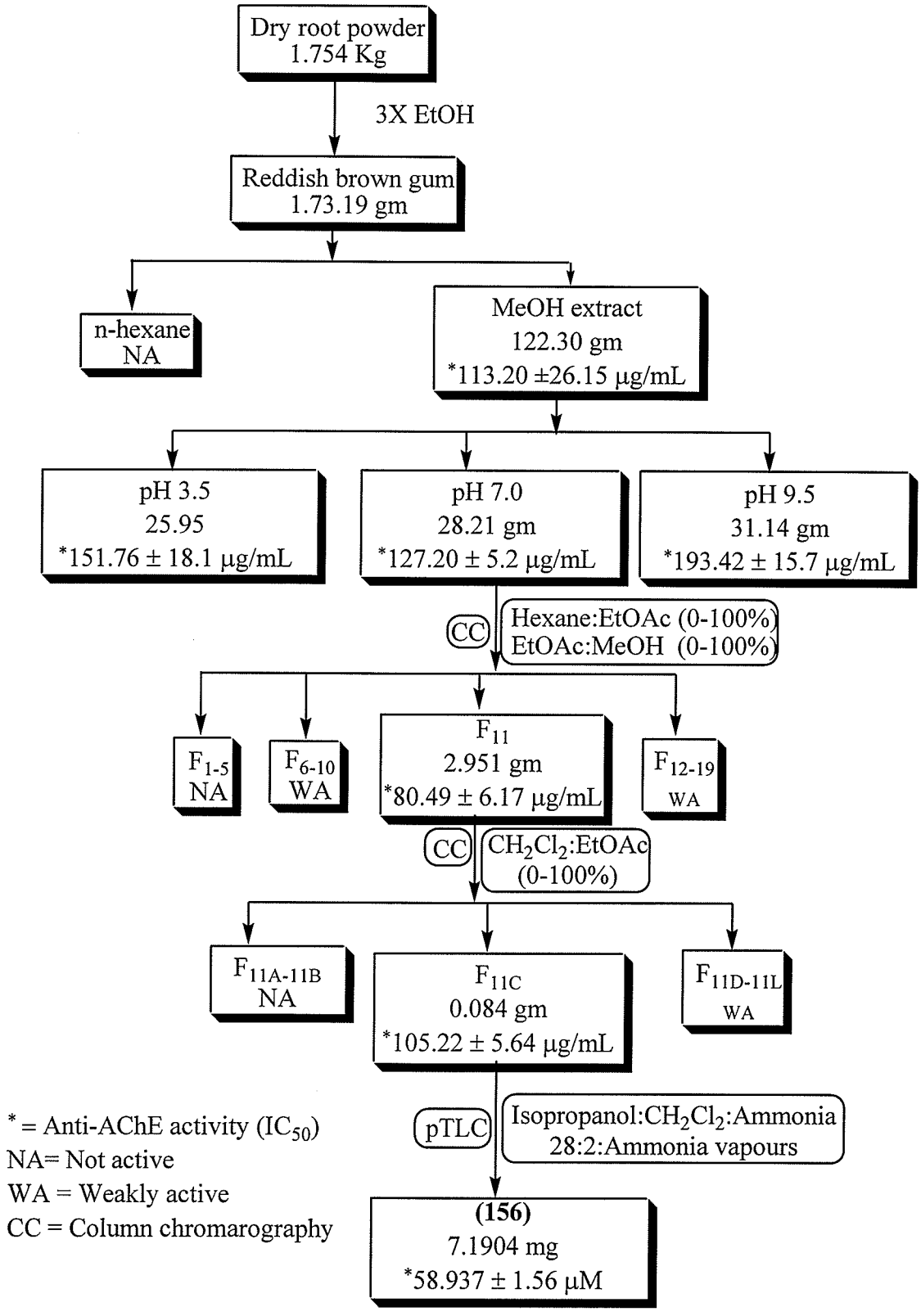

Scheme 5.2 Isolation procedure for natalensamine-A (**156**)

5.3.4 Natalensamine-A (156)

Colorless gummy solid, 7.1904 mg, 0.00041% yield, R_f = 0.21 (Isopropanol-CH_2Cl_2-28:2: ammonia vapours); $C_{28}H_{48}N_2O_2$; UV λ_{max} (MeOH) = 206 nm; IR (KBr) ν_{max} = 3436 and 1551cm^{-1}; for ^{1}H and ^{13}C-NMR spectral data see Table **5.1**. ElMS *m/z* (reI. int.%): 444 $[M]^+$ (5), 429 $[M\text{-}CH_3]^+$ (7), 399 (4), 115 (3), 72 (100), 58 (30), 44 (20).

5.4 Enzyme inhibition assay

5.4.1 Acetylcholinestrase assay

The AChE assay was conducted as described in chapter **2**, page 51.

5.5 References

[1] Cordell, G. A. *Introduction to alkaloids; A Biogenetic Approach*, Wiley intersciences, New York, **1981**, 907.

[2] Durant, J.; Vandermander, J.; Chantre, P.; Dellamonica, P. *Communication at conference on AIDS*, Vancouver, Canada, **1996** (Abstract LBB6040).

[3] Durant, J.; Chantre, P.; Gonzalez, G.; Vandermander, J.; Halfon, P.; Rousse, B. *Phytomedicine*, **1998**, 5, 1.

[4] Atta-ur-Rahman, Choudhary, M. I. *The Alkaloids*, Cordell, G. A., Ed., Academic press, San Diego, **1998**, 50, 61.

[5] Shan, p.; Mao, R.; Xu, J.; Li, J.; *J. Trad. Chin. Med.*, **1984**, 4, 15.

[6] Wang, Y. X.; Liu, J. W.; Tan, Y. H.; Sheng, B. H. *Acta Pharmacol. Sinica*, **1989**, 10, 516.

[7] Wang, Y. X.; Tan, Y. H.; Sheng, B. H. *Acta Pharmacol. Sinica*, **1992**, 13, 226.

[8] Atta-ur-Rahman, Ata, A.; Naz, S.; Choudhary, M. I.; Sener, B.; Turkoz, S. *J. Nat. Prod.*, **1999**, 62, 665.

[9] Atta-ur-Rahman, Noor-e-ain, F.; Choudhary, M. I.; Parveen, Z. *J. Nat. Prod.*, **1997**, 60, 976.

[10] Kiamuddin, M.; Hye, H. K. M. A. *Pak. J. Sci. Ind, Res.*, **1970**, 13, 59.

[11] Choudhary, M. I.; Shahnaz, S.; Parveen, S.; Khalid, A.; Ayatollahi, S. A. M.; Atta-ur-Rahman, Pervez, M. *J. Nat. Prod.*, **2003**, 66, 739.

[12] Khalid, A.; Azim, M. K.; Parveen, S.; Atta-ur-Rahman, Choudhary, M. I. *Biochem. Biophys. Res. Commn.*, **2005**, 331, 1528.

[13] Rehman, A.; Parveen, S.; Khalid, A.; Farooq, A.; Choudhary, M. I. *Phytochemistry*, **2001**, 58, 963.

[14] Baber, Z.; Ata, A.; Meshkatalsadat, M. H. *Steroids*, **2006**, 71, 1045.

[15] Atta-ur-Rahman, Parveen, S.; Asaad, K.; Farooq, A.; Ayatollahi, S. A. M.; Choudhary, M. I. *Heterocycles*, **1998**, 49, 481.

[16] Choudhary, M. I.; Shahnaz, S.; Parveen, S.; Khalid, A.; Ayatollahi, S. A. M.; Atta-ur-Rahman, Pervez, M. *Chem. & Biodivers.*, **2006**, 3, 1039.

[17] Cerny, V.; Sorm, F. *The Alkaloids*, Ed., R.H.F. Manske Academic Press, New York, **1967**, 9, 417.

[18] Herlem-Gaulier, D.; Khuong-Huu, L. F.; Goutarel, R.; Magdeleine, M. *J. Bull. Soc. Chim. Fr.*, **1968**, 2, 763.

[19] Gilani, Hussan, A.; Ghayur, Nabeel, M.; Asaad, K.; Haq, Z.; Choudhary, M. I.; Atta-ur-Rahman. *Planta Medica*, **2005**, 71, 120.

[20] Waller, G. R.; Dermer, O. C. *Biochemical Applications of Mass spectrometry*, Wiely-interscience, New York, **1980**, 779.

[21] Nakano, T.; Terao, S.; Saeki. *J. Chem. Soc.* **1966**, 1412.

[22] Choudhary, M. I.; Atta-ur-Rahman, Shamma, M. *Phytochemistry*, **1988**, 27, 271.

[23] Voticky, Z.; Paulik, V. *Collection Czechoslov. Chem. Commun.*, **1977**, 42, 541.

CHAPTER 6

Chemical studies on *Coprinus micaceus*

6.1 Introduction

Mushrooms have been used as food and pharmaceuticals for thousands of years and are well represented in pharmacopoeia of Asian traditional medicines. There are about 140,000 species of mushrooms out of which only 14000 species are known. It has been reported that 50% of these known species are considered to be edible while only 5% possess significant pharmacological properties[1,2]. A number of mushrooms such as *Poria cocos*, *Ganoderma lucidum*, *Ganoderma tsugae*, *Hericium erinaceum* are used in crude form in China, Korea, Japan and eastern Russia to cure cancer, hypertension, hepatitis, hypercholesterolemia, high blood pressure, dizziness, insomnia, anorexia, coronary heart disease, altitude sickness, fatigue and bronchial cough[3-6]. In the last decade, the aforementioned traditionally used mushrooms have been investigated in both *in vivo* and *in vitro* model systems and many pharmacologically active substances with anti-microbial, anti-viral and anti-cancer properties have been isolated[7-10]. A number of anti-tumor and immunomodulating polysaccharides have been identified from mushrooms and are in clinical practice as potent anti-cancer agents[11]. For instance lentinan (**157**), isolated from *Lentinus edodes*[12], is a polysaccharide based potent anti-cancer agent.

Some edible mushrooms such as *Agaricul bisporus* and *Ganoderma lucidum* have been chemically investigated for the isolation of biologically active compounds with potential for protecting cellular DNA from oxidative damage which is associated with coronary heart disease, cancer and age-related neurodegenerative diseases[13]. The cold

water extract of *Agaricul bisporus* and hot water extract of *Ganoderma lucidum* were found to have highest protection against oxidative damage to cellular DNA[13].

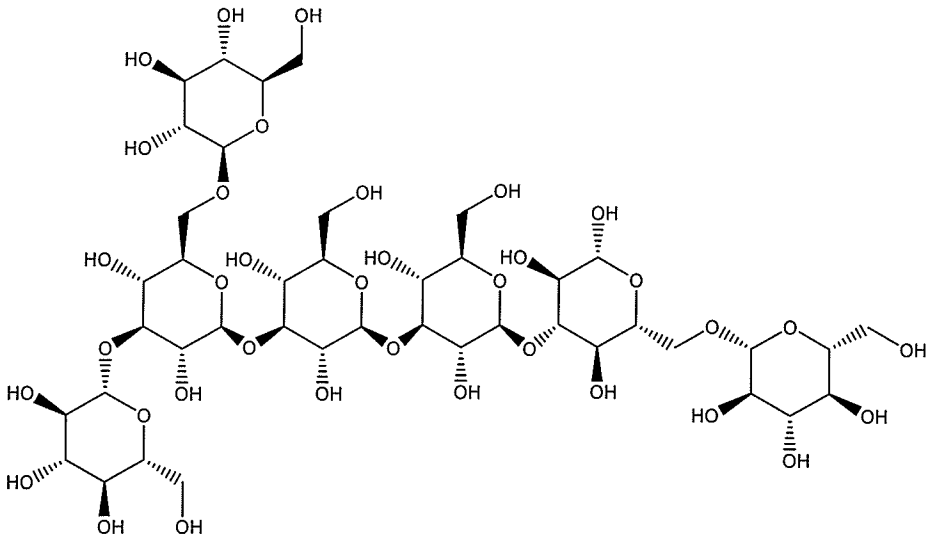

(**157**)

During the last two decades many mushroom species have been investigated for the isolation of anti-tumer polysacchrides and *L. edodes* is one of the most studied mushrooms in this regard. Chihara *et al.* reported that a water-soluble polysaccharide fraction from a fruiting body of *L. edodes* could inhibit the growth of mouse Sarcoma 180 in mice and even complete regression was observed in Swiss albino mice[14,15]. It was also studied that the excessive use of *L. edodes* can reduce the serum cholesterol level, which is directly related to hypertension, in humans[16]. An inhibitory effect on HIV replication *in vitro* was reported from an extract of the culture medium of *L. edodes* mycelia[17]. It was subsequently discovered that sulfated lentinan completely inhibit the replication of HIV[18]. Min *et al.*[19] and El-Mekkawy *et al.*[20] reported a number of anti-HIV compounds from *G. lucidum* such as ganoderic acid α (**158**), A (**159**), B (**160**), and C_1 (**161**), H (**162**); ganoderiol A (**163**), B (**164**), and F (**165**); ganoderanotriol (**166**); and lucidumol B (**167**). In addition to these compounds,

ergosterol (**168**), ergosterol peroxide (**169**), cerevisterol (**170**) and 3β-5α-dihydroxy-6β-methoxyergosta-7,22-diene (**171**) were also reported from the same fungus. The compound **165** and **166** were the most active anti-HIV agents with an IC_{50} value of 7.8 μg/mL each, whereas rest of the compounds were moderately active inhibitory agents with IC_{50} values ranging from 0.17 to 0.23 mM. Bok *et al.*[21] discovered anti-tumor sterol glycoside (**172**) by activity guided fractionation of *Cordyceps sinessis*. In this study the compound **172** was reported to be a potent inhibitor to the proliferation of K562, Jurkt, WM-1341, HL-60, and RPMI-8226 tumor cell lines by 10 to 40% at a concentration of 10μg/mL. Most recently Liu *et al.* investigated the hypoglycemically active mushroom "*Phellinus gilvus*" (IC_{50} = 20 μg/mL) and reported lanostane triterpenoids gilvus A (**173**), B (**174**), C (**175**), andD (**176**); 24-methylenelanost-8-ene-3β,22-diol (**177**); and 5α-ergosta-7,22-diene-3-one (**178**)[22].

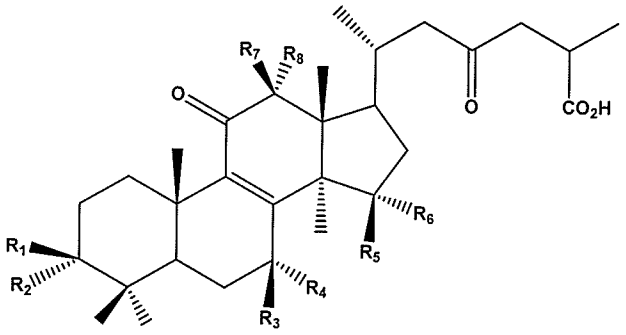

Compound	R_1	R_2	R_3	R_4	R_5	R_6	R_7	R_8
Ganoderic acid α (**158**)	OH	H	O	----	OAc	H	OH	H
Ganoderic acid A (**159**)	O	---	OH	H	H	H	OH	H
Ganoderic acid B (**160**)	OH	H	OH	H	H	H	O	---
Ganoderic acid C_1 (**161**)	O	---	OH	H	H	H	O	---
Ganoderic acid H (**162**)	OH	H	O	---	OAc	H	O	---
Cerevisterol (**170**)	OH	OH	H	OH	H	H	O	---

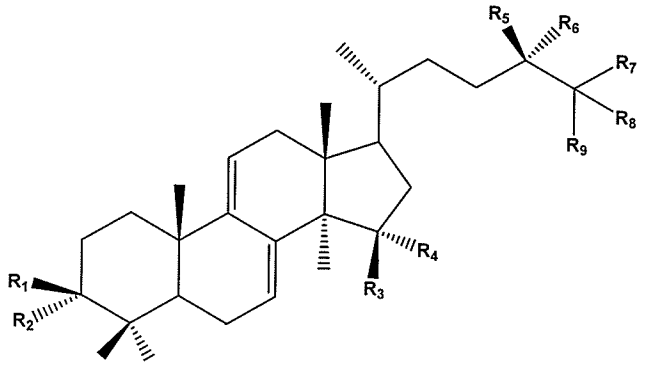

Compound	R_1	R_2	R_3	R_4	R_5	R_6	R_7	R_8	R_9
Ganoderiol A (**163**)	OH	H	H	H	H	OH	OH	CH_3	CH_2OH
Ganoderiol B (**164**)	O	---	H	OH	H	$\Delta^{24(25)}$	-	CH_2OH	CH_2OH
Ganoderiol F (**165**)	O	---	H	H	H	$\Delta^{24(25)}$	-	CH_2OH	CH_2OH
Gandermanotriol (**166**)	O		H	H	H	OH	OH	CH_3	CH_2OH
Lucidumol B (**167**)	OH	H	H	H	H	OH	CH_3	OH	CH_3

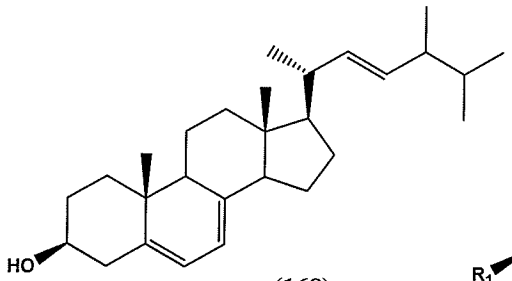

(**168**)

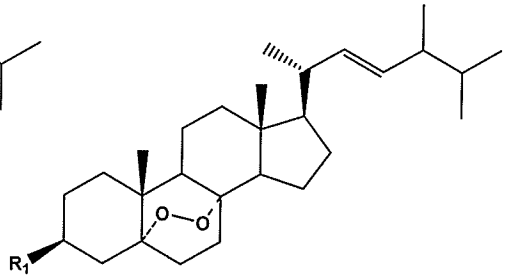

(**169**), R_1=OH, $\Delta^{6(7)}$
(**172**), R_1= O-D-glucopyranoside

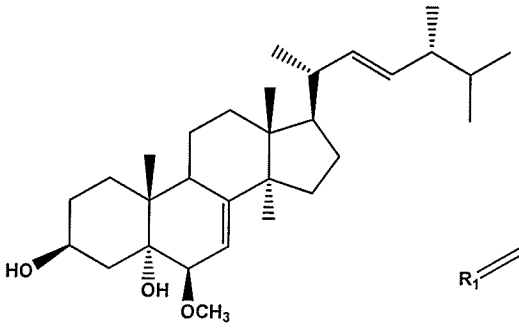

(**171**)

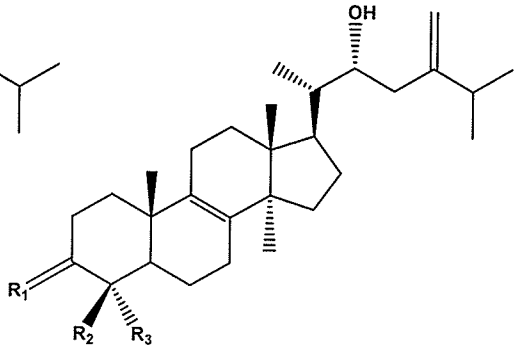

(**173**) R_1 = O R_2 = R_3 = CH_3
(**174**) R_1 = α–H β–OH R_2 = COOH, R_3 = CH_3
(**175**) R_1 = O R_2 = H, R_3= CH_3
(**177**) R_1 = α–H β–OH, R_2, R_3 = CH_3

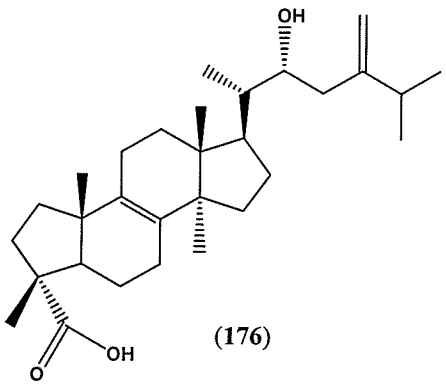

(176)

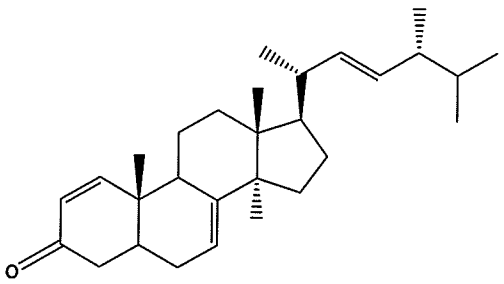

(178)

Coprinus micaceus is a saprophytic fungus commonly found in the prairie region of Canada. It is widely distributed in North America and grows in clusters, mainly in woody areas on decaying wood.

The crude methanolic extract of C. *micaceus* was screened against six pathogenic bacteria namely *Enterococcus faecalis, Staphylococcus aureus, Pseudomonas aeruginosa, Streptococcus agalactia, Corynebacterium xerosis* and *Escherichia coli* according to Kirby-Bauer antimicrobial assay[23].

In the preliminary antibacterial assay, the crude methanolic extract of C. *micaceus* showed anti-bacterial activity against five pathogenic bacteria namely, *Enterococcus faecalis, Staphylococcus aureus, Streptococcus agalactia, Corynebacterium xerosis* and *Escherichia coli.* The antibacterial activity data of the crude extract is shown in table **6.1**.

Chemical studies on the methanolic extract of *C. micaceus* resulted in the isolation of a sterol, micaceol (**179**) and (Z, Z)-4-oxo-2,5-heptadienedioic acid (**180**). In this chapter structure elucidation of these two compounds with the aid of NMR spectral data as well as their bioactivity of these compounds will be discussed.

Table 6.1 Antibacterial data of crude methanolic extract of *C. micaceus*

Bacterium	Zone of inhibition in mm	
	Crude extract 250 µg/disc	Streptomycine 10 µg/disc
E. coli	10.0	22.0
S. aureus	12.0	14.0
C. xerosis	16.5	30.0
S. agalactia	10.5	9.0
E. facecalis	8.0	Nil
P. aeruginosa	Nil	13.0

6.2 Results and discussion

6.2.1 Isolation of compounds 179 and 180

The crude methanolic extract of *C. micaceus* was subjected to chromatographic methods (column and TLC) to purify the compounds, micaceol (**179**) and (Z,Z)-4-oxo-2,5-heptadienedioic acid (**180**) (for purification see experimental section).

The structures of these compounds were established with the aid of extensive spectroscopic studies. These purified compounds (**179-180**) had shown moderate glutathione *S*-transferase inhibitory and antibacterial activities.

6.2.2 Structure elucidation of micaceol (179)

The UV spectrum of micaceol (**179**) showed a maximum absorption at 246 nm indicating the presence of a conjugated π system. The IR spectrum exhibited intense absorption bands at 3425 (OH) and 1601 (C=C) cm^{-1}. The CIMS of **179** showed the molecular ion peak at *m/z* 399 $[M+H]^+$. The HREIMS of this compound showed a molecular ion peak at *m/z* 398.3521 (calcd. 398.3549), corresponding to a molecular formula of $C_{28}H_{46}O$ which indicated the presence of six degrees of unsaturation in **179**. These six double bond equivalents were accounted for by the steroidal skeletons with two double bonds incorporated in its structure.

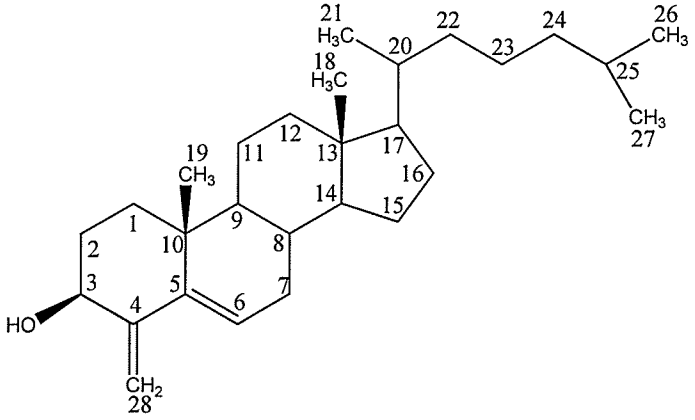

(179)

The ^{1}H-NMR spectrum ($CDCl_3$, 500 MHz) of **179** showed two singlets at δ 0.83 and 0.95, integrating for three protons each, due to the H_3-18 and H_3-19, respectively. Three three-proton doublets at δ 0.78 (J = 6.5 Hz), δ 0.79 (J = 6.5 Hz) and δ 0.85 (J = 7.0 Hz) were due to the secondary H_3-26, H_3-27 and H_3-21, respectively. H-3 resonated as a one-proton double doublet at δ 3.63 (J_1 = 10.5 and 3.5 Hz) and its downfield chemical shift value was indicative of the presence of a geminal hydroxyl functionality. A one-proton multiplet at δ 5.21 was ascribed to H-6. The H_2-28 exocyclic methylene protons appeared as two broad singlets at δ 5.40 and 5.58.

In COSY-45° spectrum, H-3 (δ 3.63) showed cross-peaks with H_2-2 (δ 2.20 and 2.41) which in turn exhibited coupling with H_2-1 (δ1.24 and 1.90). The vinylic couplings between H_2-28 (δ 5.40 and 5.58) and H-6 (δ 5.21) were also observed in the COSY-45° spectrum of **179**. H-6 (δ 5.21) showed vicinal couplings with H_2-7 (δ 2.06 and 1.53). H_3-21 (δ 0.85) exhibited cross-peaks with H-20 (δ 1.59) while H_3-26 (δ 0.78) and H_3-27 (δ 0.79) showed correlations with H-25 (δ 1.51).

The ^{13}C-NMR spectrum ($CDCl_3$, 125 MHz) of **179** showed the resonance of all 28 carbons. The C-3 resonated at δ 71.0 and its downfield chemical shift value was due to the presence of a geminal hydroxyl group. A combination of ^{1}H and ^{13}C-NMR data suggested that compound **179** has a sterol like structure as most of the ^{1}H and ^{13}C-NMR chemical shift values of **179** were similar to those of sterols reported in the literature[24-27]. The HSQC spectrum of **179** showed the one-bond shift correlations of H-3 (δ 3.63) with C-3 (δ 71.0). A signal at δ 5.21 (H-6) showed a cross-peak with the C-6 (δ 134.0). The H_2-28 exocyclic methylene protons (δ 5.40 and 5.58) showed correlations with C-28 (δ 119.1) in the HSQC spectrum. The complete ^{1}H and

^{13}C-NMR chemical shift assignment and ^{1}H/^{13}C one-bond shift correlations of compound **179**, as determined from HSQC spectrum, are presented in Table **6.2**.

In the HMBC spectrum, H_3-19 (δ 0.95) showed long-range heteronuclear couplings with C-5 (δ 146.5), while H_2-28 exocyclic methylene protons (δ 5.40 and 5.58) exhibited interactions with C-3 (δ 71.0), C-4 (δ 140.2) and C-5 (δ 146.5). These HMBC interactions strongly suggested that the C-28 methylene group was substituted at C-4 of the sterol skeleton, and this was also confirmed from the COSY-45° spectrum of **179** which displayed the vinylic couplings of H_2-28 (δ 5.40 and 5.58) with H-6 (δ 5.21). By substituting C-28 at C-4 would produce conjugated π system in **179**. The presence of a conjugated double bond was also inferred by the UV spectrum, which showed an absorption maximum at 246 nm. Important HMBC interactions of compound **179** are shown around structure **179a**.

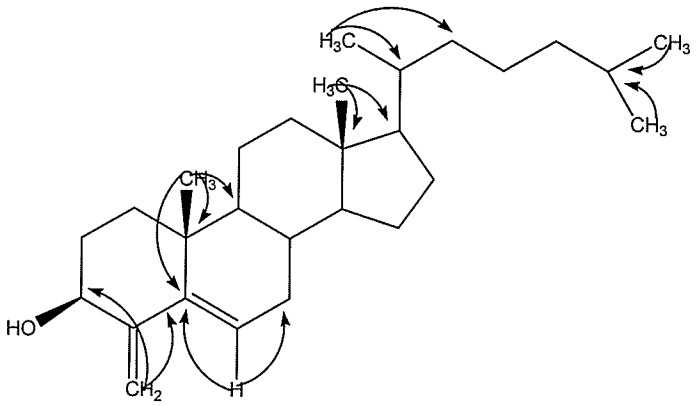

(179a)

The stereochemistry at various chiral centers of **179** was established with the aid of a NOESY spectrum, ^{1}H-^{1}H NMR coupling constants and by comparison of ^{1}H and ^{13}C-NMR chemical shift values of **179** with the reported sterols in the literature. A *cis* relationship between H-8 (δ 1.50), H_3-18 (δ 0.83) and H_3-19 (δ 0.95) was observed in the NOESY spectrum. It has been reported in the literature that H-8, H_3-18 and H_3-19

have β-orientation in sterols[27-29]. The ^{1}H and ^{13}C-NMR chemical shift values of H-8, H_3-18 and H_3-l9 were also nearly identical to those of sterols reported in the literature[27-29]. Based on these observations, β-orientation of H-8, H_3-I8 and H_3-19 was assumed. H-3 resonated as double doublet at δ 3.63 (J = 10.5 and 3.5 Hz). The coupling constant between H-2/H-3 ($J_{2e,3a}$ = 3.5 and $J_{2a,3a}$= 10.5 Hz) indicated that H-3 was axially oriented. This led to the assignment of an α-stereochemistry for H-3 and a β-orientation for C-3/OH. The stereochemistry at H-9, H-I4, and H-17 was also found to be same as reported for other sterols in the literature[28]. Based on these spectral data, structure **179** was established for this new sterol.

Table 6.2 ^{1}H and ^{13}C-NMR data of **179,** recorded at 500 and 125 MHz, respectively.

Carbon No.	^{1}H-NMR (δ)	^{13}C-NMR (δ)	DEPT Multiplicity
1	1.24, 1.90, *m*	32.0	CH_2
2	2.20, 2.41, *m*	39.0	CH_2
3	3.63, *dd*, (10.5, 3.5)	71.0	CH
4	----	140.2	C
5	----	146.5	C
6	5.21, *m*	134.0	CH
7	1.53, 2.06, *m*	27.0	CH_2
8	1.50, *m*	31.7	CH
9	1.01, *m*	51.0	CH
10	---	34.6	C
11	1.47, 1.58, *m*	22.8	CH_2
12	1.60, 1.74, *m*	29.1	CH_2
13	---	46.0	C
14	1.68, *m*	56.5	CH
15	1.65, 1.77, *m*	25.0	CH_2
16	1.49, 2.06, *m*	28.2	CH_2
17	1.57, *m*	56.5	CH
18	0.83, *s*	12.3	CH_3
19	0.95, *s*	22.8	CH_3
20	1.59, *m*	35.5	CH
21	0.85, *d,* (7.0)	18.9	CH_3
22	1.32, 1.52, *m*	36.8	CH_2
23	1.25, 1.47, *m*	23.7	CH_2
24	1.19, 1.54, *m*	39.5	CH_2
25	1.51, *m*	27.9	CH
26	0.78, *d,* (*6.5*)	22.6	CH_3
27	0.79, *d,* (*6.5*)	22.8	CH_3
28	5.40, 5.58, *brs*	119.1	CH_2

Solvent: $CDCl_3$

6.2.3 Structure elucidation of (Z,Z)-4-oxo-2,5-heptadienedioic acid (180)

The EIMS of **180** showed a molecular ion peak at *m/z* 170. Its IR spectrum showed intense absorption bands at 1610 (C=C), 1716 (C=O) and 3438 (OH) cm^{-1}. The UV spectrum of **180** exhibited absorption maxima at 259 nm suggesting the presence of an α,β-unsaturated carbonyl functionality in this compound. The combination of MS, IR, UV, ^{1}H and ^{13}C-NMR spectral data provided the molecular formula, $C_7H_6O_5$.

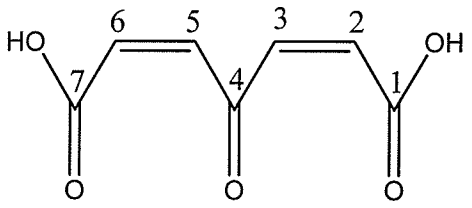

(180)

The ^{1}H-NMR spectrum (DMSO, 500 MHz) of **180** showed the presence of two doublets at δ 5.40 (J = 7.6 Hz) and δ 7.35 (J = 7.6 Hz). These two signals were ascribed to the H-2 and H-3, respectively. A broad peak at δ 11.00 due to the carboxylic acid proton was also observed in the ^{1}H-NMR spectrum.

The broad-band ^{13}C-NMR spectrum (DMSO, 125 MHz) of **180** showed the resonance of four carbons. DEPT experiment was performed to establish the multiplicity of these carbon signals and this indicated the presence of two methine carbons in **180**. Subtraction of the DEPT spectra from the broad-band ^{13}C- NMR spectrum revealed the presence of three quaternary carbons in this compound. The complete ^{13}C-NMR chemical shift assignments are shown in Table **6.3**.

The presence of a carboxylic acid group was further confirmed by the IR spectrum, which showed absorption bands at 3438 (OH) and 1716 (C=O) cm^{-1}. The high resolution FAB mass spectrum of **180** showed the molecular ion peak at *m/z* 170.0439 that provided a molecular formula, $C_7H_6O_5$ (Cald. 170.0446). An ion at *m/z* 152 was

due to the loss of a water molecule from the molecular ion peak. This loss of water molecule was due to the formation of an anhydride of compound **180** in the ionization chamber of the mass spectrometer. The mass spectral data indicated the presence of a plane of symmetry in **180** and explained the observation of signals for one half of the molecule in the ^{1}H and ^{13}C-NMR spectra. A *cis*-configuration for both double bonds of **180** was assumed on the basis of ^{1}H-^{1}H coupling constant ($J_{2,3}$ = 7.6 Hz). The ^{1}H and ^{13}C-NMR data were compared with that of (*2E,5E*)-4-oxo-2,5-heptadieneoic acid (purchased from the Sigma Aldrich) and found to be identical except for the coupling constants between H-2/H-3 and H-5/H-6. The latter exhibited *trans*-coupling constants between H-2/H-3 and H-5/H-6 for *trans*-configuration of Δ^{2-3} and Δ^{4-5}. Based on these spectral data, structure **180** was proposed for this compound. This compound was isolated as a natural product for the first time from natural source.

Table 6.3 ^{1}H and ^{13}C-NMR data of **180,** were recorded at 500 and 125 MHz.

Carbon No.	^{1}H-NMR (δ)	^{13}C-NMR (δ)	DEPT Multiplicity
1	----	166.2	C
2	5.40, *d*,(7.6)	143.0	CH
3	7.35, *d*,(7.6)	154.0	CH
4	----	190.2	C
5	7.35, *d*,(7.6)	154.0	CH
6	5.40, *d*,(7.6)	143.0	CH
7	-----	166.2	C

Solvent: DMSO

6.3 Bioactivity of chemical constituents of *Caprinus micaceus*

6.3.1 Anti-bacterial activity

The anti-bacterial activity of **179** and **180** was examined[30,31]. Compound **180** was found to have modest inhibitory activity against *Staphylococcus aureus* and *Corynebacterium xerosis* with minimal inhibitory concentration (MIC) values of 82.35 and 146μg/mL, respectively. Compound **180** was inactive in this bioassay.

6.3.2 Glutathione *S*-transferase (GST) inhibitory activity

Compound **180** showed inhibitory activity against equine liver GST. The enzyme lost (26.8 ± 0.6)% of its activity in the presence of 32 μg/mL of **180**. Lower concentrations of this compound, 16 μg/mL and 24 μg/mL resulted in (l4.1±2.5) % and (19.7±5.6) % GST inhibition, respectively. Although considered weak, the inhibition may be due to the presence of α,β-unsaturated carbonyl functionality in compound **180**, which promotes the formation of a conjugate with glutathione. GST inhibition, in this case, may be attributed to adduct formed between glutathione and **180**. GSH conjugates have been discovered for most α,β-unsaturated carbonyl compounds as effective inhibitors of various GST isoforms[32-35]. In this bioassay, compound **179** was found to be inactive.

6.4 Experimental

6.4.1 General Experimental conditions

General experimental conditions for this part of research were the same as previously discussed in chapters **2-5.**

6.4.2 Collection of mushroom

Coprinus micaceus (1.4 kg) was collected from Winnipeg, Manitoba, Canada in September 2004. Prof. Richard Staniforth, Department of Biology, the University of Winnipeg identified this mushroom as C. *micaceus.*

6.4.3 Extraction and isolation

Coprinus micaceus was dried in the air at room temperature and diced into small pieces. This organism was extracted with methanol at room temperature. The solvent was removed under reduced pressure to obtain a gum. This gum was then dissolved in water and partitioned between butanol and water. The butanol layer was further defatted with hexane. The defatted extract was concentrated by using rotavap to yield a dark brown gummy residue (24.86 g). This extract was then loaded onto a silica-gel column. The column was eluted with hexane-ethyl acetate (0-100%) and ethyl acetate-methanol (0-100%) to afford 39 fractions. Similar fractions were pooled together on the basis of analytical TLC which gave six fractions (F_1-F_6) altogether. A fraction F_2 (0.0237 g) was obtained on elution of the silica-gel column with hexane: ethyl acetate (11: 9 v/v) and was subjected to preparative thin layer chromatography using hexane: ethyl acetate (3:2 v/v) as a mobile phase to afford light yellow amorphous solid of compound **179** (7.82 mg, 0.00056%, R_f = 0.72) and brown solid of compound **180** (3.55 mg, 0.00025%, R_f = 0.46) as shown in Scheme **6.1**.

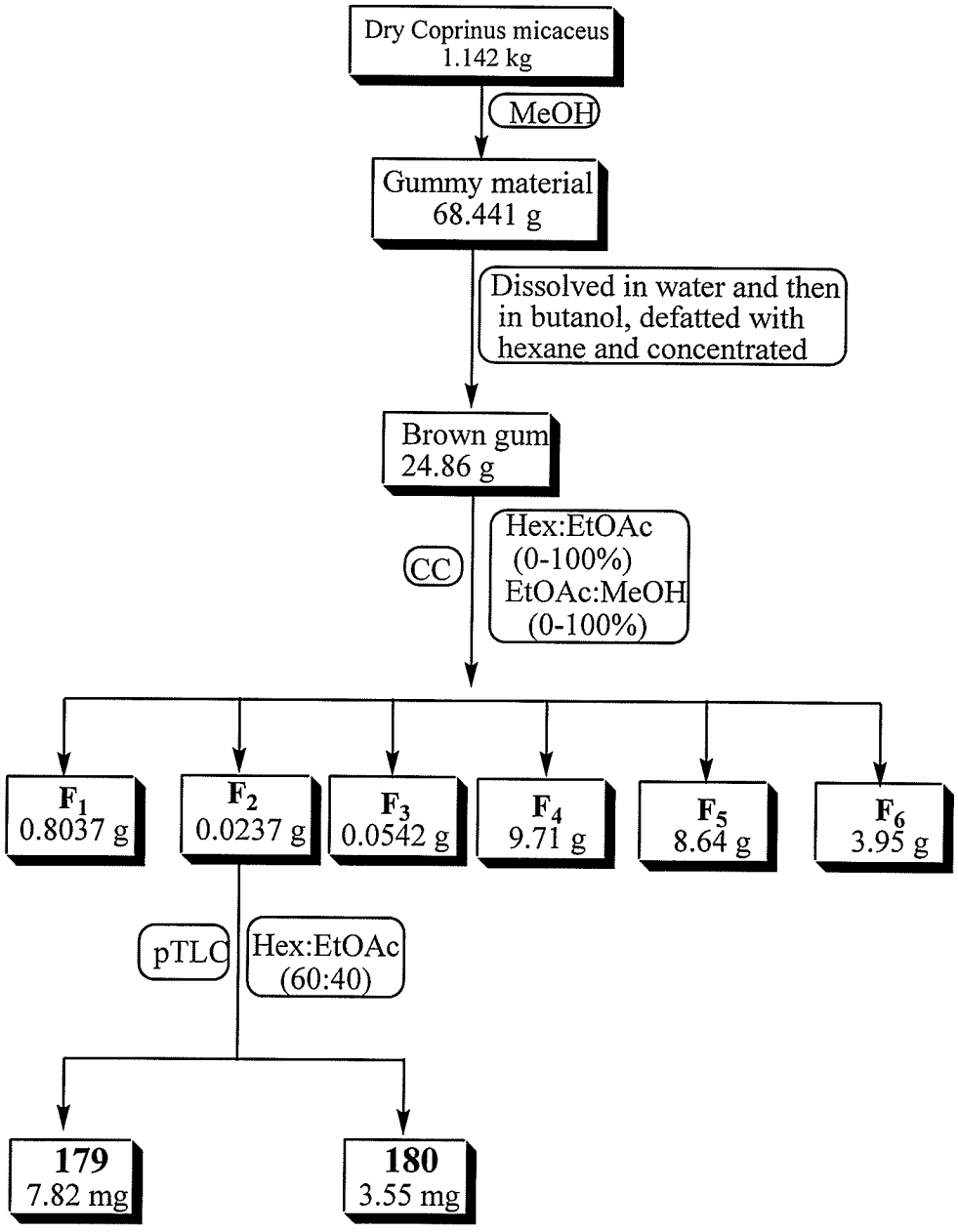

Scheme 6.1 Isolation procedure for compounds **179** and **180**

6.4.4 Micaceol (179)

Light yellow amorphous solid, 7.82 mg, % yield 0.00056%, R_f = 0.72 (hex:EtOAc, 60:40), $C_{28}H_{46}O$, $[\alpha]^{25}D$ = 45° (c = 0.12, $CHCl_3$); UV λ_{max} (EtOAc): 246 nm; IR υ_{max} (KBr): 3425 (OH), 2926 (CH), 1601 (C=C) cm^{-1}; for ^1H and ^{13}C-NMR spectral data see Table **6.2**; ElMS *m/z* (rel. int.): 398 (M^+, 5%), 383 (M^+-CH_3, 11%), 380 (M^+-H_2O, 19%), 43 (100%).

6.4.5 (Z, Z)-4-oxo-2, 5-heptadienedioic acid (180)

Brown solid, 3.55 mg, % yield 0.00025%, R_f = 0.46 (hex:EtOAc, 60:40), $C_7H_6O_5$, UV λ_{max} (MeOH): 259 nm; IR υ_{max} (KBr): 1610 (C=C), 1716 (C=O) and 3438 (OH) cm^{-1}; for ^1H and ^{13}C-NMR spectral data see Table **6.3**; ElMS *m/z* (rel. int.): 170 (M^+, 2%), 152 (M^+-H_2O, 25%).

6.4.6 Enzyme inhibition assays

6.4.6.1 Glutathione *S*-transferase inhibition assay

Glutathione *S*-transferase inhibitory activity of both compounds (**179** and **180**) was determined as described in chapter **2**, page 50.

6.4.6.2 Anti-bacterial assay

The methanolic crude extract of *C. micaceus* was screened against six pathogenic bacteria namely *Escherischia coli* (ATCC 25922), *Staphylococcus aureus* (ATCC 25933), *Corynebacterium xerosis* (ATCC 373), *Streptococcus agalactia* (ATCC 13813), *Entrococcus faecalis* (ATCC 194333) and *Pseudomonas aeruginosa* (ATCC 27853). All of these bacterial cultures were provided by Dr. Paul Holloway, Department of Biology, University of Winnipeg, Manitoba. Sterile six mm filter paper discs were loaded with 250 µg of crude methanolic extract of *C. micaceous* in sterile conditions. A negative control was also prepared by loading a disc with 450 µl of

methanol. Streptomycine (10 μg/disc) was used as positive control. A single colony from each bacterial culture was picked and inoculated into 3 mL of Muller-Hinton (MH) broth, pH 7.2 in 10 mL sterile test tubes and kept at 37C° overnight with vigorous shaking. The next morning each bacterium from freshly grown cultures was swabbed on MH agar plates. The pre-loaded paper discs along with positive and negative controls were placed on each plate for all bacterial strains as stated above and were incubated at 37C°. After 24 hours the zone of inhibition around each disc was measured. The results are tabulated in Table **6.1**.

Both purified compounds **179** and **180** were also tested against *E. coli*, *S. aureus*, *C. xerosis*, *S. agalactia*, and *E. faecalis* by following the above stated methodology. The compound **180** was inactive while the compound **179** showed positive results at a concentration of 50μg/disc against *S. aureus* and *C. xerosis*. Consequently the Minimu Inhibitory Concentration (MIC) of **179** that can inhibit the visible growth of *S. aureus* and *C. xerosis* was determined using a two fold serial dilution assay[36]. The overnight cultures of both bacteria (*S. aureus* and *C. xerosis*) were diluted to 0.5 Mc-Farland standard turbidity by using MH-broth. A stock solution of of **179** was prepared by dissolving 1.318 mg in minimum amount of THF and was diluted with sterile distilled water up to 1 mL. This stock solution was divided into two equal portions. Two fold serial dilutions from each portion were made in the concentration range of 0.64-658.8 μg/mL by using bacterial suspension (10^5 colony forming units-CFU/mL) in 10 mL sterile test tubes. A Positive growth control (equal volume of MH-both, 100 μl of THF and bacterial suspension), blank or sterile control (1 mL of MH-broth) and reference/ standard control-chloramphenical were also prepared. The tubes were incubated at 37C° for 18 hours on a gyrorotary shaker (135 rpm). After incubation period, the

optical density (OD_{620}) of each was measured. No growth was observed in blank control.

6.5 References

[1] Chang, S. T. *Int. J. Med. Mushrooms*, **1999**, 1, 1.

[2] Reshetnikov, S. V.; Wasser, S. P.; Tan, K. K. *Int. J. Med. Mushrooms*, **2001**, 3, 361.

[3] Hobbs, C. *Medicinal Mushroom: An Exploration of Tradition, Healing and culture*, 2nd ed., Botanica Press, Santa Cruz, CA, **1995**.

[4] Jones, K. R. *Ancient Herb for Modern Times*, 2nd ed., Sylvan Press, Seattle, **1996**.

[5] McKenna, D. J. *Natural Dietary Supplements: A Desktop Reference*, Institute for Natural Product Research, St. Croix, U. S., Virgin Islands, **1998**.

[6] Chang, H. M.; But, R. P. *Pharmacology and Applications of Chinese Materia Medica* 1, World Scientific: Singapore, **1986**, 642.

[7] Collins, R. A.; Ng, T. B. *Life Sci.,* **1997**, 60, 383.

[8] Smania, A.; Monache, F. D.; Logueričio-Leite, C.; Smania, E. F. A.; Geber , A. L. *Int. J. Med. Mush.*, **2001**, 3, 87.

[9] Suay, I.; Aernal, F.; Asenio, F. J.; Basilio, A.; Cabello, M. A.; Diez, M. T.; Garcia, J. B.; Gonzalez del Val, A.; Gorrochategui, J.; Hernandez, P.; Pelaez, F.; Vicente, M. F. *Antionie van Leeuwenhoek,* **2000**, 78, 129.

[10] Suzuki, H.; Iiyarria, K.; Yoshida, O.; Yamazaki, S.; Yamamoto, N.; Toda, S. *Agric. Bio. Chem.*, **1990**, 54, 479.

[11] Mizuno, T. *Int. J. Med. Mushrooms*, **2002**, 4, 32.

[12] Wasser, S. P. *Appl. Microbial. Biotechnol.,* **2002**, 60, 258.

[13] Shi, Y. L.; James, A. E.; Benzie, I. F. F.; Buswell, J. A. *Teratogenesis Carcinogensis Mutoagensis*, **2002**, 22, 103.

[14] Chihara, G.; Hamuro, J.; Maeda, Y.; Arai, Y.; Fukuoka, F. *Cancer Res.*, **1970**, 30, 2776.

[15] Chihara, G.; Maeda, y.; Humuro, J.; Sasaki, T.; Fukuka, F. *Nature,* **1969**, 222, 687.

[16] Suzuki, S.; Oshima, S. *Mushroom Sci.*, **1976**, 9 (Part I), 463.

[17] Tsunoda, A.; Ishida, N.; *Ann. N. Y. Acad. Sci.*, **1969**, 173, 719.

[18] Yoshida., O.; Nakashima, K.; Yoshida, T.; Kaneko, Y.; Yamamoto, I.; Matsuzaki, K.; Uryu, T.; Yamamoto, N.; Yoshida, O.; Nakashima, K.; Yoshida, T.; Kaneko, Y.; Yamamoto, I.; Matsuzaki, K.; Uryu, T.; Yamamoto, N. *Biochem. Phann.*, **1988**, 37, 2887.

[19] Min, C. N.; Nakamura, N.; Miyashiro, H.; Bae, K. W.; Hattori, M. *Chem. Pharm. Bull.*, **1998**, 46, 1607.

[20] El-Mekkawy, S.; Meselhy, M. R.; Nakamura, N.; Tezuka, Y.; Hattori, M.; Kakiuchi, N.; Shimotohno, K.; Kawahara, T.; Otake, T. *Phytochemistry,* **1998**, 49, 1651.

[21] Bok, J. W.; Lermer, L.; Chilton, J.; Klingeman, H. G.; Towers, G. H. N. *Phytochemistry*, **1999**, 51, 891.

[22] Liu, H.; Tasi, T.; Chang, T.; Chou, C.; Lin, L. *Phytochemistry*, **2009**, 70, 558.

[23] Ishikawa, N. K.; Fukushi, Y.; Yamaji, K.; Tahara, S.; Takahashi, k.; *J. Nat. Prod.*, **2001**, 64, 932.

[24] Yamada, Y.; Suzuki, S.; Iguchi, K.; Kikuchi, H.; Tsakitani, Y.; Horiai, H.; Nakanishi, H. *Chem. Pharm. Bull.*, **1980**, 28, 473.

[25] Pettit, G. R.; Numata, A.; Cragg, G. M.; Herald, D. L.; Takada, T.; Iwamoto, Riesen, C. R.; Schmidt, J. M.; Doubek, D. L.; Goswarni, A. *J. Nat. Prod.*, **2000**, 63, 72.

[26] Kobayashi, M.; Hayashi, T.; Hayashi, K.; Tanabe, M.; Nakagawa, T.; Mitsuhshi, H. *Chem. Pharm. Bull.*, **1983**, 31. 1848.

[27] Masaru, K.; Takaaki, H.; Furnie, N.; Hiroshi, M. *Steroids*, **1979**, 34, 285.

[28] Li, Y.; Ishibashi, M.; Satake, M.; Chen, X.; Oshima, Y.; Ohizumi, Y. *J. Nat. Prod.*, **2003**, 66, 696.

[29] Liiourneux, Y.; Khuong-Huu, Q.; Gut, M.; Lukacs, G. *J. Org. Chem.*, **1975**, 40, 1674.

[30] Iscan, G.; Kirimer, N.; Kurkcuoglu, M.; Baser, H. C. K.; Demirci, F. *J. Agric. Food Chem.*, **2002**, 50, 3943.

[31] Holt, R. J. *J. Clin. Path.*, **1975**, 18, 767.

[32] Burg, D.; Filippov, D. V.; Hermanns, R.; van der Marel, G. A.; van Boom, J. H.; Mulder, G. *J. Bioorg. Med. Chem.*, **2002**,10, 195.

[33] Schmidt, T. *J. Planta Med.*, **2000**, 66, 106.

[34] Zhao, G.; Yu, T.; Wang, R.; Wang, X.; Jing, Y. *Bioorg. Med. Chem.*, **2005**, 13, 4056.

[35] Habig, W. H.; Pabst, M. J.; Jakoby, W.B. *J. Biol. Chem.*, **1974**, 249, 7130.

[36] National Committee for Clinical Laboratory Standards. *Methods for dilution antimicrobial susceptibility tests for bacteria that grow aerobically.* 3rd ed., approved standard, **1993**, NCCLS document M7-A3 NCCLS, Villanova, Pennsylvania, USA.

CHAPTER 7

Conclusions

The overall goal of this project was to perform phytochemical studies on medicinally important plants (*Vitex pinnata*, *Artocarpus nobilis*, *Barleria prionitis* and *Buxus natalensis*) and saprophytic fungus (*Coprinus micaceus*) in order to isolate their chemical constituents and to evaluate them for AChE and GST inhibitory activities. These studies afforded six new natural products, [6″-glucosepednucullariside (**88**), artocarpurate A (**109**), atocarpurate B (**110**), natalensamine A (**156**), micaceol (**179**) and (Z, Z)-4-oxo-2,5-heptadienedioic acid (**180**)] and fourteen known compounds [pedunculariside (**89**), agnuside (**90**), *p*-hydroxy benzoic acid (**91**), cyclolaudenyl acetate (**111**), lupeol acetate (**112**), β-amyrine acetate (**113**), 12, 13-dihydromicromeric acid (**114**), artonins E (**115**), artobiloxanthone (**116**), barlerin (**127**), shanzhiside methyl ester (**128**), lupeol (**129**), betulinic acid (**130**) and pipataline (**131**)]. These studies provided new sources for the previously described pharmaceutically active compounds. Examples include pedunculariside, agnuside, cyclolaudenyl acetate, lupeol acetate, β-amyrine acetate, 12,13-dihydromicromeric acid, lupeol and pipataline. All of the purified compounds were found to exhibit different levels of GST and AChE inhibitory activities. The bioactivity data indicated that flavonoids have potent GST inhibitory activities. Further GST inhibition studies on other structurely related flavonoids are warranted in order to explore their potential biomedical applications. All of these compounds exhibit moderate to weak AChE inhibitions. These compounds may be used as a template to synthesize different analogues that might have potent AChE inhibitory activity. For instance Sauvaître

et al. has recently reported a potent selective AChE inhibitor "oxazine" with IC_{50} value of 0.029 μM. Oxazine was synthesized from a natural product, *N*-3-isobutyrylcycloxobuxidine-F, which was a weak AChE inhibitor (IC_{50} >10 μM)[1]. Compound **131** was structurally modified into three derivatives, 7,8-epoxypipataline (**131**), 7-amino-8-hydroxy pipataline (**133**) and 7, 8-dibromopipataline (**134**) and were evaluated for AChE inhibitory activity. The derivative (**133**) showed improved AChE inhibitory activity compared to the parent compound **131**. Additionally we had also discovered anti-oxidant activities of 6″-glucosepeduncullariside (**88**), pedunculariside (**89**), agnuside (**90**), *p*-hydroxy benzoic acid (**91**), artonins E (**115**), artobiloxanthone (**116**).

7.1 References

[1] Sauvaître, T.; Barlier, M.; Herlim, D.; Gresh, N.; Chiaroni, A.; Guenard, D.; Guillou, C. *J. Med. Chem.*, **2007**, 50, 5311.

^{1}H-NMR spectrum of 6”-glucosepeduncullariside (**88**)

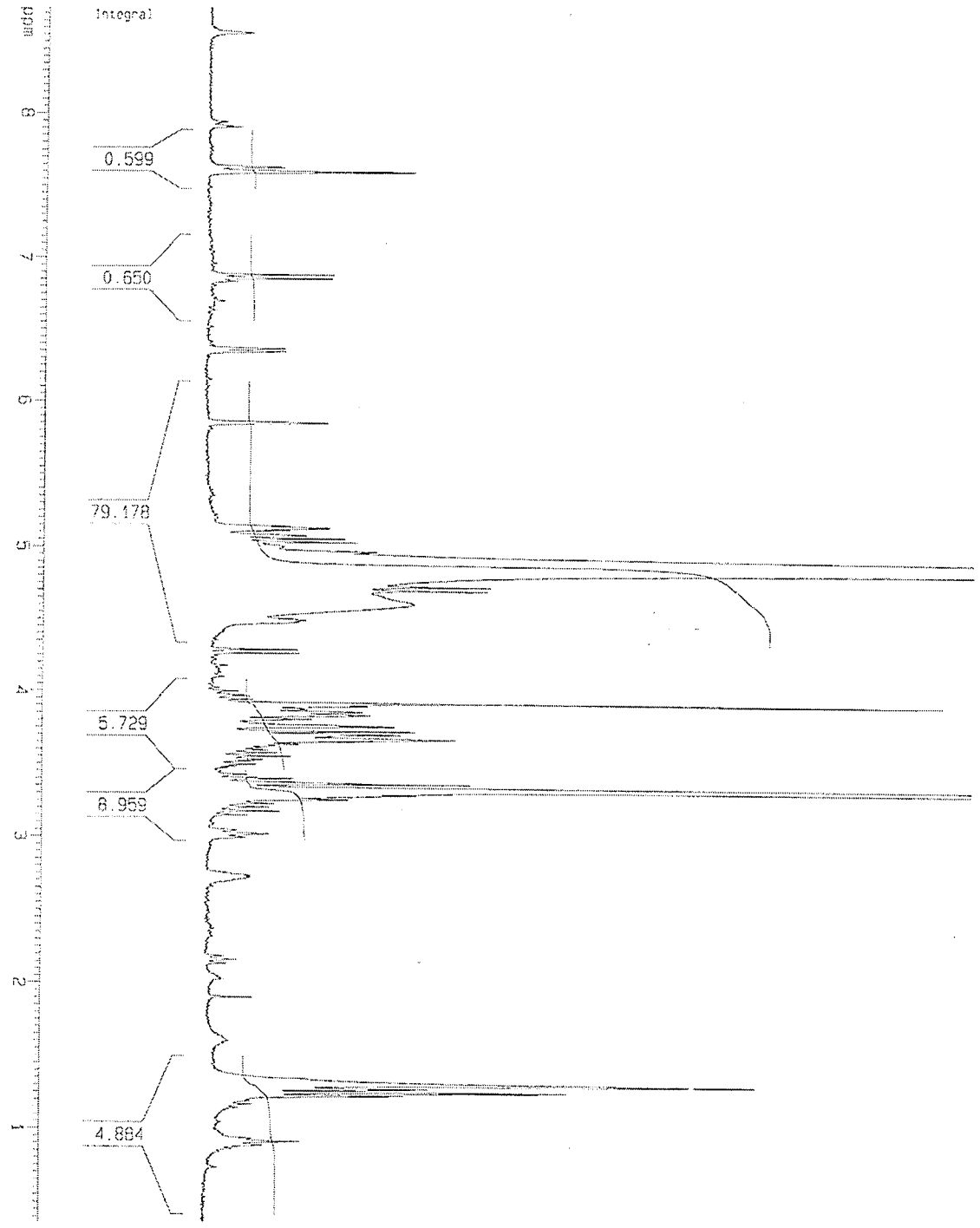

^{13}C-NMR spectrum of 6”-glucosepeduncullariside (**88**)

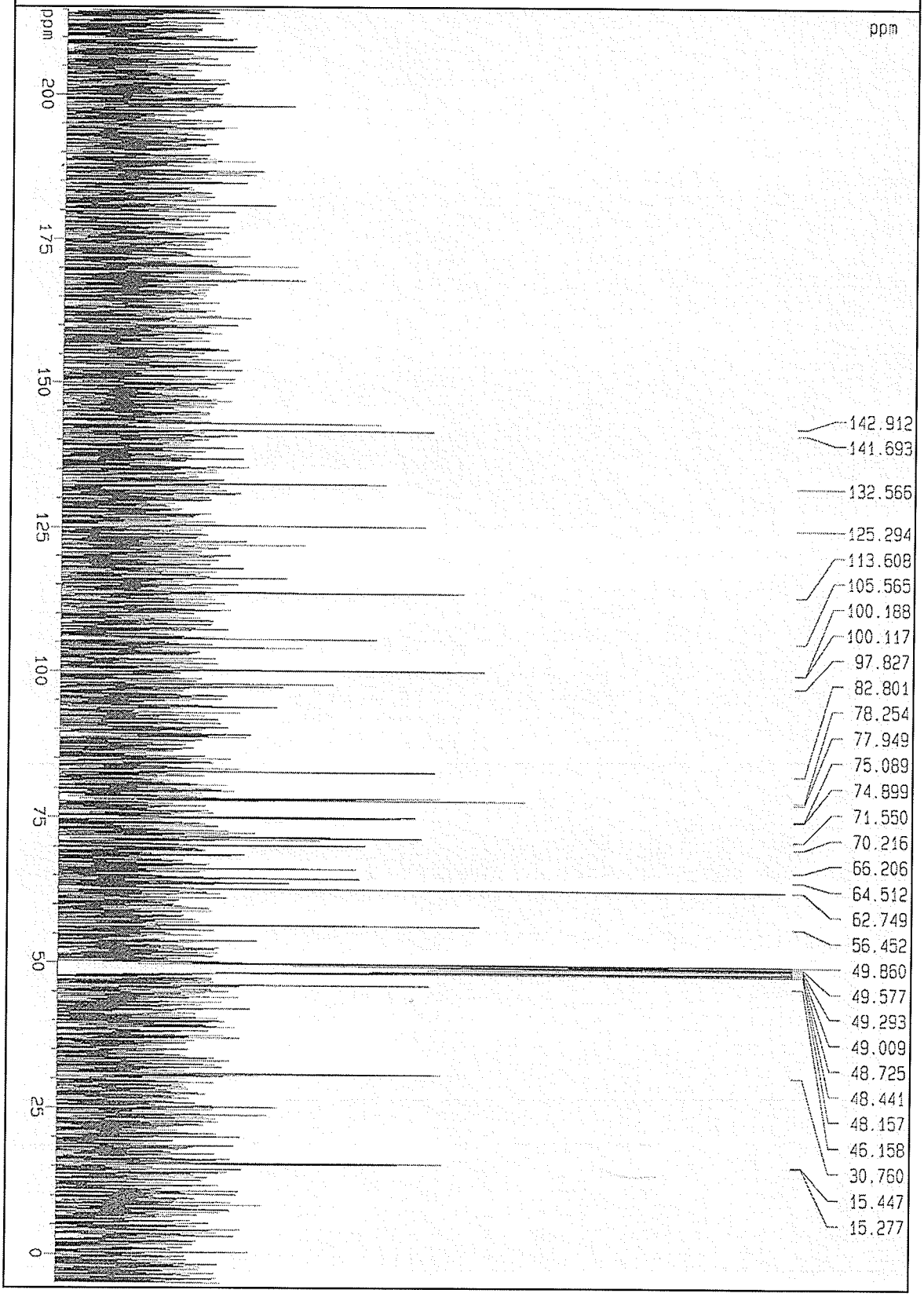

^{1}H-NMR spectrum of pedunculariside (**89**)

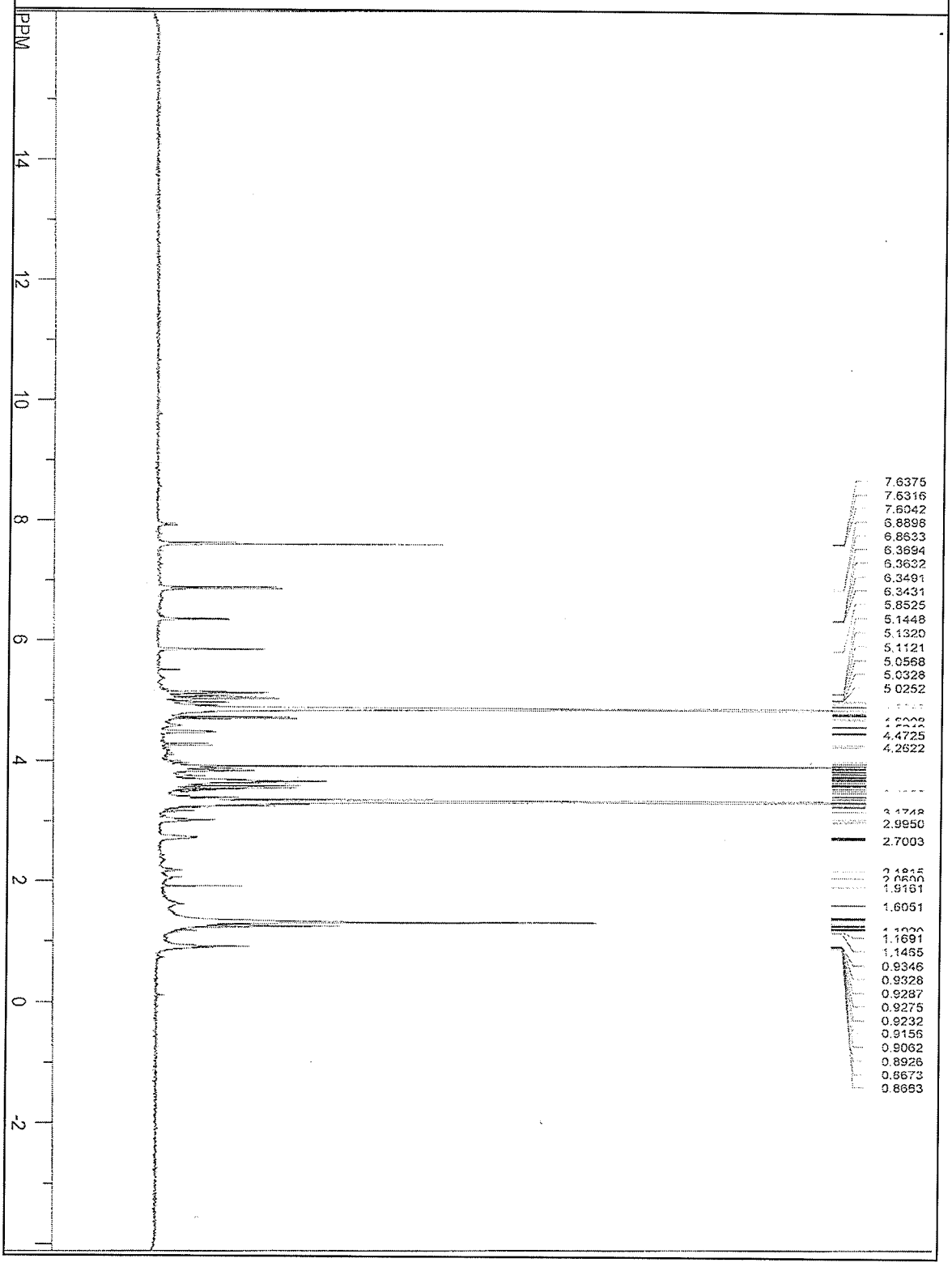

^{13}C-NMR spectrum of pedunculariside (**89**)

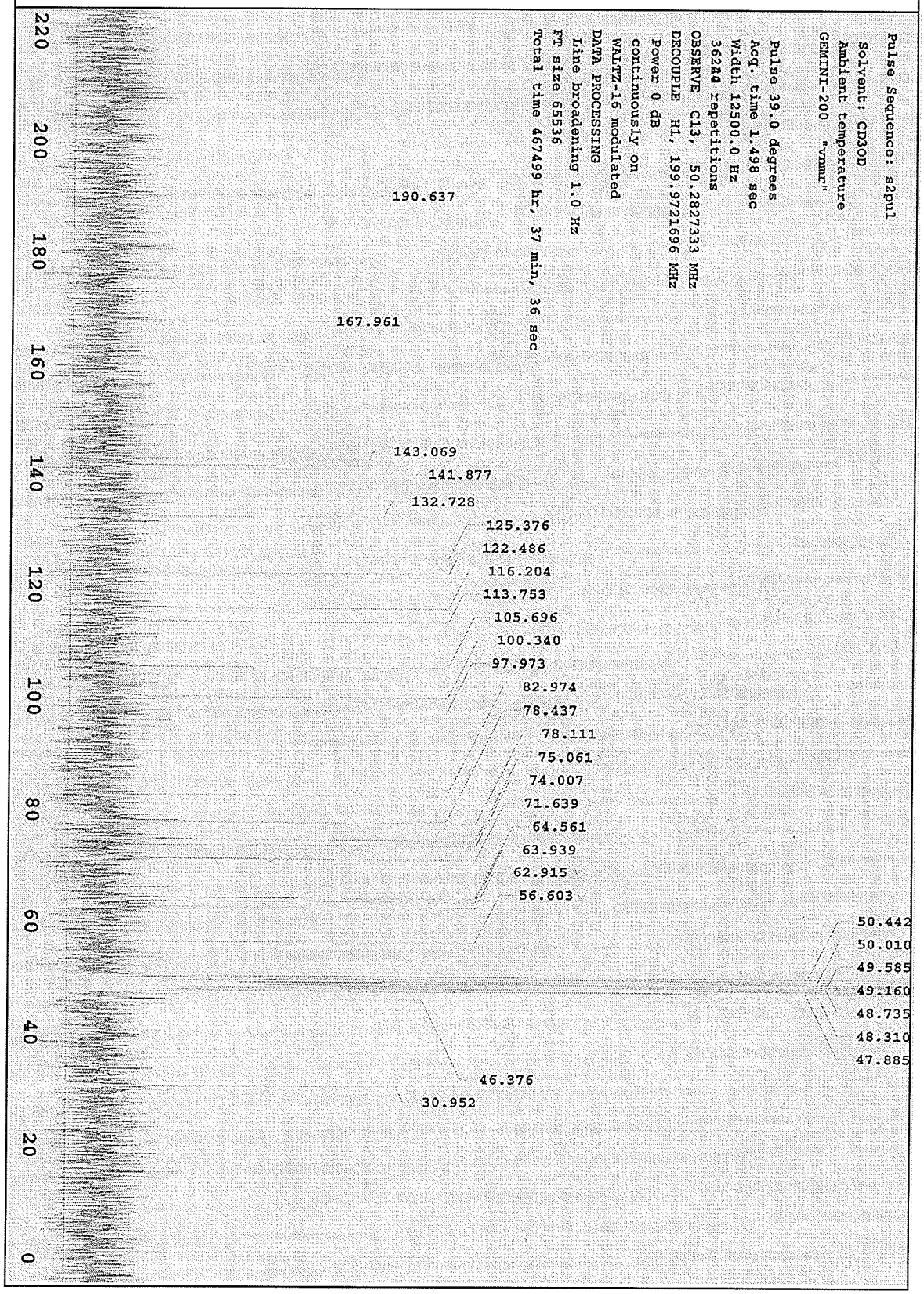

^{1}H-NMR spectrum of agnuside (**90**)

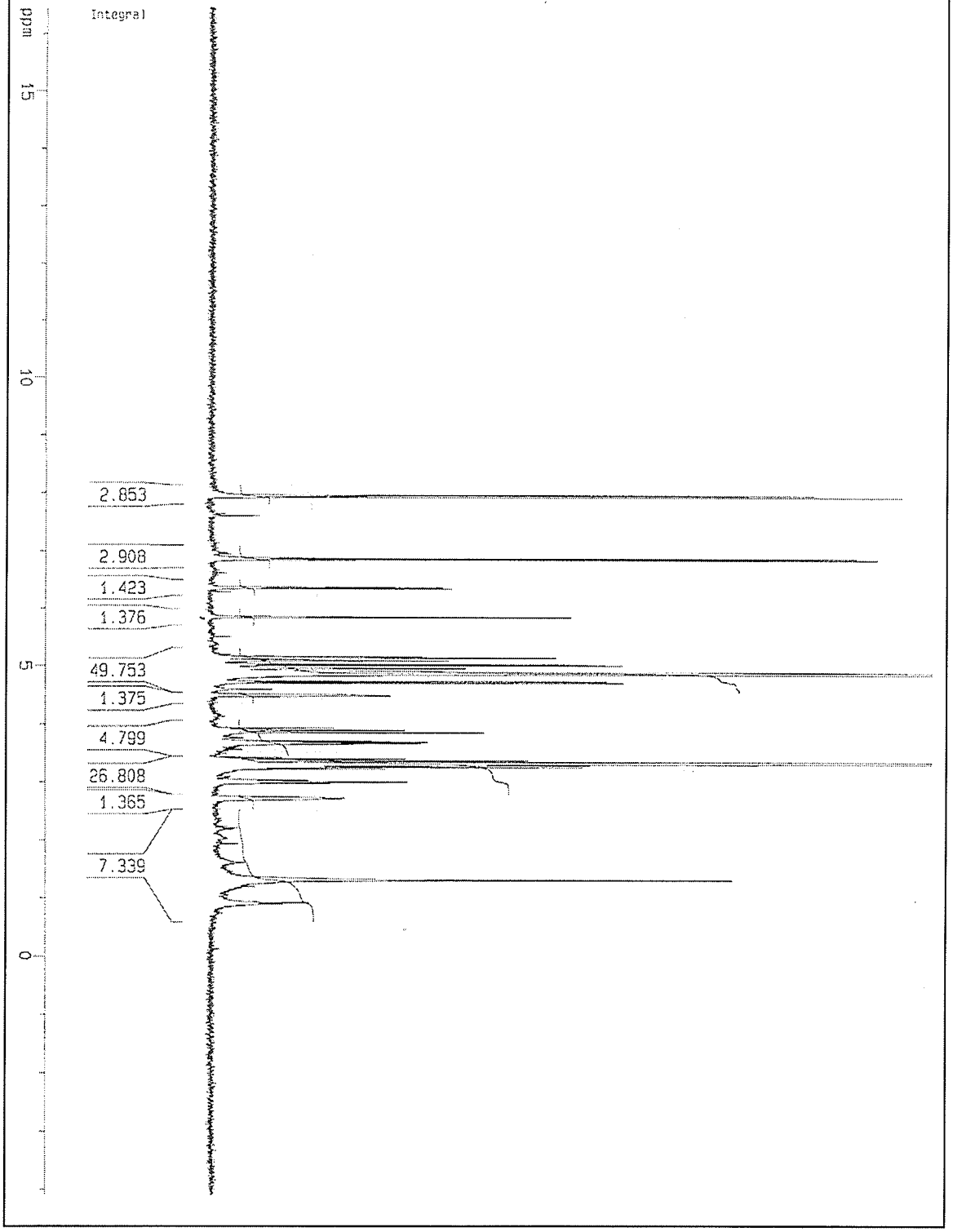

^{13}C-NMR spectrum of agnuside (**90**)

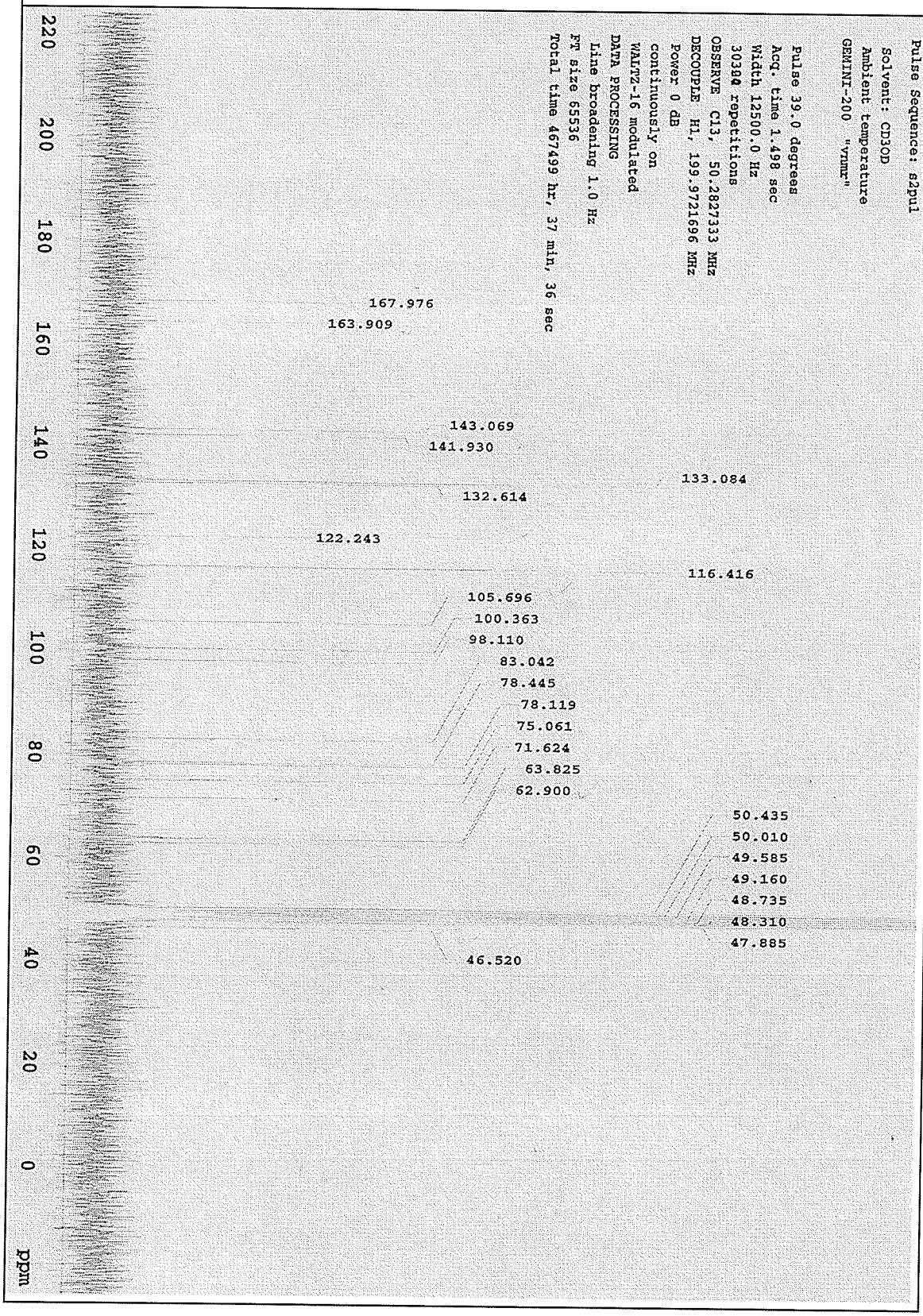

^{1}H-NMR spectrum of *p*-hydroxy benzoic acid (**91**)

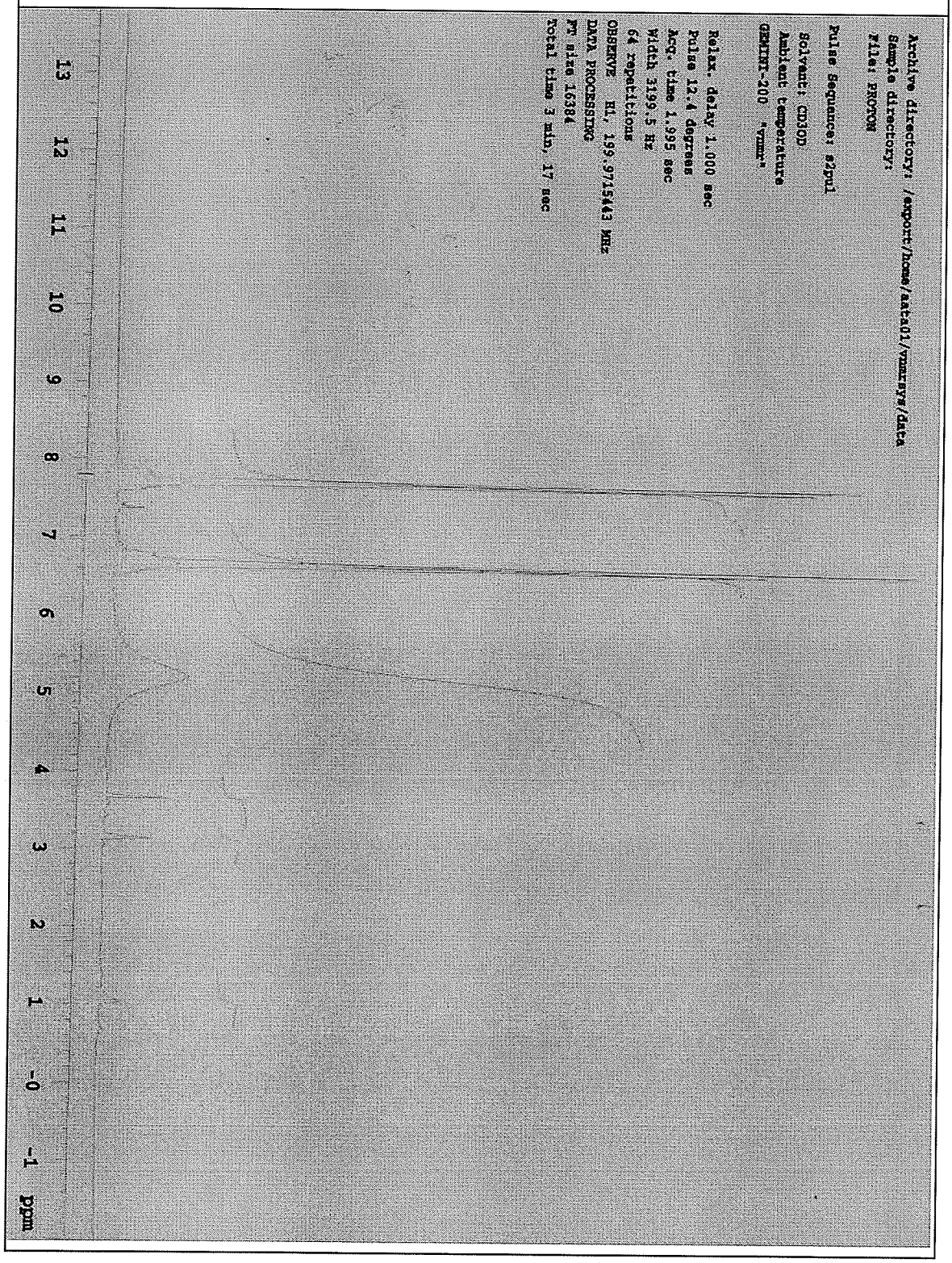

^{13}C-NMR spectrum of *p*-hydroxy benzoic acid (**91**)

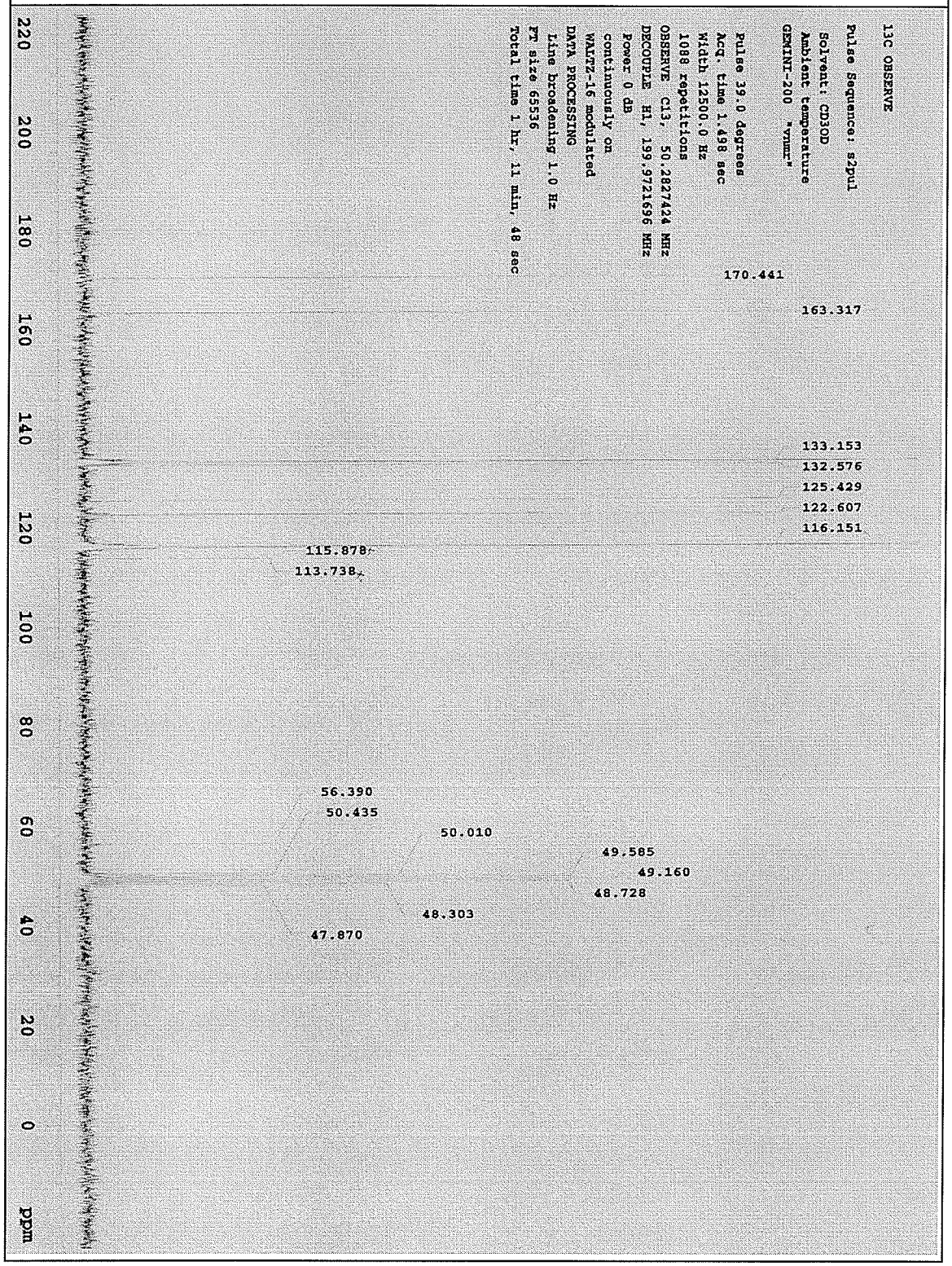

^{1}H-NMR spectrum of artocarpuate A (**109**)

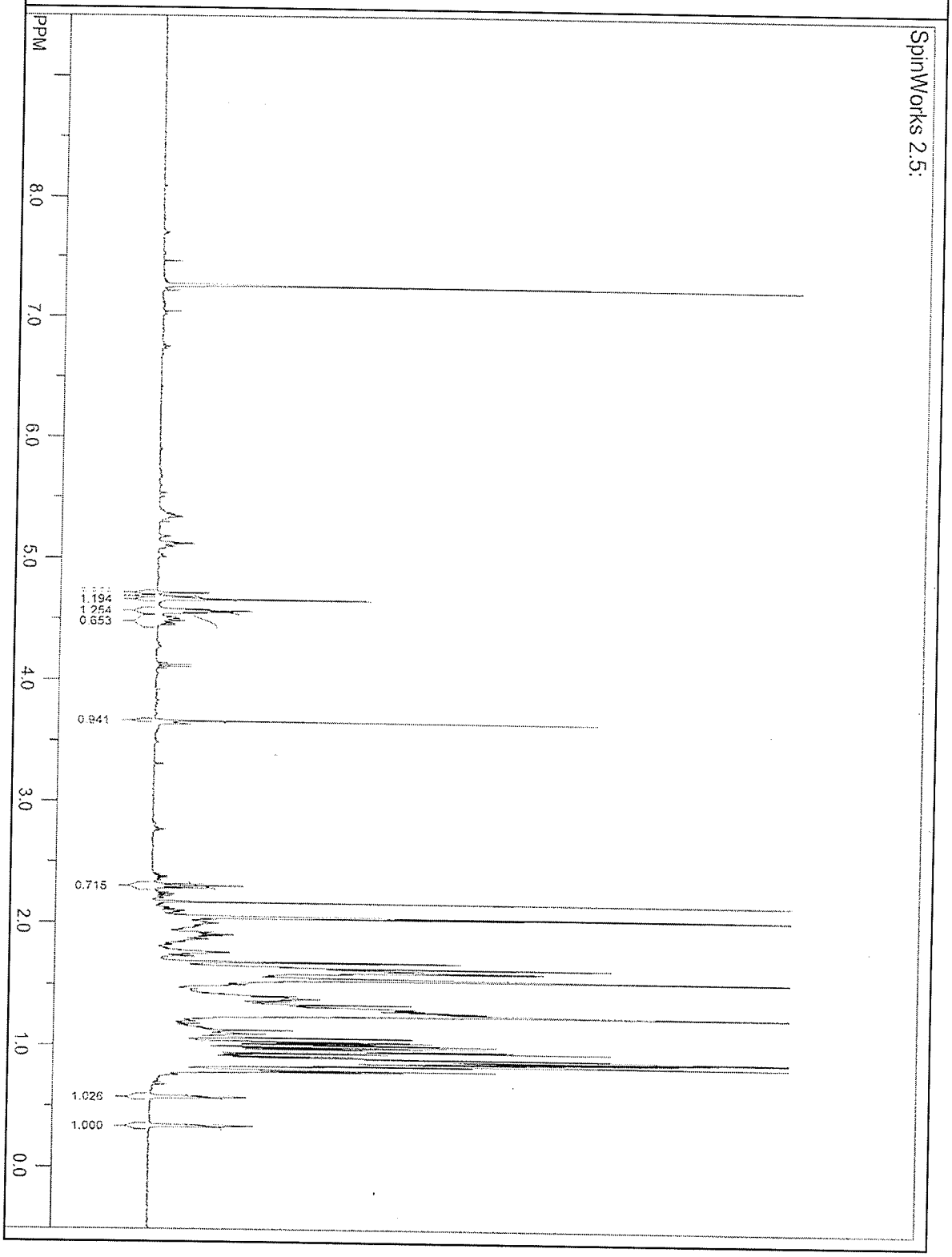

^{13}C-NMR spectrum of artocarpuate A (**109**)

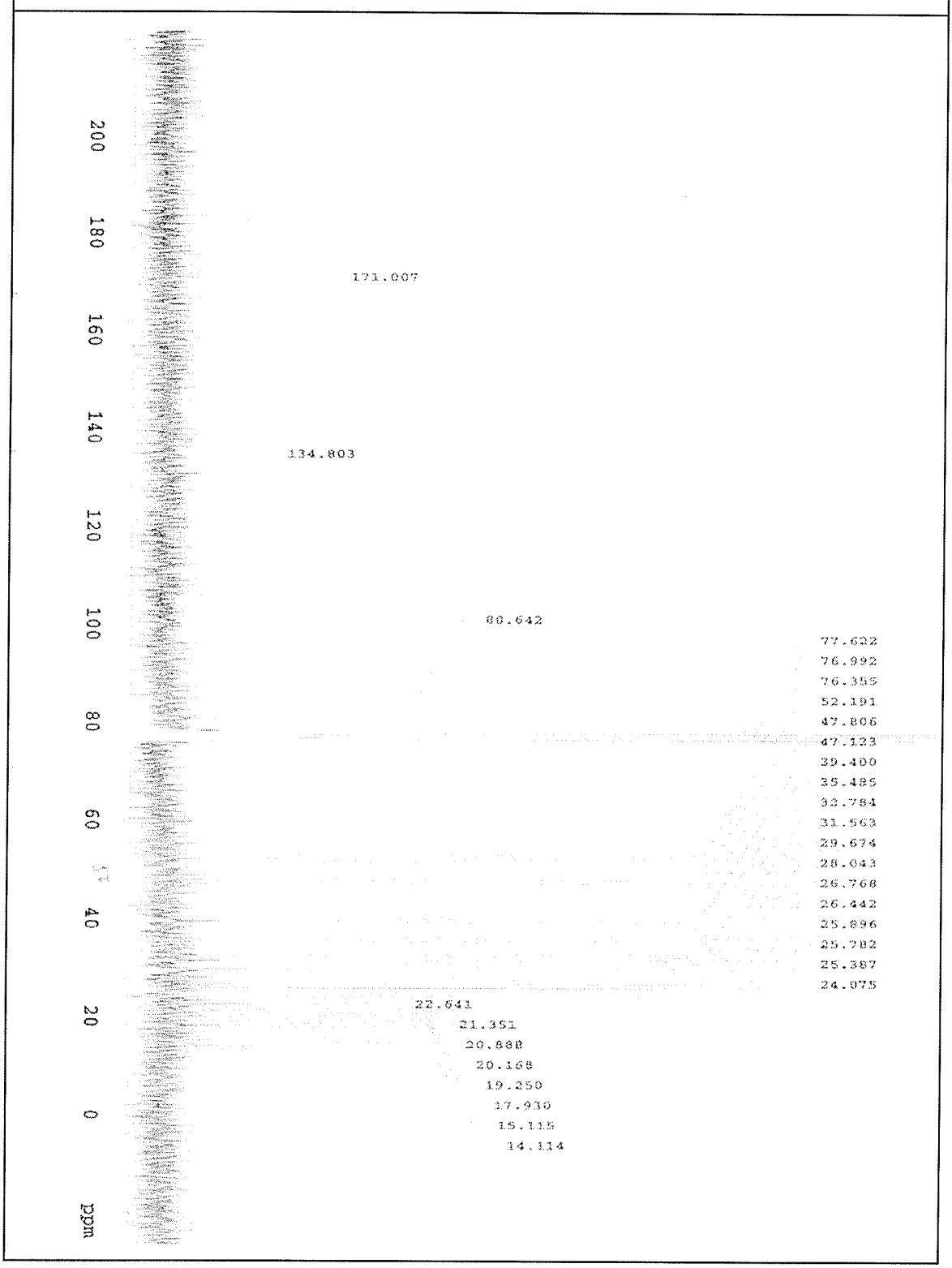

^{1}H-NMR spectrum of artocarpuate B (**110**)

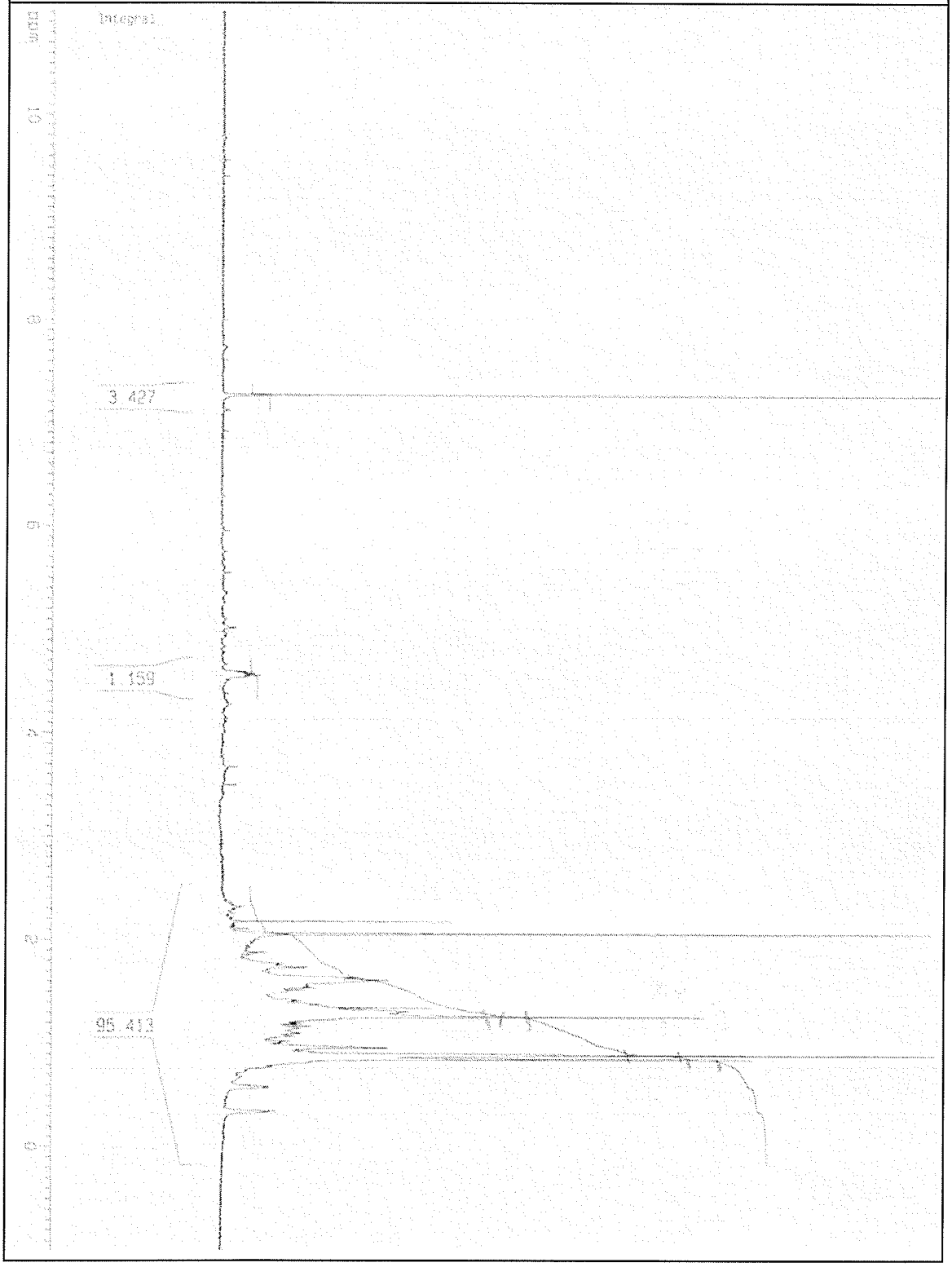

^{13}C-NMR spectrum of artocarpuate B (**110**)

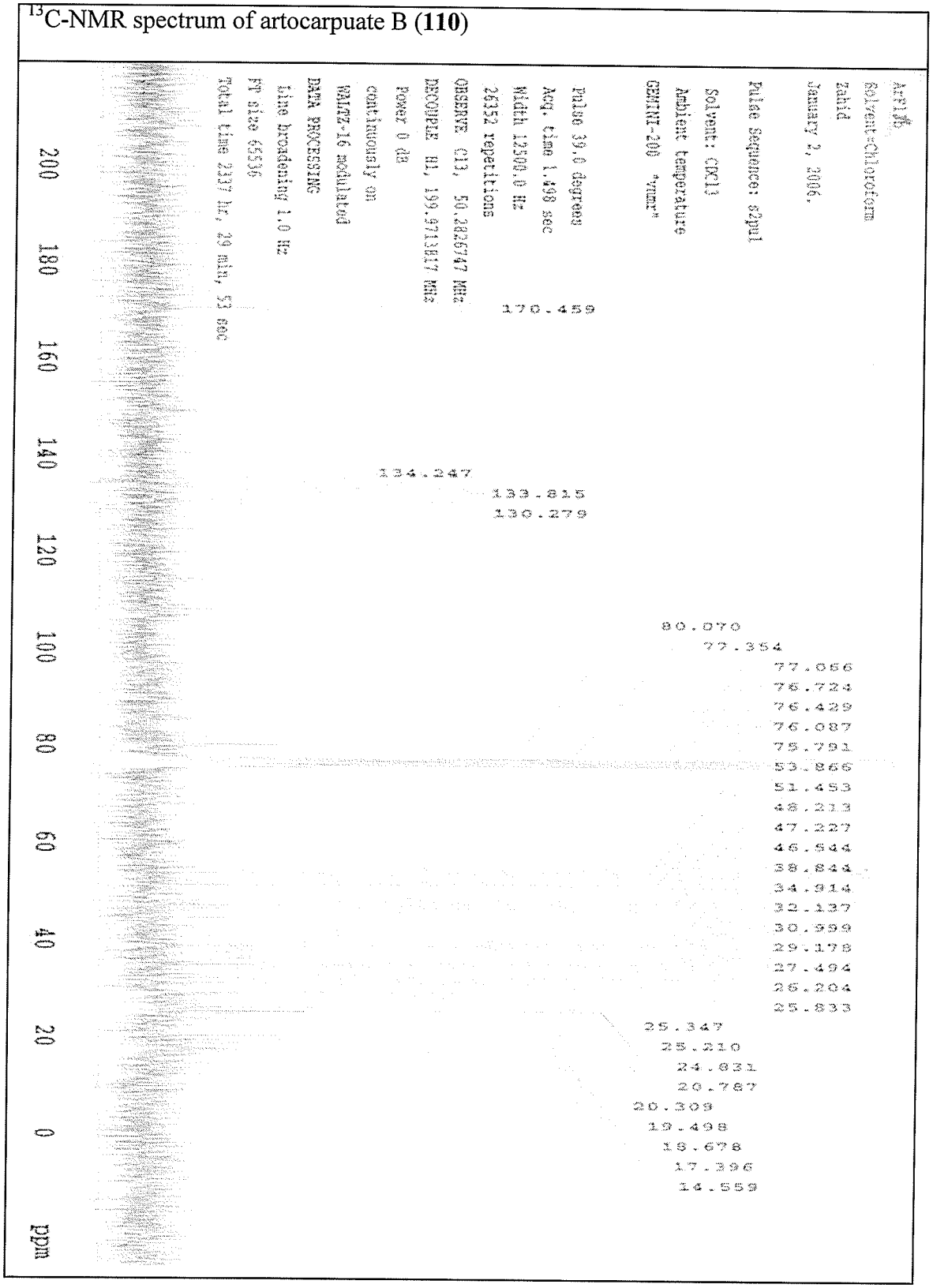

^{1}H-NMR spectrum of cyclolaudenyl acetate (**111**)

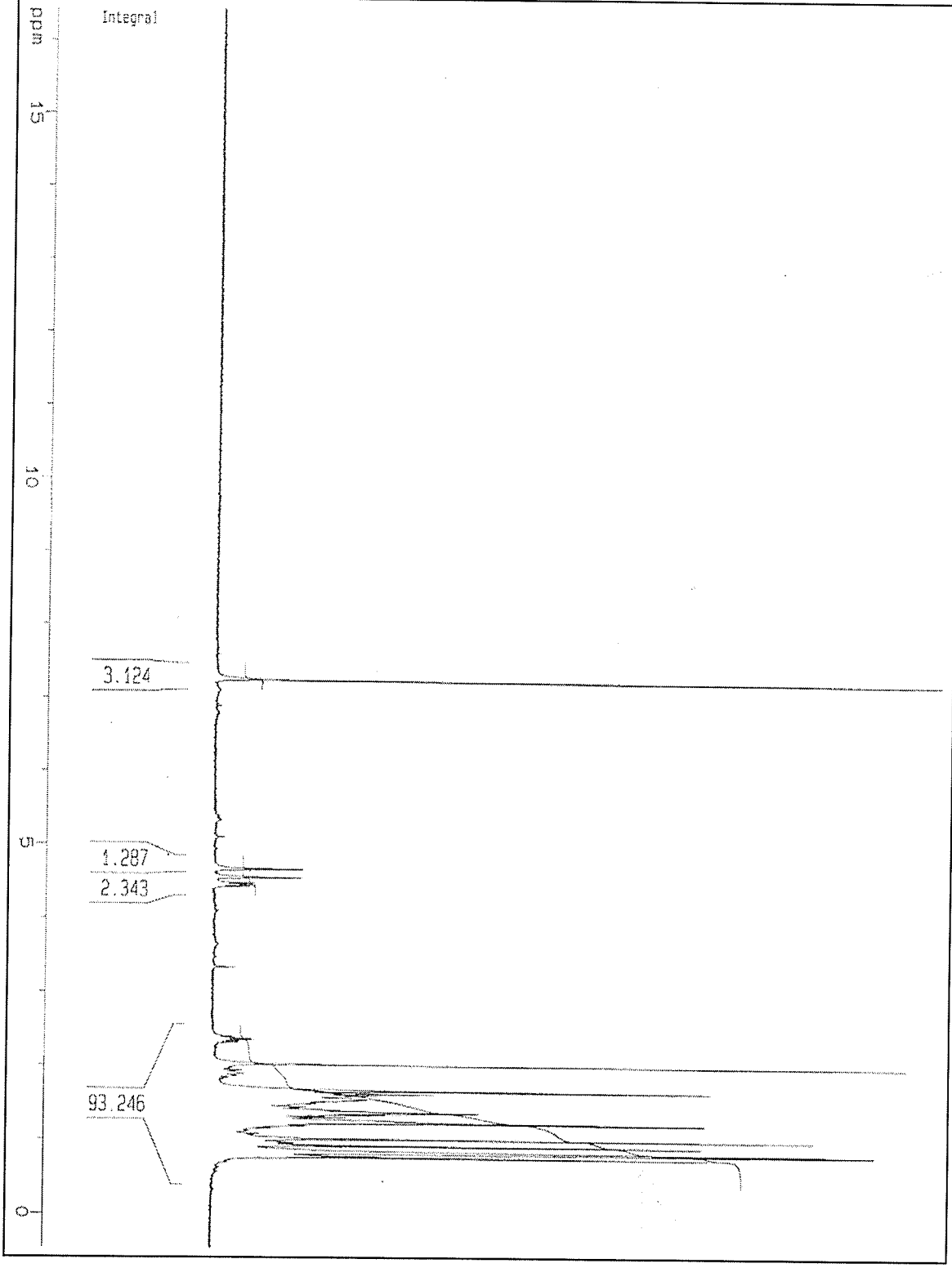

^{13}C-NMR spectrum of cyclolaudenyl acetate (**111**)

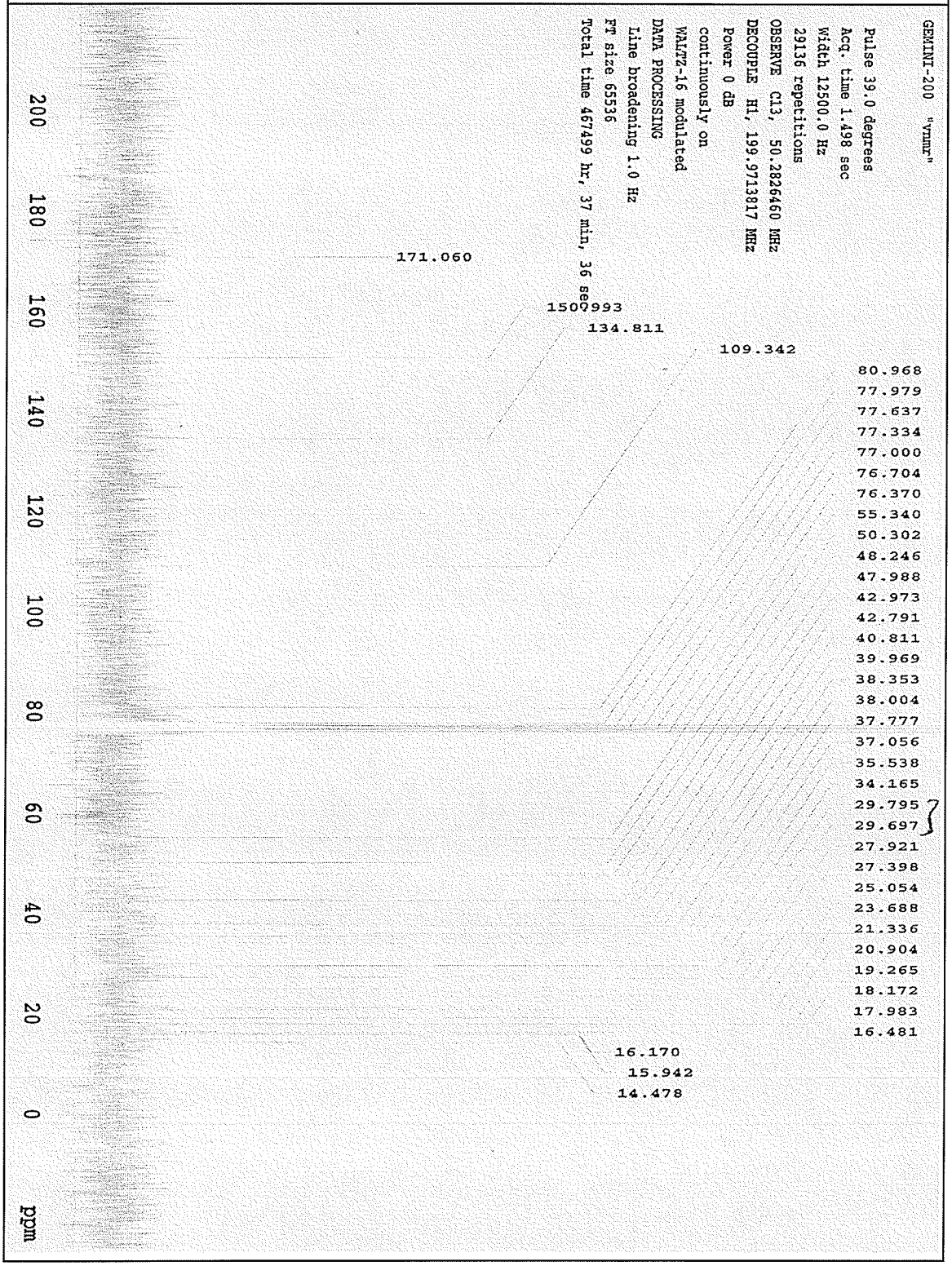

^{1}H-NMR spectrum of lupeol acetate (**112**)

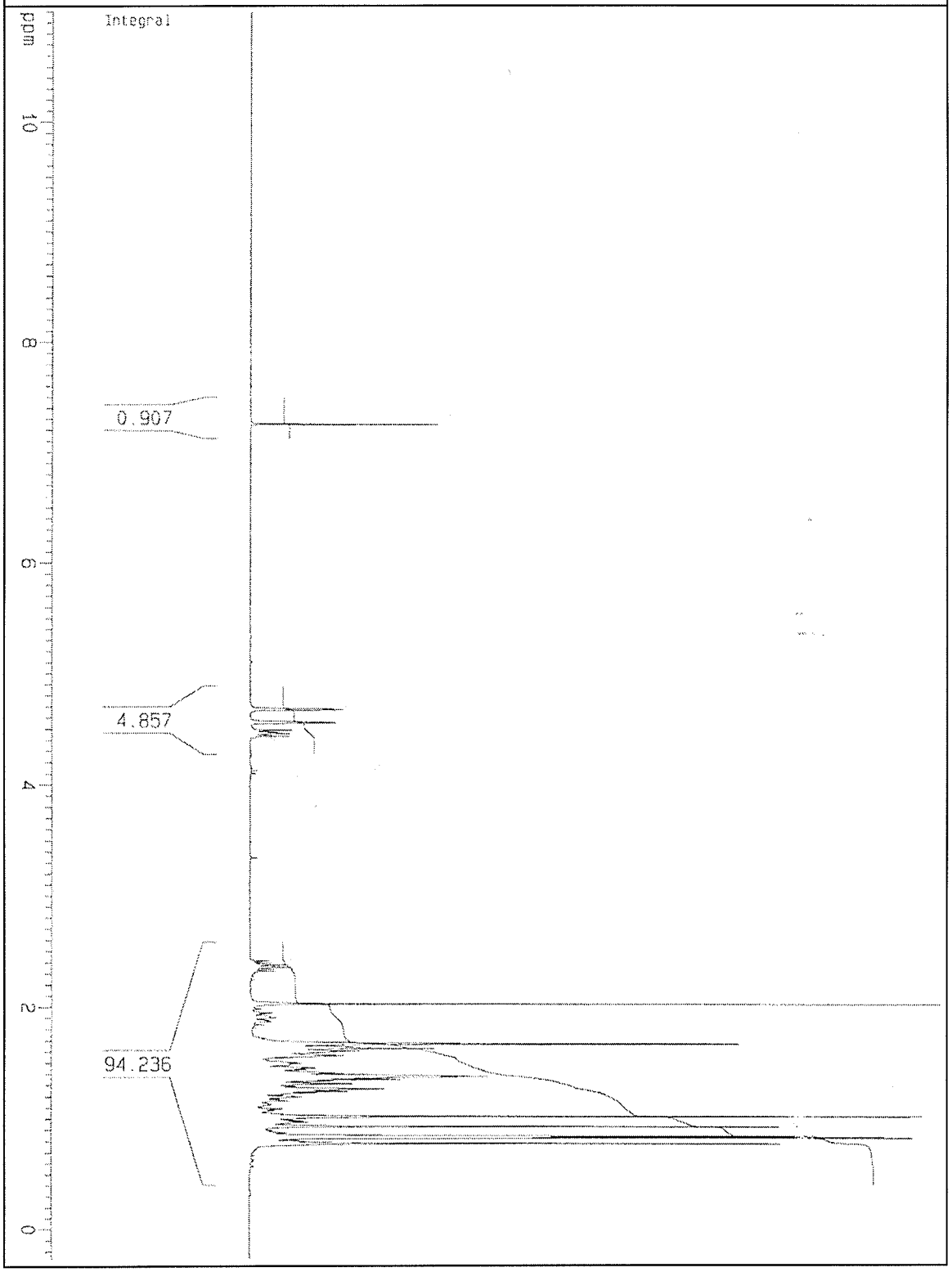

^{13}C-NMR spectrum of lupeol acetate (**112**)

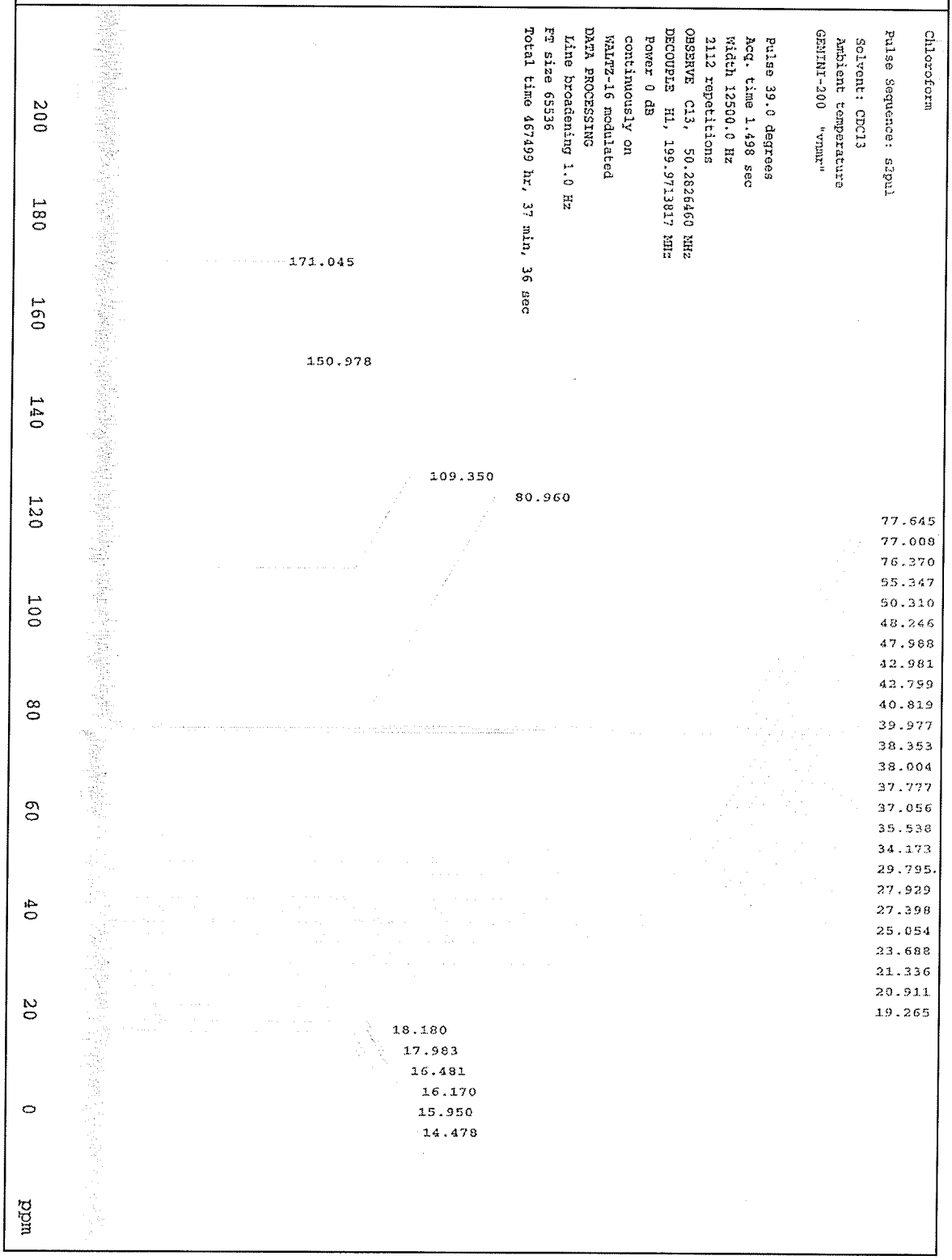

^{1}H-NMR spectrum of β-amyrine acetate (**113**)

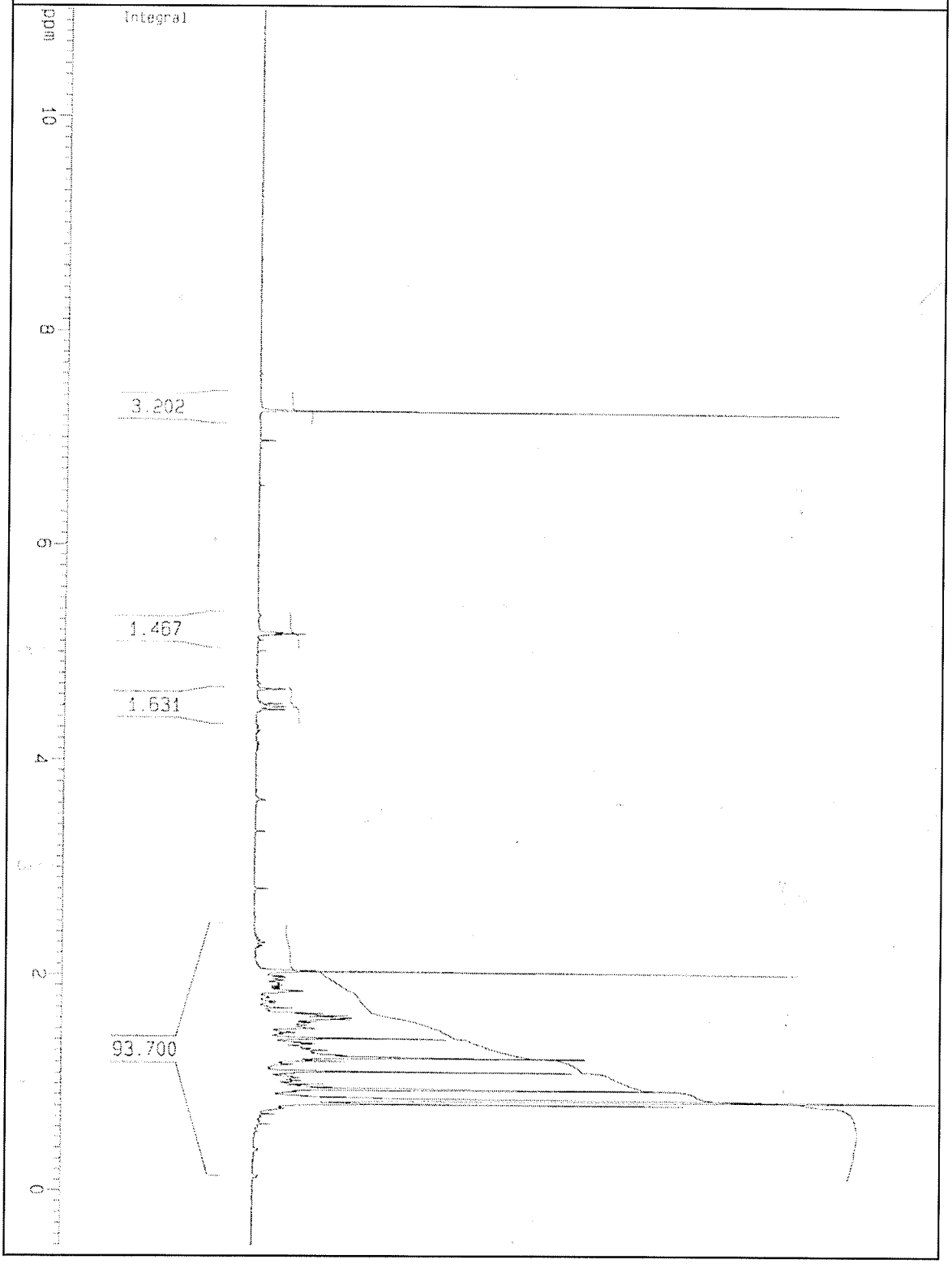

^{13}C-NMR spectrum of β-amyrine acetate (**113**)

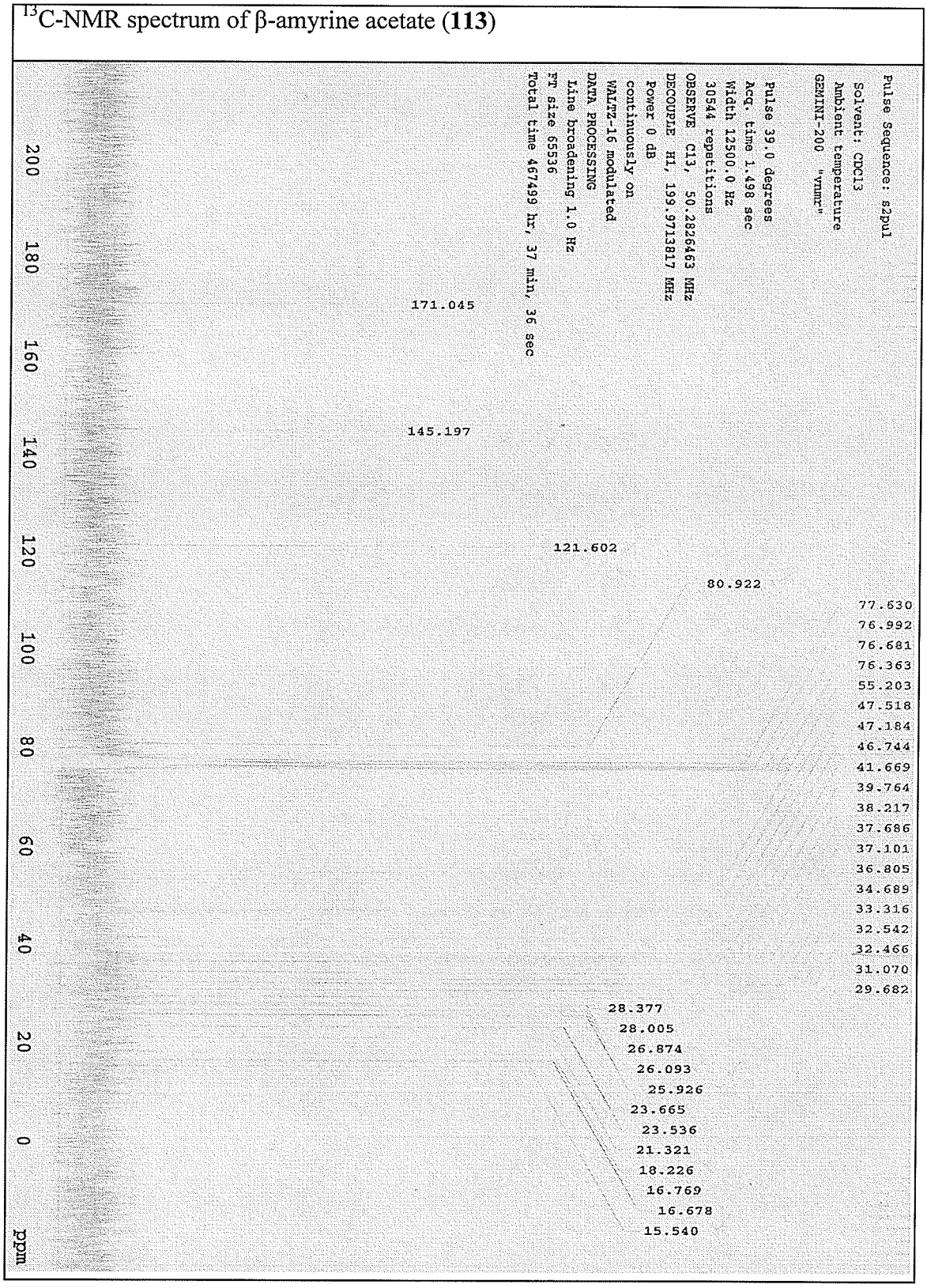

^{1}H-NMR spectrum of 12,13-didydromicromeric acid (**114**)

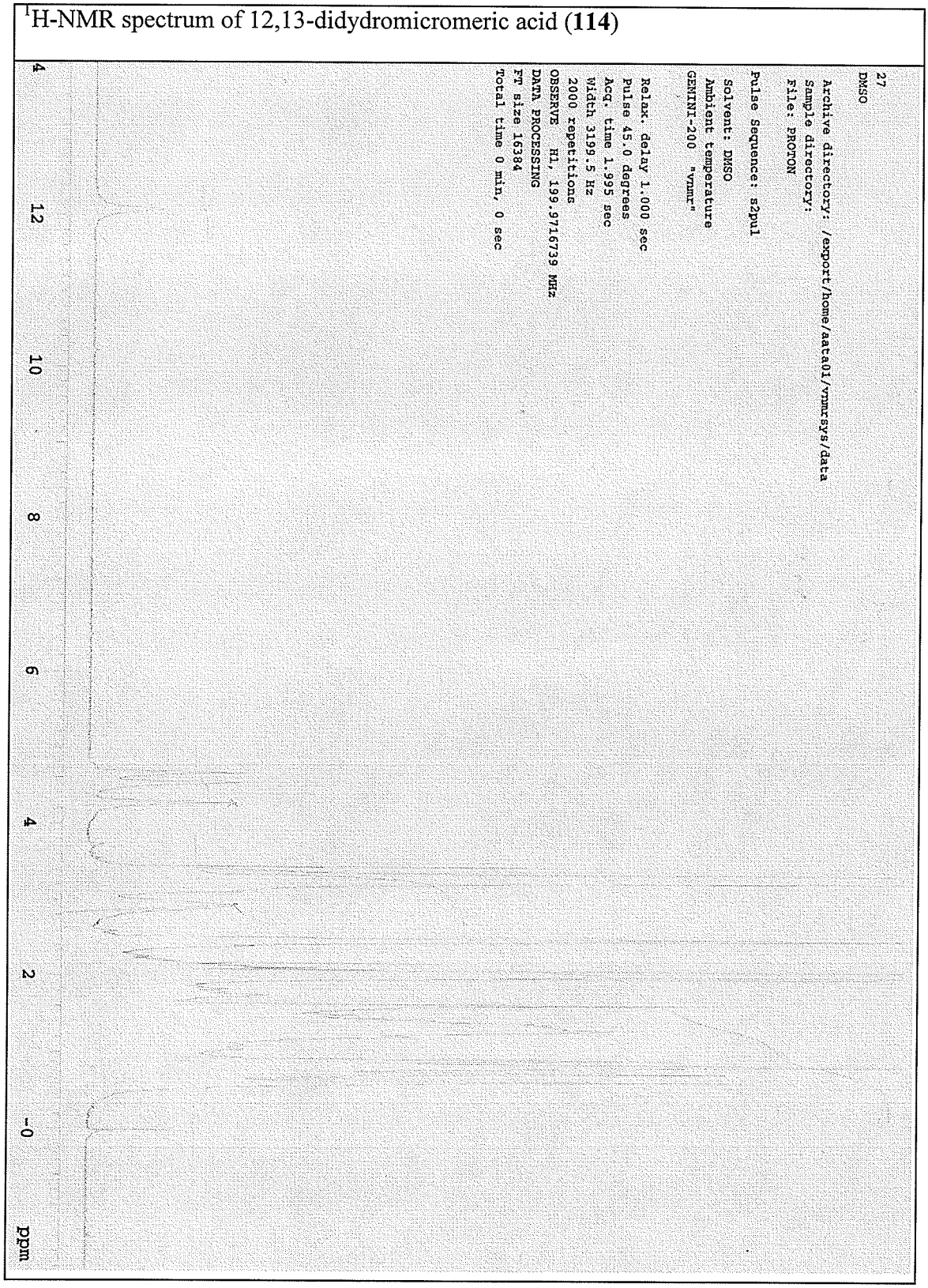

^{13}C-NMR spectrum of 12,13-didydromicromeric acid (**114**)

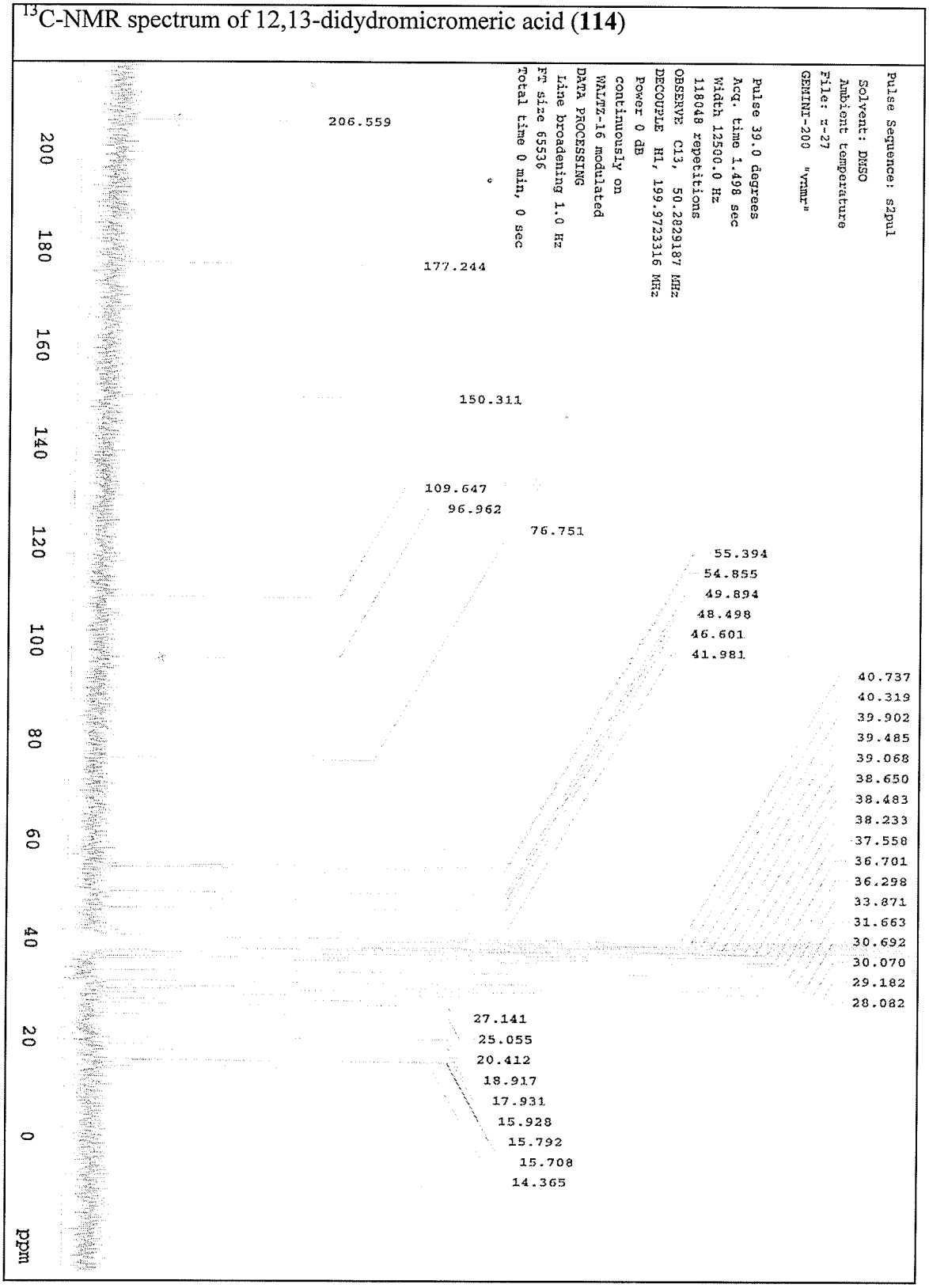

^{1}H-NMR spectrum of artonins E (**115**)

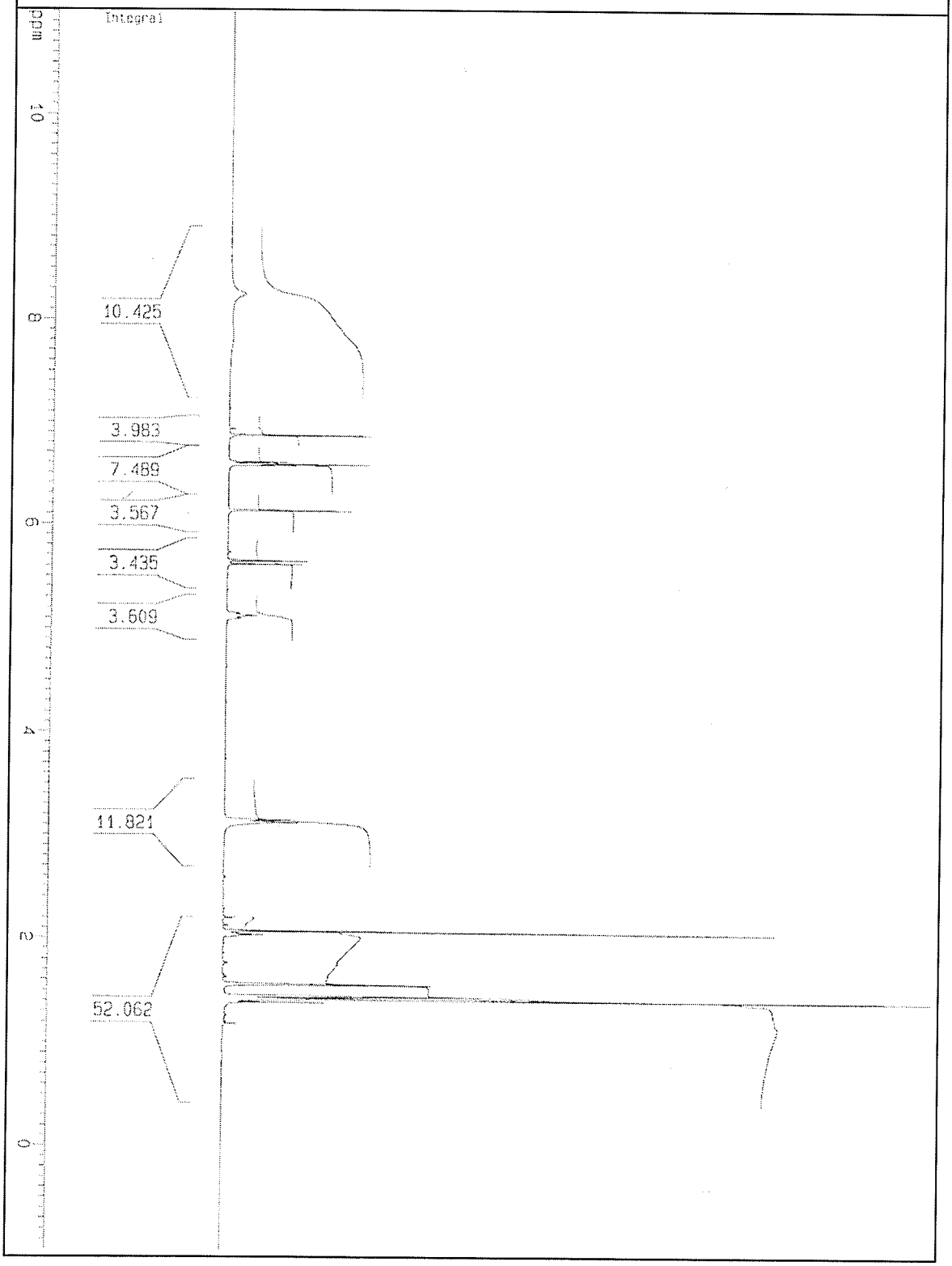

^{13}C-NMR spectrum of artonins E (**115**)

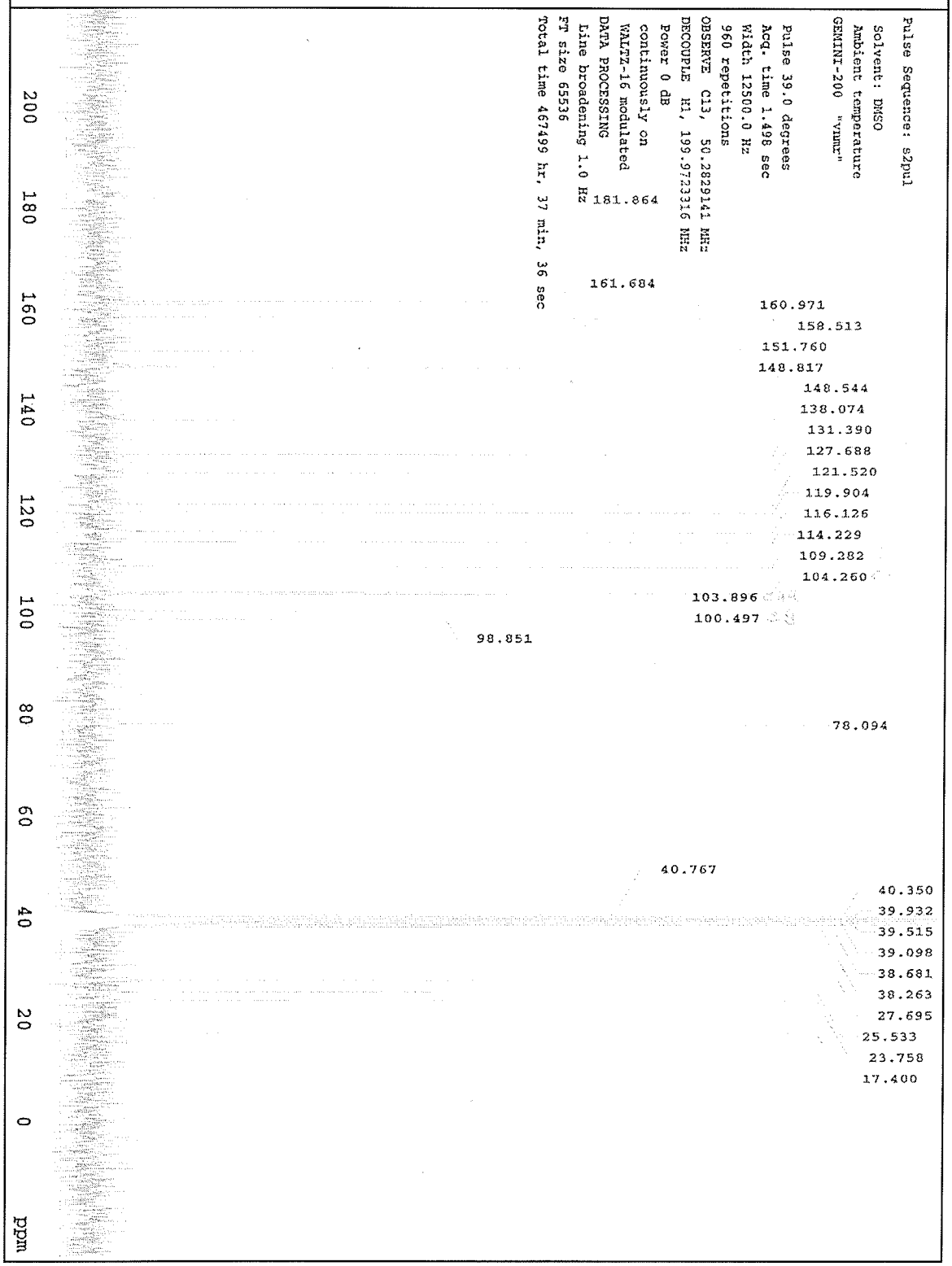

^{1}H-NMR spectrum of artobiloxanthone (**116**)

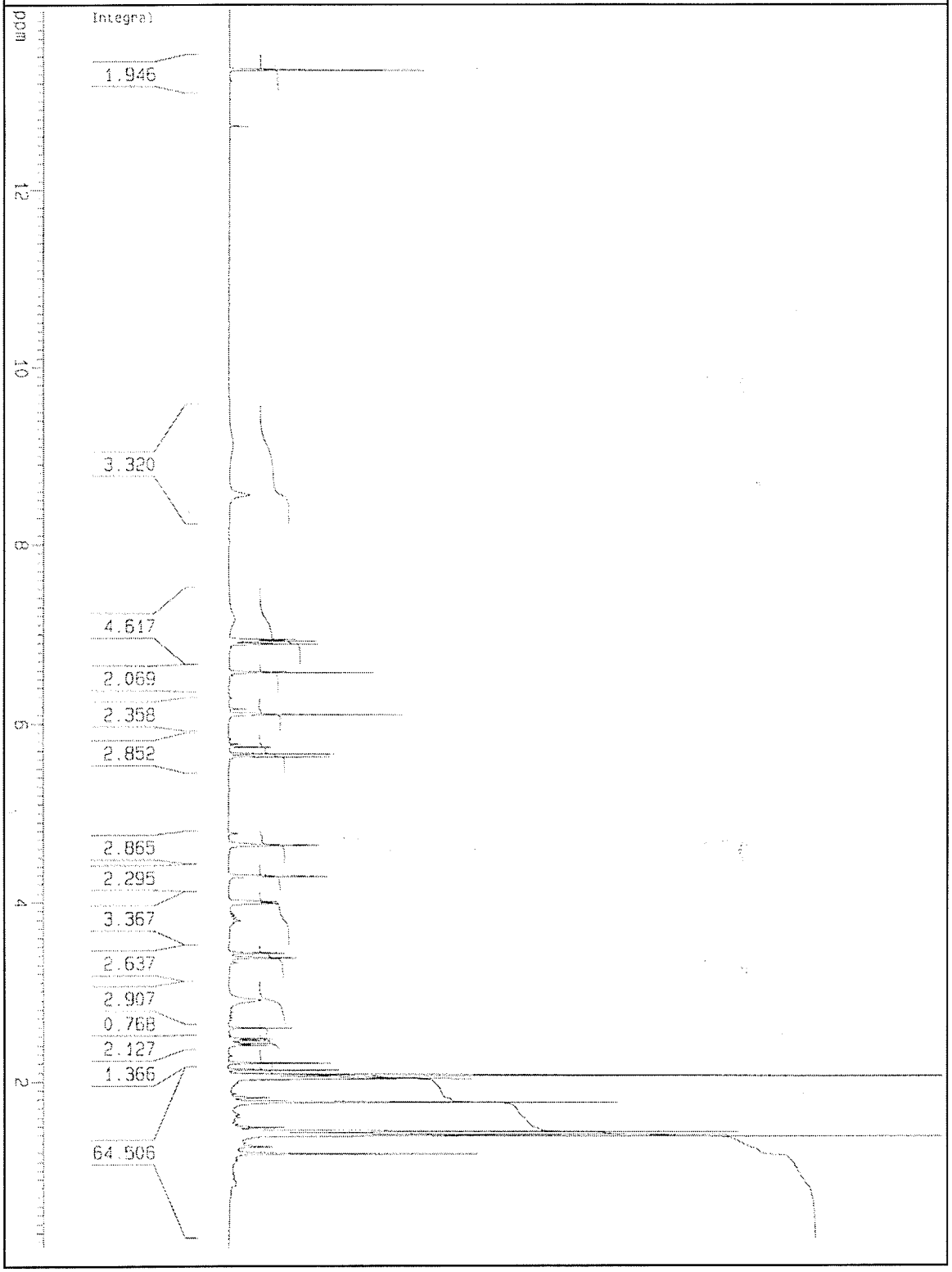

^{13}C-NMR spectrum of artobiloxanthone (**116**)

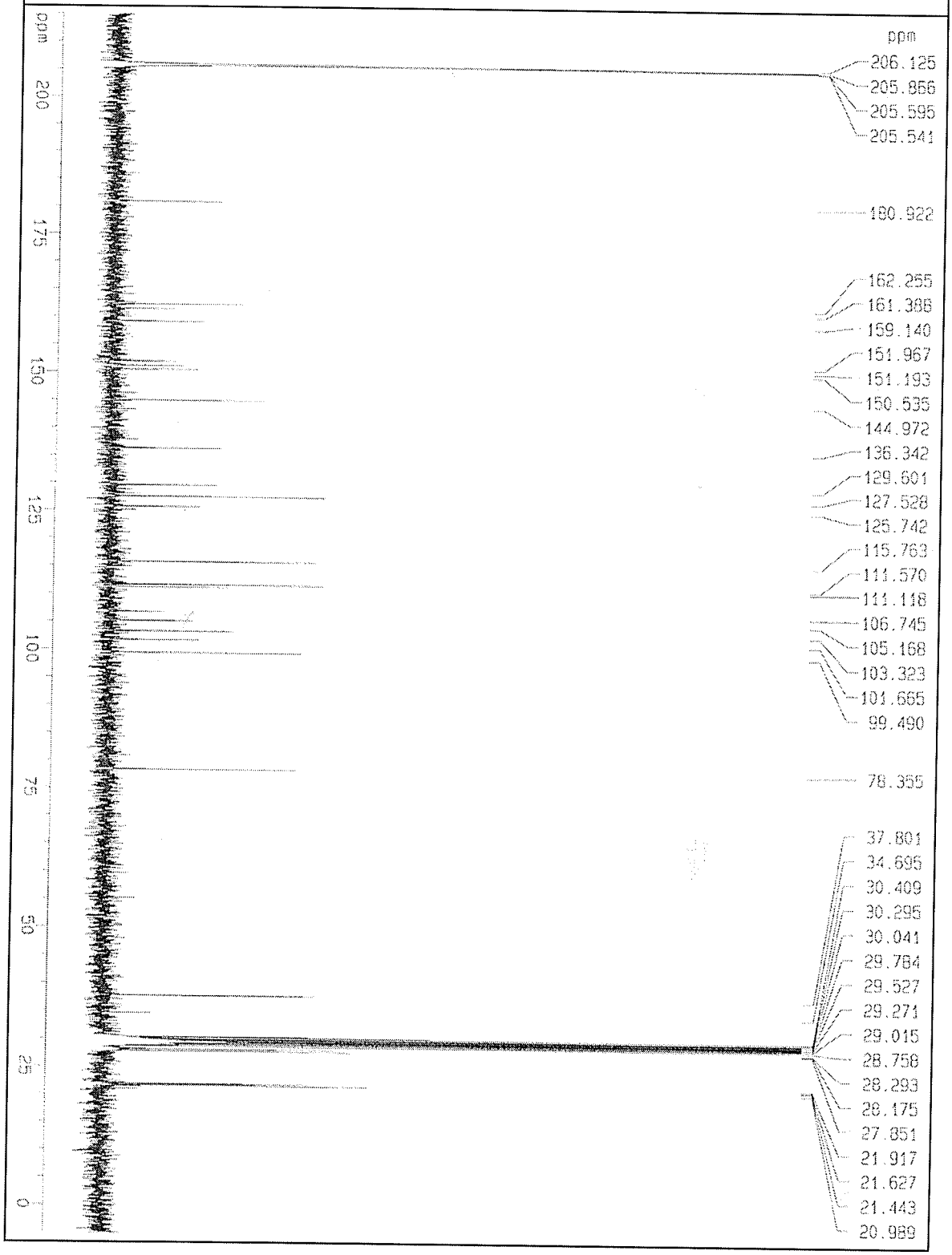

^{1}H-NMR spectrum of barlerin (**127**)

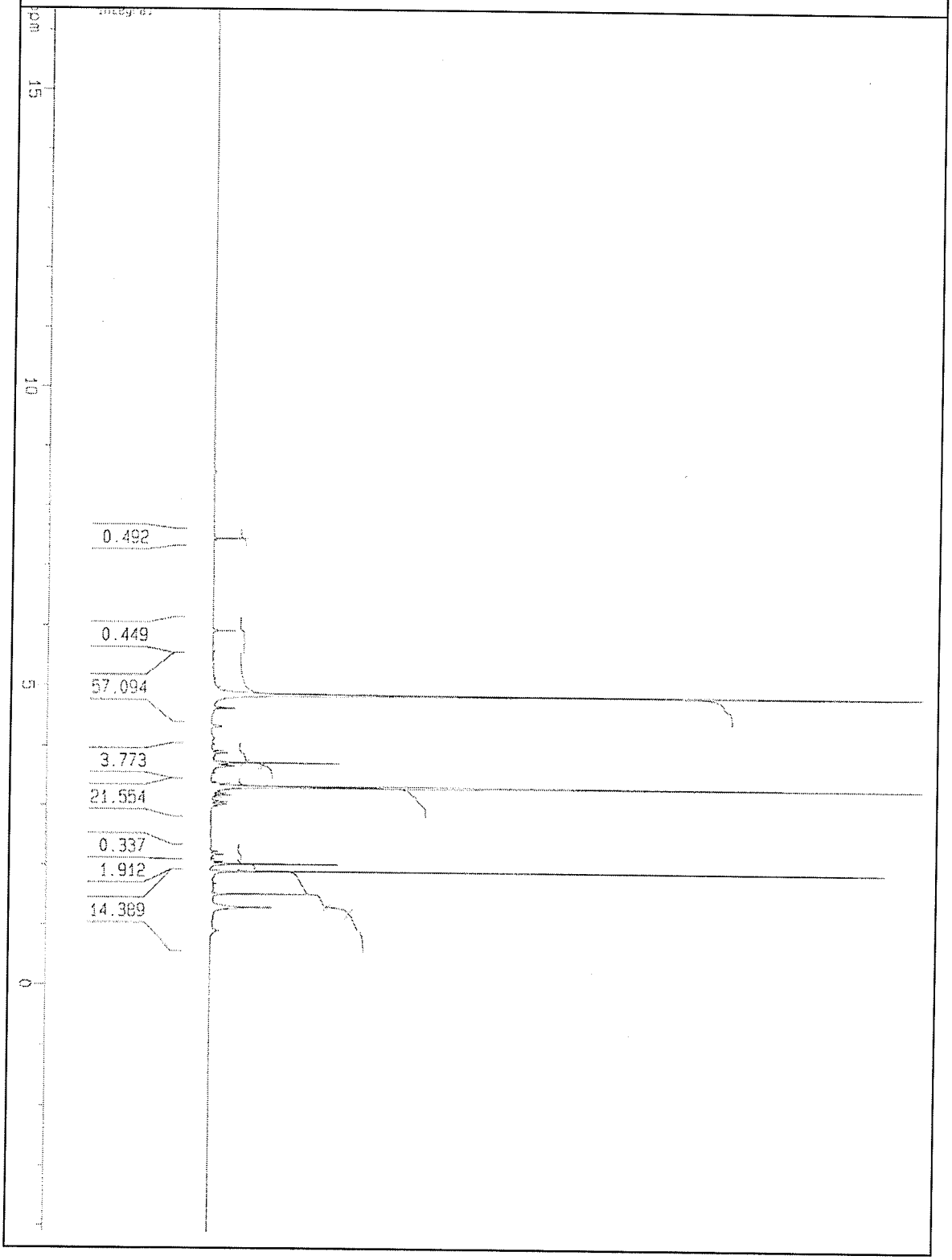

^{13}C-NMR spectrum of barlerin (**127**)

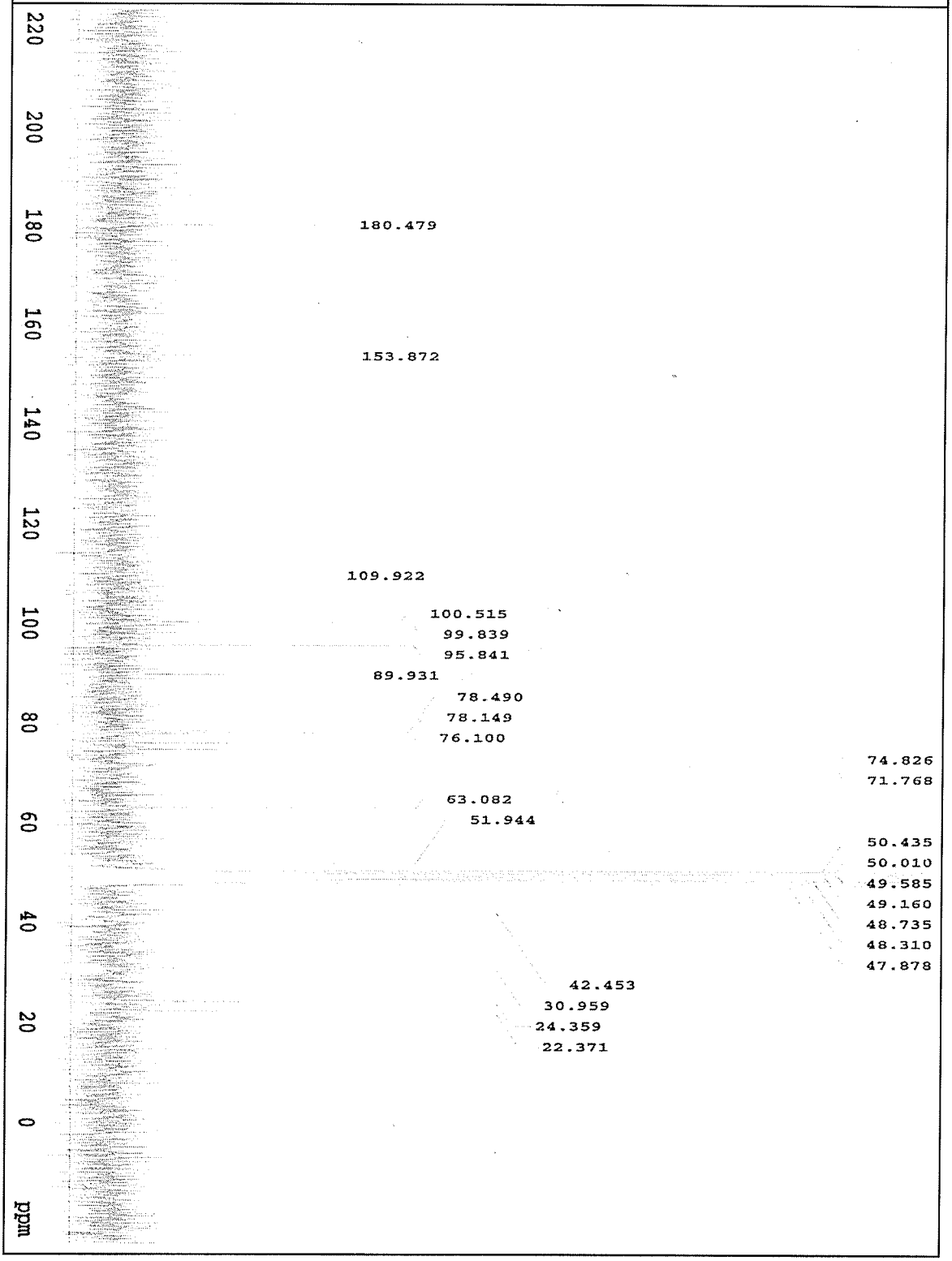

^{1}H-NMR spectrum of shanzhiside methyl ester (**128**)

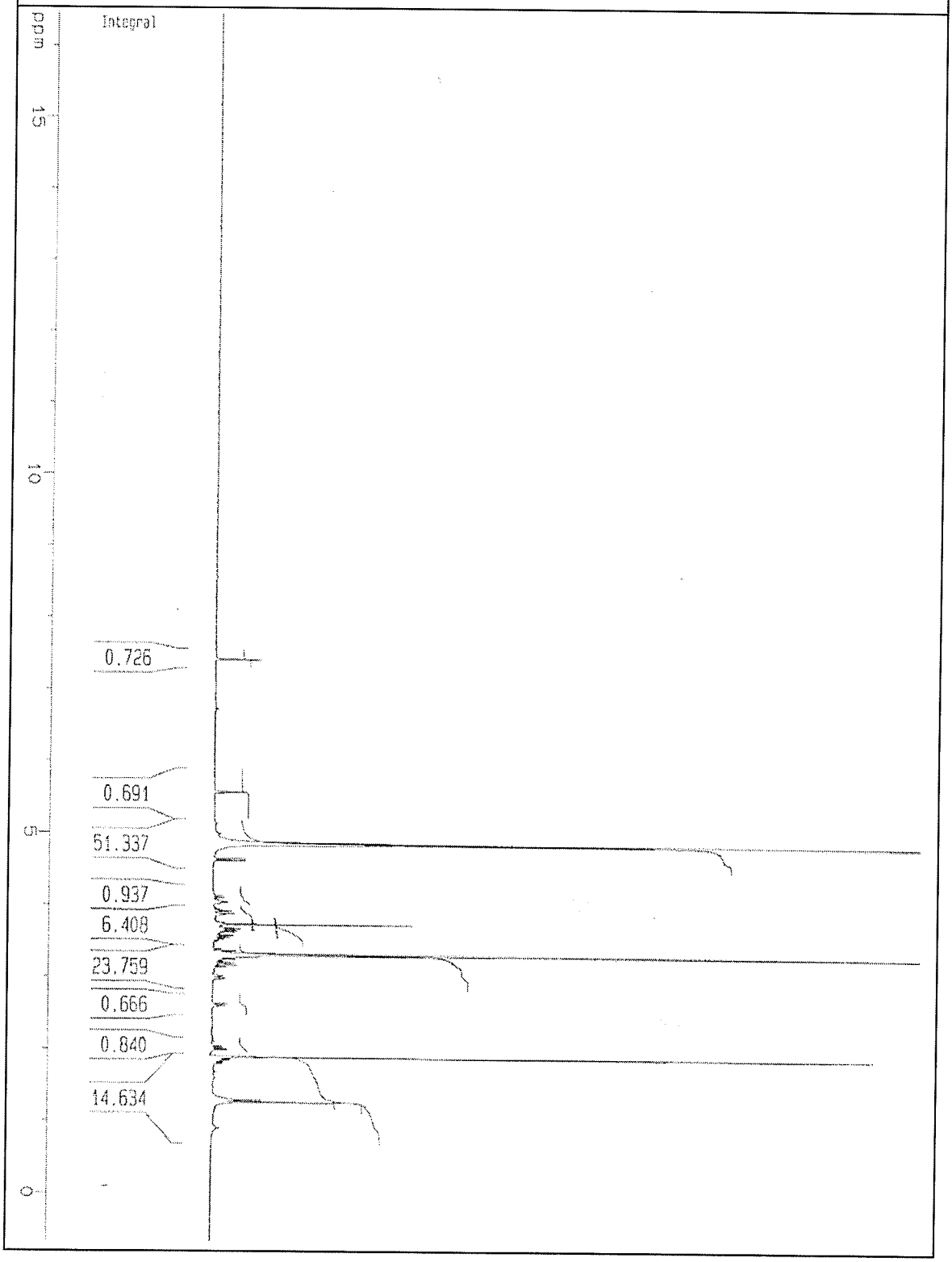

^{13}C-NMR spectrum of shanzhiside methyl ester (**128**)

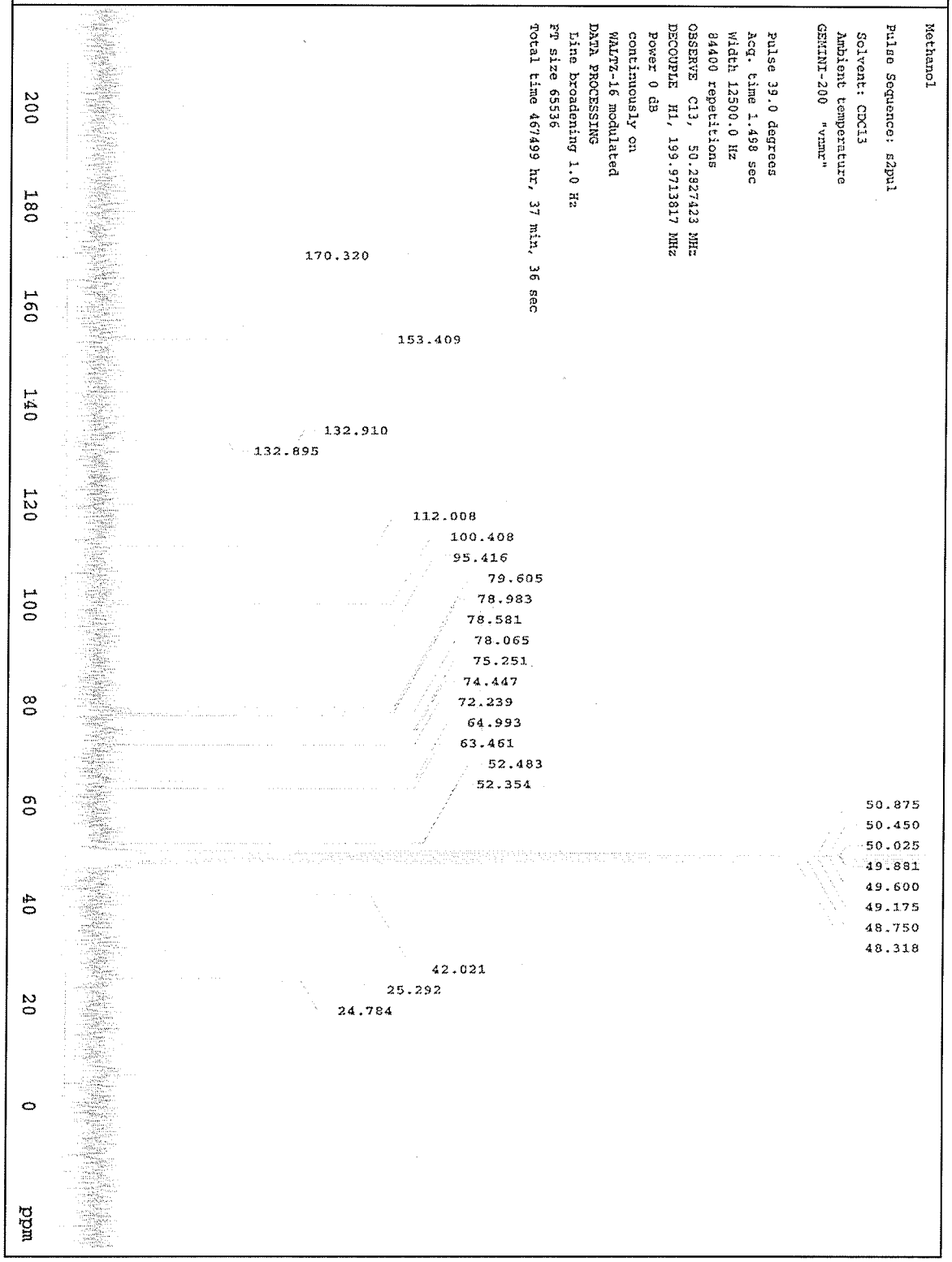

^{1}H-NMR spectrum of lupeol (**129**)

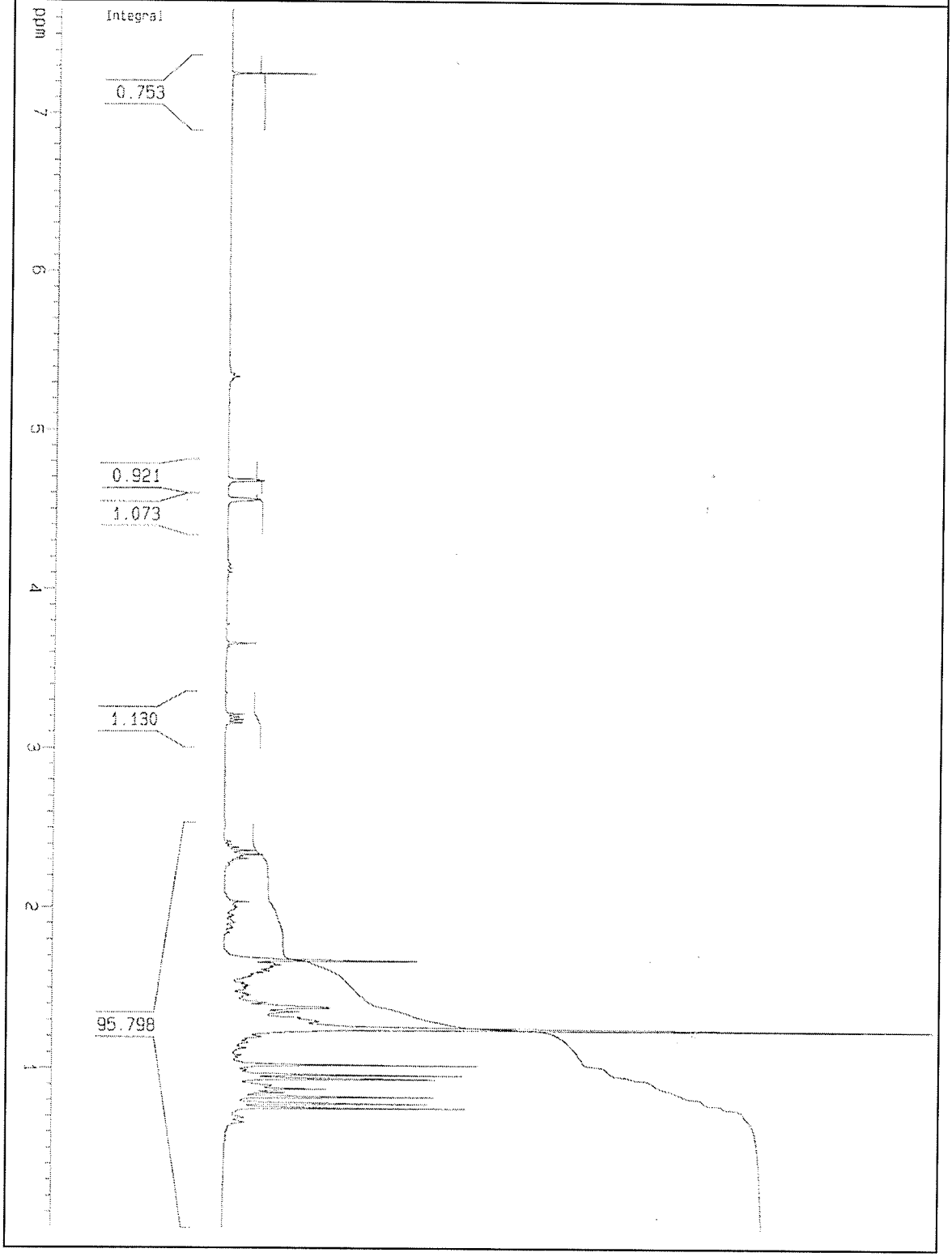

^{13}C-NMR spectrum of lupeol (**129**)

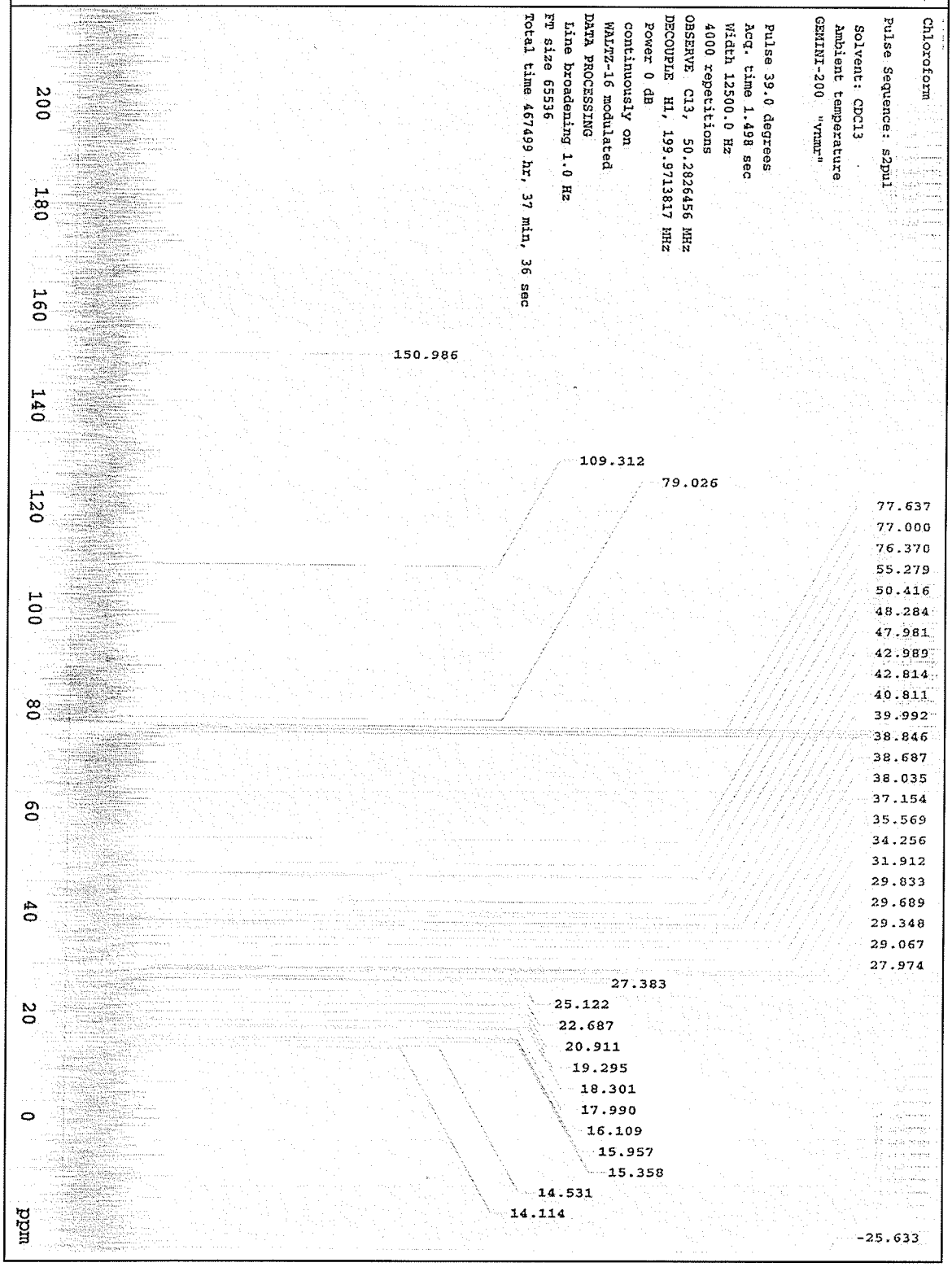

^{1}H-NMR spectrum of bitulinic acid (**130**)

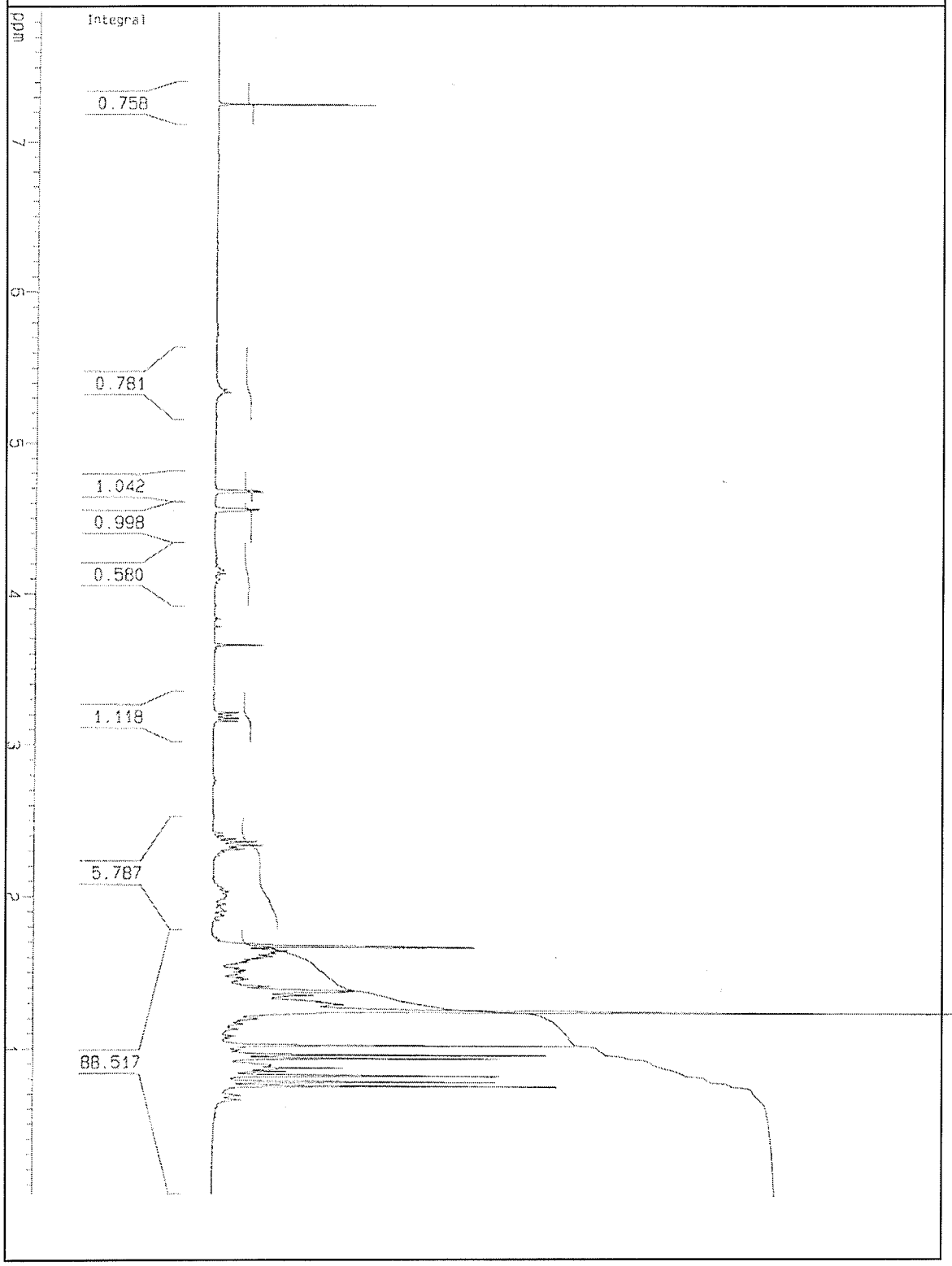

^{13}C-NMR spectrum of bitulinic acid (**130**)

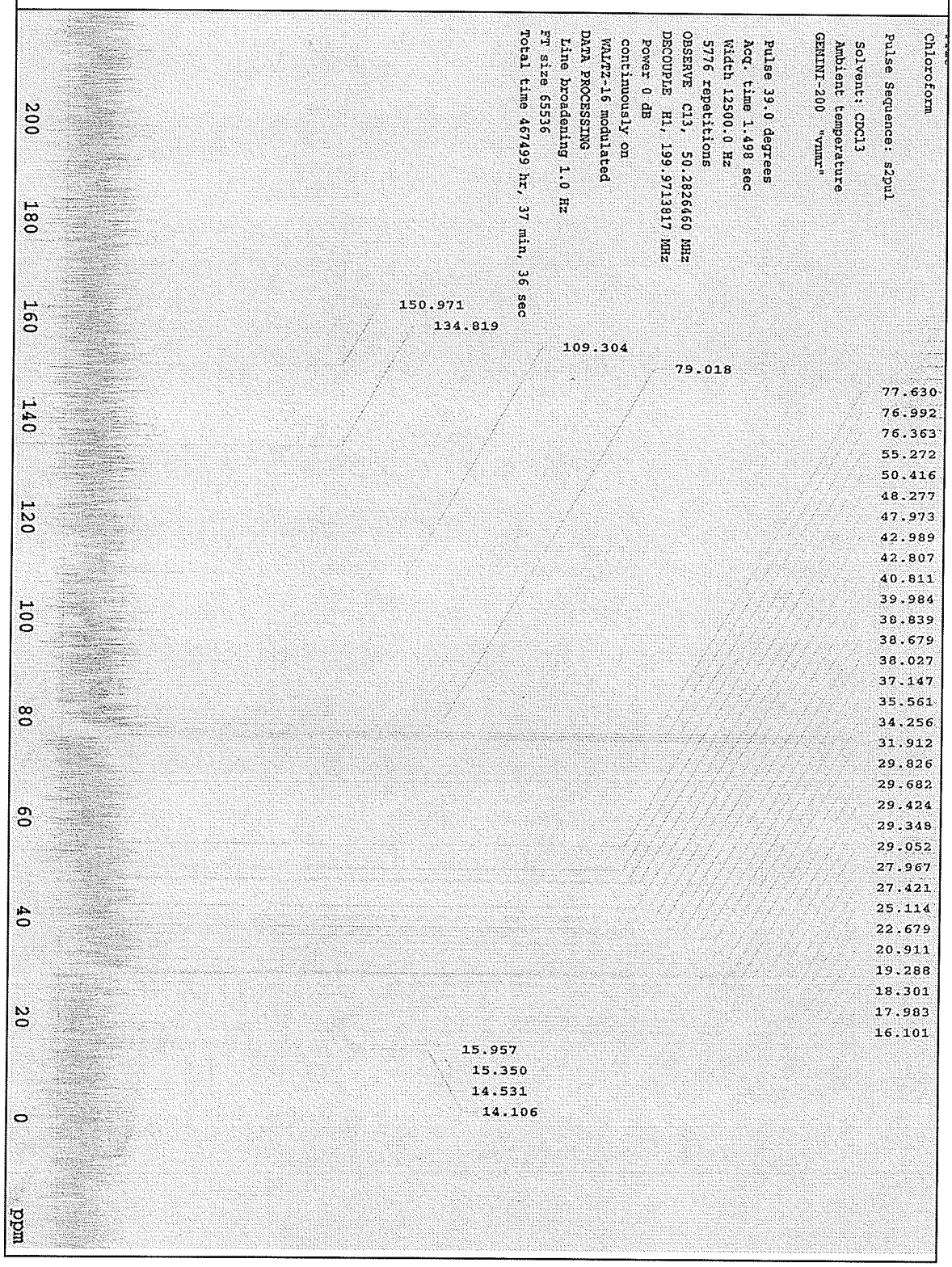

^{1}H-NMR spectrum of pipataline (**131**)

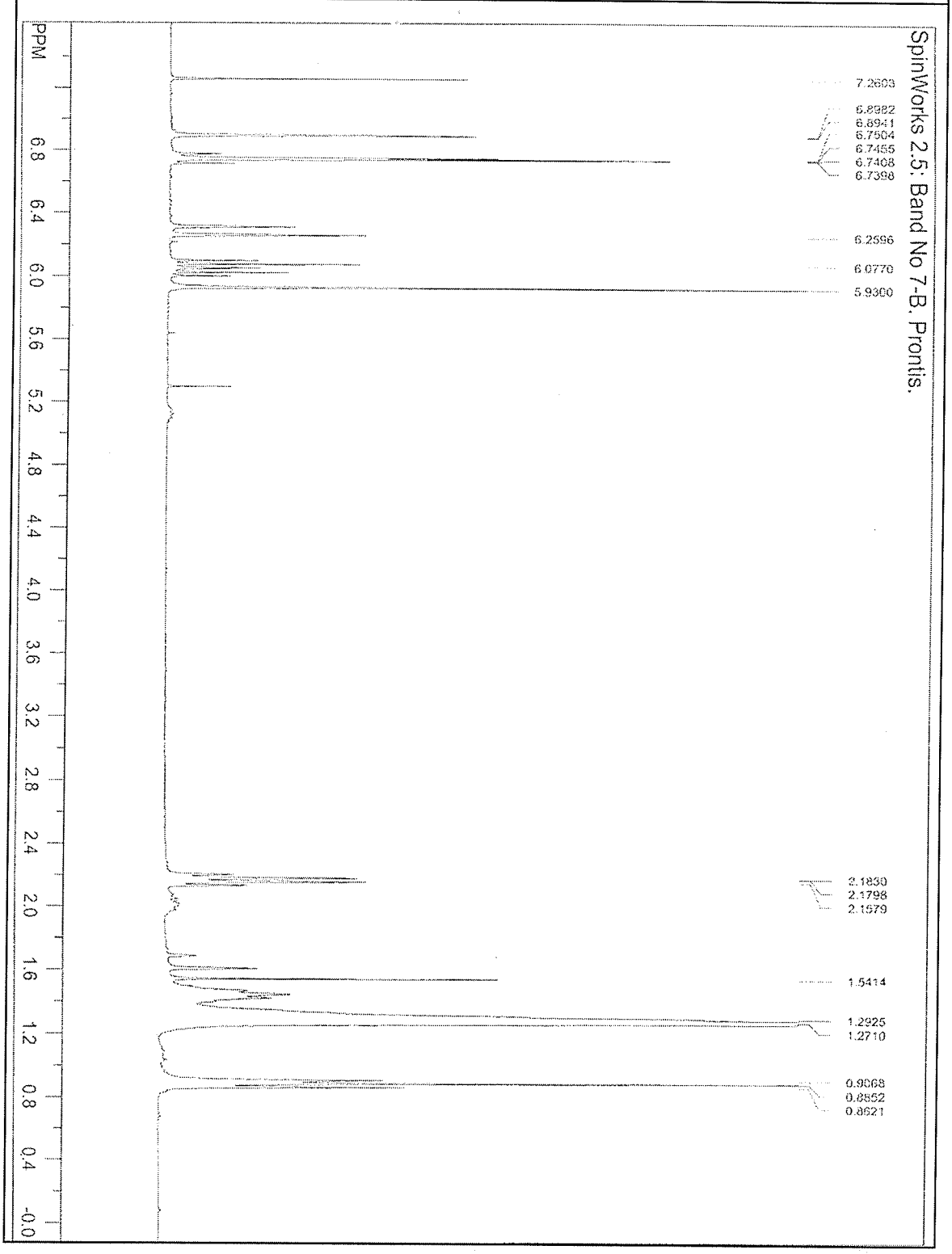

^{13}C-NMR spectrum of pipataline (**131**)

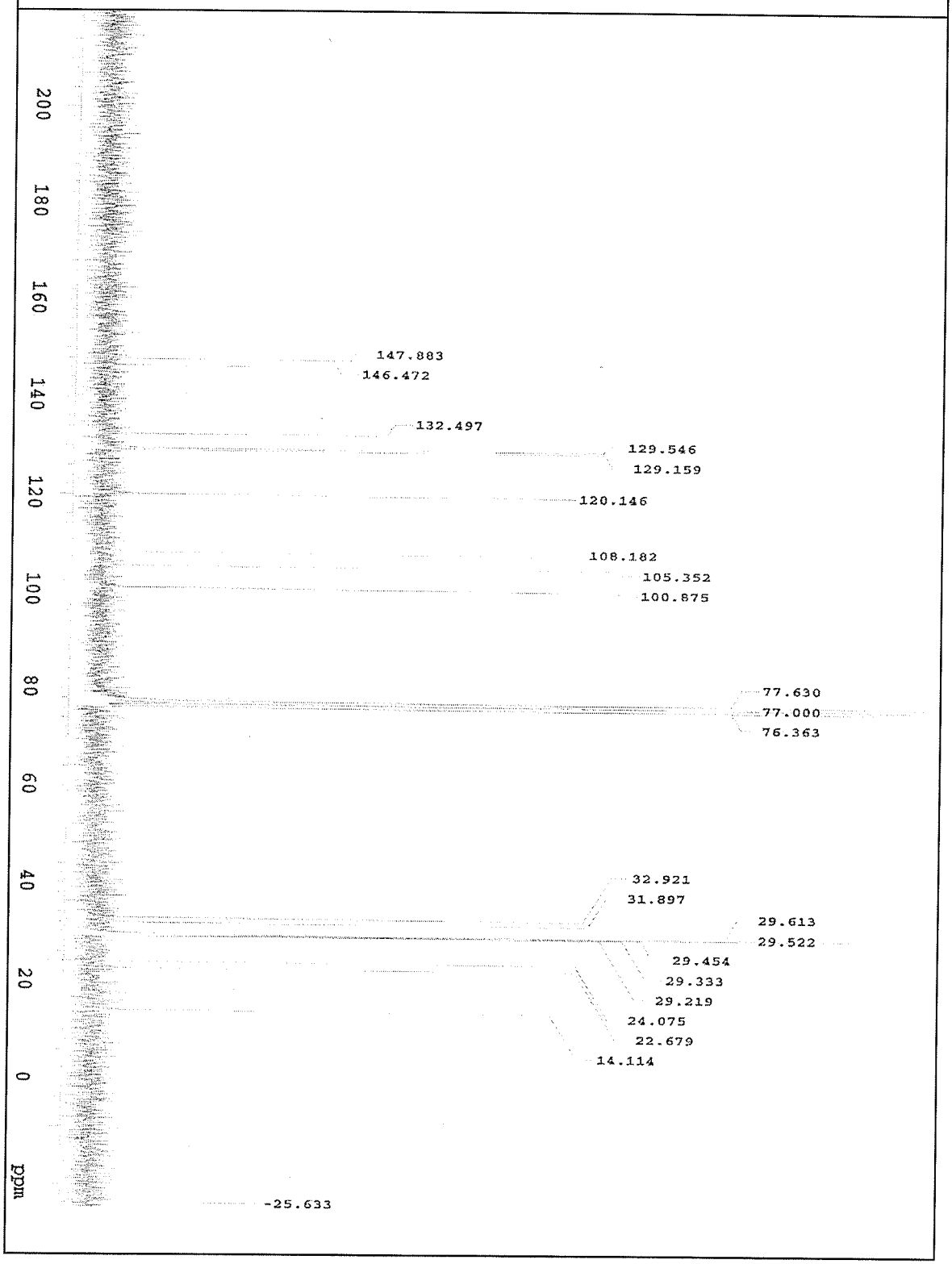

^{1}H-NMR spectrum of 7, 8-epoxypipataline (**132**)

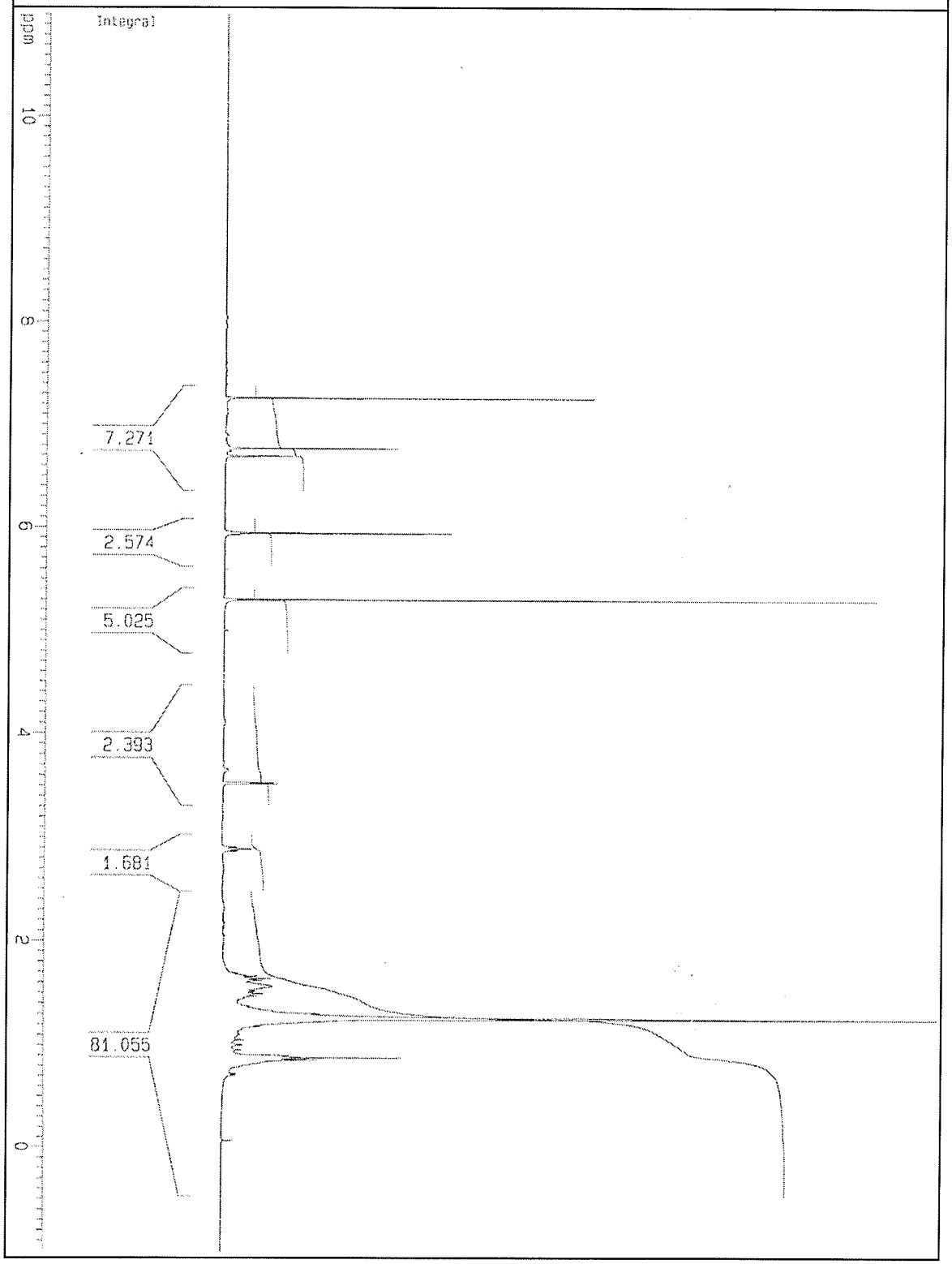

^{13}C-NMR spectrum of 7, 8-epoxypipataline (**132**)

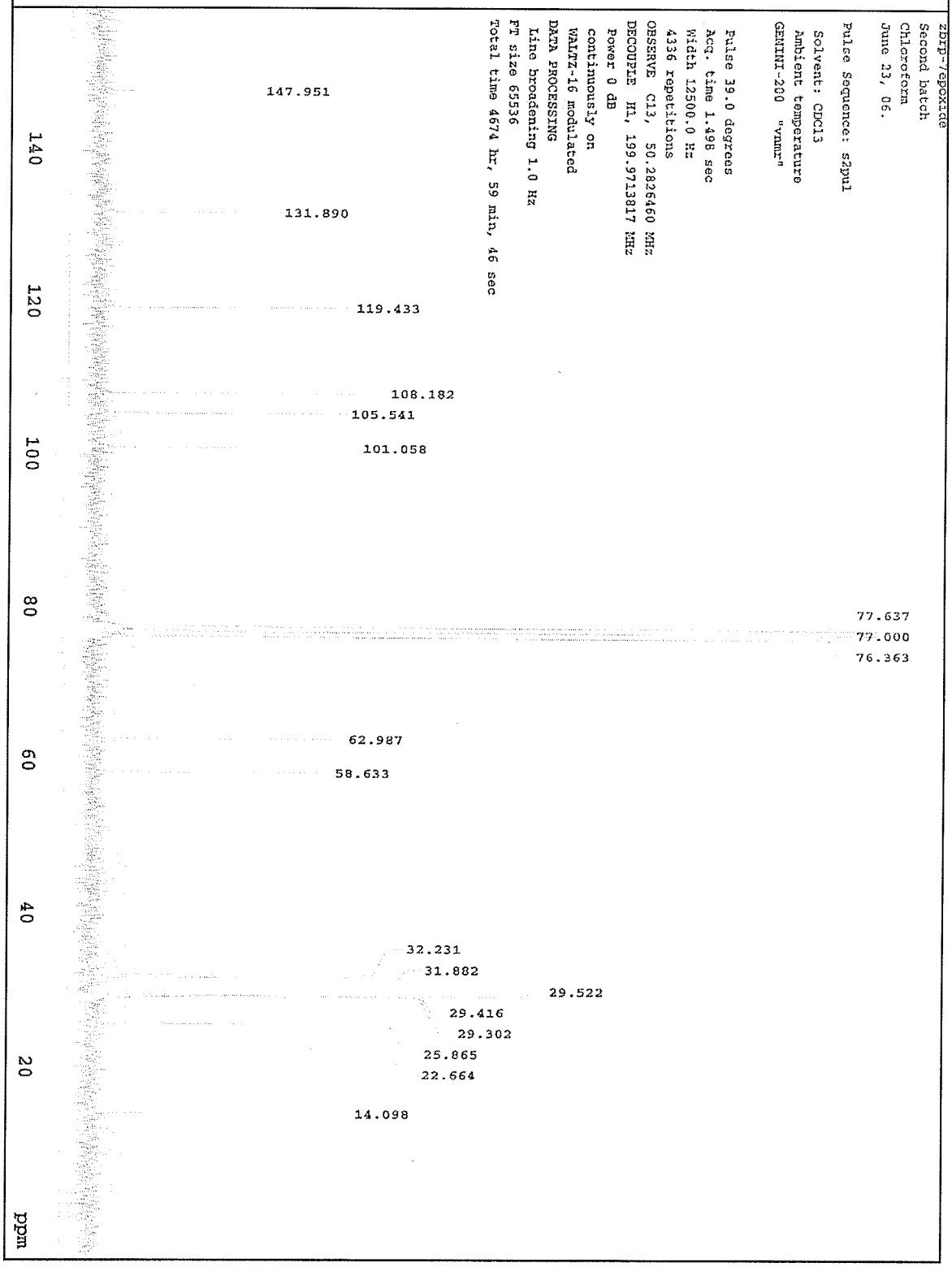

^{1}H-NMR spectrum of 7-amino-8-hydroxypipataline (**133**)

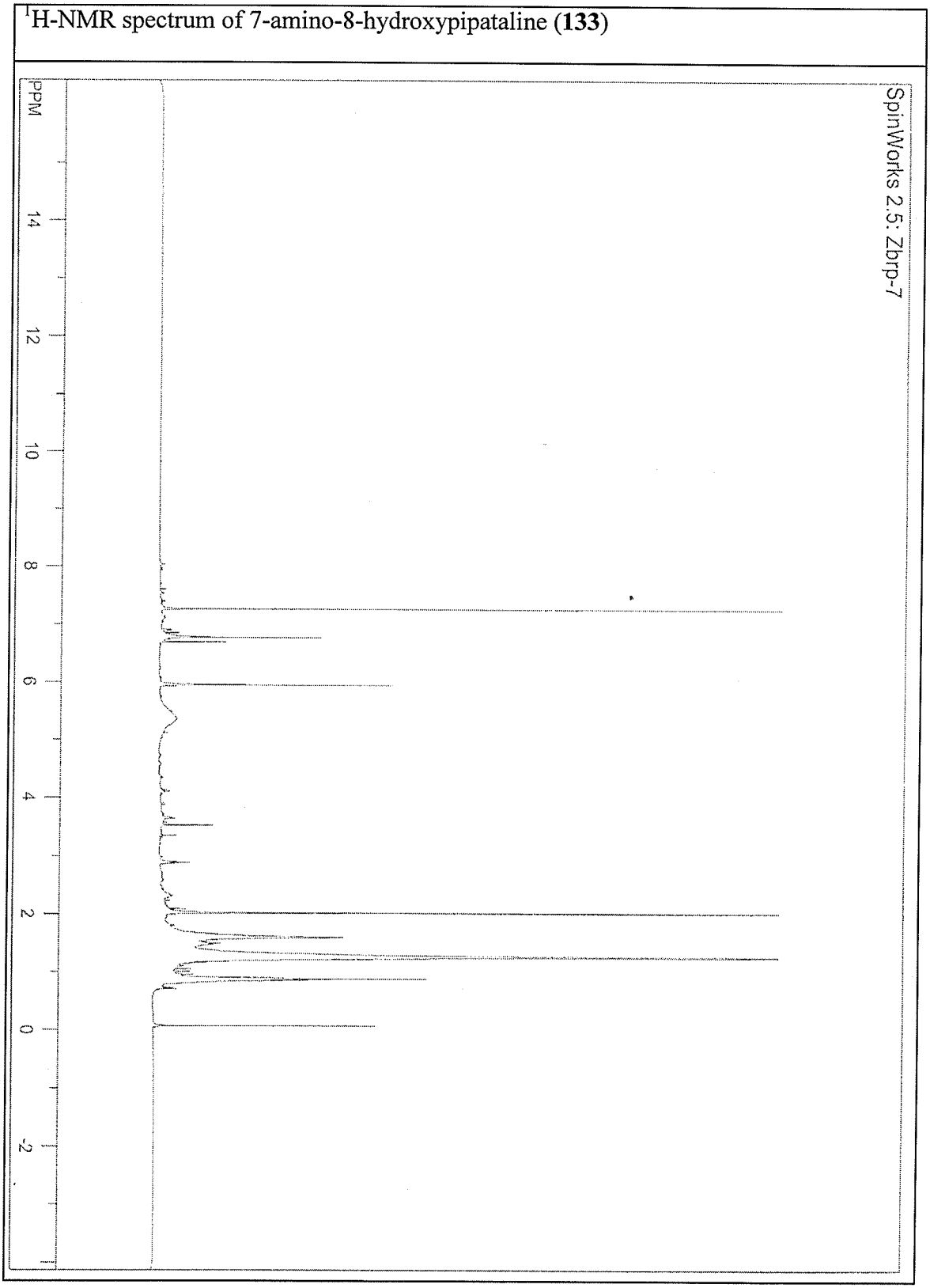

^{13}C-NMR spectrum of 7-amino-8-hydroxypipataline (**133**)

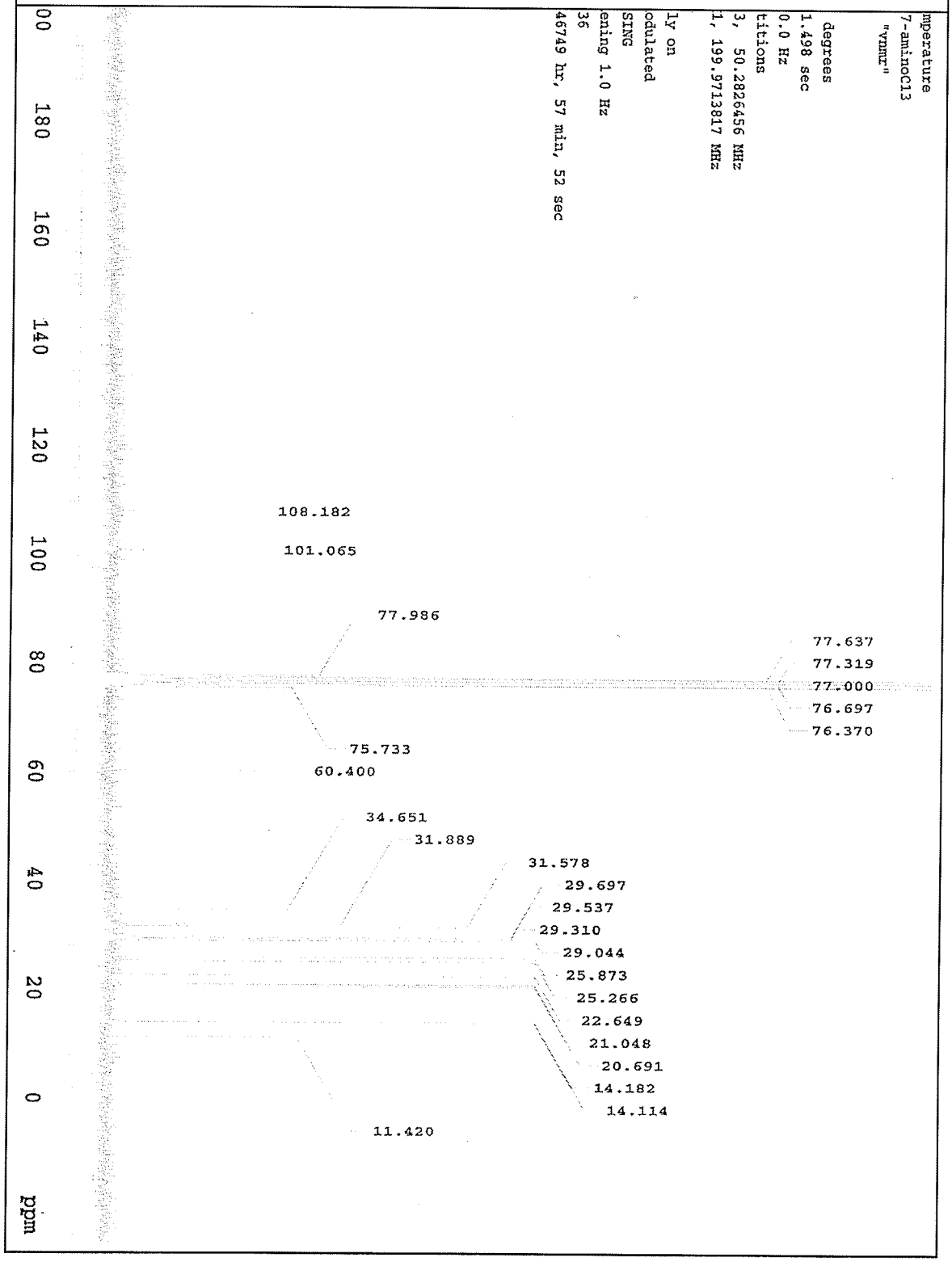

^{1}H-NMR spectrum of 7, 8-dibromopipataline (**134**)

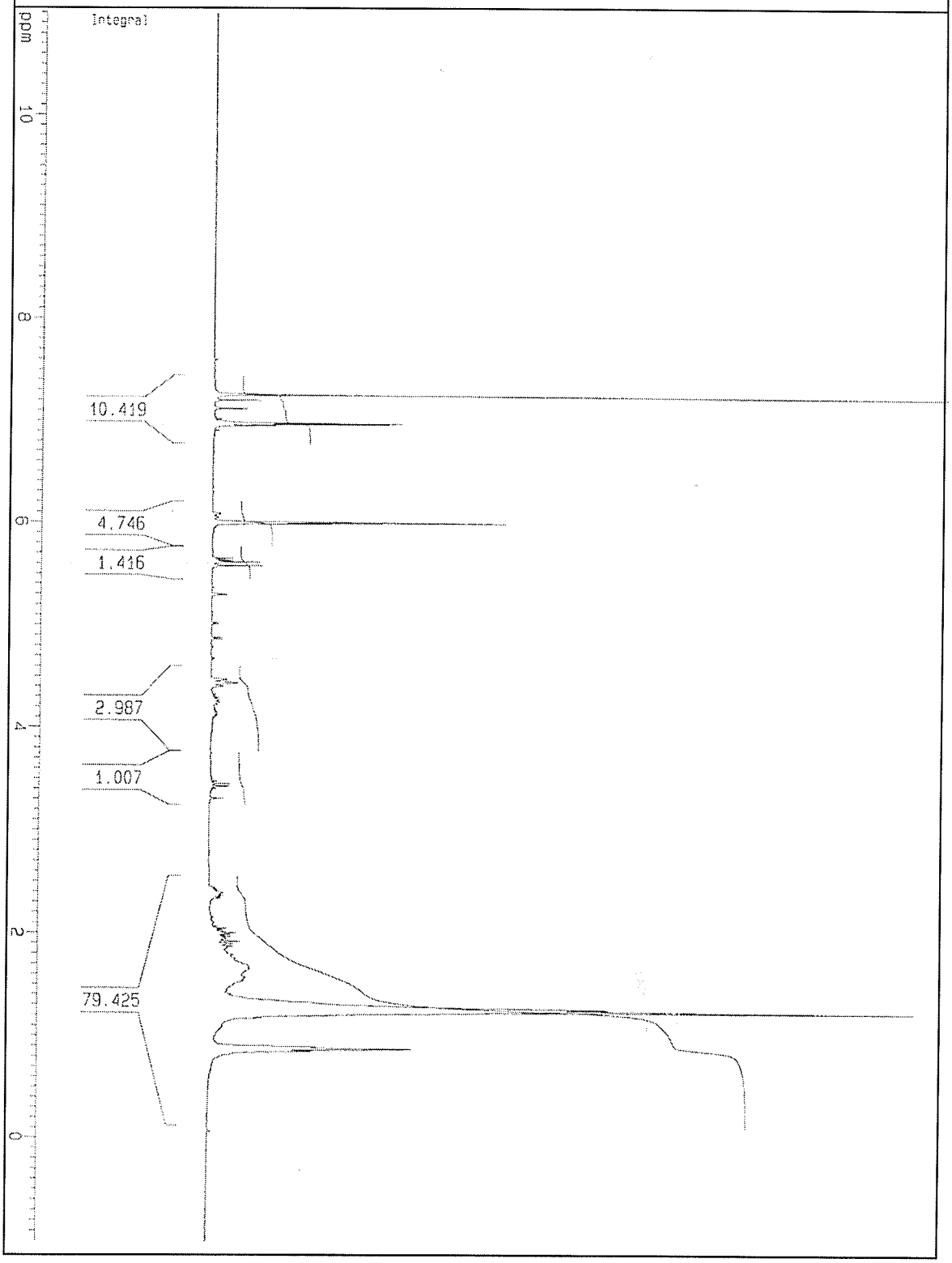

^{13}C-NMR spectrum of 7, 8-dibromopipataline (**134**)

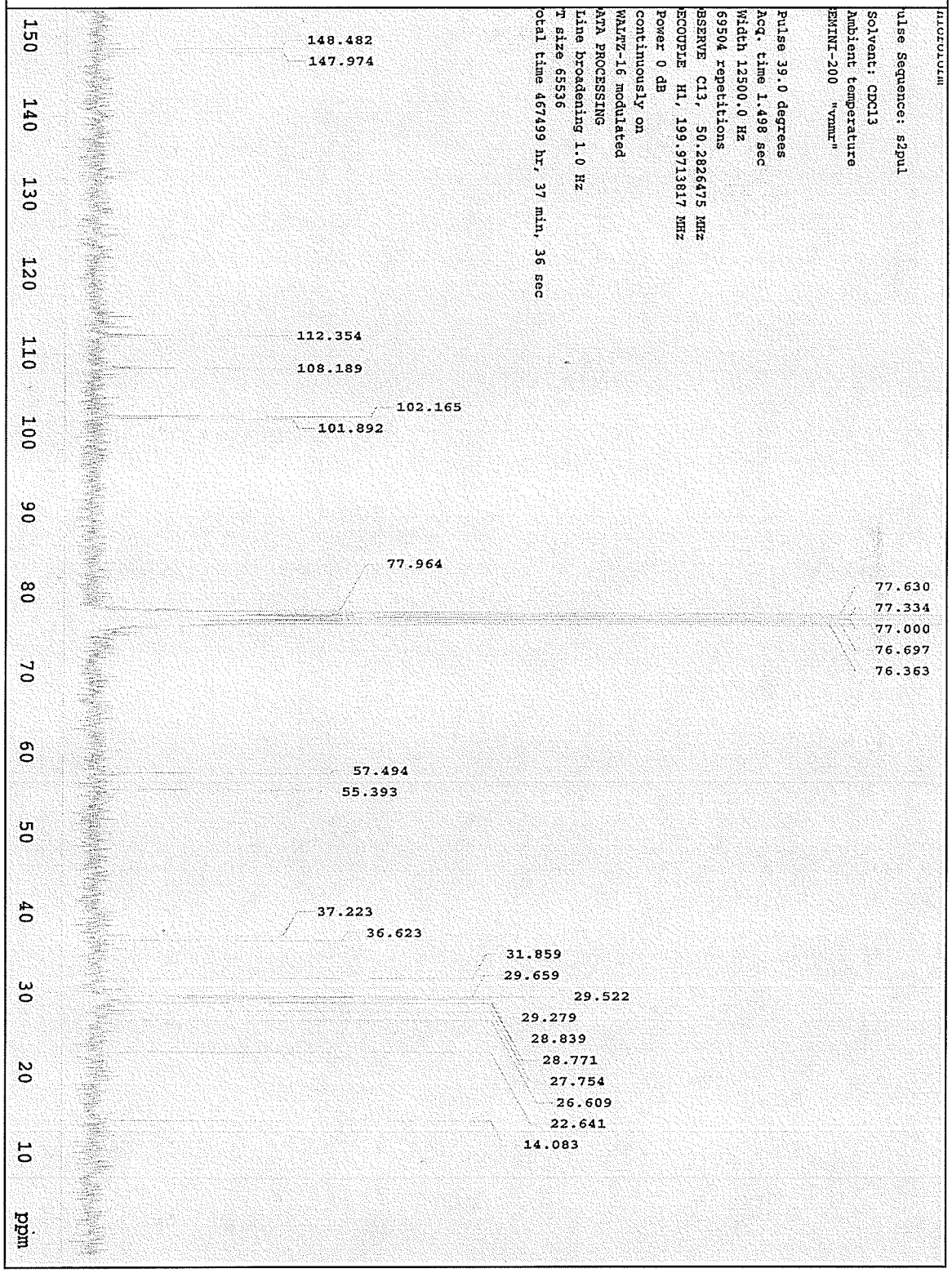

^{1}H-NMR spectrum of natalensamine-A (**156**)

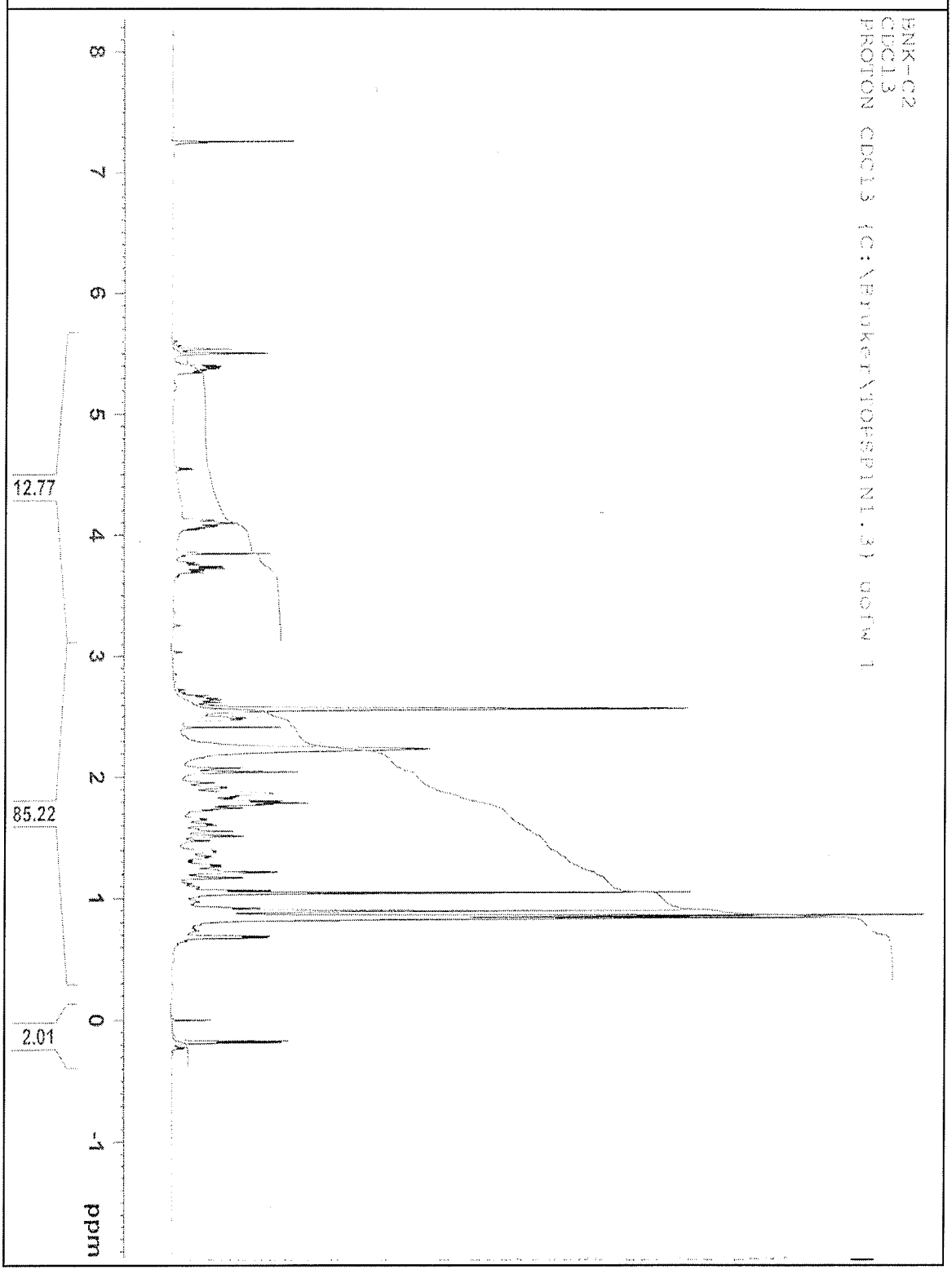

^{13}C-NMR spectrum of natalensamine-A (**156**)

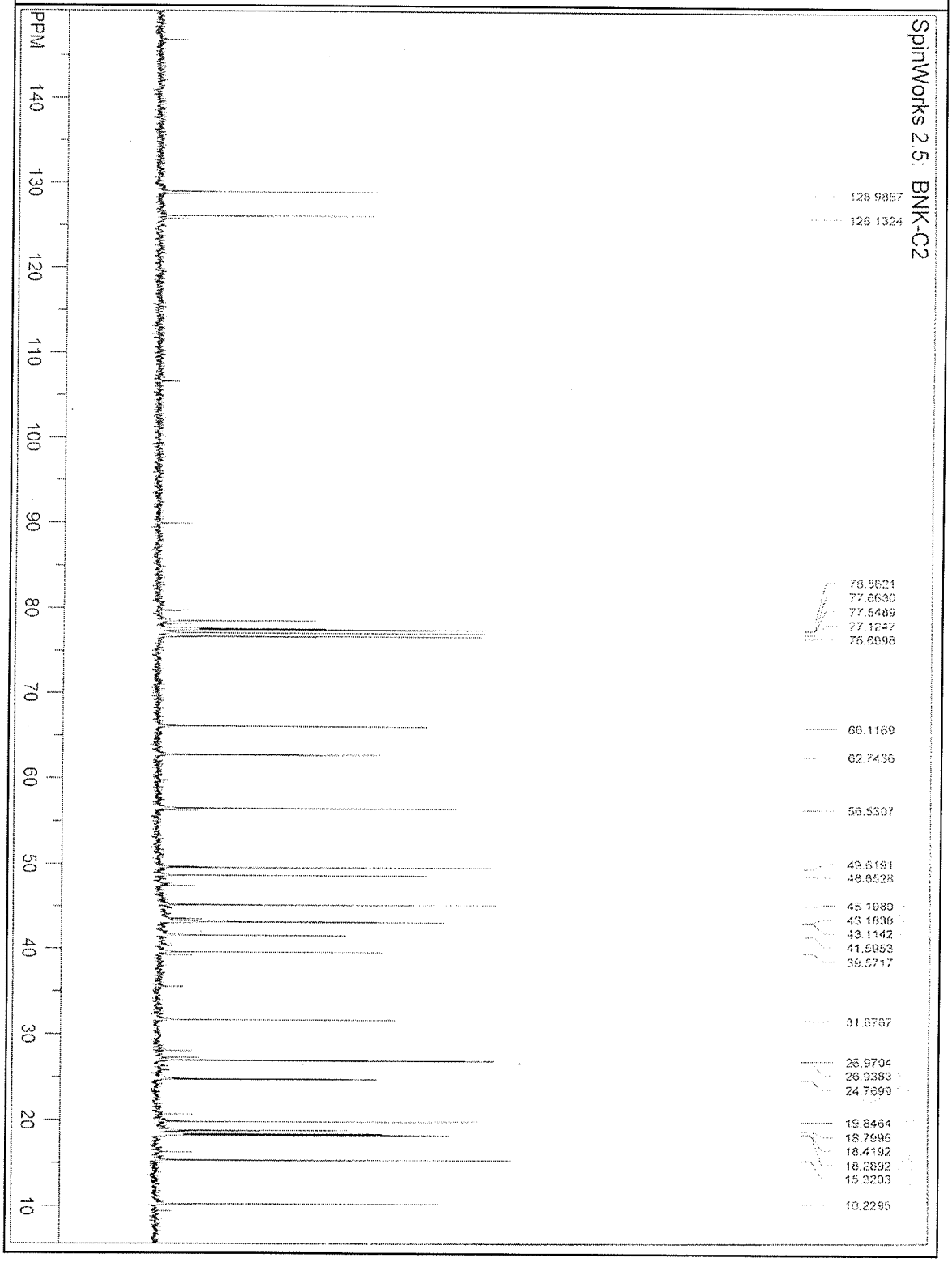

^{1}H-NMR spectrum of micaceol (**179**)

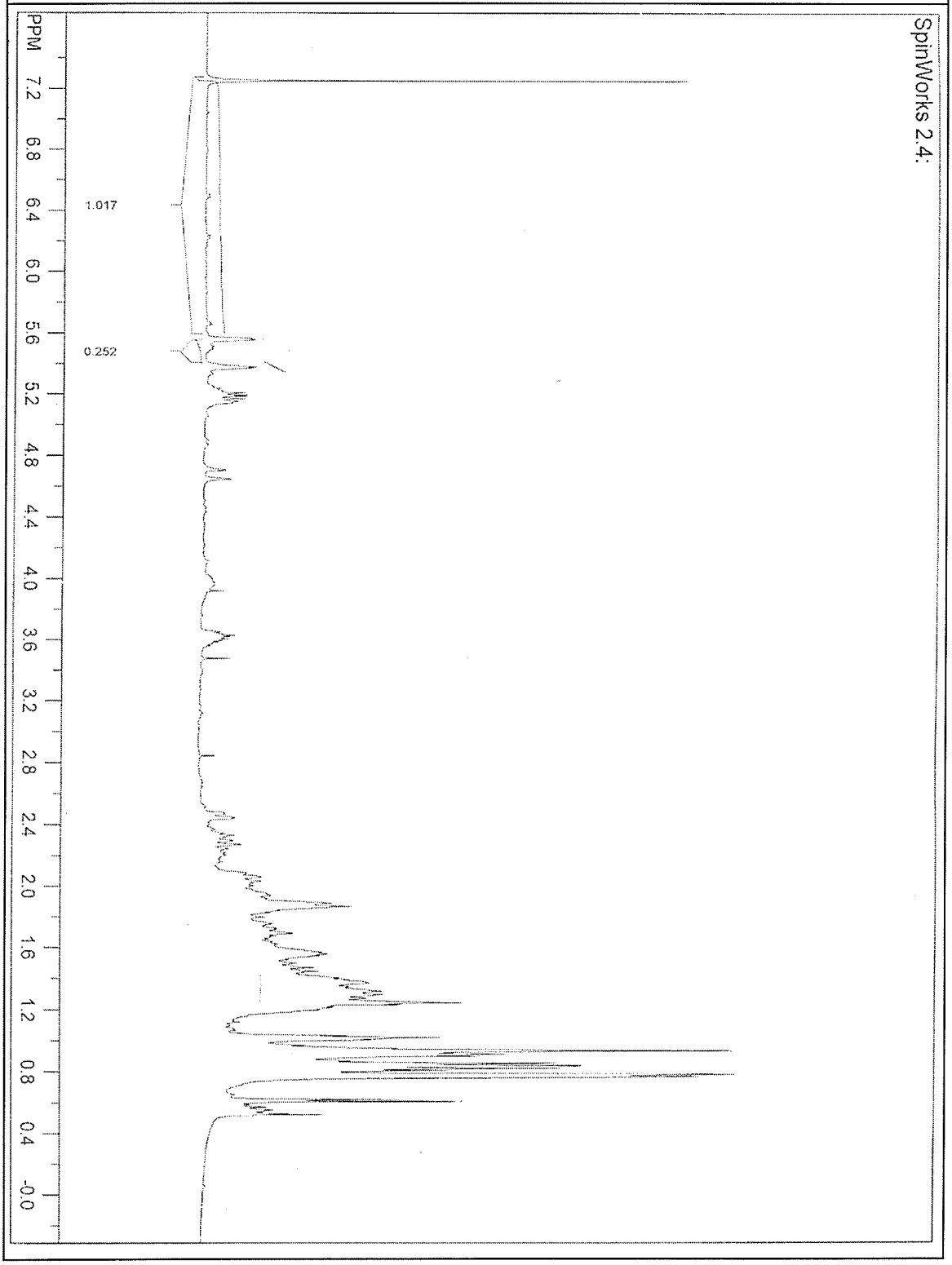

HSQC spectrum of micaceol (**179**)

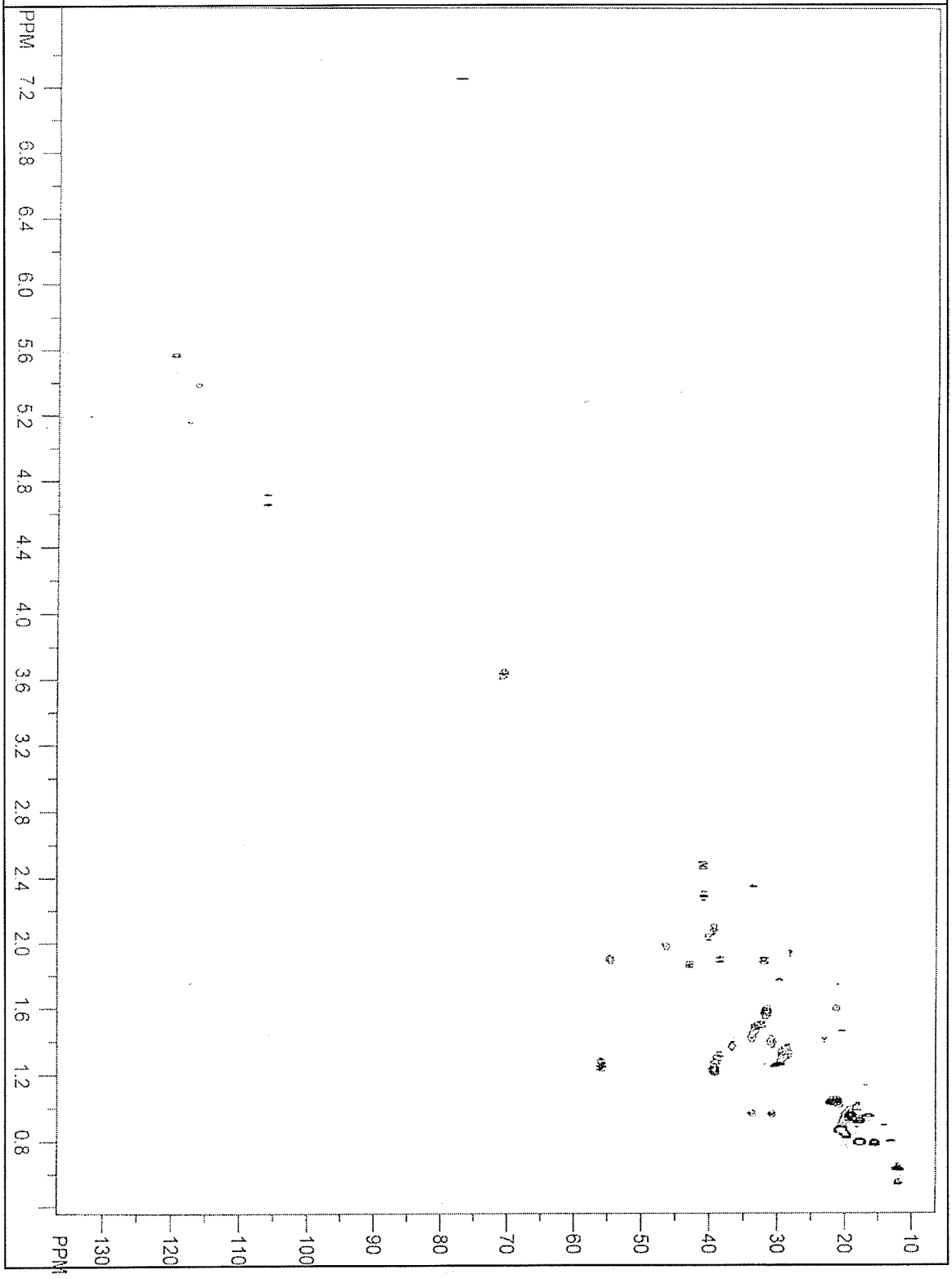

HMBC Spectrum of micaceol (**179**)

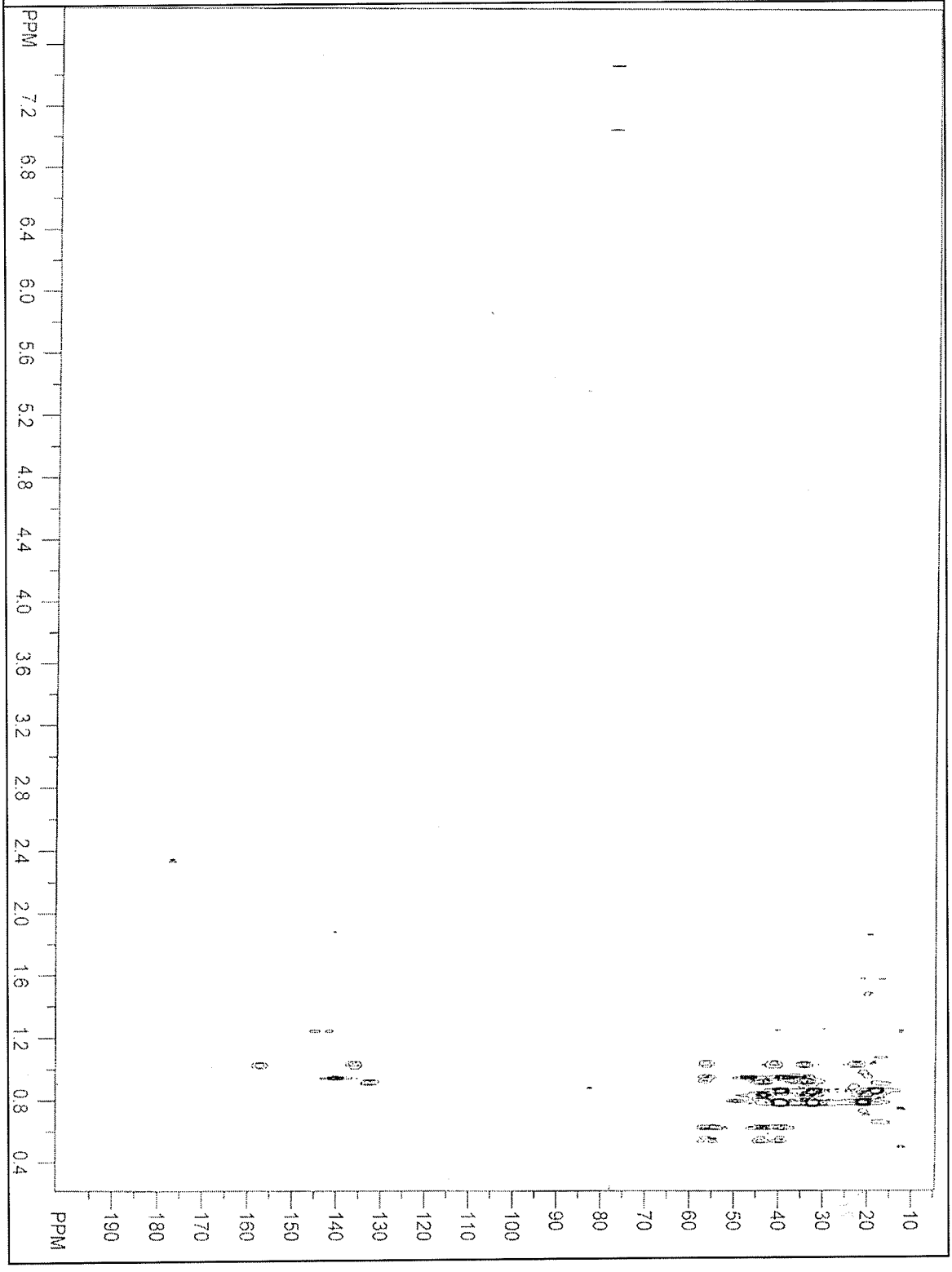

^{1}H-NMR spectrum of (Z, Z)-4-oxo-2, 5-heptadienedioic acid (**180**)

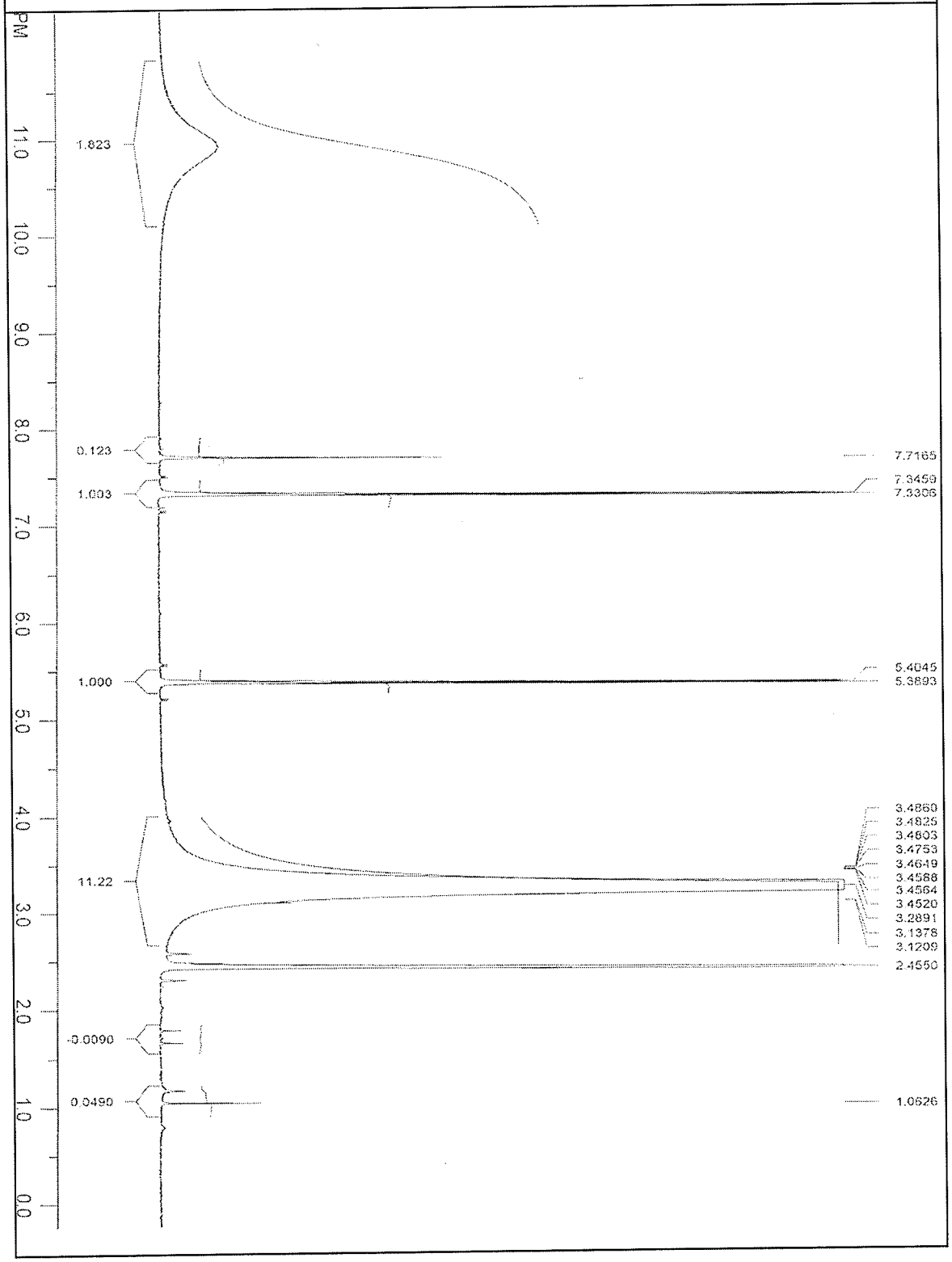

^{13}C-NMR spectrum of (Z, Z)-4-oxo-2, 5-heptadienedioic acid (**180**)